The Effect of Shear Stress on Bovine Nucleus Pulposus Cells

A thesis submitted to the Faculty of Science, Agriculture and Engineering for the Degree of Doctor of Philosophy

by

Cate Wilson MEng, BSc (Hons)

School of Mechanical and Systems Engineering

Newcastle University

March 2019

Abstract

Low back pain affects most people at some point in their lives, and intervertebral disc degeneration is a common cause of this pain. The nucleus pulposus is the first structure to fail in intervertebral disc degeneration. Gaining a greater understanding of the nucleus pulposus cell and its response to mechanical stimuli may be useful in tailoring the next cell-based regenerative therapy and preventative therapies. The nucleus pulposus is a highly hydrated, porous tissue and changes in spinal loading create fluid movement throughout the tissue, which causes fluid shear stress on the tissue and cells. This research has investigated shear stress rates of 0.1, 1.0 and 4.0 dyne/cm^2 on bovine nucleus pulposus cells. Steady and pulsed flow were studied over 1, 4, 8 and 24 hours using Ibidi VI$^{0.4}$ chambers. Results showed shear stress affects the morphology and gene expression of bovine nucleus pulposus cells. Morphological changes associated with cell detachment and reduced proliferation were seen in cells exposed to 1.0 dyne/cm for 4 and 8 hours and 4.0 dyne/cm^2 for 1, 4 and 8 hours. After 24 hours in 1.0 dyne/cm^2 and 4.0 dyne/cm^2 all cells had detached from the Ibidi VI$^{0.4}$ slides. There was an increase in cell proliferation in cells exposed to 0.1 dyne/cm^2 for 4 hours in steady flow and no change in cell number compared to control at 1, 8 and 24 hours in steady and pulsed flow. Changes in gene expression in 4.0 dyne/cm^2 flow were consistent with changes associated with catabolic metabolism; downregulation of collagen 2 and aggrecan and upregulation of aggrecanase 1 and 2. Results comparing steady and pulsed flow and gene expression changes at 0.1 and 1.0 dyne/cm^2 were inconclusive, further studies with a larger sample size could help to clarify these effects. These findings are important in guiding researchers in the development of optimal perfusion bioreactor conditions for cell-seeded nucleus pulposus regeneration therapies. The implications for research to increase our understanding of fluid flow through the intervertebral disc during exercise as a preventative measure for disc degeneration are also discussed.

Acknowledgements

I would like to express my special appreciation and thanks to Professor Tom Joyce and Dr. Phil Hyde whom have been a constant source of support and guidance throughout my research. Thank you to the Musculoskeletal Research Group, for their support and resources, especially Dr. Mark Birch and Mr. Kenneth Rankin and to Dr. Ria Toumpaniari, Dr. Simon Partridge and Joanna Pangou for the generosity with their time and support. Dr. Alex Laude in Bioimaging for his assistance with the microscopy and Dr. Saikat Jana, Brian Abraham and Oana Bretcanu in Bioengineering for their help and support. I would like to express my appreciation to Ken Madden and the technical team at the School of Mechanical and Systems Engineering of Newcastle University.

Table of Contents

Table of Figures

List of Tables

Nomenclature

AF Annulus fibrosus

ANOVA Analysis of variance

DAPI 4', 6-diamidino-2-phenylindole

DMEM Dulbecco's modified eagle's medium

DMSO Dimethyl sulphoxide

EDL Electric Double Layer

Ψ Electric potential

EOF Electro-Osmotic Flow

ECM Extracellular matrix

FBS Fetal bovine serum

FCD Fixed charge density

GAPDH Glyceraldehyde 3-phosphate dehydrogenase

GAG Glycosaminoglycan

IVD Intervertebral disc

IDD Internal Disc Disruption

MSCs Mesenchymal stem cells

Mequiv Milliequivalents

NICE National Institute for Health and Care Excellence

NSCLBP Non-specific chronic low back pain

NSAIDs Non-steroidal anti-inflammatories

NP Nucleus pulposus

PPFC Parallel plate flow chambers

PBS Phosphate Buffered Saline

PG Proteoglycan

RT-PCR Reverse transcriptase polymerase chain reaction

SEM Scanning electron microscope

ζ Zeta potential

Chapter 1. Introduction

1.1 Research context

This research investigates the use of mechanical stimuli by way of fluid shear stress to affect the morphology and metabolism of nucleus pulposus cells. The aim of which is to gain knowledge which may facilitate novel cell-based bioengineering approaches for the treatment of low back pain. Low back pain affects 80% of the population at some point in their lives (Andersson, 1999) and causes more global disability than any other condition (Hoy et al., 2014). Annual healthcare costs associated with chronic low back pain treatment cost the UK £2.8 billion per year (Hong et al., 2013). A more recent study in the US found low back pain and neck pain to be the third biggest healthcare spend at $87.6 billion per year. Discogenic pain; that is pain arising from the intervertebral disc, has been shown to be the most common cause of chronic low back pain in adults, accounting for between 26-42% of patients (DePalma et al., 2011). The intervertebral discs lie between the vertebrae of the spine, they are hydrated fibrocartilaginous structures which give stability while allowing movement in the spine, and also act as spacers giving height to the interforaminal spaces wherein the spinal nerves lie (Palastanga, 2012). The main cause of discogenic pain is now widely thought to be due to internal disc disruption, which manifests as degradation of the internal matrix of the disc and fissures which extend from the centre of the disc to the outer part of the disc (Adams, 2013). The outer third of the disc is innervated and fissures or degraded disc matrix in contact with these nerves can illicit pain (Adams, 2013).

The intervertebral disc is a highly hydrated porous structure, consisting of a matrix of mainly collagen and the proteoglycan known as aggrecan, which is hydrophilic. Nucleus pulposus cells lie within this collagen-aggrecan matrix of the NP and are responsible for maintaining the matrix through synthesis of anabolic and catabolic proteins in a balanced system (Bogduk, 2011). The environment surrounding the cells is paramount to their correct functioning and maintenance of the disc matrix. The cells in the intervertebral disc experience mechanical stimuli through postural changes, spinal loading and movement. Cells experience compression and elongation through physical movement of the disc matrix they lie within and shear stress from movement of interstitial fluid surrounding them. Fluid movement into and out from the disc as well as through the matrix of the disc (intra-fibrillar) is the focus

of this research, there will likely be fluid movement inside collagen fibres as well (inter-fibrillar) but this is not discussed.

The mechanism of flow into and through the disc matrix is complex. It is affected by the concentration of aggrecan, the hydration of the disc, the porosity of the disc and the concentration of the interstitial fluid (Ferguson et al., 2004, Accadbled et al., 2008, Farrell and Riches, 2011, Nield and Bejan, 2013, Gu and Yao, 2003). Therefore, it may be considered likely that different flow types and flow speeds (shear stress values) could be experienced by the cells. This could be especially so in conditions such as internal disc disruption where the structure of the disc matrix breaks down and leads to fissures, which would increase the volumetric flow through the matrix due to an increased pore size while decreasing the fluid shear stress due to a decreased fluid velocity. Analysing the effect of different flow types and fluid shear stress values and over a series of time points would be useful in identifying dynamic environments which may be beneficial or detrimental for cell health.

The challenge facing clinicians in the treatment of low back pain is that often the condition is so far escalated by the time pain is felt and the patient seeks treatment that the options are limited. Current treatments for discogenic pain, discussed in Chapter 2 are aimed at reducing patient symptoms rather than curing the underlying cause of the pain. Novel research has turned to cell-based regenerative medicine with an aim to find treatments for discogenic pain focussed on the possible repair and regeneration of the intervertebral disc tissue. These include cell-seeded scaffolds which can be inserted into the degraded nucleus pulposus (Fernandez et al., 2016). In order to ensure a healthy environment for cells and to promote cell growth and uniform distribution on the scaffold, the temperature, pH, nutrient concentration and solute concentration surrounding the cells need to be maintained, this is done so through a bioreactor (Walter et al., 2014). The role of bioreactors has developed over the years from static containers in which the aim was to optimise conditions for cell growth to dynamic bioreactors, which try to mimic in vivo conditions, including mass transfer and mechanical stimulation. As in static bioreactors they must provide an optimum environment for cell requirements, including temperature, pH and ensure correct concentrations of oxygen content, nutrient content, growth factor supply. They also ensure waste product removal to maintain the balance required to maintain cell

health and metabolism and the exposure of cells to mechanical stimuli through loading or shear stress (Bancroft et al., 2003, Raimondi et al., 2016, Ding et al., 2016).

1.2 Research focus

Mechanotransduction is the mechanism by which cells turn mechanical signals into biochemical signals. NP cells in vivo are anchored to their extracellular matrix through focal adhesions. Changes in mechanical stimuli through loading of the intervertebral disc have been shown to affect the metabolism of NP cells (Le Maitre et al., 2009, Wang et al., 2011, Neidlinger-Wilke et al., 2006). However, there is only one other research study on the effect of shear stress as a mechanical stimuli on NP cells (Wang et al., 2011). There is a large body of research on the effect of shear stress on cells in other body tissues, for example in endothelial cells of the vascular system (Chatzizisis et al., 2007, Traub and Berk, 1998), and more recently chondrocytes (Gharravi et al., 2016, Wan et al., 2013) and stem cells (Sonam et al., 2016, Raimondi et al., 2016); and it has been demonstrated this fluid movement causes mechanotransduction in cells which can help to maintain the balance in metabolism required for a healthy tissue matrix or can cause degenerative effects.

This research aims to build on the gap in current knowledge regarding the effect of shear stress on NP cells and with perfusion bioreactors becoming ever more popular in the field of bioengineering any information which could guide the successful use and development of these novel bioreactors should be utilised. Increasing research knowledge of the influence of shear stress on NP cells and furthermore if different regimes of flow; including type of flow, speed of flow and duration of flow applied to NP cells will be of value to the bioengineering research community working to develop novel cell-based treatments for discogenic pain. The main research question to be answered is; does fluid shear stress affect nucleus pulposus morphology and gene expression? Further questions emerging from this are; does the type of fluid shear stress (steady or pulsed) affect NP morphology and gene expression? Does the shear stress rate affect NP morphology and gene expression? And if so, does the length of time cells are exposed to the shear stress have an influence on the cell morphology and metabolism?

Answers to these questions will also give a greater understanding of the role of shear stress on NP cells which will likely increase the body of knowledge surrounding mechanotransduction of NP cells with respect to the effect of shear stress on the morphological and metabolic response of NP cells to shear stress. This should also help to guide researchers using perfusion bioreactors on flow regimes in which to expose cell-seeded scaffolds, including information on the type of flow, the speed of flow and the duration of flow.

1.3 Brief methodology

In order to create a dynamic flow environment over the cells, they will be grown in a parallel plate flow chamber. The cells are grown in a monolayer and adhere to the bottom surface of the slide and then a thin film of fluid is driven over them using a pump. A monolayer is used so that the appearance of the cells can be more easily studied. The small size of the channel allows a laminar flow of which the characteristics can be used to determine the shear stress that the cells experience in the flow chamber from a known volumetric flow rate. Two types of pumps will be used in this research to create two different types of fluid flow; steady and pulsed. In order to determine the NP cell condition under flow regimes, the morphology and metabolism of the NP cells will be assessed. Assessing morphological changes of the cells will allow tracking of any changes in cell number; which could indicate if cells have proliferated (increased in number) or detached from the slide (decreased in number). The number of focal adhesions per cell will also be assessed. Focal adhesions are responsible for adherence of cells to the flow chamber (Geiger et al., 2009). Nucleus pulposus cells respond to mechanical stimuli in their environment through focal adhesions, which are junctions between inner and the extra-cellular matrix (Nettles et al., 2004). The shape of the cells will be tracked by analysing the cell circularity, the “roundness” of the cell which is a value between 1 and 0, with 1 signifying a circle and 0 signifying a straight line. Assessing the possible synthesis of proteins by the cell through analysing the gene expression would give an indication about the metabolism of the cell and if a change in environment through shear stress would change the proteins synthesized by the cell. The gene expressions that will be studied are of collagen 1, collagen 2 and aggrecan, all of which are genes found in anabolic metabolism and are responsible for building the matrix of the intervertebral disc and aggrecanase 1 and aggrecanase 2 which are associated with catabolic

metabolism of cells, involved in the breakdown of the hydrophilic protein aggrecan. A balance between these anabolic and catabolic processes is essential for the correct functioning of the intervertebral disc (Grunhagen et al., 2006). Analysis of the morphology and metabolism by the methodology briefly discussed will answer the research questions and help to fill a gap in knowledge surrounding the response of NP cells to fluid shear stress.

1.4 Outline of chapters

This chapter has detailed a brief overview of the purpose of the project and gap in research. Chapter two details a more in depth look at some of the background topics discussed in this chapter and literature review as a basis for the rationale for this project. Chapter three details the methodology chosen for the study, the rationale for the choice of flow chamber and pumps are discussed, and the methods of quantifying any changes seen in the cells are described. Chapter four will detail the results that were obtained for the 8 dependent variables under the 3 independent variable conditions. Mixed ANOVAs, one-way ANOVAs and Repeated Measured ANOVAs will be used to compare between-subject results and within-subject results. Chapter five will discuss the results analysed and link these findings to the greater research area as discussed in the literature review. Limitations of the project and future work will also be discussed at this point. Finally, chapter six will draw the main conclusions found from the research and how this can aid in the field of bioengineering of novel intervertebral disc treatments.

Chapter 2. Background

The early focus of this chapter in section 2.1 describes the anatomy and function of the nucleus pulposus. It begins with the general structure of a spinal segment through to the more detailed structure and function of the vertebral endplates and intervertebral disc. The structure and function of the healthy nucleus pulposus matrix is then described including the mechanisms by which fluid flows to and from the nucleus pulposus and how the healthy nucleus pulposus maintains nutrition and hydration. Description of the nucleus pulposus cells, down to the delicate detail of the DNA contained within the nucleus of the cell is then described. Section 2.2 outlines the regulation of the nucleus pulposus matrix and how the surrounding environment of a cell can alter the proteins that it synthesises through mechanical forces (such as fluid shear stress) and biochemical processes. Section 2.3 outlines what happens when the matrix of the nucleus pulposus degrades, the processes of intervertebral disc degeneration, discogenic pain and disc prolapse and treatment options are discussed. Section 2.4 discusses novel cell-based therapies as an exciting new area of research in the possible treatment of IDD leading onto the aims and objectives of the research. The chapter concludes with section 2.5 in which the findings of the chapter are drawn together to justify the aims and objectives of the research undertaken.

2.1 The Structure and Function of the Nucleus Pulposus of the Lumbar Spine

2.1.1 Nucleus pulposus structure

The nucleus pulposus lies within the intervertebral discs of the spine, there are 23 intervertebral discs in the spinal column, as shown in figure 2.1a. The discs act as spacers between the vertebrae to maintain the intervertebral foramen and allow movement with stability through the spine (Costi et al., 2007). Vertebral endplates lie between the disc and the vertebrae. Facet joints link the vertebrae together at the posterior aspect of the spine (Palastanga, 2012). The intervertebral discs contain the nucleus pulposus and annulus fibrosus and create intervertebral foramen, spaces between the vertebrae, wherein lie the spinal nerves. The role of the intervertebral disc (IVD) is to allow supportive movement and load transfer. The vertebral endplates are permeable and allow the transfer of nutrients and fluids between the vertebral body and the nucleus pulposus. Ligaments surround the facet joints and support the

anterior and posterior of the spine. Muscles are attached to the spine itself and surround the spine to give support and facilitate movement. Back pain arising from the lumbar spine is the focus of this research. The lumbar spine consists of the lowest 5 vertebrae as shown in figure 2.1.

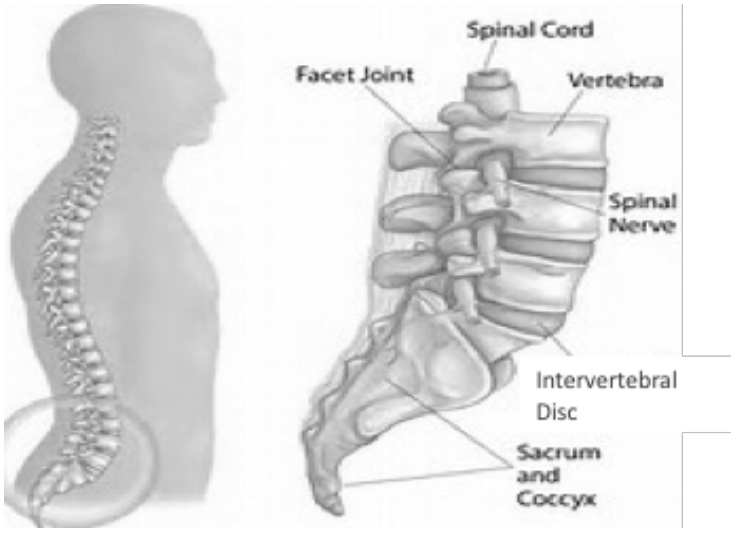

a) **b)**

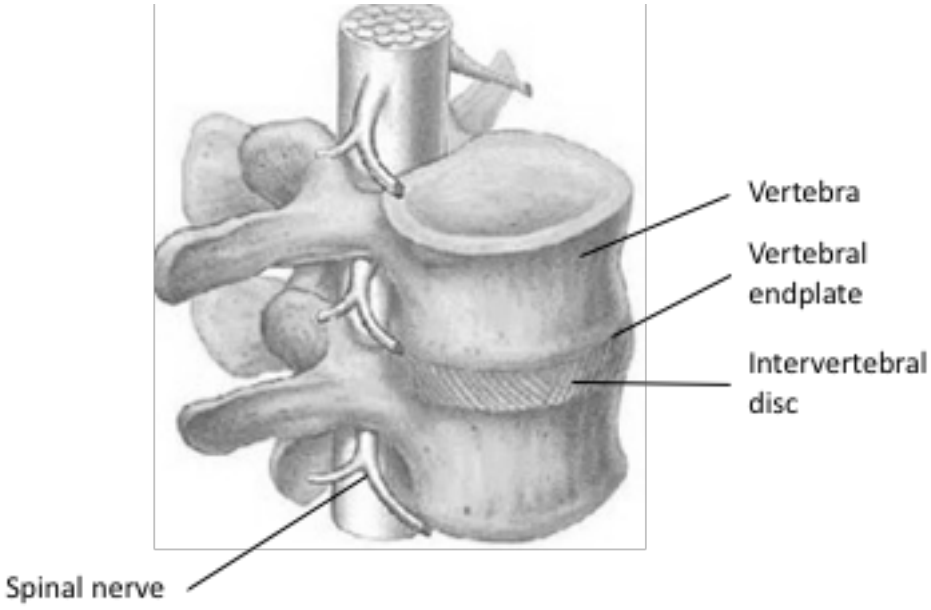

c)

Figure 2.1 a) The spinal column, b) the lumbar spine c) a spinal segment (Palastanga, 2012)

The focus of the research undertaken was on fluid flow in the nucleus pulposus. The nucleus pulposus is in direct contact with the vertebral endplate and annulus fibrosus, which are integral to its structure and function. The annulus fibrosus and nucleus pulpous make up the intervertebral disc. The intervertebral disc consists of the nucleus pulposus surrounded by the annulus fibrosus. The first published dissection of the intervertebral disc was performed by Coventry (1945) and detailed a poroelastic structure made up of layers of a fibrocartilaginous collagen and proteoglycan matrix. Thirty years later scanning electron microscope (SEM) images of human discs of various ages detailed an adult human annulus with a regular network of collagen fibrils on average 0.1-0.2 μm thick with a regular periodicity of on average 600 angstrom in width and a less structured nucleus pulposus with a loose network of collagen fibres (Inoue and Takeda, 1975).

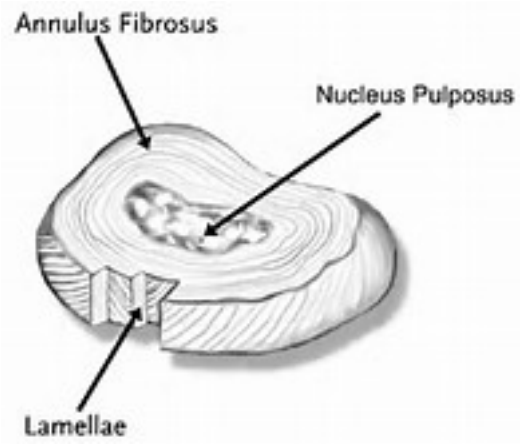

Figure 2.2 The Intervertebral Disc the gel-like centre (NP) and the outer cartilaginous layers (lamellae) of the AF

The main components of the intervertebral disc are water, collagen and proteoglycan and these components are integral to the functioning of the disc. In a healthy intervertebral disc, the annulus fibrosus consists of 10-20 lamellae arranged in concentric rings. They are orientated at 120^{o}-130^{o} to each other and the direction from layer to layer changes to give the disc anisotropy which adds to its strong tensile properties in 6 degrees of freedom. The healthy annulus pulposus (AP) contains up to 70 % water (Bogduk, 2011). The nucleus is a less well organized, but more hydrated structure, containing irregularly arranged collagen fibres and up to 80 % water (Urban and Maroudas, 1981). The high water content of the disc is due to

a proteoglycan called aggrecan, which is a hydrophilic protein, and is crucial for the correct functioning of the intervertebral disc (Melrose et al., 2008).

2.1.2 Nucleus pulposus nutrition

The endplate is essential for IVD nutrition, it is a structure less than 1 mm thick which is situated between the intervertebral disc and the vertebra. It consists of a hyaline cartilage layer; the cartilage endplate (CEP) and an osseous layer; the bony endplate (BEP) (Malandrino et al., 2014). The cartilage layer consists of collagen I and II, proteoglycans, water and chondrocyte cells. The collagen fibres are aligned horizontally. The bony part consists of fused trabecular bone, is porous and contains osteocytes (Lotz et al., 2013). The endplate covers the full superior and inferior surfaces of the nucleus pulposus and the inner half of the annulus fibrosus, as shown in figure 2.3. The collagen fibres of the inner half of the annulus fibrous run through the endplate. This causes the attachment of the intervertebral disc to the endplate to be much stronger than the attachment of the vertebral body to the endplate (Inoue and Takeda, 1975). The endplate is infiltrated by capillaries from which nutrients can flow to and from and diffuse into the intervertebral disc (Crock et al., 1973). This is essential for the nutrition of the endplate and intervertebral disc (Holm et al., 1981).

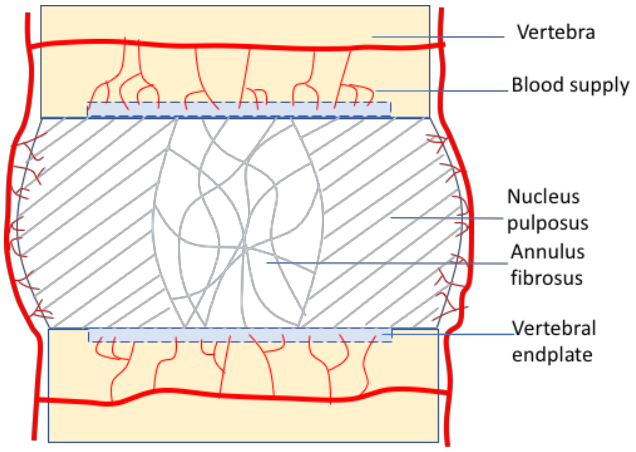

Figure 2.3 The Intervertebral Endplates and Vascular Supply

Cells must be surrounded by the correct environment to function effectively which requires an adequate nutrient supply. Electrolytes are essential to control cell membrane stability; oxygen and glucose are essential as energy sources for ATP; and growth factors are essential for cell proliferation. Nutrition for nucleus pulposus cells is essential to maintain a healthy nucleus pulposus matrix. However, the

nucleus pulposus does not have a direct blood supply, so depends on neighbouring blood supplies in the endplate and outer annulus for transport of nutrients. Interstitial fluid within the IVD consists of water dissolved with electrolytes; Na^+, Cl^-, Ca^{2+}, larger molecules; cytokines and growth factors, and small solutes; oxygen, carbon dioxide, glucose, and lactate.

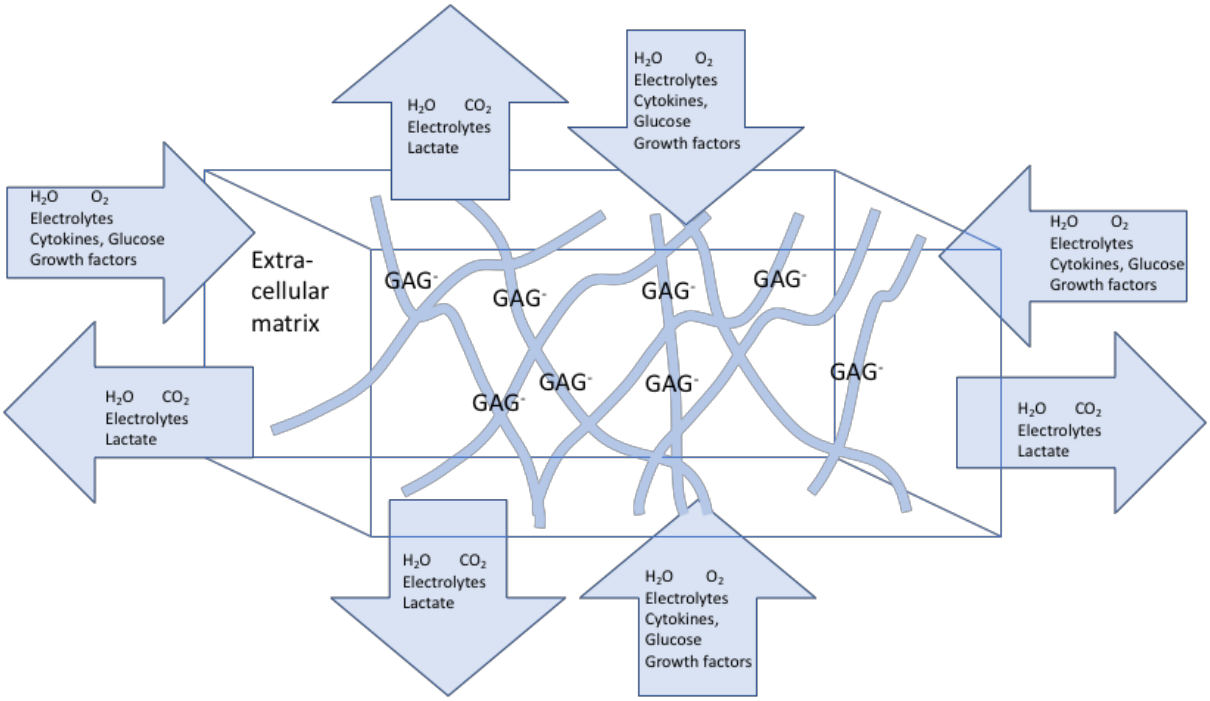

Figure 2.4 Nutrition to and from the intervertebral disc

The electrolytes and small solutes freely pass through the vertebral endplate and disc by diffusion caused by concentration gradients (Urban, 1977, Ferguson et al., 2004). As oxygen and glucose are metabolised by the cells their concentration in the matrix will decrease, maintaining a concentration gradient. Equally, as carbon dioxide is produced by the cells and its concentration increases, so will the concentration gradient be present for carbon dioxide to be expelled from the disc. Small nutrients and ions, such as Na^+, Cl^-, K^+, Ca^{2+}, O_2, CO_2 and glucose diffuse to and from the capillaries in the bony end plate, through the cartilage end plate and to and from the nucleus pulposus. These small nutrients are also able to diffuse to and from the annulus fibrosus due to the capillary supply in the outer layers of the annulus fibrosus and from there can diffuse into the nucleus pulposus. Larger molecules such as cytokines, which are important for regulation of cell processes (Park and Park, 2016),

travel through the disc due to ‘Pressure-Driven Flow’, caused by pressure changes in the disc creating fluid movement.

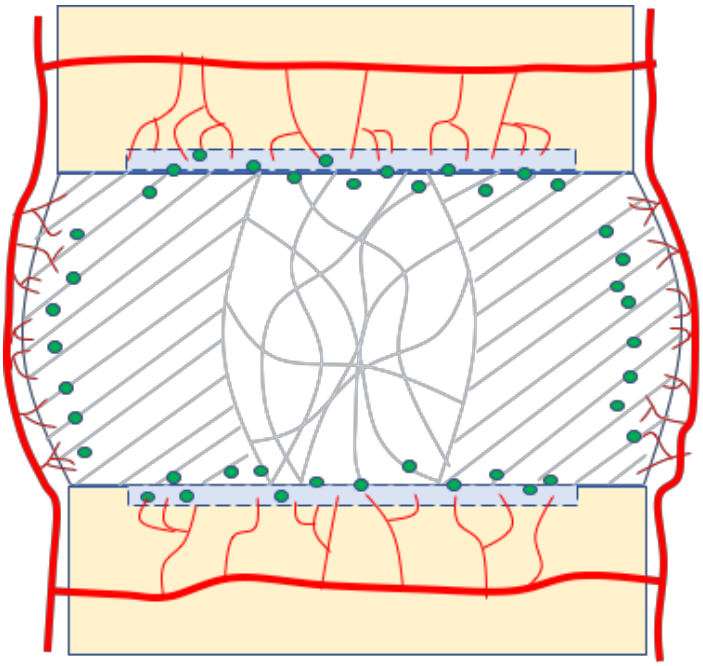

Figure 2.5 Flow of nutrients (green dots) to and from the intervertebral disc from the surrounding blood supply.

Nutrients will flow through the quickest route to get to the disc and this can be influenced by spinal posture and movement (Ferguson et al., 2004). Studies investigating postures which could help nutrition of the disc showed that flexed postures favoured movement into the posterior of the disc and upright postures favoured fluid movement into the anterior of the disc. Flattening the lordosis of the lumbar spine when sitting and lifting heavy weights may be more advantageous due to flexion improving transport of metabolites and reducing stress on the facet joints. However, flexion also increases stress on the anterior annulus fibrosus and increases hydrostatic pressure at low load levels so may not be advisable for prolonged postures. (Adams and Hutton, 1983, Adams et al., 1986a).

2.1.3 Intradiscal pressure

The central portion of the nucleus pulposus originates from the notochord of the developing foetus. Its periphery is derived from the mesenchyme and is fibrocartilaginous. At birth, notochordal cells are still present but these reduce with age and in most cases are no longer present from four years of age (Bogduk, 2011).

The nucleus pulposus matrix consists mainly of collagen II, the proteoglycan known as aggrecan, and water. In smaller abundance, there is also collagen I and the proteoglycan known as versican present. The structure of proteoglycans causes them to be highly hydrophilic. They consist of keratin sulphate and chondroitin sulphate glycosaminoglycan (GAG) chains which are made up of numerous carboxyl and sulphate groups, these groups become negatively charged when dissolved in the interstitial fluid which bathes the disc (Varki et al., 1999, Hillsley and Frangos, 1994). These negative charges attract the dipole of the hydrogen on the water molecules which holds water in the disc. To a lesser extent, the shape of the long proteoglycan (PG) strands also help to trap water molecules.

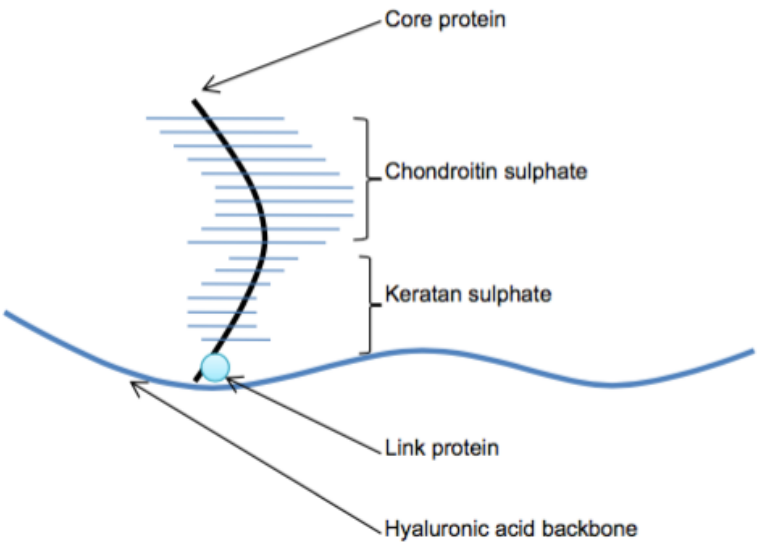

Figure 2.6 General proteoglycan structure showing attachment of the core protein to the hyaluronic acid back bone by a link protein

As shown above in figure 2.6 and 2.7, proteoglycans consist of chains of glycosaminoglycans (GAGs, for example chondroitin sulphate and keratan sulphate) linked to proteins.

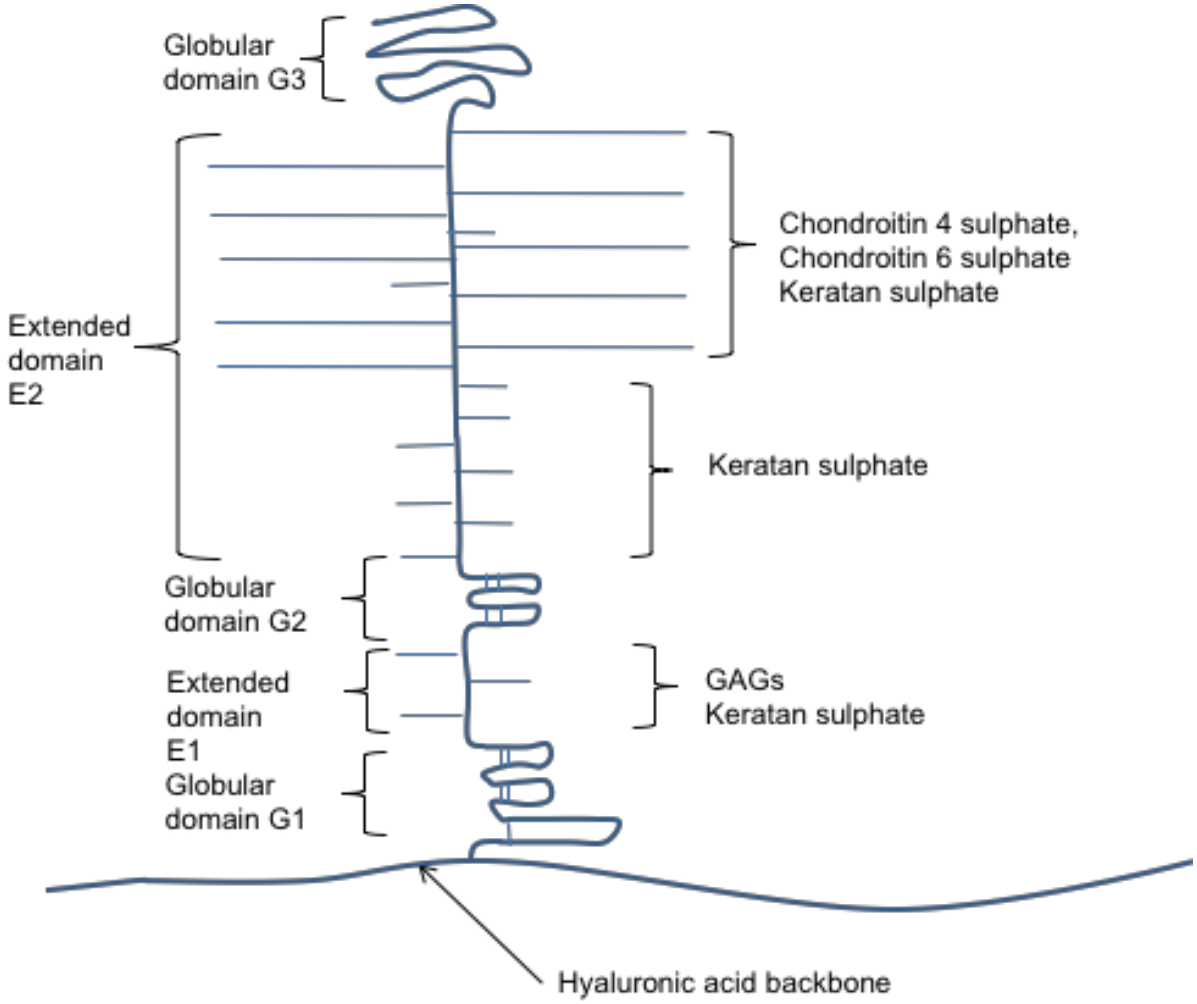

Figure 2.7 Detailed structure and shape of aggrecan molecule

Figure 2.7 shows the molecular structure of the two types of chondroitin sulphate (4 and 6) and keratan sulphate as well as the structure of hyaluronic acid which makes up the backbone of the GAG. This shows the COOH and SO_4 groups which become COO^- and SO_3^- in fluid and create the hydrophilic nature of the GAGs.

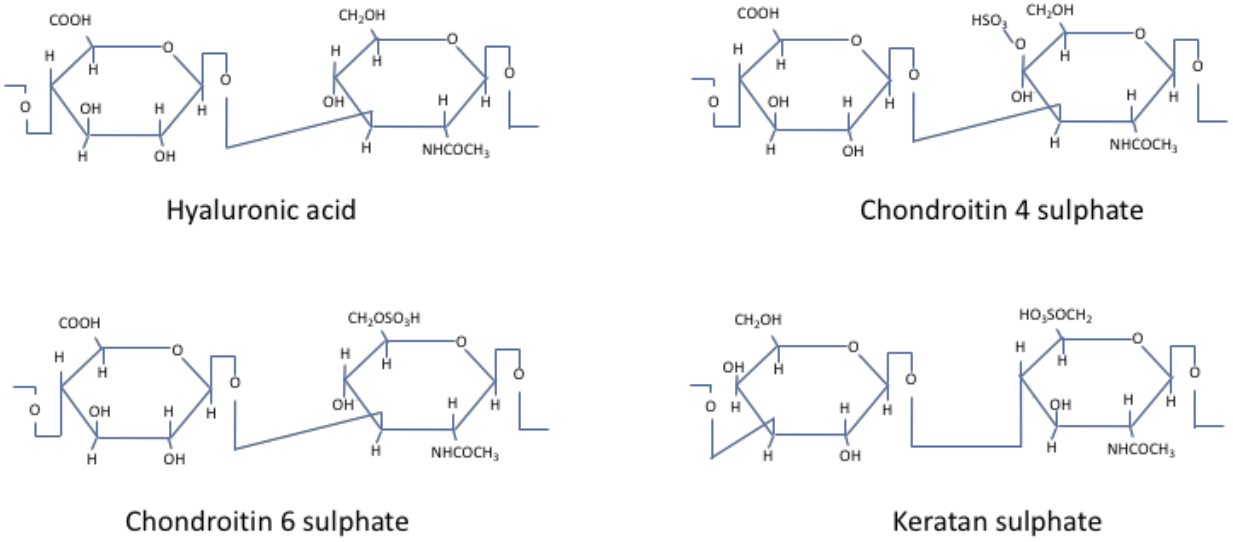

Figure 2.8 Structure of 4 GAGs contained in aggrecan

One of the fundamental functions of the nucleus pulposus is its ability to with stand and distribute load through the intervertebral disc. As mentioned, water, collagen and proteoglycan are the main components of the IVD and give the disc its structure and allow it to function normally. Due to the high water content of the nucleus pulposus, in its simplest form it can be thought of as a ball of fluid which can be deformed but not compressed (Iatridis et al., 1996). In a healthy, hydrated disc, when pressure is exerted on the disc through muscle forces and spinal movement, pressure is first exerted on to the nucleus pulposus which sits just proud of the annulus fibrosus which then exerts pressure against the annulus fibrosus, see figure 2.7. In a healthy AF, the high tensile properties of its collagen fibres prevent deformation and oppose the pressure exerted on them. Vertebral endplates create the same opposition of pressure and this causes the intradiscal pressure in the nucleus pulposus to increase (Nachemson and Morris, 1964b).

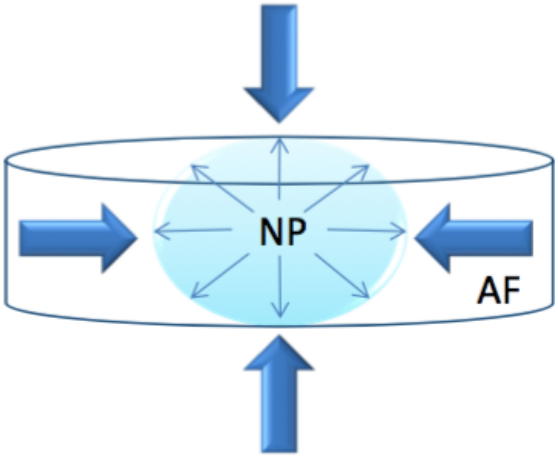

Figure 2.9 Schematic drawing depicting compression of IVD due to muscle forces and intradiscal pressure created as a result

Intradiscal pressure has been measured during in-vivo studies where a pressure transducer needle was inserted into the centre of the NP in live human subjects. During these studies pressure in the centre of the disc ranged from 0.1MPa to 1.1MPa. The lowest readings were yielded when the person was supine lying and the highest readings were in flexed standing with loading (Nachemson and Morris, 1964b, Wilke et al., 1999). The NP will withstand the pressure exerted on it until the intradiscal pressure exceeds the osmotic pressure created through the hydrophilic nature of the proteoglycan (Wognum et al., 2006). This is called the fixed charge density (FCD) and is a measure of the negative charges (carboxyl and sulphate groups) attached to the disc matrix. The unit is measured per unit volume and is often written in units of milliequivalents (mequiv) which is the amount of substance required to supply one mole of electrons in a redox reaction (Urban and Maroudas, 1979). When the pressure exerted on the disc exceeds the osmotic pressure resulting from the FCD then, due to the porous nature of the disc matrix, fluid flows from the disc and due to the reduced pressure of the NP resulting in axial load acting directly through the AF instead of being shared with the NP, bulging of the AF occurs (Hickey and Hukins, 1980). Fixed charged density has been measured and found to reduce as the IVD aged, 0.28mequiv/g in 27-year-old disc compared to 0.18-0.24 mequiv/g in 74-year-old disc. It was highest in the NP and fell steeply in the outer annulus to about 0.07-0.13 mequiv/g (Urban and Maroudas, 1979).

2.1.4 Nucleus pulposus fluid movement

Fluid flow into the disc occurs through the porous vertebral endplates directly to the nucleus pulposus and from the outer annulus fibrosus to the inner annulus fibrosus and then to the nucleus pulposus. Fluid flow out of the disc follows the same pathways in reverse. The movement of fluid through the collagen fibrils of the extracellular matrix is termed interfibrillar flow. Fluid also flows within the collagen fibres, known as intrafibrillar, although this is not covered in this research. For the purpose of discussing the mechanism of flow to and from the disc in this section; mechanisms which draw fluid into the disc from outside the disc and then through interfibrillar flow within the extracellular matrix of the disc to the nucleus pulposus, and the reverse mechanism which extrudes fluid out from the nucleus pulposus to the outside of the disc are discussed. In discussing fluid shear stress through fluid flow over the NP cells, see section 2.6, interfibrillar fluid flow through the extracellular matrix of the NP is the focus.

Flow to and within the disc is complex but can be described by 4 mechanisms. Mechanisms 1-3 are termed diffusio-osmotic flow and mechanism 4 is pressure-driven flow. Mechanisms 1 and 2 are governed by carboxyl and sulphate groups on the glycosaminoglycan dissociate due to the water molecules in the interstitial fluid to create negatively charged COO^- and SO_3^- (Linn and Sokoloff, 1965). This creates two methods of water movement into and within the disc, in mechanism 1 the dipole nature of the water molecules are attracted to the negative charges and in mechanism 2 the K^+ and Na^+ ions which were dissociated from their negative Cl^- counterpart are also drawn towards the carboxyl and sulphate groups which creates an osmotic gradient which draws water through osmosis (Gu et al., 1998).

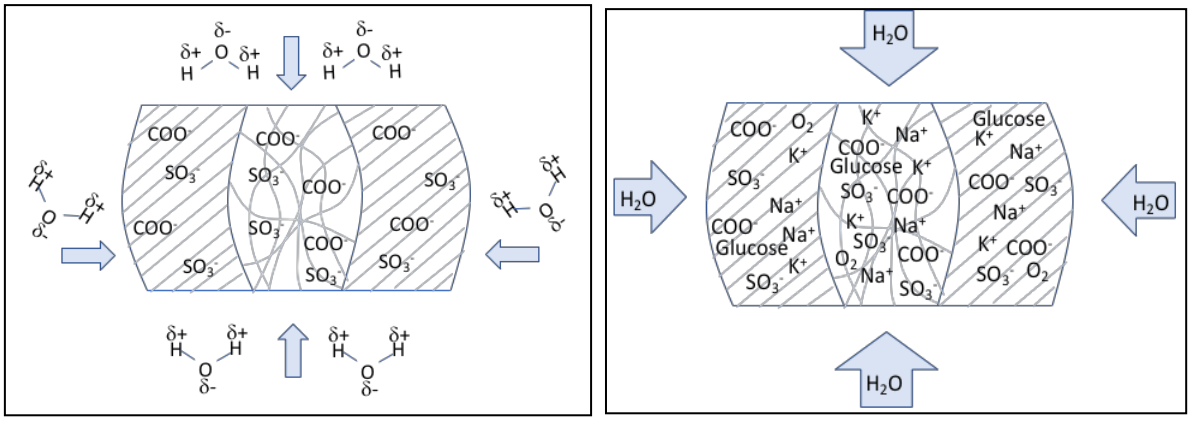

a) b)

Figure 2.10 a) dipole of water molecule, attracted to negative charge of COO^- and SO_3^-, from GAGs, b) high electrolyte concentration within disc due to influx of K^+ and Na^+ causes water to flow in down a concentration gradient.

Mechanism 3 is due to the small pore size in the disc causing electro-osmosis effects at the solid-fluid boundary which effects the cations and anions in the interstitial fluid. The negatively charged ions in the tissue cause the cations near the tissue surface to be attracted to the wall, this creates an electric double layer (EDL) which has a higher cation content (Lai and Mow, 1999). The fixed charge density (FCD) in the NP is higher than in the AF so there is an attraction of cations though the outer pores (AF) in the disc matrix to the inner (NP), this attraction of cations creates a bulk flow in the fluid (Urban and Maroudas, 1979). The charged nature of the fluid and disc tissue are integral to their role in movement of fluid through the disc through Electro-Osmotic Flow (EOF). EOF creates fluid flow through and within the disc due to the negative charge of the tissue. The cations (positive ions) in the fluid are drawn to the channel which form the Stern Layer, a boundary of strongly attracted cations attached to the wall. The next boundary is the layer with a greater concentration of cations than anions, but they are not adhered to the channel wall, this is known as the diffuse layer. These two boundaries make up the Electric Double Layer (EDL), shown in figure 2.11. The addition of an electric field at the end of the channel, such as in the high aggrecan content of the IVD matrix on the EOF creates movement of the excess of free ions in the diffuse layer which induces a bulk flow, so draws fluid towards the aggrecan and maintains the hydration of the disc (Mitra, 2012).

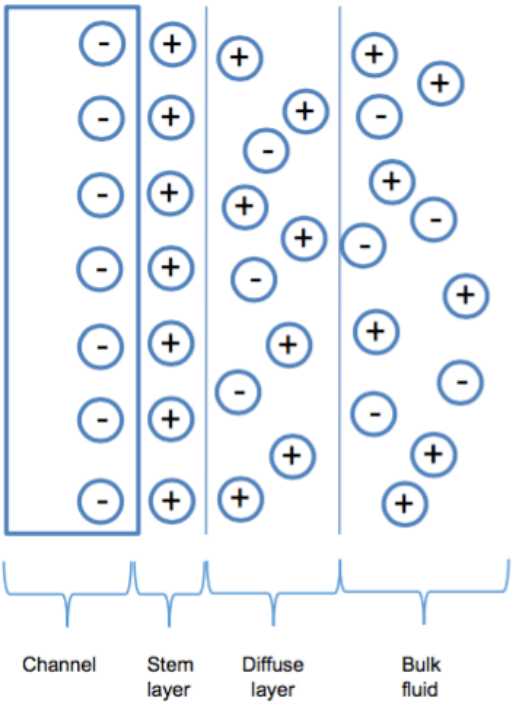

Figure 2.11 The Electric Double Layer (EDL), as present on the solid-liquid boundary in negatively charged biological tissue, such as the IVD (Mitra, 2012).

The fourth method of fluid delivery is through pressure driven flow through diurnal changes (sitting, standing, lying down, creating pressure changes over the disc) (Malko et al., 1999) and spinal movements. This has been discussed in section 2.2 in relation to the movement of larger solutes, growth factors and cytokines through the disc, but is also a mechanism of flow of fluid into and out of the disc. The disc has been shown to imbibe fluid overnight and increase in height by 10% compared to disc height at the end of the day (Zander et al., 2010)

.

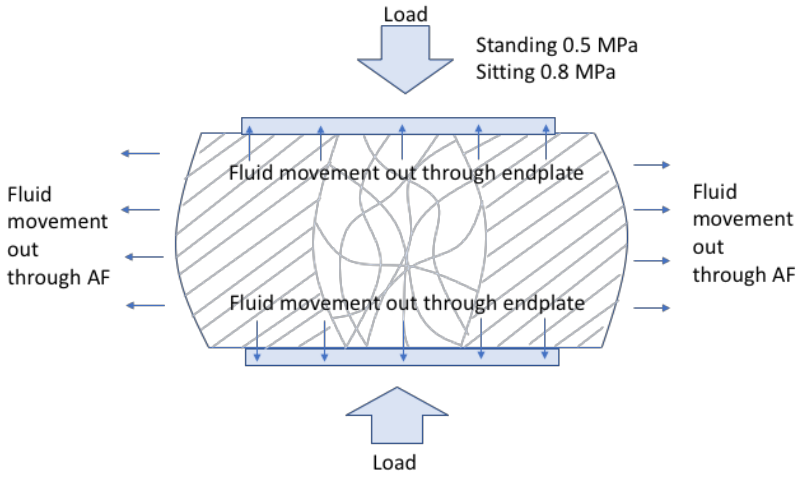

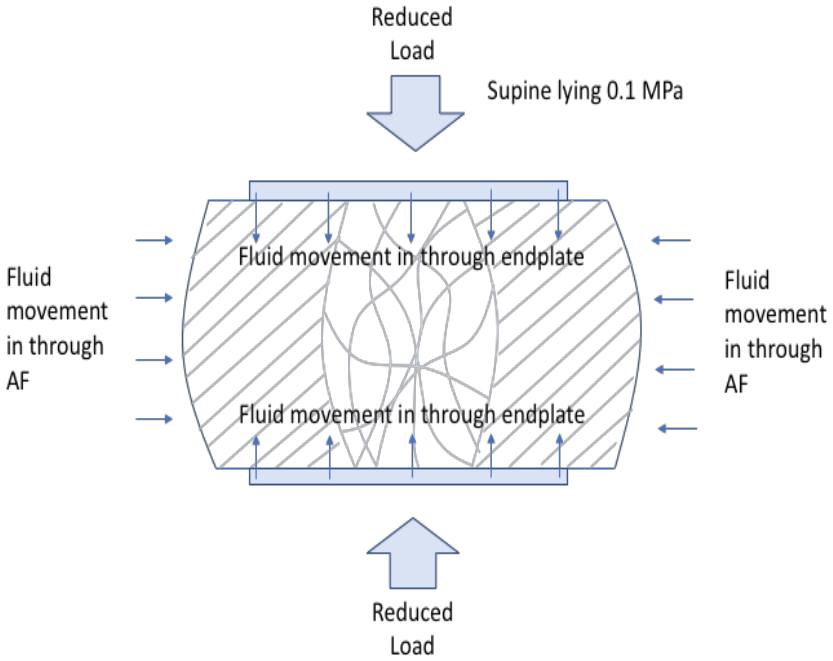

Figure 2.12 Fluid movement through endplates and AF through pressure-driven flow

Pressure–driven fluid flow also affects the EDL mentioned previously, resulting in the flow of cation-heavy diffuse layer to the end of the channel creating a flow of cations at the surface against the pressure driven flow (Mitra, 2012). This is known as the streaming potential and creates an additional electro-viscous effect which can cause the actual flowrate to be lower than the expected flow rate (Li, 2001) which adds to the complexity of fluid flow in the disc, this is discussed further in limitations in Chapter 5.

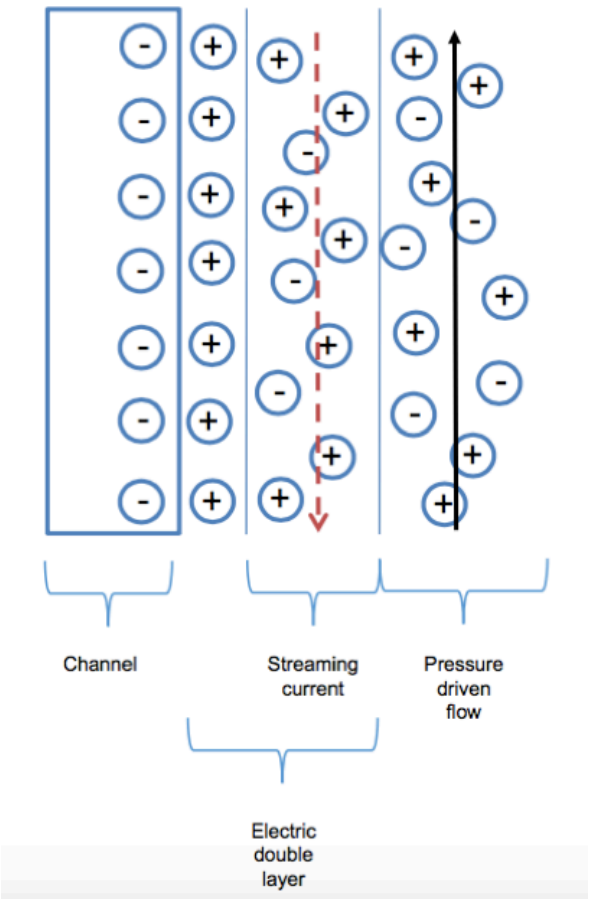

Figure 2.13 The Streaming Potential as is present in negatively charged biological tissue, such as the IVD. Pressure driven flow creates a streaming potential close to the solid-liquid boundary which can affect fluid flow rates

As fluid is driven through the pores in the disc matrix, an individual pore can be thought of as a microfluidic channel where counterions in the diffuse layer are driven to the end of the channel, resulting in a greater counterion concentration at the end of the channel which in turn results in a flow of counterions in the opposite direction, to the direction of pressure driven flow. This flow in the opposite direction is known as 'The Streaming Current' and the potential it develops is known as 'The Streaming Potential', shown in figure 2.13. The streaming potential has been used to measure the amount of degeneration in the intervertebral disc using needle electrodes (Iatridis et al., 2009, Fujisaki et al., 2011, Iatridis et al., 2003). It is responsible for higher viscous effects in microfluidic channels than would be found in macroscopic channels, leading to reduced velocity and increased pressure drop than may be expected.

In a relatively healthy disc, mechanisms 1-3, which are dependent on the negative charge in the disc and ionic content of the interstitial fluid, would be expected to cause fluid to flow towards the highest FCD, through the AF and vertebral endplate to the NP. Mechanism 4 would be expected to cause fluid to flow into and out from the disc. The ability of the nucleus pulposus to maintain its complex structure and hydration relies on the complex nature of its extra cellular matrix. Section 2.2 discusses how the nucleus pulpous cells regulate the nucleus pulposus matrix.

2.2 Regulation of the Healthy Nucleus Pulposus Matrix in the Lumbar Spine

2.2.1 Nucleus pulposus cells

The matrix of the disc is a sensitive structure which is kept stable by the continually functioning processes of the cells within it. The phenotype of a cell (the observable characteristics) is determined by its genotype (the genetic coding) and the environment surrounding the cell (the extracellular matrix), which can influence the gene expression of a cell. The gene expression is the term given to the process by which the information from a gene is used in the synthesis of a gene product (usually a protein) (Johnson, 2015). This synthesis is often described as anabolic metabolism (the building of molecules from smaller units, for example in the IVD the synthesis of aggrecan and collagen) or catabolic metabolism (the synthesis of molecules into smaller units; for example in the IVD the synthesis of aggrecanases which break down aggrecan, or collagenases which break down collagen) (Neidlinger-Wilke et al., 2006).

Cells make up only approximately 1% of the disc material, but are essential for the functioning of a healthy disc. Cells are the building blocks of the body, they are responsible for tissue growth, tissue maintenance and tissue healing (Johnson, 2015). In the intervertebral disc the cells sit within the collagen-proteoglycan extracellular matrix. Cells in the intervertebral disc are less populated than other areas of the body, with 5,000 cells/cm^3, in comparison to chondrocytes in knee cartilage at 40,000,000 cells/cm^3 (Horner et al., 2002) or osteoblast in bone at 11, 000, 000 cells/cm^3 (Egan et al., 1991). Human nucleus pulposus cells share a common phenotype with articular chondrocytes, expressing similar genes. However, they also demonstrate morphological and physiologic differences which are not yet fully understood (Minogue et al., 2010). The DNA in the healthy NP cell is

responsible for the manufacture mainly of collagen and aggrecan. Collagen types I-VI are present in the human body and the most prevalent in the disc are types II followed by type I. Aggrecan is the most prevalent proteoglycan, followed by versican. Aggrecan is hydrophilic and extremely important to the functioning of the intervertebral disc due to its ability to keep the disc hydrated (Minogue et al., 2010), as seen in section 2.2. Nucleus pulposus cells sit within the collagen fibrils of the matrix. NP cells originate from the notochord of the developing foetus. Immature NP cells have large vacuoles, a high abundance of F-actin and are densely populated. Vacuoles are spaces which a cell uses to store nutrients needed for cell survival or waste products to prevent a cell becoming contaminated. F-actin is a protein which is critical in the role of cellular functions, such as regulating cell transcription to determining cell shape. However, even in early adolescence these cells have been shown to change. The cells of the NP are shown to be chondrocyte-like, it is thought these cells migrate to the NP from the vertebral endplates, although there are some studies which declare these cells may be the original cells which have differentiated to become more chondrocyte-like than their notochord derived predecessors. Cells in the mature human NP display cytoplasmic processes which are also seen in the NP cells of the bovine disc and high levels of Vimentin, which is a key intermediate filament, required for cell adhesion and signalling. Cytoplasmic processes have been shown to be present in areas of high loading, such as in the NP, in human and bovine subjects.

NP cells, like all eukaryotes, possess an encased nucleus, within this is stored the Deoxyribonucleic acid (DNA) from which the proteins of the NP are made, as shown in figure 2.13. The DNA of all cells consist of long, paired, polymer chains, formed of the same four nucleotides. Nucleotides consist of a sugar (name deoxyribose) with a phosphate group attached and one of the four following bases adenine (A), thymine (T), cytosine (C) and guanine (G).

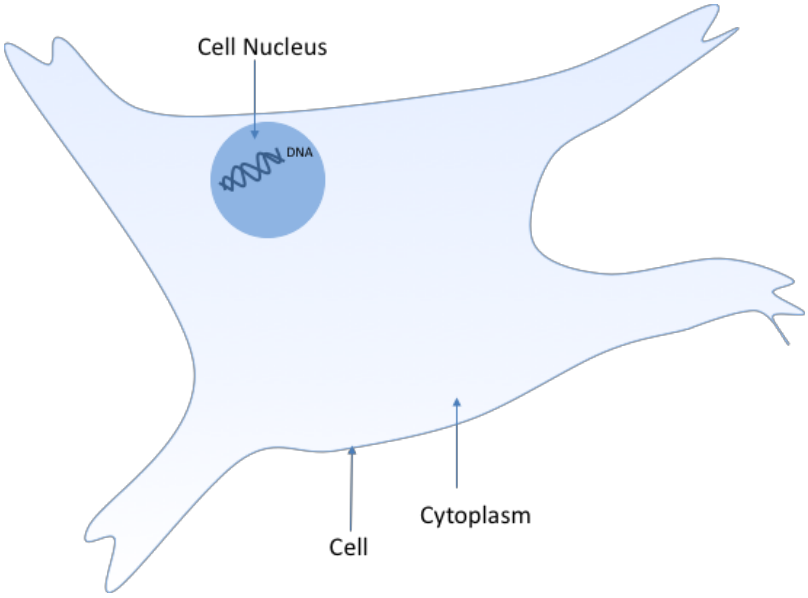

Figure 2.14 Nucleus pulposus cell, showing DNA contained within the nucleus

Each sugar on the nucleotide is linked to another sugar by the phosphate group which results in a chain of sugar-phosphate with bases protruding from it. This leads to a single strand of DNA, see figure 2.14. In the living cell DNA is synthesized as a double stranded helix however, the bases of one strand linking to the bases of another strand. These bases can only pair up in a certain way, A binds to T and C binds to G. In this way, the well-known structure of the double helix of DNA is formed. The bonds holding the bases together are weak in comparison to the sugar-phosphate bonds and this allows the double strand DNA to be separated to single strand, without affecting the sugar-phosphate ‘back-bone’. These single strands can then serve as 2 templates for the formation of 2 new double strands of DNA. In this way DNA replication is accomplished which ensures that each new cell has contains its own copy of DNA. This is essential for cell division during growth or repair of the nucleus pulposus matrix, which is discussed in the following section.

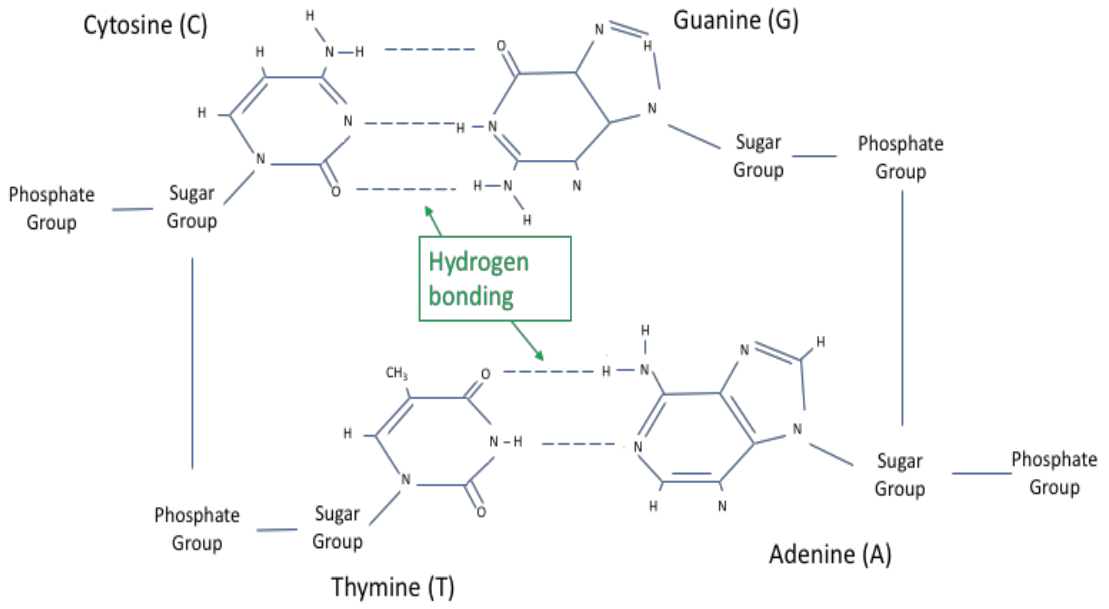

Figure 2.15 The 4 nucleotides of DNA, dotted lines depict hydrogen bonding between the bases. The sugar and phosphate groups link to make the DNA backbone.

2.2.2 Protein synthesis

The two main structures (except for water) found in the nucleus pulposus; collagen II and aggrecan, are proteins. Synthesis of proteins by the cells in the nucleus pulposus matrix occurs in two phases; transcription and translation. Transcription takes place within the nucleus of the cell, during transcription ribonucleic acid (RNA) is synthesised from DNA in 3 steps; initiation, elongation and termination. During initiation the DNA double strand is split. Each DNA strand has a sequence near the beginning of the gene known as a ‘promoter’. RNA polymerase links to this promoter sequence and separates the double DNA strand. This creates 2 single strands of DNA which are used in the next step; elongation. RNA polymerase ‘reads’ the sequence on one of the single strands of DNA, the polymerase builds a strand of RNA which complements the DNA sequence. In a similar way to DNA base pairing, C binds to G, but for RNA the base uracil (U) replaces thymine (T), so A binds to U (rather than T) (Johnson, 2015).

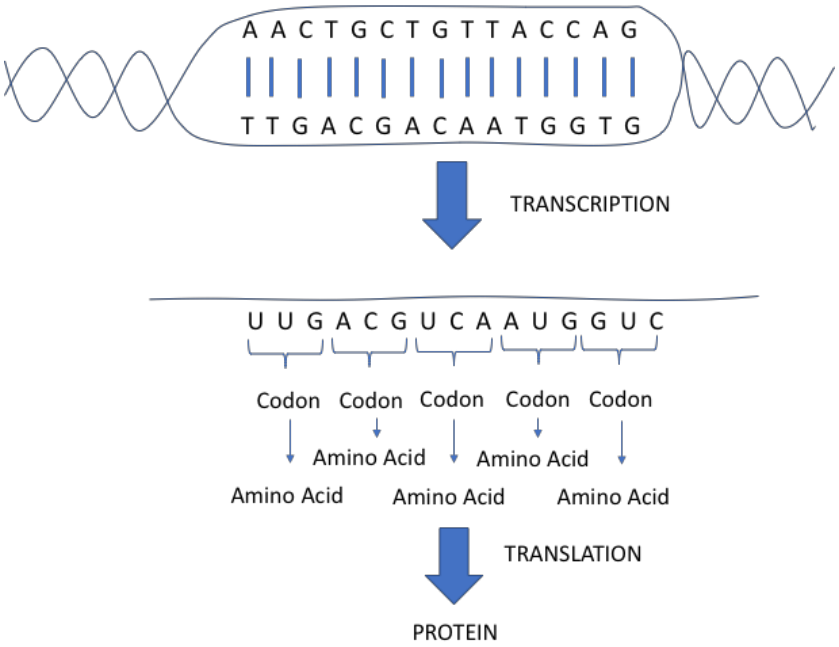

Figure 2.16 DNA transcription and translation in the nucleus of the cell

This continues until the third step; termination. Sequences of nucleotides, known as terminators, halt the elongation process, once transcribes and the release the strand from the RNA polymerase. This strand, known as the messenger RNA (mRNA) then moves out of the cell to the cytoplasm where translation occurs, synthesising a protein from the RNA strand. The RNA strand attaches to a ribosome where protein synthesis takes place. Every 3 bases on the mRNA strand are known as a codon and form an amino acid. Another RNA strand, known as transfer RNA (tRNA) is involved now in translation, it transports amino acids to the ribosome, matching the codons in the mRNA to their corresponding amino acid, peptide bonds form between these amino acids to form a protein molecule. The protein molecule is then excreted from the cell membrane through exocytosis, a process by which the amino acid chain making up the protein molecule is engulfed by the cell membrane and passes from inside the cell to the extra-cellular matrix (Johnson, 2015).

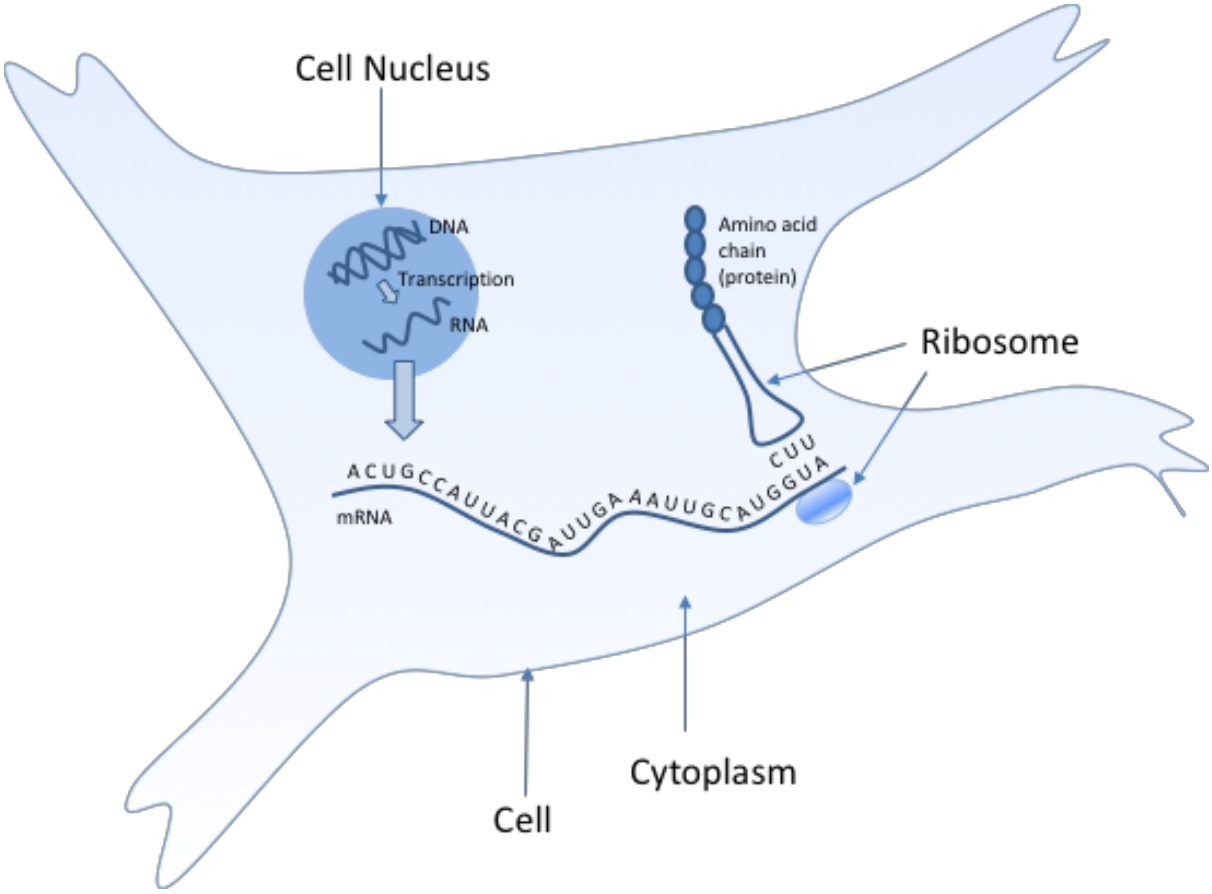

Figure 2.17 Protein synthesis from mRNA by ribosome in the cytoplasm

2.2.3 Cell function in the NP

NP cells naturally go through changes in response to their environment or their inherent processes. These physiologic changes in the cells are in turn responsible for the matrix proteins in the extra-cellular matrix surrounding the cell. Cell proliferation, or cell growth is the term used to describe a cell dividing. In nucleus pulposus cells this process is known as mitosis and describes the way one cell divides in to two cells, the proliferation of NP cells is therefore exponential (Lee, 2016). Cell growth is mediated by growth factors. Cell senescence is the term used to describe cells which no longer divide, they are alive and able to perform other physiological processes, but do not proliferate. The vast majority of cells display senescence, in culture this has been shown after approximately 50 population doublings, the cells then fail to divide again. Cancer cells do not display senescence and it is thought that senescence may be a preventative mechanism against cancer. Once a cell shows

senescence then no stimuli has been found which will reverse the senescence except for the inactivation of tumour suppressor genes (Campisi, 2013).

Cell apoptosis, or cell death is a natural process that occurs when a cell is no longer needed by a tissue, the cell dies neatly, and its contents are digested by other cells. This is not to be confused with cell necrosis which is cell death due to injury and is usually associated by an inflammatory response in the tissue. In necrosis the cell contents burst or leak over other cells affecting their processes (Johnson, 2015).

Cell differentiation is the term used to describe the process by which cells become more specialized in their function. The ability of a cell to differentiate into other types of cell is called the cell potency. A fertilized human cell for example is totipotent, meaning they can differentiate into any type of cell in the foetus or human body, embryonic stem cells are termed pluripotent as they can differentiate into any adult cell in the human body. Multipotent cells are able to differentiate into several cell types in the body, for example human umbilical cord blood has cells have been differentiated into nerve cells. Oligopotent cells have the ability to differentiate into only a few cells types, for example some vascular stem cells which can differentiate into smooth muscle and endothelial cells. Most cells in the body, including the chondrocyte-like cells of the adult nucleus pulposus, are not stem cells so do not have the ability to differentiate into a different type of cell. However, they do have the ability to change their gene expression, depending on their environment, a process known as mechanotransduction (Johnson, 2015).

2.2.4 Cell metabolism in the NP

Normal cellular processes mediate a balance between anabolic metabolism and catabolic metabolism to control synthesis in the matrix by the disc cells. As the cells naturally age, so changes occur which affect this balance and lead to natural age-related changes in the disc. The cells of the nucleus pulposus alter mostly in the first few years of life. The cells of the NP at birth are notochordal, but after a few years they have changed to the chondrocyte-like cells seen in the adult nucleus pulposus (Setton and Chen, 2004). This is the case in other mammalian species, such as bovine. It is not known definitely whether these chondrocyte-like cells have differentiated from notochord cells, or whether the notochord cells have died and

been replaced by chondrocyte cells which have migrated from the vertebral endplates or inner annulus (Risbud et al., 2010, Kim et al., 2003, Kim et al., 2009) . It is interesting that not all mammalian species follow this pattern, porcine models maintain notochord cells into adulthood, and do not show the same level of degeneration seen in discs without notochord cells. Chondrodystrophic canine breeds, such as beagles, do not maintain notochord cells into adult hood and show early signs of disc degeneration, non-chondrodystrophic canine breeds maintain notochord cells into adult life and do not show signs of early degeneration (Smolders et al., 2013). The reason for the change in cells is thought to be as a result of the shrinkage of the already small blood supply to the nucleus pulposus soon after birth. This concept appears to have been supported by Guehring et al., (2009) in an animal model study which compared the response of notochord cells (NC) and chondrocyte-like mature nucleus pulposus cells (NMPCs) to deprivation on nutrients and found the notochord cells to be adversely affected nutrient deprivation compared to the chondrocyte-like cells. As the cells change from notochord to chondrocyte-like so do does the matrix they synthesize. The biggest change is the aggrecan content which reduces from 65 % in young adults to 30 % by the age of 60 (Buckwalter, 1995). This reduction is due to a decrease is aggrecan synthesis as well as a degradation of aggrecans, resulting in shorter chains. There is also an increase in collagen I fibres in the nucleus pulposus which are thicker and more rigid than the collagen II fibres originally present. This also leads to more collagen-aggrecan bonding, which leaves less sulphate and carboxyl ion groups available for the attraction of water into the disc. Leading to dehydration of the disc which is shown on an MRI scan as a disc which is darker in colour than a disc which is well hydrated (Bushell et al., 1977). Interestingly this reduction in water content, does not lead to disc thinning, due to a simultaneous increase in collagen I, causing the disc to be more rigid and collagen rich, so leading to a stiffer, but not thinner disc.

The NP are responsible for the production of proteins which are responsible for the replacement of collagen in the disc and reduction or chondroitin sulphate. The cells are affected as the blood supply to the disc changes in the first 10 years of life and by their natural senescence as they age. The role of the changing environment and its effect on the cell is known as mechanotransduction and is discussed in the next section.

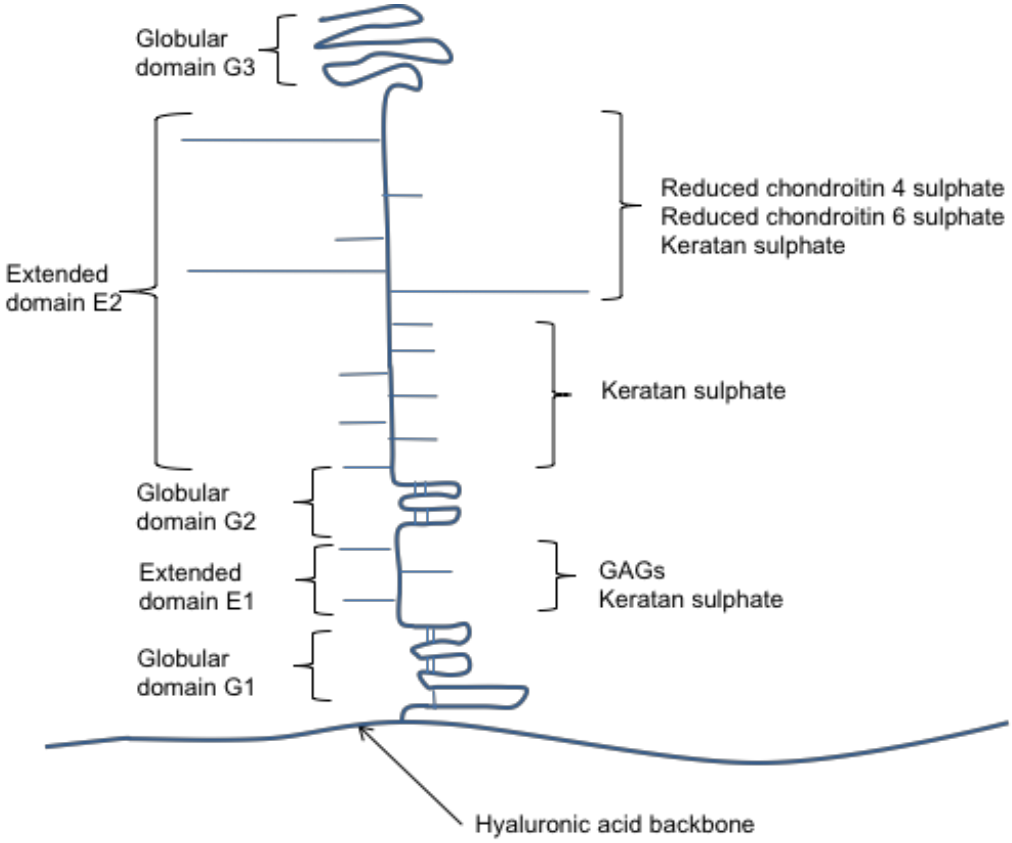

Figure 2.18 Aggrecan with the long chains of chondroitin 4 sulphate and chondroitin 6 sulphate chains degraded by aggrecanases compared to figure 2.7, resulting in a reduction in water binding ability.

2.2.5 Mechanotransduction in the NP cell

Mechanotransduction describes the way in which cells interact with their environment and change mechanical forces into biochemical processes (Wang et al., 1993). Application of mechanical stimuli such as pressure changes and fluid shear stress activate mechanosensitive ion channels, heterotrimeric G proteins, protein kinases and other membrane-associated signal-transduction molecules (Yoshizumi et al., 2003). This influences the gene expression of the cell causing alterations in the protein synthesis of the cell to the extra cellular matrix (Wang et al., 2009). Human intervertebral disc cells share a common phenotype with articular chondrocytes, expressing similar genes. However, they also demonstrate morphological and physiologic differences which are not yet fully understood (Minogue et al., 2010). The DNA in the healthy nucleus pulposus cell is responsible for the manufacture mainly of collagen II and aggrecan. Aggrecan is the most prevalent proteoglycan, followed by versican. Aggrecan is hydrophilic and extremely important to the functioning of the

intervertebral disc due to its ability to keep the disc hydrated (Minogue et al., 2010). Integrins are an essential part of the mechanotransductive process, they are cell adhesion molecules that regulate interactions between a cell and its surroundings. . Integrins are key players by which cells interact with their environment (Nettles et al., 2004). They bind cells to their extra cellular matrix through their cytoskeleton, see figure 2.19. They consist of an alpha and a beta sub-unit combined con-covalently (Nettles et al., 2004) which attach to ligands in the extra cellular matrix, such as fibronectin (Gilchrist et al., 2011), to create junctions known as known as focal adhesions

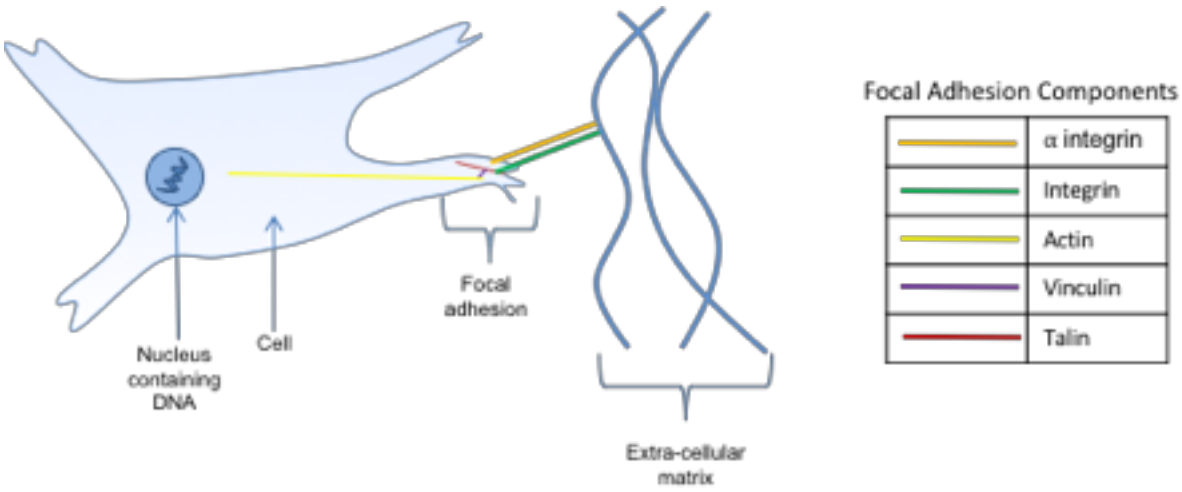

Figure 2.19 Focal adhesion components showing vinculin (in purple) as an integral part.

Cells have also been shown to react to their environment through cell-cell interactions, but as the cell density in the nucleus pulposus is so low the more likely mechanism through which intervertebral disc cells react to their environment would be cell-matrix interactions (Gilbert et al., 2016). Most cell-matrix interactions are connected to a contractile actin network that tends to pull the junctions inward (Horzum et al., 2014). When the cells are attached to a rigid matrix it strongly resists these pulling forces, the cell-matrix junction can sense the resulting high tension and triggers a response in which it recruits additional integrins and other proteins to increase the ability of the junction to withstand that tension. In a degenerated disc, the matrix loses its structure; therefore, the cell-matrix interactions would be altered.

There is also a difference between cell behaviour in the more rigid structure of the annulus fibrosus and the less rigid structure of the nucleus pulposus. Cell attachment to a relatively soft matrix generates less tension and therefore a less robust response. These mechanisms allow cells to sense and respond to differences in the rigidity of extracellular matrices in different tissues (Johnson, 2015). The responsive pathways in NP are yet to be fully realised, but attempts have been made to investigate which pathways may be present under mechanical loading (Guehring et al., 2006) and nutritional modifications (Jünger et al., 2009).

The normal age-related changes of the intervertebral disc were discussed in section 2.2.4 and in this section the role of mechanotransduction in changing the proteins synthesized by the cell. If the environment of the cell differs further from what is considered normal then the proteins synthesised by the cells will differ again and can lead to destruction of the intervertebral disc which can lead to low back pain, the next section discusses some mechanisms of low back pain for which the intervertebral disc is involved.

2.3 Low Back Pain from the IVD

There are many causes of low back pain, this research is involved with the causes of low back pain from the intervertebral disc. Disc degeneration is discussed and the painful conditions of stenosis that can be associated with it in the end stages. Discogenic pain, meaning pain arising from the disc itself and associated with internal disc disruption is discussed. Finally, disc prolapse where the contents of the disc the disc interferes with the surrounding structures leading to pain of the surrounding structures or referred pain. The latter two conditions can be symptomatic in younger patients, they can be sudden in onset and are associated with vertebral endplate and disc injury, rather than a diffuse, progressive condition as seen in disc degeneration.

2.3.1 Disc degeneration

Disc narrowing is a condition associated with intervertebral disc degeneration which can illicit low back pain or referred lower limb symptoms. Adams and Roughley (2006) distinguished intervertebral disc degeneration from normal ageing processes as “an aberrant cell mediated response to progressive structural failure” further

stating that a degenerate disc is one “with structural failure combined with accelerated or advanced signs of ageing”. They determine degenerative disc disease as a degenerate disc which is also painful. Underlying causes of disc degeneration are genetic inheritance, aging, nutritional compromise (due to endplate damage or smoking) and loading history (Adams and Roughley, 2006). Loading history in this context relates to heavy repetitive loading of the spine when intradiscal pressures are greatest (Nachemson and Morris, 1964a) and can lead to microtrauma in the disc. Weightlifters have been shown to have degenerative changes throughout the spine when compared with runners (Videman et al., 1995), however normal physiological loading through movement, or exercise has been shown to have a beneficial effect, runners have been shown to have less spinal degeneration than controls (Belavý et al., 2017). Early signs of degeneration are an increase in collagen II synthesis in the nucleus pulposus, which may be indicative of a repair mechanism by the cells of the NP. Following this an increase in collagen I in the NP is seen. A decrease in aggrecan synthesis follows on from and this leads to an altered ratio of CS to KS in the disc, as shown in figure 2.16. This leads to dehydration of the disc which is the first sign of degeneration, but this would not usually be a painful condition. The next stages of degeneration involve degradation of the matrix leading to structural failure. This occurs through the production of ADAMTS (a disintegrin and metalloprotease with thrombospondin motifs) and MMPs (matrix metalloproteinases) ADAMTS and MMPs are numbered according to which sites they cleave on the proteins. In greatest abundance in the disc are MMP7 and MMP13 which degrade collagen II and aggrecan and ADAMTS 4 (also known as aggrecanase 1) and ADAMTS 5 (also known as aggrecanase II) which degrade aggrecan. ADAMTS have been shown to be more aggressive in cleavage of aggrecan in the non-degenerated disc and MMPs have been shown to degrade aggrecan in the degenerated disc (Iatridis et al., 2011, Tian et al., 2013).

The vertebral endplate is susceptible to weakening and damage through repeated compression and microdamage, especially in later life. In a non-degenerated disc, the nucleus pulposus bulges against the vertebral endplates, which withstand the pressure and are an integral part of the correct functioning of the disc (Adams et al., 1986b). As the vertebral endplates weaken they can no longer withstand this pressure and decompress the nucleus which transfers loading to the annulus

fibrosus instead, which can bulge inwards to the nucleus pulposus. If the nucleus pulposus bulges into the vertebral endplate it can damage the endplate causing what is termed a Schmorl's node (Malandrino et al., 2014).

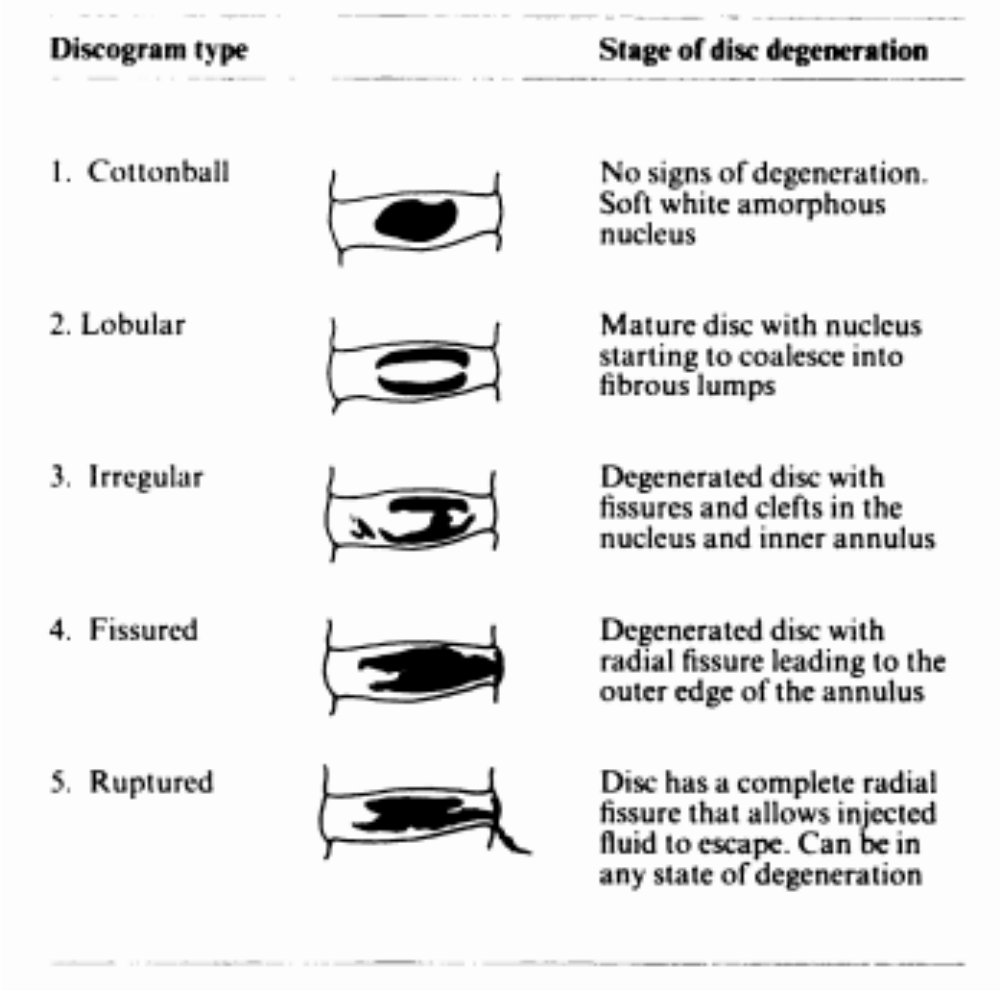

Discogram type		Stage of disc degeneration
1. Cottonball		No signs of degeneration. Soft white amorphous nucleus
2. Lobular		Mature disc with nucleus starting to coalesce into fibrous lumps
3. Irregular		Degenerated disc with fissures and clefts in the nucleus and inner annulus
4. Fissured		Degenerated disc with radial fissure leading to the outer edge of the annulus
5. Ruptured		Disc has a complete radial fissure that allows injected fluid to escape. Can be in any state of degeneration

Figure 2.20 From Adams et al., (1986b). The stages of degeneration as revealed by discograms.

The vertebral endplates have been described as the spine's "weak links" (Adams and Roughley, 2006) and endplate damage can be caused due to microdamage through repeated compressive loading. As the disc dehydrates, it tends to bulge into the vertebral bodies, this reduces the pressure on the nucleus pulposus which causes loading to be exerted onto the annulus. The inner annulus tends to bulge inwards towards the nucleus, which no longer withstands this pressure and the outer annulus bulges radially like a flat tyre. A young, healthy disc will tend not to bulge due to the ability of the nucleus pulposus to withstand the pressure exerted on it and a very hydrated disc with not have the ability to bulge due to the increased stiffness, so

moderately degenerate discs tend to bulge more. Severely degenerate discs, however will decrease in height, this narrowing leads to a reduced space for the spinal nerves to lie and is often associated with osteophyte growth in osteoarthritis which can further impinge the nerves. Disc prolapse, and disc narrowing can lead to impingement of the spinal nerves and referred lower limb pain which can be an indication for surgical intervention. Nerve and blood vessels have also been shown to grow into a degenerated disc. This is in part due to a decreased aggrecan content which has been shown to prevent the ingrowth of nerves, there is also a claim that blood vessel ingrowth it is an attempt at repair of the disc (Freemont et al., 1997, Melrose et al., 2002).

2.3.2 Discogenic pain

Internal disc disruption (IDD) was a term coined by Crock et al (1973) and describes a process of localised nucleus pulposus degradation followed by annulus fissures which can lead to pain. IDD is a focal disorder affecting only one area of the annulus fibrosus and can be as a result of trauma. The process differs from degeneration in that it is not a diffuse process affecting the entire disc and differs from disc prolapse in that the fissure remains contained within the disc (Bogduk, 2011). Low back pain arising from IDD is termed discogenic as it is pain arising from the disc itself rather than pain arising from the structural failure of the disc affecting structures outside of the disc. IDD is characterised by a breakdown of the matrix of the nucleus pulposus and fissures from the nucleus to the annulus forming through which the nuclear material can seep. It has been shown to be present in 30 – 50 % of patients with low back pain (Schwarzer et al., 1995). The degradation of matrix is thought to occur most commonly due initially to endplate fracture which in vivo In is thought to occur due to injuries of forced compression or flexion of the spine with or without rotation, such as falling onto the pelvis or coccyx from a standing position, or road traffic collisions or horse-riding accidents where the spine may be forcibly compressed or flexed with or without rotation (Rolander and Blair, 1975).

The grading system for fissures is shown in figure 2.21. The intervertebral disc is innervated in the outer two-thirds of the annulus, but not the inner third and not the nucleus pulposus, so a patient would not experience pain until a grade II or grade III fissure was present.

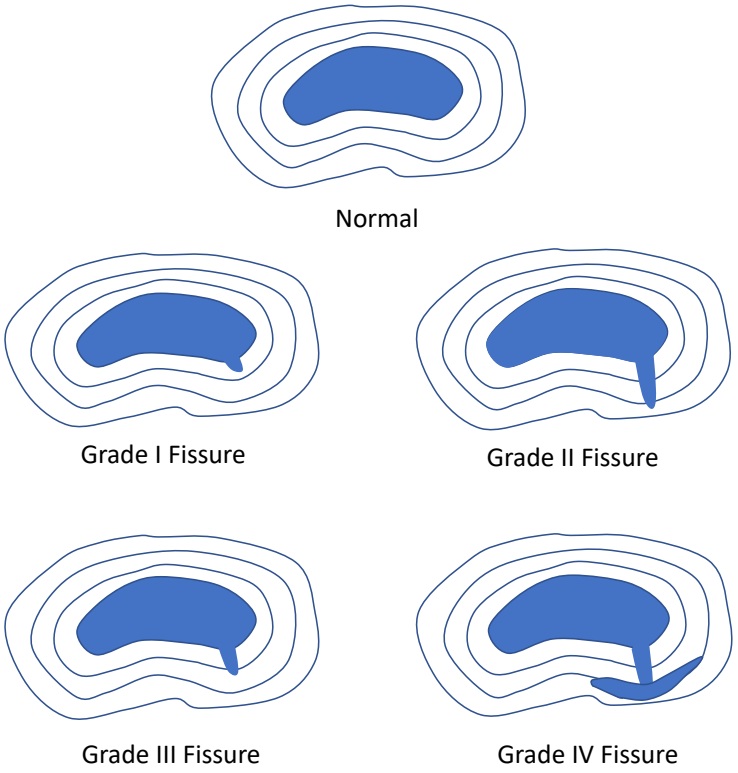

Figure 2.21 Fissures in internal disc disruption (IDD) and their grading. The rings notate the thirds of the annulus, grade I fissures affect the inner third of the annulus, grade II extends to the mid third of the annulus, grade III fissures extends to the outer third of the annulus and grade IV which extends circumferentially around the annulus (Bogduk, 2011).

2.3.3 Disc Prolapse

Annular tears in the intervertebral disc have been shown in vitro by cyclic loading in bending and compression tears can occur. There are three classifications of annulus tears circumferential, peripheral and radial and they are present in discs from increasingly commonly from 10 years of age (Boos et al., 2002). Disc tears show increased metabolism levels which are responsible for scar formation of the disc however larger tears cannot heal and are part of the degenerative cascade of events and structural failure which can lead to low back pain. Radial fissures progress from the nucleus to the annulus and most commonly in the posterior aspect or anteroposterior aspect of the disc (Osti et al., 1992). In a degenerated disc when the nucleus pulposus of the disc has been less structured and fissures are present, then nuclear material can seep from the disc through these tears resulting in a disc

bulging and eventual protrusion, extrusion or sequestration known as disc prolapse (Adams and Hutton, 1982, Buckwalter, 1995). Radial fissures can allow seeping of the nucleus pulposus to the annulus. A disc herniation can be painful or non-painful, the contents of the degenerated nucleus pulposus have been shown to illicit pain when in contact with nerve endings. A herniation can then lead onto a protrusion of the disc material from the disc and eventual sequestration when the disc material leaves the disc altogether. A disc protrusion (often called a prolapse) is a rare and painful event, but when it does happen its most common occurrence is at 30-40 years of age. In an aged disc the nuclear material would be too dehydrated and the disc too stiff to allow matrix movement from the disc. There are three terms used to characterize disc prolapse; protrusion, extrusion and sequestration, as shown in figure 2.22. Protrusion defines an intact disc, but with a bulging annulus. Extrusion defines a ruptured annulus with nuclear content which has seeped out from the nucleus pulposus, but remains in contact with the disc. Sequestration defines a prolapsed disc in which the disc contents have left the disc and are no longer in contact with it (Adams, 2013).

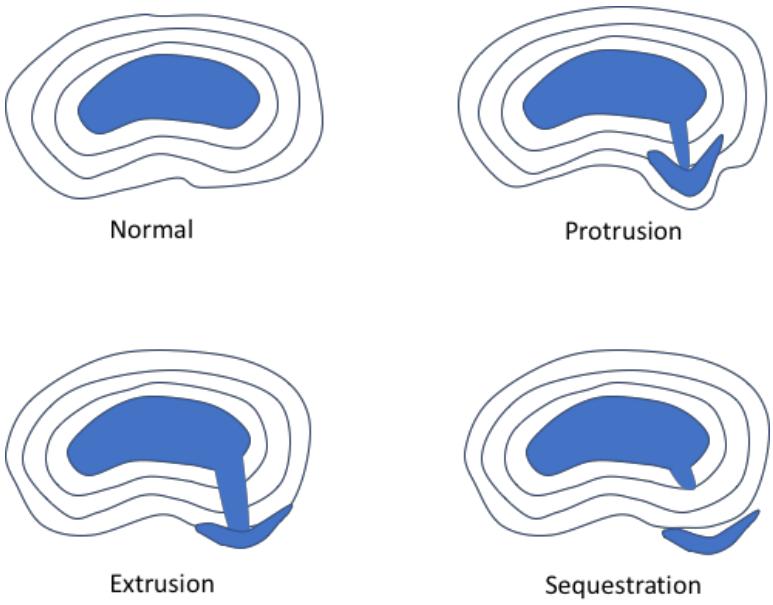

Figure 2.22 The stages of disc prolapse. Adapted from Adams (2013).

2.3.4 Current Treatments

The most recent NICE (National Institute for Health and Care Excellence) guidelines published in November 2016 recommend self-management, exercise, manual

therapy (in conjunction with exercise), NSAIDs (Non-steroidal anti-inflammatory drugs) and psychological therapy for the non-invasive treatment of low back pain with or without sciatica (pain felt in the leg from the lower back). If non-invasive treatment is not successful then radiofrequency denervation, epidurals and spinal decompression may be considered and spinal fusion can be offered as part of a clinical trial (NICE, 2016).

The painful conditions outlined in sections 2.3.1 and 2.3.2 are often so far progressed that options for treatment are limited. Spinal stenosis is associated with disc narrowing and osteophyte formation resulting in a reduction in the space of the spinal canal, lateral nerve canals or neural foramina wherein the spinal nerves lie and is one of the most common spinal disorders in patient over 65 years of age (Chou et al., 2007). If non-invasive treatments do not relieve the patient's pain then laminotomy procedures, where the laminar is formed from one or several segments may be carried out to relieve the pressure on the spinal nerves. Spinal fusion now only recommended as part of a clinical trial (NICE, 2016), this is in part due to issues with adjacent facet disease, whereby the joints above or below the fused spinal segment, bear a great burden of movement and loading resulting in early onset degenerative disease of the facet joints in particular. Intervertebral disc replacement was poised as the next gold standard for low back pain treatment (Enker et al., 1993, Lemaire et al., 1997). Although results have shown improvement compared to spinal fusion at 1, 2, 5 and 10-year follow-up (Enker et al., 1993, Tropiano et al., 2003, Chung et al., 2006, Berg et al., 2009, Guyer et al., 2009) and it continues to be used worldwide and in private practice in the UK, it is not recommended for use by NICE guidelines. Part of the issue arising from disc replacements using plastics, metals or other non-biological biomaterials are that as the spine naturally stiffens with age, the replaced disc will maintain its mechanical properties so will be more flexible than the rest of the spine which could lead to similar biomechanical problems as seen in adjacent level IDD with fusion (Hilibrand and Robbins, 2004, Park et al., 2004). Recent research studies on its effectiveness show more promising results (Garcia et al., 2015, Rihn et al., 2017, Mattei et al., 2017), and has been shown to reduce the likelihood of adjacent segment disease in the lumbar spine seen with fusion surgery (Rainey et al., 2012, Zigler et al., 2018) but its cost effectiveness when compared to non-invasive treatments has been questioned (Johnsen et al., 2014).

There are several different methods of spinal fusion, but their role is to achieve a solid arthrodesis in the segment. This can be achieved using a combination of bones grafts from the pelvis, metal work screws through the vertebral above and below the disc or cage devices. The disc may also be removed, especially if it is suspected discogenic pain is not as a result of disc movement, otherwise that pain could still be present following the surgery. However, fusion has recently also been shown to have no benefit when compared to non-operative interventions (Mannion et al., 2016).

These surgical interventions can also be indicated for discogenic pain, but this condition firstly requires correct diagnosis which requires a discography (Schwarzer et al., 1995). A contrast medium is injected into the nucleus pulposus and a positive test would be the patients confirming their pain being reproduced by the injection. The contrast medium also outlines the disc matrix, so fissures can be seen more easily. There is a slight risk of discitis (disc infection) through discography, so there needs to be a strong indication for performing the technique (Bogduk, 2011).

Disc prolapse is an indication for decompression surgery if the lower limb symptoms are worse than the low back symptoms and especially if symptoms of cauda equina are present. Decompression surgery removes the disc contents which may be causing pressure on the spinal nerves. Decompression surgery can involve removing a disc protrusion through microdiscectomy which removes the area of the disc which is causing the compression (Adams, 2013). Larger prolapses may require a laminectomy where part of the laminar is removed so the full disc prolapsed can be accessed. Cauda equina symptoms can present with sciatica and lower limb pain and include saddle anaesthesia and lower limb and bladder/bowel motor weakness with sensory deficit, in the worst cases this can progress to incontinence which may be permanent or paraplegia (Adams, 2013). Cauda equina is termed a red flag symptom and due to the serious of the symptoms surgical intervention is recommended within 48 hours, with diagnosis on MRI scan.

The development of regenerative medicine over the past 30 years has seen experimental development in cell-based treatments for the intervertebral disc. Cell-based treatments for low back pain are still in their development stage in the UK and are not currently being used as standard treatments. For those patients where

current treatment methods are not available to aid conditions causing discogenic pain, then these cell-based treatments may be the next novel course of treatment. This will be discussed further in section 2.5.1 The common theme with the painful conditions discussed is the involvement of the localised degradation or widespread degeneration of the nucleus pulposus. Involving the breakdown of the extra-cellular matrix and the loss of function of the usually hydrophilic NP matrix. Although the natural ageing process involves changes in the NP, these changes involve replacement of aggrecan and collagen II within the NP with collagen I. These ageing processes on their own would not likely lead to large annular fissures, disc prolapse and disc narrowing so would not illicit pain. Cell-based treatments are being developed which hope to halt or reverse some of the processes in the IVD that lead to pain by regenerating the nucleus pulposus and annulus fibrosus and these will be discussed now. Research also shows that static loading of the spine, possibly through inactivity can lead to degradation of the nuclear matrix and this is an area which is of great interest when looking for prevention strategies of low back pain (Ohshima et al., 1995, Wang et al., 2007). This breakdown of the nuclear matrix of the disc is the focus of this research so will be discussed in more detail now.

2.4 Targeting Treatments for Intervertebral Disc Health through Cell-Therapy

2.4.1 Cell-based studies for Intervertebral disc health

The past 30 years has seen a development of cell-based treatments as a way to try treat low back pain. The nucleus pulposus is usually the first part of the disc to be affected by degenerative and pathological changes in the disc, studies over the past 30 years have increased the understanding of effects of a changing environment on the nucleus pulposus cells. By changing the environment surrounding the nucleus pulposus cells then changes can be made to the proteins that are synthesised. Cells respond to their surrounding environment by regulating the steps of protein synthesis, to control the proteins that are expressed from a DNA strand (gene). This process is known as gene expression. Gene expression can be influenced throughout the protein synthesis sequence, from transcription to translation. In NP cells, as in most other eukaryotic cells, these processes are complex and not fully understood yet. However, studies have been carried out to show how gene expression in NP cells is affected by their biochemical and mechanical environment, a process known as mechanotransduction. These processes can be altered to

manipulate the environment of the cell and so change the gene expression of the cell.

2.4.2 Cell- based Loading studies

In a study of six bovine caudal intervertebral discs, aggrecan synthesis rates of bovine caudal intervertebral discs were shown to double when stimulated by 2.5MPa, whereas pressures of up to 7.5MPa caused aggrecan synthesis rates to decrease (Ishihara et al., 1996). Similar results were shown in a study with 14 IVD specimens, a pressure of 0.3MPa resulted in an anabolic effect on cells and 3MPa or greater resulted in catabolic effects (Handa et al., 1997). In-vivo animal models have also generated similar results. A study with 32 white rabbits involved fitting an external device fixed to the spine to load and distract the intervertebral discs, signs of regeneration of the discs were seen in terms of disc height and cell number (Kroeber et al., 2005). A study by the same group in the following year of 18 rabbits using MRI, gene and protein expression levels showed that distraction resulted in disc rehydration, increased extracellular matrix synthesis and protein expressing cells (Guehring et al., 2006). The effects of distraction could aid nutrition of the intervertebral disc. Glucose supply has been shown to be essential for the anabolic maintenance of the intervertebral disc, more so than mechanical stimulation alone (Rinkler et al., 2010). More recent research has investigated responses of cells within the intact spinal segment, testing the segments in flexion and extension and then analysing the gene expression following testing. The study found that loading increased the catabolic products matrix metalloproteinases (MMPs) and that variation between specimens was seen in term of the response to loading (Hartman et al., 2015)

2.4.3 Topology and topography cell-based studies

Cell shape is governed by its environment and in two-dimensional studies can be defined by the term circularity, where 0 would depict a linear cell and 1 a circular cell, and the closer the cell shape tends towards a circle the closer the value tends towards 1. Cells in suspension tend to be spherical and cells in a matrix, such as in cartilage or the IVD tend to be adhered to the matrix and have cell-matrix or cell-cell focal adhesions which cause them to be non-spherical. Cell circularity has been studied by immunostaining of the cytoskeleton and imaging (Eskin et al., 1984,

Helmlinger et al., 1991, Malek and Izumo, 1996, Whited and Rylander, 2014). Images can then be viewed in software such as ImageJ which can provide quantitative analysis of the shape of the cell and focal adhesions (Horzum et al., 2014). The adhesion to the matrix is essential for the functioning of a cell, such as osteoblasts, fibroblasts, endothelial cells, and chondrocytes whose role it is to respond to mechanical stimuli in the musculoskeletal environment. Cells have been shown to change their shape and line up in the direction of shear flow, but they have also been shown to change shape to become tangential to the direction of flow (Eskin et al., 1984). The uniformity of cell scaffolds has been shown to have a beneficial effect on cell adherence with uniform topography causing greater adhesion of cells in shear flow when compared with random topography (Huang et al., 2013, Whited and Rylander, 2014, Sonam et al., 2016). Pore size of scaffolds have been shown to effect cell functioning, although the most beneficial pore size for cell health has not yet been ascertained. Pore sizes of 200-400 μm have been shown to be important for the differentiation of chondrocytes (Boyan et al., 1996) and pores of 300 μm have been shown to stimulate the expression of chondrogenic genes (Matsiko et al., 2015). Shear flow has been shown to causes changes in gene expression in endothelial cells (Brooks et al., 2002), osteoblasts (Sharp et al., 2009, Tate et al., 1998) and mesenchymal stem cells (Sonam et al., 2016). The effect of shear flow has been tested on IVD cells from the annulus fibrosus in two published studies which were mentioned previously (Chou et al., 2016, Elfervig et al., 2001). The application of shear flow to cell-seeded porous scaffold in perfusion bioreactors is of great interest in developing cell-seeded scaffolds for biological tissue regeneration (Hossain et al., 2015, Raimondi et al., 2016).

2.4.4 Cell-seeded scaffolds

Novel therapies are being developed which utilize cell therapies to aid regeneration of the intervertebral disc and growth of a biological disc. There has been an increasing trend in research into IVD regeneration in the past two decades. Transplanting cells into a degenerated disc to try to encourage intervertebral disc healing has had some success in animal studies (Ganey et al., 2003). Several groups are working on developing IVD cell constructs using autologous IVD cells or mesenchymal stem cells, or both, which could be injected into the IVD for regeneration (Vadala et al., 2016, Sakai et al., 2003, Bertram et al., 2005,

Richardson et al., 2006). Stem cells differentiated from adipose tissue have been more successful than those generated from bone marrow for IVD regeneration (Minogue et al., 2010, Hohaus et al., 2008). Initial tests for cell regeneration injected autologous cells into the intervertebral disc but cell death occurred (Hohaus et al., 2008). Cell seeded scaffolds have had more success (Tong et al., 2016). The scaffolds were usually collagen and the purpose of adding a scaffold for regeneration rather than just injecting cells into the area is to give the cells a better chance of survival and growth, as has been demonstrated in other cell types (Gomes et al., 2006, Whited and Rylander, 2014, Raimondi et al., 2016). Cross linked scaffolds with a combination of collagen and chemicals such as Genipin can add to their mechanical strength and have been shown to be better than non-cross-linked scaffolds (Nikkhoo et al., 2016, Halloran et al., 2008, Roughley et al., 2006). Co-culture systems using a mixture of mesenchymal stem cells with intervertebral disc cells have shown a greater success than either cell by themselves (Ouyang et al., 2016). Bioreactors are now being used to try to create the most beneficial conditions for cell growth on scaffolds prior to scaffold implantation and to aid differentiation of MSCs. The understanding that cells in the body are rarely under static conditions is now being incorporated into in vitro research, with perfusion bioreactors allowing fluid flow through the cell-seeded scaffolds. Bioreactors have advanced over the past few years to include mechanical stimulation such as shear fluid flow to the cells on the scaffolds (Walter et al., 2014, Hossain et al., 2015). These studies have looked at regeneration of tissue for tendon and cartilage repair. One of the challenges facing researchers and clinicians in the development of scaffolds for IVD regeneration involved the implantation of the scaffold, which can be through an original annular tear, but then in facilitating the scaffold to stay in the disc and not migrate out from the same tear. This could be overcome by using suture techniques to repair the tear, although difficulty has been shown in maintaining IVD pressure even with these sutures in place(Chiang et al., 2012).

In more recent years the focus of mechanotransduction has been directed towards mesenchymal stem cells (MSCs) and their ability to differentiate (Richardson et al., 2006, Zhu et al., 2016, Vadala et al., 2016). The extracellular matrix defines differentiation of MSCs (Hadden and Choi, 2016) and pore size and topography of scaffolds have been shown to affect differentiation of MSCs into chondrocytes (Di

Luca et al., 2016). The most effective pore size has not yet been ascertained. A larger pore size allows the cell to migrate into a scaffold more easily, but a smaller pore size may allow greater cell adhesion to the surface.

2.4.5 Shear stress studies

There have been two papers published on the effects of shear fluid flow over AF cells. 'Flexflo' apparatus was used to test the effect of shear flow ranging from 1-25 dyne/cm^2 for 1-3 minutes with growth factor beta-1 compared to shear flow only, the study found that beta-1 sensitizes AF cells to shear stress (Elfervig et al., 2001). A more recent study of shear stress over AF cells demonstrated an increase in anabolic processes at 10 dyne/cm^2 when compared with no flow or 1 dyne/cm^2 (Chou et al., 2016). One study has been published which studied shear stress on nucleus pulposus rat cells at 1 dyne/cm^2, which found no change in gene expression for aggrecan and increase in gene expression for lumican compared to no flow (Wang et al., 2011). The study of nucleus pulposus cells under various flow rates and steady and pulsatile flow in this thesis has not previously been studied. This novel research which will add to the current body of knowledge. The units of dyne/cm^2 are frequently used as a measure of shear stress and is derived from the CGS unit for force. 1 dyne is equivalent to 1 gram accelerated by 1 cm per second squared. 1 dyne/cm^2 is the equivalent to 0.000001 bar or 0.0000001 MPa. It is used almost exclusively in literature for fluid shear stress in cell-based studies so has been used in this research for consistency.

2.5 Aims and objectives

The focus of this research is fluid flow within the extra-cellular matrix and over the cells within that matrix, known as inter-fibrillar fluid flow, see figure 2.23.

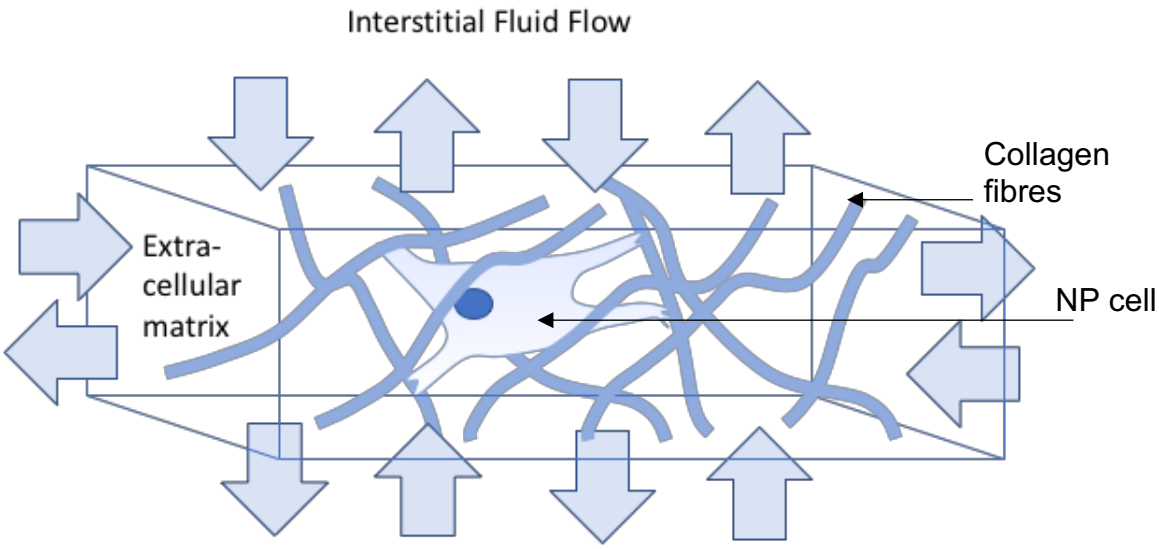

Figure 2.23 Diagram depicting a section of extra-cellular matrix containing a cell and collagen fibres. Arrows signal interstitial fluid flow through the extra-cellular matrix.

As interstitial fluid moves through the extracellular matrix and over the cells a solid-fluid boundary layer. Friction forces at the boundary caused due to the adhesive forces between a solid and liquid being larger than the cohesive forces in the fluid result in a force acting parallel to the cell surface, which is known as the fluid shear stress, see figure 2.25. The fluid shear stress is proportional to the viscosity and velocity of the fluid and as it acts on the cell surface effects the focal adhesions of the cell which can alter the biochemical signals through the process known as mechanotransduction. When the fluid molecules pull on the integrin receptors at the cell-fluid interface, as shown in figure 2.24 this can alter the biochemical processes of the cell, changing the morphology and gene expression, so leading to changes in proteins synthesized by the cell.

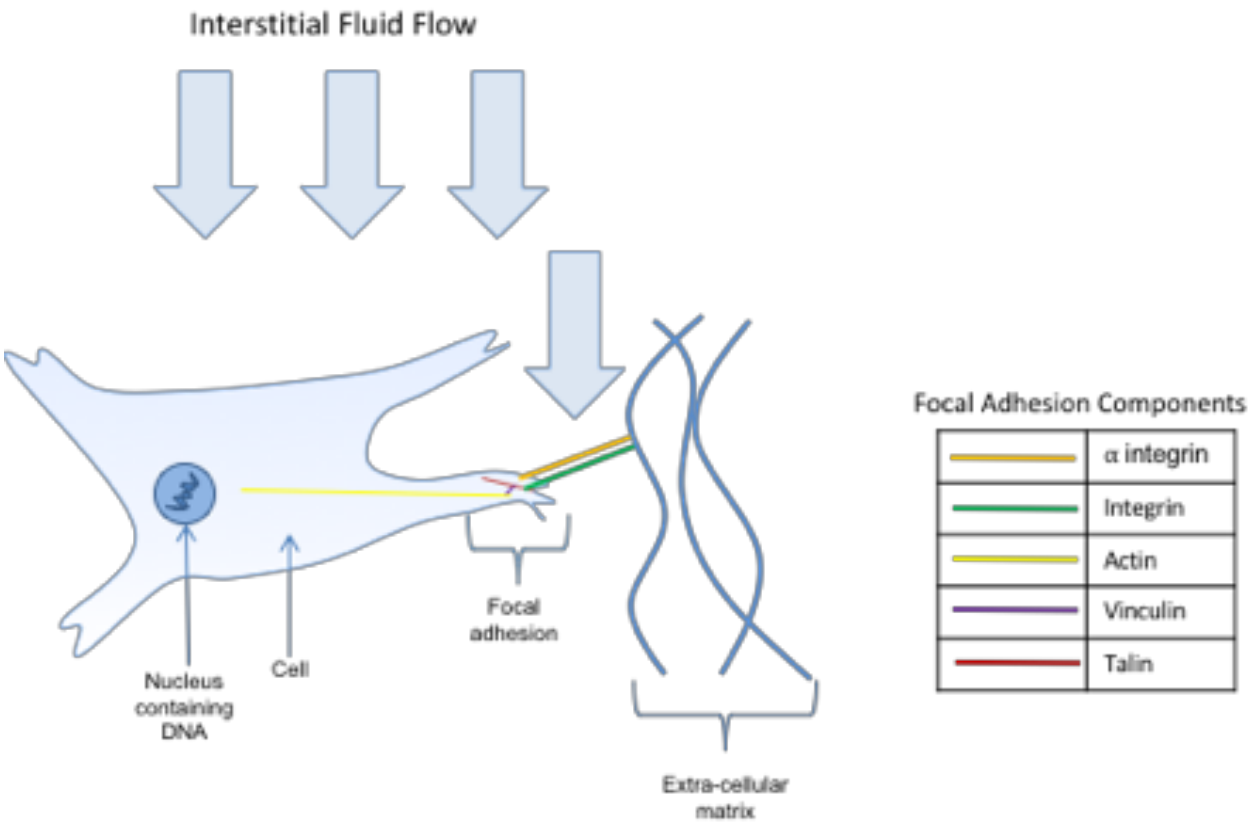

Figure 2.24 Depicts fluid flowing between a cell and ECM over the focal adhesion on the cell surface.

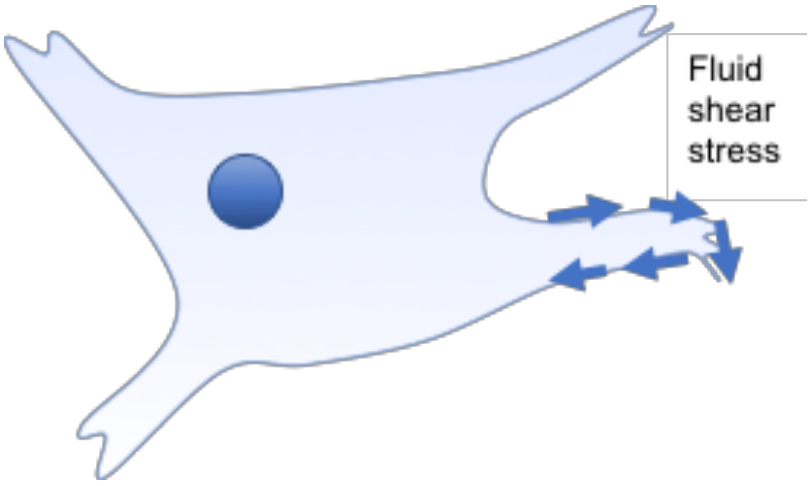

Figure 2.25 Fluid shear stress created parallel to the surface of the cell as fluid flows over it.

The challenge facing clinicians in the treatment of low back pain is that often the condition is so far escalated by the time pain is felt and the patient seeks treatment

that the options are limited. Novel cell-based therapies may help to expand the treatment options available. These novel therapies often entail growing cells in a bioreactor. Bioreactor designs are evolving in their complexity, and the development of dynamic bioreactors allows cells to be exposed to mechanical forces, such as fluid shear stress in a perfusion bioreactor. This helps create an environment more akin to the in vivo environment of the cell. The mechanism of fluid flow through the IVD is so complex (determined by ECM density, FCD concentration, IVD hydration and pressure changes) that cells are likely to experience a range of shear stress conditions in vivo. Knowledge of shear stress conditions which are beneficial or detrimental to NP cell health would be beneficial for the body of knowledge surrounding mechanotransduction but would also be useful for researchers and clinicians developing NP cell-based therapies in dynamic bioreactors. There is a current gap in knowledge regarding the effect of shear stress on NP cell health. A greater understanding of the role of shear stress in NP cell morphology and gene expression will guide researchers when developing bioreactor regimes for the growth of intervertebral disc cells. To answer the questions elucidated in this chapter, a range of shear stress conditions will be investigated. The objectives of this research are to ask if the shear stress conditions chosen affect NP cell morphology and gene expression. If the conditions do have an effect on the NP cells, the following 3 questions are to be answered. Does the type of shear stress affect cell morphology and gene expression? Does the rate of shear stress affect cell morphology and gene expression? Does the duration of time the cells are exposed to a shear stress affect the cell morphology and gene expression? The overall aim of the research would be to highlight shear stress conditions which would be detrimental or beneficial to cell health and if possible, devise a regime which would be beneficial in the use of perfusion bioreactors.

The above aims will be accomplished by focusing on the following objectives:

1. Bovine NP cells will be harvested from oxtails by sequential digestion and grown in a monolayer on flow chambers. Experimental set-up will include a syringe pump to create a steady flow, a peristaltic pump to create a pulsed flow and controls with no flow.

2. The cells will be exposed to a control (no flow), steady flow and pulsed flow to analyse the effect of flow type. Morphology (cell number, focal adhesion number and cell circularity) will be assessed through immunostaining and results will be analysed using one-way ANOVA with post-hoc Tukey if significant results are found.
3. The cells will be exposed to shear stress rates of 0.1, 1.0 and 4.0 dyne/cm^2 to analyse the effect of shear stress rate. Morphology (cell number, focal adhesion number and cell circularity) will be assessed through immunostaining and results will be analysed using one-way ANOVA with post-hoc Tukey if significant results are found.
4. The cells will be exposed to shear stress for 1, 4, 8 and 24 hours to analyse the effect of duration. Morphology (cell number, focal adhesion number and cell circularity) will be assessed through immunostaining and results will be analysed using one-way ANOVA with post-hoc Tukey if significant results are found.
5. The cells will be exposed a control, steady flow and pulsed flow to analyse the effect of flow type. Gene expression (of collagen 1, collagen 2, aggrecan, aggrecanase 1 and aggrecanase 2) will be analysed using qRT-PCR techniques and results will be analysed using one-way ANOVA with post-hoc Tukey if significant results are found.
6. The cells will be exposed to shear stress rates of 0.1, 1.0 and 4.0 dyne/cm^2 to analyse the effect of shear stress rate. Gene expression (of collagen 1, collagen 2, aggrecan, aggrecanase 1 and aggrecanase 2) will be assessed through qRT-PCR and results will be analysed using one-way ANOVA with post-hoc Tukey if significant results are found.
7. The cells will be exposed to shear stress for 1, 4, 8 and 24 hours to analyse the effect of duration Gene expression (of collagen 1, collagen 2, aggrecan, aggrecanase 1 and aggrecanase 2) will be assessed through qRT-PCR and results will be analysed using one-way ANOVA with post-hoc Tukey if significant results are found.

Chapter 3. Methodology

3.1 Research Approach

The aim of this study was to investigate the effect of shear stress on bovine nucleus pulposus (NP) cells. Cell studies were carried out at the Musculoskeletal Research Group at Newcastle University Medical School, 4th Floor Cookson Building. Fluid flows passively through the nucleus pulposus due to the hydrophilic nature of proteoglycan in the nucleus pulposus matrix. Fluid also flows through pressure driven flow created by changes in spinal posture and loading. Cells in the nucleus pulposus are embedded in a fibrous matrix of mainly collagen and proteoglycan; fluid flows through the pores in the matrix and over the cells, creating shear stress on the cell surface. Shear stress varies with varying flow rate and it is hypothesized that differing flow rates and flow types may have differing effects on the way nucleus pulposus cells function. This study has chosen three shear stress values, 0.1, 1.0 and 4.0 dyne/cm^2 and flow types; steady and pulsed, to analyse the effect that differing shear stresses may have on the morphology and phenotype of bovine nucleus pulposus cells.

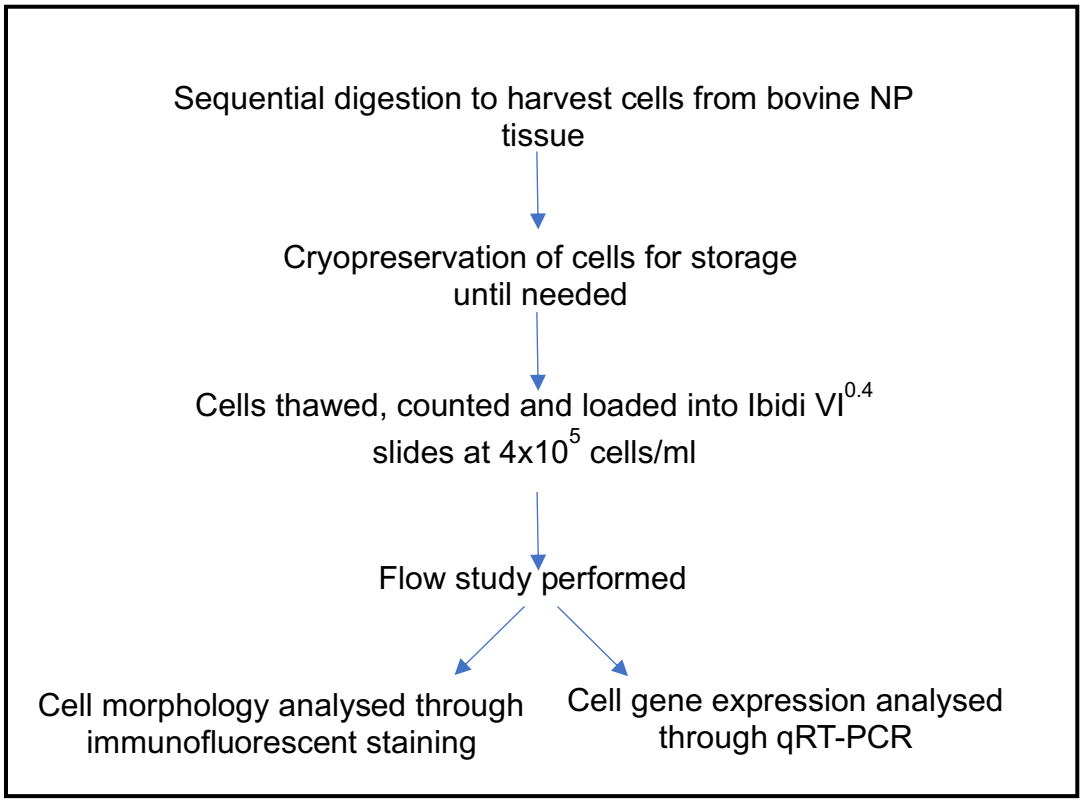

Figure 3.1 Flow diagram of research methodology

The effects of shear stress on cells has been commonly studied using parallel plate flow chambers (PPFC) which uses a rectangular channel through which to pass fluid over cells (Levesque and Nerem, 1985, Brown and Larson, 2001, Khismatullin and Truskey, 2004, Bacabac et al., 2005). A PPFC is used to create a flow profile over a monolayer of cells, where all the cells experience the same shear stress. The first PPFC was designed by (Hochmuth et al., 1971) to study red and white blood cells under flow and historically the thin channel was created between two plates, the height of which was determined either by a stainless steel plate, or ring with either clamps, screws or a vacuum to seal the chamber (Brown and Larson, 2001). Modern designs have created PPFC by moulding which has allowed smaller channel dimensions, this allows for a reduction in the reagents used in flow studies which is important in reducing the cost of experiments. The chamber chosen in these flow studies were Leur $VI^{0.4}$ slides, manufactured by Ibidi. 'Leur' relates to the connector at the channel ends, 'VI' relates to there being 6 PPFC channels on each slide and '0.4' relates to the height of the channels; 0.4mm. Live, healthy NP cells adhere to the bottom of the channel in a monolayer over 2-3 hours after seeding, fluid is passed over the cells to create a shear stress on the surface of the cell. A monolayer was preferable to allow more effective analysis of cell morphology.

Historically, flow through a PPFC channel was created by a pressure head, but a pumping system is now more commonly used to adequately control the flow of fluid over the cells. The research approach in this study required both a steady flow and a pulsed flow. A Harvard PHD2000 syringe pump was used to create a steady flow and a GE P1 peristaltic pump was used to create a pulsed flow which would allow the two flow types to be compared. Shear stress values were chosen and flow rate settings for the pumps could then be calculated from the flow profile through the Ibidi $VI^{0.4}$ slide. The governing equations and method for calculating the flow rate is discussed in section 3.2.1.

The equipment set-up, calibration and experimental conditions are discussed in sections 3.3, 3.4 and 3.5, respectively. A bovine cell model was used in the research. Intervertebral disc bovine cells have been found to be similar in morphology to human (Alini et al., 2008) and similar in gene expression (Wilke, 2008) and are frequently used as animal models in spinal research. Cells were harvested from the

tails of 18-months old bovine calves. Once the cells were harvested, they were cryogenically frozen and stored until use. When required they were then thawed and loaded in the Ibidi Leur VI$^{0.4}$ slides following the method described in section 3.6.

In order to understand the effect of shear stress on the cells, their morphology was analysed using immunofluorescent staining. This protein staining method allows the analysis of different components of the cell. Staining for DAPI, Phalloidin and Vinculin were carried out and images of the cells were then taken under a microscope and imported into ImageJ software which allowed quantitative analysis. DAPI was used to stain the nucleus of the cell which were then counted and used to analyse if cell proliferation or cell death had occurred during the flow study. If any cells had died during the flow study, they would detach from the Ibidi slide and be washed away in the flow, so the cell number would be reduced when compared to the control Ibidi slide with no flow. Similarly, if cells had proliferated during the flow study then the number of cells would increase when compared to the control slide. Phalloidin staining of the cytoskeleton was used to detect changes in cell shape and circularity. Cell shape can give an indication of the health of the cell, a more circular cell is seen as focal adhesions are lost, prior to cell detachment from the slide which can be a precursor to cell death in the NP cell. Vinculin staining was used to analyse the presence of the focal adhesions. ImageJ was used to quantify any changes. Methods for immunostaining and ImageJ are detailed in section 3.7.

To understand the effect of shear stress on the phenotype of the cell, quantitative reverse transcriptase-polymerase chain reaction (qRT-PCR) was used. qRT-PCR is a standard procedure for analysing gene expression. It involves breaking down the DNA in the nucleus of the cell to single stands of RNA and adding RNA strands of a known gene which then forms complimentary DNA (cDNA), which is then amplified to a quantify that can be measured. It is the current choice of analysis for gene expression (Johnson, 2015). The two common methods of qRT-PCR are TaqMan and SYBR green. King (2002) report SYBR green as being widely used because of the ease in designing the assays and its relatively low set up and running costs. (Cao et al., 2013) compared TaqMan and SYBR green procedures for animal cells, they found both assays to be reliable, but that SYBR green generates higher gene expression values than TaqMan, so they stress the importance of stating which

assay is being used in the analysis and using the same analysis when comparing sets of results. SYBR green was used for this research and the method is described in section 3.8. Statistical analyses of the results are discussed in section 3.9. Limitations of the experimental design are discussed later in the thesis in Chapter 5.

3.2 Parallel plate flow chamber

3.2.1 Shear Stress

Calculating the velocity profile, flow rate and shear stress for flow in a rectangular channel, such as Ibidi Leur VI$^{0.4}$ slides, is complex due to the necessity to solve for a three-dimensional flow, as the end effects of the sides of the chamber cannot be ignored. The values were calculated for steady flow and the same flow rate was then used as an average flow rate for the pulsed flow studies. The dimensions of the rectangular duct are height of gap 2H, and width of 2W, as shown in figure 3.1.

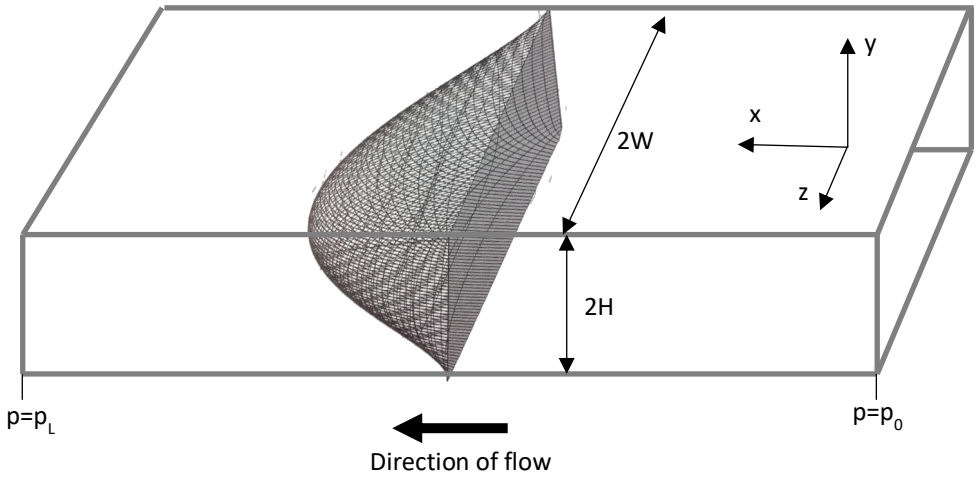

Figure 3.2 Three-dimensional flow through a rectangular channel as in a parallel plate flow chamber

The differential equations have been solved by Ibidi for their chambers using advanced mathematical techniques and equation (1) is used to calculate the flowrate for a given shear stress at the bottom wall of the Ibidi slide, where the cells are adhered to, as shown in figure 3.2.

$$Q = \frac{\tau}{\mu * 176.1}$$

(1)

Where Q is the flow rate (ml/min), τ the shear stress (dyne/cm^2) and μ the dynamic viscosity of the fluid (dyne.s/cm^2). 176.1 is a constant derived by advanced mathematically solutions and provided by Ibidi for the chosen Leur VI$^{0.4}$ slide. The units used have been advised by Ibidi and correlate with the constant value 176.1 supplied by them.

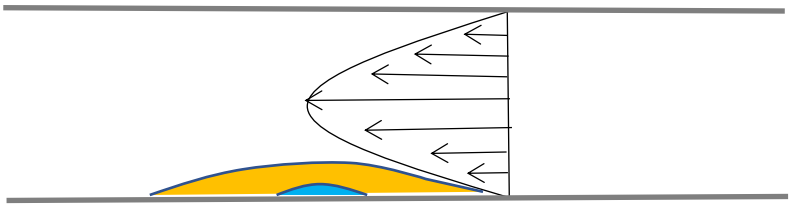

Figure 3.3 Cross section through the centre of a parallel plate flow chamber, with a cell shown adhered to floor of the chamber and experiencing shear stress from the surrounding fluid

Although equation (1), supplied by Ibidi, has been used to calculate the required flow rates, it is useful to have an understanding of how the solution has been derived, the equations used to solve for flowrate and shear stress are shown in published work by Cornish (1928) and Morrison (2013) and are used in the solution below.

The continuity equation and Navier-Stokes equation are applied to solve for velocity, ν and shear stress τ. The flow is modelled as steady, well developed, Newtonian and incompressible and a no-slip boundary is assumed. The continuity equation for the flow in figure 3.2 is

$$0 = \frac{\partial v_x}{\partial x} + \frac{\partial v_y}{\partial y} + \frac{\partial v_z}{\partial z} \tag{2}$$

The flow is only in the x direction so the y and z components of ν are zero.

$$\underline{v} = \begin{pmatrix} v_x \\ 0 \\ 0 \end{pmatrix}_{xyz}$$

(3)

So, the continuity equation cancels to

$$\frac{\partial v_x}{\partial x} = 0$$

(4)

The Navier-Stokes equation is used for the momentum conservation for an incompressible Newtonian fluid is

$$\rho \left(\frac{\partial \underline{v}}{\partial t} + \underline{v}.\nabla \underline{v}\right) = -\nabla p + \mu \nabla^2 \underline{v} + \rho \underline{g}$$

(5)

$$\rho \left(\frac{\partial v_x}{\partial t} + v_1 \frac{\partial v_x}{\partial x} + v_2 \frac{\partial v_x}{\partial y} + v_3 \frac{\partial v_x}{\partial z}\right) = -\frac{\partial p}{\partial x} + \mu \left(\frac{\partial^2 v_x}{\partial x^2} + v_2 \frac{\partial^2 v_x}{\partial y^2} + v_3 \frac{\partial^2 v_x}{\partial z^2}\right) + \rho g_x$$

(6)

$$\rho \left(\frac{\partial v_y}{\partial t} + v_1 \frac{\partial v_y}{\partial x} + v_2 \frac{\partial v_y}{\partial y} + v_3 \frac{\partial v_y}{\partial z}\right) = -\frac{\partial p}{\partial y} + \mu \left(\frac{\partial^2 v_y}{\partial x^2} + v_2 \frac{\partial^2 v_y}{\partial y^2} + v_3 \frac{\partial^2 v_y}{\partial z^2}\right) + \rho g_y$$

(7)

$$\rho \left(\frac{\partial v_z}{\partial t} + v_1 \frac{\partial v_z}{\partial x} + v_2 \frac{\partial v_z}{\partial y} + v_3 \frac{\partial v_z}{\partial z}\right) = -\frac{\partial p}{\partial z} + \mu \left(\frac{\partial^2 v_z}{\partial x^2} + v_2 \frac{\partial^2 v_z}{\partial y^2} + v_3 \frac{\partial^2 v_z}{\partial z^2}\right) + \rho g_z$$

(8)

Simplifying these equations by neglecting gravity, cancelling all y and z terms and substituting equation (4)

$$\frac{\partial v_x}{\partial x} = 0$$

(4)

$$\rho \frac{\partial v_x}{\partial t} = -\frac{\partial p}{\partial x} + \mu \left(\frac{\partial^2 v_x}{\partial y^2} + \frac{\partial^2 v_x}{\partial z^2}\right)$$

(9)

$$0 = -\frac{\partial p}{\partial y}$$

(10)

$$0 = -\frac{\partial p}{\partial z}$$

(11)

Equation (8) can be simplified further, assuming the flow is at steady state then the time derivative term is zero.

$$0 = -\frac{\partial p}{\partial x} + \mu\left(\frac{\partial^2 v_x}{\partial y^2} + \frac{\partial^2 v_x}{\partial z^2}\right)$$

(12)

Rearranging equation (11)

$$\frac{\partial p}{\partial x} = \mu\left(\frac{\partial^2 v_x}{\partial y^2} + \frac{\partial^2 v_x}{\partial z^2}\right)$$

(13)

Equations (9) and (10) indicate that there is no change in pressure in the y and z direction, therefore pressure is a function of x only and from the continuity equation, velocity is a function of y and z only and not x. Taking this into consideration equation (13) can hold only if the left and right hand of the equation are equal to the same constant, for which we have given the symbol λ

$$\frac{dp}{dx} = \lambda$$

(14)

Note the change from partial derivative to total derivative as pressure is a function of x only and not, y and z.

$$\mu\left(\frac{\partial^2 v_x}{\partial y^2} + \frac{\partial^2 v_x}{\partial z^2}\right) = \lambda$$

(15)

As we are concerned with the flow over the cells, we are concerned with the wall shear stress at the bottom wall of the channel. Assuming the no-slip boundary at the wall then where x = 0, p = p_0 and x = L, p = p_L

Then for the pressure profile equation (13) integrates to give

$$p(x) = \left(\frac{p_L - p_0}{L}\right)x + p_0 \tag{16}$$

From equations (13) and (15)

$$\lambda = \frac{(p_L - p_0)}{L} \tag{17}$$

So, the velocity profile the equation can be written as

$$\left(\frac{\partial^2 v_x}{\partial y^2} + \frac{\partial^2 v_x}{\partial z^2}\right) = -\frac{(p_L - p_0)}{L} = -\frac{\Delta p}{\mu L} \tag{18}$$

This is called the Poisson equation and unlike in tube flow or slit flow, this equation cannot be simplified further as the no-slip boundary conditions at each of the four walls must be taken into consideration in the velocity profile for three-dimensional flow. From figure 3.2, for all values of y and z

$$y = \pm H \qquad v_x = 0$$
$$z = \pm W \qquad v_x = 0$$

For a rectangular channel the functions f(y) and g(z) are trigonometric functions and the method used to solve the equation uses orthogonal functions which leads to the following solution, provided by the manufacturer, Ibidi, and the derivation is published in Cornish (1928). The derivation has been adapted to meet the annotation in figure 3.2.

$$v(y,z) = -\frac{1}{\eta}\frac{dp}{dx}\left\{\frac{W^2}{2} - \frac{z^2}{2} - \sum_{n=0}^{\infty}\frac{(-1)^n(2W^2)}{(2n+1)^3}\left(\frac{2}{\pi}\right)^3\frac{cosh\left[(2n+1)\left(\frac{\pi z}{2W}\right)\right]}{cosh\left[(2n+1)\left(\frac{\pi H}{2W}\right)\right]}cos\left[\frac{(2n+1)\pi y}{2W}\right]\right\}$$

(19)

The equation for flow rate through the channel, Q, is

$$\mathrm{Q} = -\frac{1}{\eta}\frac{dp}{dx}\left\{\frac{4}{3}HW^3 - 8W^4\left(\frac{2}{\pi}\right)^5\sum_{n=0}^{\infty}\frac{1}{(2n+1)^5}tanh\left[\frac{(2n+1)\pi H}{2W}\right]\right\}$$

(20)

Where, as shown in figure 3.2, 2H is the height of the channel in the y direction, 2W is the width of the channel in the z direction and x is the direction of flow, η is the dynamic viscosity of the fluid.

Substituting

$$q = \frac{4}{3}\,HW^3 - 8W^4\left(\frac{2}{\pi}\right)^5\sum_{n=0}^{\infty}\frac{1}{(2n+1)^5}tanh\left[\frac{(2n+1)\pi H}{2W}\right]$$

(21)

Into equation (19) gives

$$\frac{dp}{dx} = -\eta\frac{\Phi}{q}$$

(22)

The shear stress profile is given by the equation

$$\tau(y,z) = \eta\frac{\partial v(y,z)}{\partial z}\Big|_{y=-H}$$
$$= \eta\left(-\frac{1}{\eta}\frac{dp}{dx}\sum_{n=0}^{\infty}\frac{(-1)^n W\pi}{(2n+1)^2}\left(\frac{2^3}{\pi}\right)\frac{sinh\left[(2n+1)\frac{\pi y}{2W}\right]}{cosh\left[(2n+1)\frac{\pi H}{2W}\right]}cos\left[\frac{(2n+1)\pi z}{2W}\right]\right)\Bigg|_{y=-H}$$

(23)

Substituting equation (22) gives

$$\tau(y,z) = \eta\left(-\frac{1}{\eta}\left(-\eta\frac{\mathrm{Q}}{q}\right)\sum_{n=0}^{\infty}\frac{(-1)^n W\pi}{(2n+1)^2}\left(\frac{2^3}{\pi}\right)\frac{sinh\left[(2n+1)\frac{\pi y}{2W}\right]}{cosh\left[(2n+1)\frac{\pi H}{2W}\right]}cos\left[\frac{(2n+1)\pi z}{2W}\right]\right)\Bigg|_{y=-H}$$

(24)

Which rearranges to

$$\tau(y,z) = \eta \frac{Q}{q} \sum_{n=0}^{\infty} \frac{(-1)^n W\pi}{(2n+1)^2} \left(\frac{2^3}{\pi}\right) \frac{sinh\left[(2n+1)\frac{\pi y}{2W}\right]}{cosh\left[(2n+1)\frac{\pi H}{2W}\right]} cos\left[\frac{(2n+1)\pi z}{2W}\right]\Bigg|_{y=-H} \quad (25)$$

The cells are attached to the bottom of the channel. The wall shear stress, τ, at the bottom and centre of the channel at y = -H, z = 0 is

$$\tau(z=0, y=-H) = \eta \frac{Q}{q} \left\{ \sum_{n=0}^{\infty} \frac{(-1)^n W\pi}{(2n+1)^2} \left(\frac{2}{\pi}\right)^3 tanh\left[(2n+1)\frac{\pi H}{2W}\right] \right\} \quad (26)$$

As discussed previously, the solution has been solved by the manufacturer of the flow channels chosen, Ibidi, who provided equation (1) including the constant 176.1 for the specific flow chamber used, the Ibidi Leur VI$^{0.4}$ slide. Units to be used to solve the equation and to calculate the flow rate in ml/min were specified by Ibidi. Dynamic viscosity, μ, of cell culture medium at 37 °C, were to be given in units of dyne.s/cm^2, which is 0.0072 dyne.s/cm^2. Shear stress was to be given in units of dyne/cm^2, which were chosen as 0.1, 1 and 4 dyne/cm^2.

$$Q = \frac{\tau}{\mu * 176.1} \quad (1)$$

3.2.2 Ibidi Leur VI$^{0.4}$ slides

Ibidi Leur VI$^{0.4}$ slides are μ-slides (inverted slides) in which the bottom surface is patterned with 'IbiTreat' which encourages adherence of the cells, see figure 3.4 and table 3.1. Cells were loaded in suspension into the channels, see figure 3.5 and adhered to the surface within 2-3 hours, see figure 3.6.

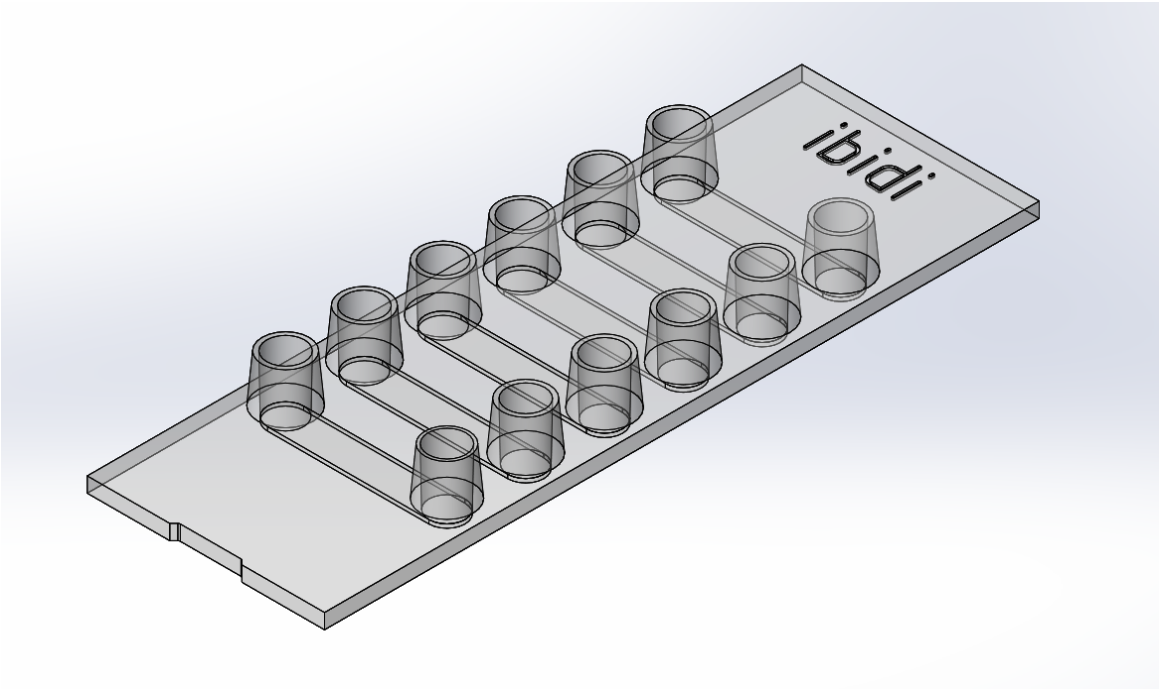

Figure 3.4 CAD render of Ibidi VI$^{0.4}$ slide

Channels per slide	6
Channel length	17 mm
Channel height	0.4 mm
Channel width	3.8 mm
Cell growth area per channel	0.6 cm^2
Volume per reservoir	60 µl

Table 3.1 Ibidi VI$^{0.4}$ slide dimensions

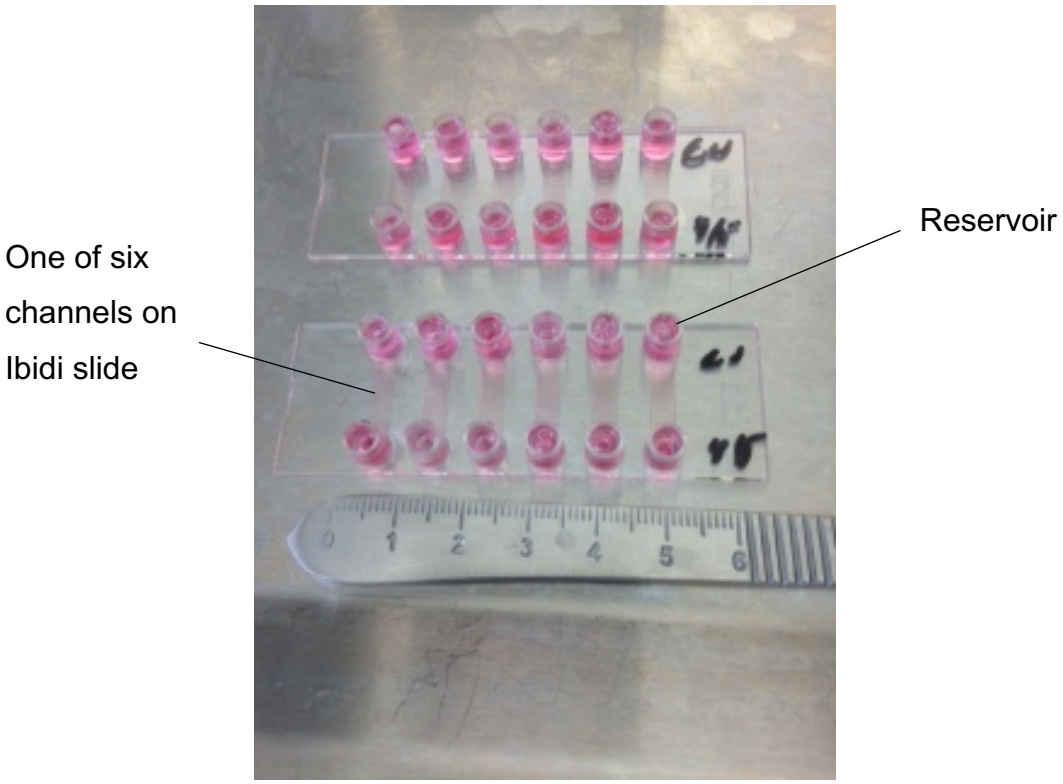

Figure 3.5 Two Ibidi VI$^{0.4}$ slides, showing six channels on each, filled with cell culture media and NP cells, adjacent implement scale is in centimetres.

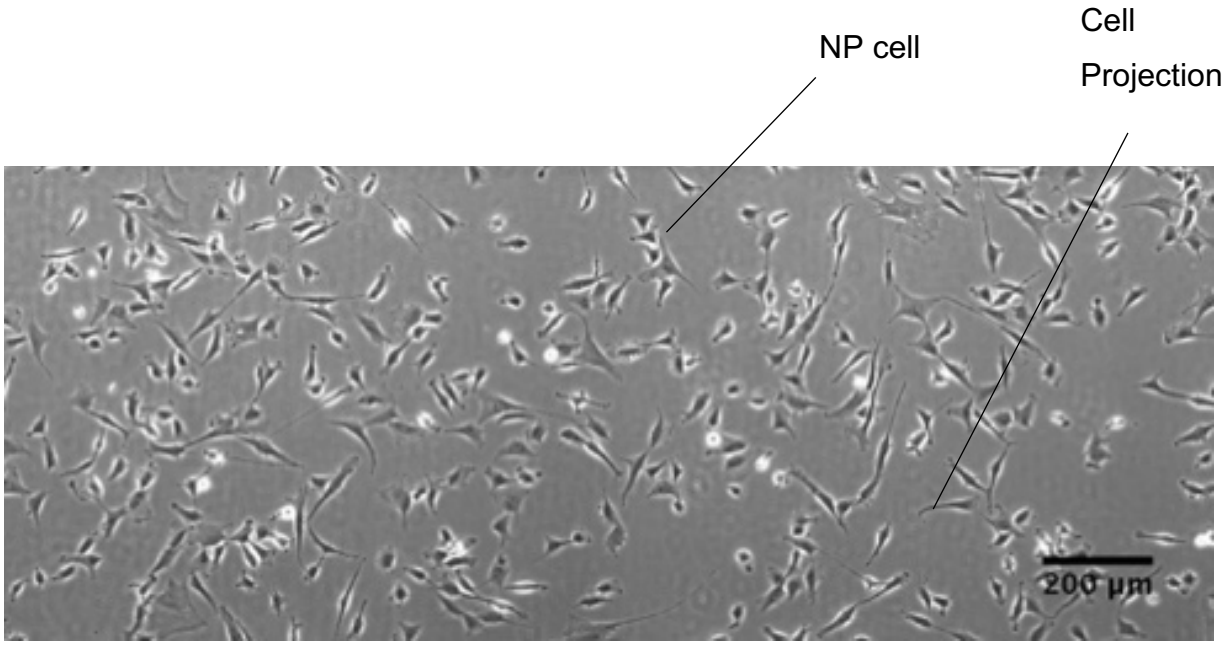

Figure 3.6 Brightfield, Nikon Biostation microscope image, showing mono-layer of bovine NP cells adhered onto Ibidi Leur VI0.4 Slides after 4 hours.

3.3 Pressure Driven flow

3.3.1 Harvard syringe pump

Figure 3.7 Harvard PHD2000 syringe pump. Showing syringes in situ and digital display for setting required flow rate.

A Harvard PHD2000 Syringe Pump was used to deliver the steady flow rate. The pump was chosen for its capacity to deliver low flow rates. The syringe pump used was an infuse-only pump which allows the movement of fluid in one direction only, infuse/withdraw syringe pumps are also available. Syringe pumps are driven by a stepper motor, which allows the delivery of small, precise quantities of fluids. A lead screw is threaded through a pusher block; as the lead screw turns, the pusher block moves towards the syringe and pushes the syringe, infusing fluid from the syringe. The Harvard syringe pump manufacturer guidelines state an accuracy of ± 0.05%. However, due to the stepper motor driving the pusher block it is recommended a syringe with as small a quantity as practically possible for the experiment is used to ensure a more continuous delivery of fluid at low flow rates. A smaller syringe lead to greater number of refills during the experiment, so a compromise between the two factors was sought. A 25 ml Hamilton 1000 series Gastight Glass syringe was used to store and infuse the cell culture medium for the 0.1 ml/min flow rate and a 100 ml Hamilton 1000 series Gastight Glass syringe was used for 0.8 ml/min and 3.2 ml/min

flow. These syringe volumes would ensure a continuous flow rate. An Elveflow bubble trap was used to eliminate air bubbles in the system as these have been shown to significantly affect the expected flow conditions (Sung and Shuler, 2009).

3.3.2 Peristaltic pump

Figure 3.8 GE P1 peristaltic pump, showing turn dial for setting required flow rate.

Peristaltic pumps are positive displacement pumps, driven by a stepper motor. The fluid lies within a tube and rollers exert pressure onto a tube compressing it. As the roller continues to move, thereby relaxing pressure on that part of the tube, fluid is drawn into the tube. The same roller then pushes the fluid on the opposite side away from the roller and along the tube. Due to the occlusion and release of the tubing containing fluid used to drive the fluid through the pump, a pulsed flow is created which was desired for the pulsed flow studies. A GE P1 peristaltic pump was chosen and manufacturers state an accuracy of ± 5%. The flow rate mentioned for the peristaltic pump flow is an average flow rate, recorded over the course of an hour, as described in section 3.4 on calibration. The pulsations created by the mechanism of the pump are affected by the material of the tubing and inner diameter of the tubing. Although the design of many modern peristaltic pumps is such to decrease

pulsations, the pulsed flow experiments required pulsations to be present. The softer the tubing the greater the occlusion and the greater the pulsations and the smaller the diameter the greater the occlusion and the greater the pulsations. There were 6 rollers which exert pressure on the tube, Cole Palmer Silicone Tubing of inner diameter 1mm was used which, this gives the maximum the pressure of the rollers occluding this tubing as 10%, as advised by the manufacturers. An Elveflow bubble trap was used to eliminate air bubbles in the system. The revolutions per minute (rpm) of the roller cage were recorded for each of the 3 average flow rates following calibration and from this the pulse frequency and wave form could be determined. The flow rates and wave forms are discussed further in section 3.5.2; figure 3.10.

Equipment	Make	Model	Serial No
Peristaltic pump	GE	P-1	135765
Syringe pump	Harvard	PHD2000 Infuse	B26746

Table 3.2 Specifications of pumps used

3.4 Calibration

Weighted-fluid calibrations were used as an in-direct method of calibrating the flow rate in the experimental set-up and the accuracy of the flow studies. While direct measurement techniques for microfluidic flow rates up to 3.3 ml/min are available to purchase, they are a relatively new technology, and relatively expensive. The reasons they were not used in this current calibration and throughout the flow experiments are discussed further in the limitations section, Chapter 5. The experimental set up, as shown in figure 3.9, to include the pump, tubing and bubble trap was calibrated using weighted-fluid calibrations to reduce the likelihood of accountable errors and determine the accuracy of the set up. Calibrations were carried out using an Amput digital precision electronic balance with readings to 0.001 g, a 200 ml Rocwing borosilicate glass beaker, 1 mm inner diameter Cole Palmer silicone tubing, Elveflow bubble trap and a TopElek electronic timer. Calibration experiments were carried out at 37 ^{o}C with cell culture medium to match the actual test conditions and determine the flowrate at the entrance to the Ibidi flow chamber. Calibration required some trial and error initially to find the correct dial setting for the

required flowrate until a repeatable and accurate flowrate was achieved. The Harvard syringe pump has a digital display which made calibration easier, the peristaltic pump was more difficult to calibrate as the flow rate set up was a turn dial, which is obviously more prone to inaccuracy when setting. The glass beaker was placed on the electronic balance and the tubing from the pump was placed in the beaker. The required flow rate was chosen, the pump was switched on and simultaneously the timer was started. After 1 hour the calibration was stopped, the liquid weight recorded, and the actual flow rate calculated. The flow rate settings on the pump were then adjusted accordingly and the calibration repeated until the correct actual flowrate was achieved. When the correct flowrate was achieved, the pump setting was fixed for that flowrate and then the procedure repeated 20 times to establish the accuracy of the set up. The flow rate calculated for the steady flow syringe pump was a continuous flow rate, the flow rate calculated for the pulsed peristaltic pump was an average flow rate. The flow rate accuracy was limited to one decimal place due to the lower accuracy of the peristaltic pump, this is discussed further in limitations in Chapter 5.

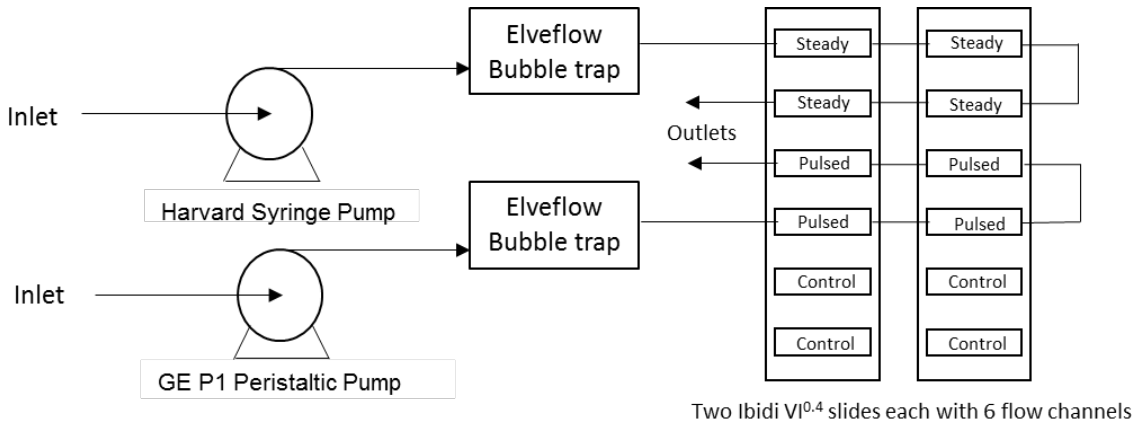

Figure 3.9 Schematic diagram showing experimental set up

3.5 Test Conditions

3.5.1 Shear Stress Values

Shear stress is proportional to fluid velocity and inversely proportional to channel/pore size as discussed in Chapter 2 (section 2.8.1). Deciding which shear stress values would best reflect those in the nucleus pulposus and so should be used in the cell studies, was difficult. Shear stress values have been more easily determined in other areas of the body with the ability to measure the fluid velocity and pore size directly in vivo. For example, Doppler velocimetry has been used to determine flow rate in blood vessels (Vennemann et al., 2007). Published values for velocity through an intervertebral disc have been approximated using CFD as 5 μm/s (Ferguson et al., 2004) and 13.7μm/s (Mow et al., 1980). Although the periodicity of collagen fibres in the annulus fibrosus of the disc has been approximated as 600 Angstrom (Inoue and Takeda, 1975), so could be used to determine an approximate pore size, these values are not available for the nucleus pulposus. Furthermore, due to the elasticity of the disc tissue, the actual pore size in the nucleus pulposus changes depending on fluid content and spinal loading. As discussed in Chapter 2, values for the shear stress cells experience in the disc are not available at this time. As computational modelling of the disc progresses, it would be hoped these values would be available at some point in the future.

In choosing appropriate shear stress values, a previous published study by Wang (2011) studied 1 dyne/cm^2 shear stress over nucleus pulposus cells, so the same value shear stress was chosen as a comparable study. A value of a magnitude ten times smaller would be useful to determine if there was a fold change in the effects, hence 0.1 dyne/cm^2 was chosen as the lowest value. In determining a higher flowrate 10 dyne/cm^2 was determined to be too high for the experimental set up over a 24-hour period as a syringe loading regime of 8 ml/min would have lead to frequent opening of the hypoxic incubator to replace the syringe volume and would have lead to greater inaccuracies introduced in the oxygen content and temperature of the incubator. A shear stress of 4 dyne/cm^2 as an upper limit was chosen as a practical compromise.

3.5.2 Flow types

Steady flow rates created by the syringe pump could be likened to flow in the disc resulting from electroosmotic flow which is passive and dependent on the FCD and ionic content of the fluid. Pulsed flow rates created by the peristaltic pump could be likened the frequent changes in flow such as in spinal loading of a degraded nucleus pulposus, as discussed in Chapter 2. Investigating the effect of unsteady flow with the same average flow rate as the steady flow studies, but the frequent acceleration and deceleration created by the occlusion and release of the peristaltic pump mechanism was of interest. The flow rate driven through a GE P1 peristaltic pump is pulsed as shown in the figure 3.10.

Following calibration, the rpm for each of the flow rates were counted manually and recorded for 1 hour. Markers where placed on the roller cage at 30^o intervals and the rpm was recorded to the nearest 30^o increment. Rpm values for average flow rates 0.1ml/min, 0.8ml/min and 3.2 ml/min, were recorded as $\frac{7}{12}$, $4\frac{8}{12}$, and $18\frac{8}{12}$ rpm respectively. Taking into account the pulsation of 10 % as given by the manufacturers, the predicted wave forms for the three flow rates are shown in figure 3.10. Direct measurement of the flow rate or pressure would allow measurement of the actual wave form, but this equipment was not available, these limitations are discussed further in Section 5.

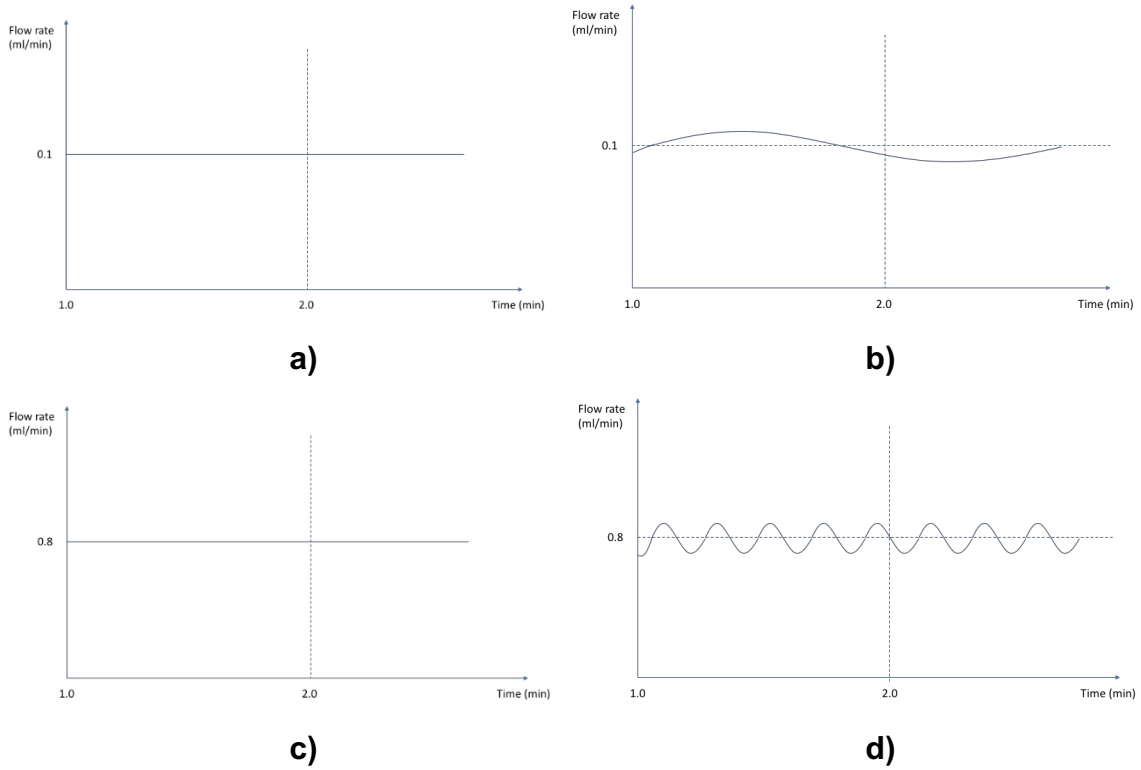

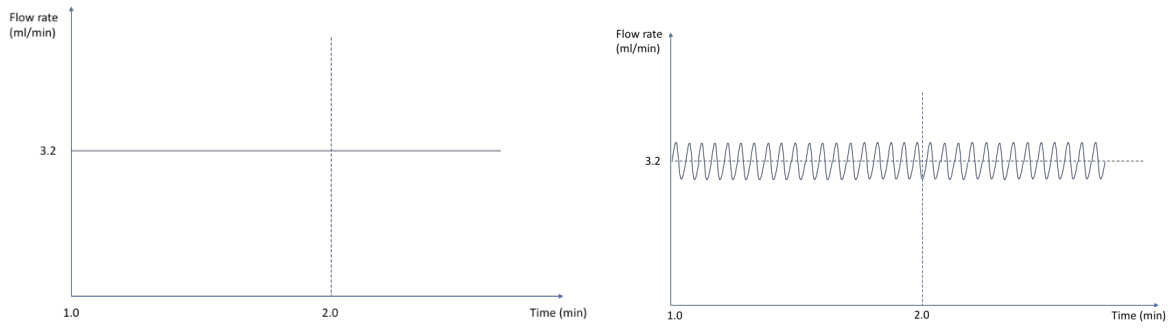

e) **f)**

Figure 3.10 Dotted horizontal line in b, d and f depicts average flow rate for GE P1 Peristaltic Pump, at 0.1, 0.8 and 3.2 ml/min respectively, solid wave line depicts predicted actual flow rate. Solid horizontal line in a, c and e depicts predicted continuous flow rate of Harvard PHD2000 Syringe Pump at 0.1, 0.8 and 3.2 ml/min respectively.

3.5.3 Time points

Time points chosen for the experiment were 1, 4, 8 and 24-hour. The 1-hour time point was chosen to see if there were any very early indicators of gene expression changes, morphological changes were not expected at this time. The 4-hour time point, and 8-hour time points were useful in discussing diurnal changes, such as fluid imbibement to the disc during sleeping or fluid exudation when sitting during work hours. The 24-hour time point was chosen to see if morphological changes in cell shape could be seen and to study the effect of shear stress on the proliferation of NP cells.

Chamber Conditions	Average Shear stress (dyne/cm^2)	Volumetric flow rate (ml/min)	Time Point (hrs)	Flow type
Ibidi Leur VI$^{0.4}$ 2% O_2 (Hypoxic) 37^o C 5% Humidity	0.1	0.1	1, 4, 8, 24	Steady and pulsed
	1.0	0.8	1, 4, 8, 24	Steady and pulsed
	4.0	3.2	1, 4, 8, 24	Steady and pulsed

Table 3.3 Summary of test conditions

3.5.4 Sample size

Statistical power analysis was carried out to estimate sample size based on data from published studies on gene expression response of intervertebral disc cells to cyclic strain (Gilbert et al., 2010) and shear stress (Wang et al., 1993) using GPower 3.1. Using Cohen's 1988 criteria, effect sizes ranged from medium to very large. An alpha value of 0.05 and power of 0.8 was inputted to GPower which calculated recommended biological sample sizes ranging from 3-7. Due to the complexity of the qRT-PCR experimental procedures carried out and the technicality of the experimental set up, it was decided that 4 technical replicates would be carried out on each experimental condition to account for human error. A biological sample size of 4 was used. This lead to 288 experiments for each of the four biological specimens, 144 studying cell morphology (immunostaining) and 144 studying gene expression (qRT-PCR), as shown in figure 3.11. To harvest cells from 4 biological specimens, 8 specimens were used as the procedure to harvest bovine cells from the disc tissue, detailed in the next section, was successful 50% of the time, failure was as a result of bacterial infections. Although the biological specimens were all taken from 18-month-old male calves, slaughtered in the same abattoir, biological replication was included to ensure any changes in results due to biological differences that may occur between specimens were considered. The experimental procedures used in harvesting the cells and in analysing gene expression were costly. The sample size was kept to 4 to allow for enough technical replication of experiments while not unnecessarily inflating the cost of the project.

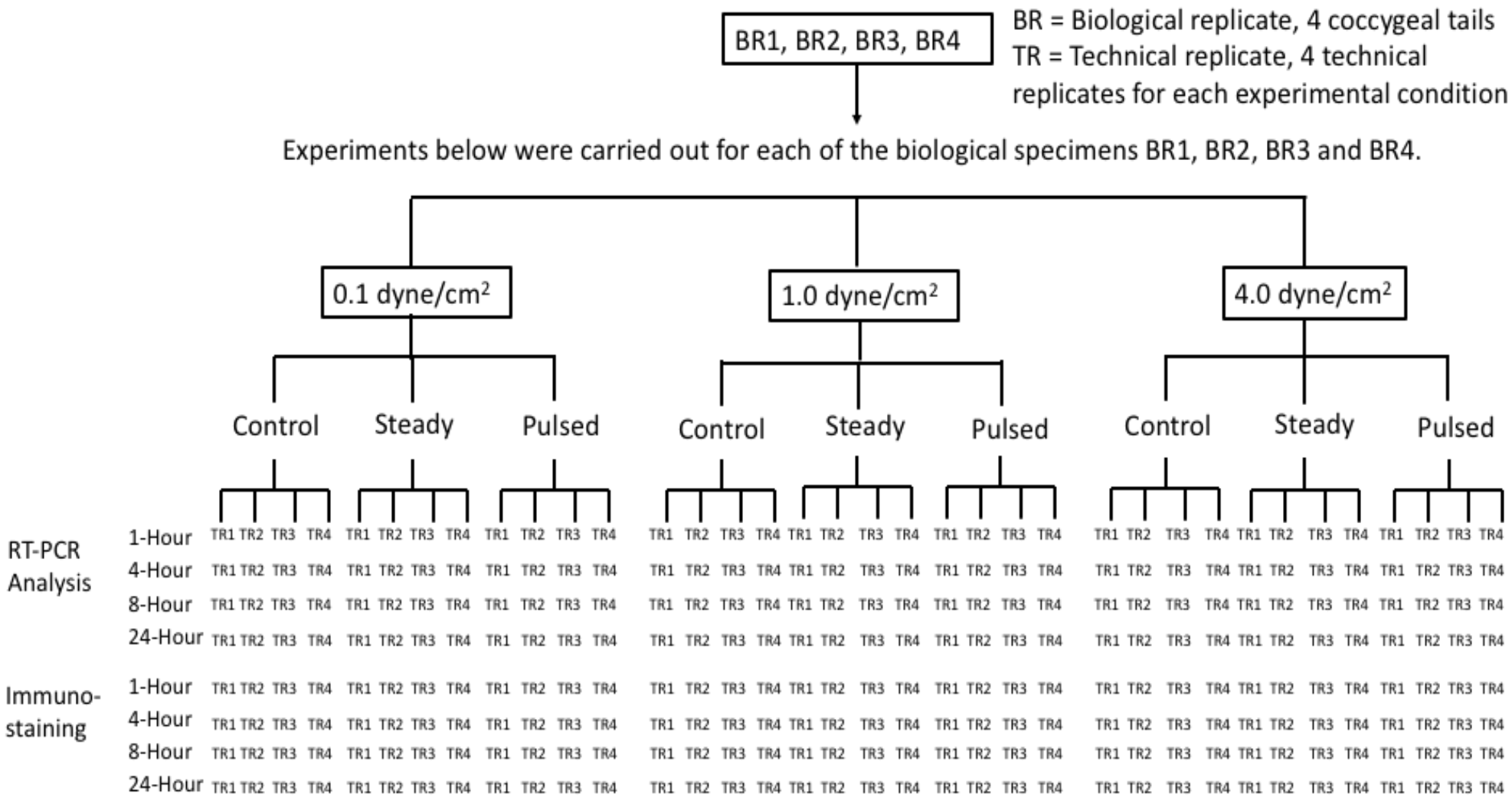

Figure 3.11 Showing biological replicates and technical replicates carried out. 288 experiments per biological specimen, including controls. Repeated for each of the 4 specimens, 1152 runs in total. 576 for qRT-PCR analysis and 576 for immunostaining analysis

3.6 Bovine nucleus pulposus cell isolation and culture

3.6.1 Cell harvesting from tissue

Cells were harvested from bovine tails and then cryopreserved until needed for the flow experiments. Sequential digestion is a common method used to harvest cells from disc tissue (Lee et al., 2015, Kraus and Lufkin, 2016). It entails the use of enzymes to digest the bonds formed between the collagen and proteoglycan in the disc tissue to release the cells from the extra-cellular matrix. Oxtails from 18 month-old calves were collected from Burradon Abattoir, Killingworth, Newcastle-Upon-Tyne within 8 hours of slaughter. Cell isolation and culture was carried out in the Musculoskeletal Research Group Laboratory, 4th floor Cookson Building, Newcastle Medical School.

3.6.2 Materials and methods

Reagent	Role	Source	Manufacturer
Dulbecco's Modified Eagle Medium (DMEM)	Salt based liquid for cell culture	Liquid solution	Sigma Aldrich
Foetal Bovine Serum (FBS)	Proteins to aid cell health	Bovine	Gibco
L-Glutamate (Gl)	Amino Acid	Human	Sigma-Aldrich
Penicillin Streptomycin (PS)	Antibiotic	Bacteria	Sigma-Aldrich
Trypsin	Used to detach cells from flasks	Mouse	Sigma-Aldrich
Dimethyl Sulfoxide (DMSO)	Cryopreservation of cells	Organic solvent	Sigma-Aldrich
Phosphate Buffered Saline (PBS)	Buffer solution to maintain cell conditions	Salt solution	Gibco
Collagenase	Break down collagen fibres in tissue	Bacteria	Gibco
Pronase-E	Breaks down protein in tissue	Bacteria	Merck Millipore

Table 3.4 Regents used in the cell isolation and culture

Equipment	Make	Model	Serial No
Laminar Flow Hood	Thermofisher	Class II	-
Roller mixer	Stuart	SRT9	45673
Centrifuge	Thermofisher	Heraeus Megafuge	B664738
Hypoxic incubator	Sanyo	MCO-18AIC	K47635
Cryogenic freezer	CBS	Classic 6002	264788
Fridge	Lec	LSR288UK	674853L
Freezer	Lec	LSF232UK	74655L
Heated water bath	VWR	1213	677455

Table 3.5 Equipment used in cell isolation and culture

Under a sterile Thermofisher Class II Laminar Flow Hood coccygeal discs Co2-Co4 were removed by slicing through the intervertebral disc and removing the central nucleus pulposus tissue, see figure 3.12. Nucleus pulposus tissue was separated from the rest of the disc, see figure 3.13, and cut into 1 mm^3 sections using a 1.5-inch scalpel blade. Cells were harvested using the following protocol, adapted from (Guilak et al., 1999) and (Horner and Urban, 2001).

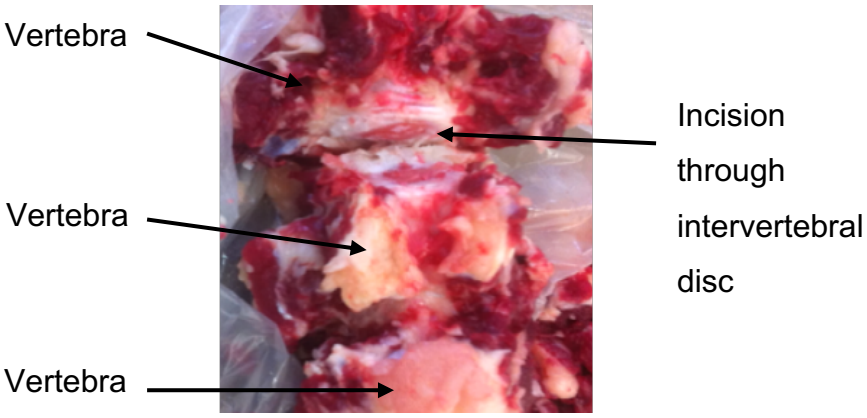

Figure 3.12 Dissection of 18-month-old bovine tail

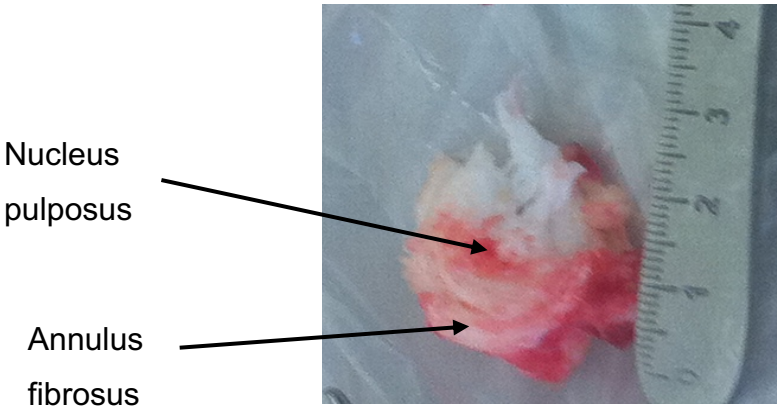

Figure 3.13 Intervertebral disc dissected from bovine tail, adjacent implement is in centimetres

Initially 5 ml of Dulbecco's Modified Eagle Medium (DMEM) with 1% Glutamate (Gl) and 1 % Penicillin Streptococcus (PS) was placed into a BD falcon flask and 2.5 % (0.125g) Pronase E added. The disc samples were added to the same falcon flask and placed on a Stuart Roller Mixer at 37 ^{o}C for 1 hour. A further 15 ml DMEM with Gl and PS (as above) was added with 0.125 % (0.025g) collagenase and the flask again placed on a shaker at 37^{o} C overnight. 100 µm BD filters were placed onto a falcon flask and the incubated container contents poured through the filter to remove the tissue debris. The filter was then removed, and the falcon flask lid replaced and placed in a centrifuge at 1300 rpm for 10 mins. The supernatant was then removed and 20 mls PBS was added to flasks and centrifuged again at 1300 rpm for 10 mins. The supernatant was removed again to leave a cell pellet at the bottom of the falcon flask to which 20 ml 'cell culture media' containing DMEM, 10% FBS, 1% Gl and 1%

PS was added. The cell suspension was then transferred into a 75 cm^2 Corning cell culture flask and placed in a Sanyo MCO-18AIC incubator at 37^o C and 2% O_2.

3.6.3 Incubation

A Sanyo MCO-18AIC hypoxic incubator at a set temperature of 37^o C and with 5 % humidity was used with the ability to change the oxygen content. The IVD does not have a direct blood supply and therefore the oxygen content in the disc is less than other areas in the body. Normoxic oxygen levels are 20 %, research has shown that the hypoxic oxygen levels likely to be experienced by the NP cells in vivo will be approximately 2 % (Stoyanov et al., 2010). Studies by (Feng et al., 2013) and (Wang et al., 2016) compared gene expression under normoxia versus hypoxia and demonstrated NP cells to respond with upregulation of anabolic metabolism in hypoxia and downregulation of anabolic metabolism in normoxia. Therefore, it was important that hypoxic conditions were used for the studies. Ibidi slides are well suited to hypoxic set-up as the slide material of 170 µm thickness allows gaseous exchange through the chamber (Ibidi, 2015).

3.6.4 Cryopreservation and thawing of cells

It was often necessary to freeze cells in between experimental testing as continuing growth would allow the passage number to reach a high value and a high passage number has been shown to effect gene expression (Darling and Athanasiou, 2005). To freeze cells, they were centrifuged at 1300 rpm, supernatant removed and then dimethyl sulphoxide (DMSO) was added which allows the cells to be preserved at 193 K (-80 ^{o}C) and lower in liquid nitrogen. Cells were then slowly cooled by placing in a Lec fridge at 4^o C for 30 mins and then a Lec freezer at -18^o C overnight prior to being placed in a CBS cryogenic freezer at 193 K (-80^o C). When cells were required again they were removed from the cryogenic freezer and quickly thawed using a VWR water bath at 37^o C for 3-5 mins or until the vial contents could be seen to be thawed. 10 ml DMEM were then added, and the cells centrifuged at 1300 rpm. The supernatant was removed to eradicate the remaining DMSO and the cells then suspended in more DMEM with FBS, transferred to a cell culture flask and placed in a Sanyo MCO-18AIC incubator at 37^o C and 2 % O_2 (Yokoyama, 2001) .

3.6.5 Cell loading into Ibidi VI$^{0.4}$ slide

Ibidi VI$^{0.4}$ slides have 6 flow channels on each slide and can be used in series, each experiment involved 4 technical replicates for the control, the steady flow and the pulsed flow for both the immunostaining and the morphology experiments. Therefore, four slides were set up in series; two for the morphological experiments and two slides for the immunostaining. Allowing 8 flow channels control; 4 for the morphological analysis and 4 for the immunostaining, 8 flow channels connected to the Harvard syringe pump for the steady flow; 4 for the morphology and 4 for the immunostaining, and 8 flow channels connected to the GE P1 peristaltic pump for the pulsed flow; 4 for the morphology and 4 for the immunostaining. The number of cells seeded on to the test slide was important, too many cells and a monolayer would not be present, however enough cells need to be present to provide genetic material for qRT-PCR analysis. A monolayer culture between 3-7 X10^5 cells/ml is recommended (Ibidi, 2015). Cells were seeded at 4x10^5 cells/ml so that any proliferation of cells as they adhered overnight would still result in a monolayer for testing. Following thawing, cells were incubated and allowed to proliferate for up to a week until a monolayer of 80% coverage was formed. Culture media was removed from the flask and the cells were washed twice with Phosphate Buffered Solution (PBS) which was then removed, and 1.5 ml of Trypsin added. The flask was placed in a Sanyo MCO-18AIC incubator at 37^o C for 2-3 mins and then removed from the incubator, 8.5 mls DMEM containing 10 % FBS, 1 % Gl and 1 % PS was then added. The cell suspension was centrifuged at 1300 rpm and the supernatant containing media and DMSO removed. The pellet was then re-suspended in 1 ml cell culture medium and mixed with a pipette to allow an even distribution of cells.

To establish the cell number, 100 μl of cell suspension was removed and mixed with 100 μl Trypan Blue and placed on an Abcam haemocytometer. The haemocytometer was placed under x10 Leica Brightfield microscope, trypan blue enters cell wall of any dead cells which would then show as blue, live and dead cells were counted using a manual counter and the Abcam haemocytometer. Using the gridlines on the haemocytometer, as shown in figure 3.14, live cells were counted which were within the top left hand 16 squares (shown in blue square), any cells touching the left-hand side and bottom lines of the square were included in the count. Those on the right-

hand side and top left were not included in the count. The number of cells was written down and then the count moved to the 16 squares on the top right, and the count repeated, and then the bottom left and bottom right. The average was taken of the 4 counts and then this number was multiplied by 10000. This accounts for the depth of the cell of suspension in the haemocytometer. The value was then multiplied by 2 to take into account the dilution factor from the addition of the trypan blue, the resulting value has a unit of cells/ml.

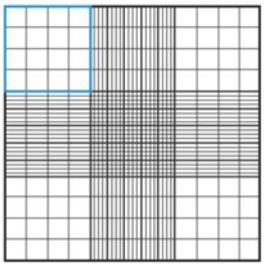

Figure 3.14 Gridlines on an Abcam Haemocytometer used for cell counting.

Once the original cell number in the 1 ml of cell suspension had been determined the cell suspension was then diluted to create a cell suspension of 4 x 10^5 cells/ml for Ibidi VI$^{0.4}$ slide loading.

An unused Ibidi Leur VI$^{0.4}$ slide was placed in the Sanyo MCO-18AIC hypoxic incubator at 37^o C and 5 % humidity and 2 % O_2 for 30 minutes to acclimatise prior to the experiment which helped to prevent air bubbles. The Ibidi slide was then removed to the sterile laminar flow hood and 30 µl volume of a 4 x10^5 cells/ml cell suspension was added to each Ibidi VI$^{0.4}$ channel, the Ibidi slide was then placed back into the hypoxic incubator. After four hours, the cells were checked under a microscope to confirm they had adhered. If the cells had not adhered, it was decided there was a problem with the cells viability and the test did not commence, another vial of cells was removed from the freezer, thawed and section 3.6.5 was repeated. If the cells had adhered they would change from a circular shape to an elongated shape. At this point, the Ibidi slide was placed in the sterile laminar flow hood again and 60 µl of cell culture media was added to each channel which pooled in the channel reservoirs, the Ibidi slide was then returned to the hypoxic incubator and left overnight. The following morning the cells were observed under a Leica Brightfield microscope again prior to testing to ensure they were still adhered. If they were still

adhered, the flow study equipment was set up as in figure 3.9 in the hypoxic incubator and the flow study commenced. For each flow experiment 4 control channels, 4 steady flow channels and 4 pulsed flow channels were set up, the steady and pulsed pumps were operated simultaneously for an experiment.

3.7 Cell Morphology Analysis

3.7.1 Materials and methods

Reagent	Role	Source	Manufacturer
PBS	Wash the cells	N/A	Sigma-Aldrich
4% Paraformaldehyde	Set the cells	N/A	Sigma-Aldrich
PBS and Tween 20:20	Permeabilize the cell wall	N/A	ThermoFisher
Goat Serum	Blocking agent	Goat	ThermoFisher
Anti-Vinculin	Stain vinculin in focal adhesions	Rabbit	MerckMillipore
FITC-conjugated	Conjugates to antibody	Horseradish	MerckMillipore
TRITC-conjugated Phalloidin	Stain actin filaments	Death cap mushroom	MerckMillipore
DAPI	Stain nuclei	N/A	MerckMillipore
Mounting Media	Prolong staining	N/A	Ibidi

Table 3.6 Reagents used for immunofluorescent staining

Equipment	Make	Model	Serial No
Confocal Microscope	Nikon	AIR	331588319
ImageJ software	NIH	N/A	N/A

Table 3.7 Equipment used in immunofluorescent imaging

Following flow testing the cells were washed three times with PBS and 4 % paraformaldehyde was applied to the cells and left for 20 minutes. To allow immunofluorescent stain to pass through the cell wall PBS with Tween (a non-ionic surfactant) was applied to the cells for 5 mins (Oliver and Jamur, 2010). The surfactant allows the protein in the stain to pass through the cell wall. The cells were then washed twice with PBS. A blocking solution was then added to the cells for 30 mins, goat serum was used as the blocking solution to prevent non-specific or background staining. The primary antibody, Anti-Vinculin, which stains the focal

adhesions, was diluted to 1:300 in blocking solution and added to the cells for 1 hour at room temperature (Millipore, 2009). The cells were then washed again three times in PBS. The secondary antibody, FITC-conjugated, and TRITC-conjugated Phalloidin, which stains the cytoskeleton, were diluted at 1:300 and 1:500 respectively in PBS and incubated on the cells for 60 mins at room temperature. The cells were then washed again three times in PBS (Millipore, 2009). The final stain, DAPI, which stains the nucleus of the cells, was diluted at 1:500 in PBS and incubated with the cells on the laboratory bench for 5 mins at room temperature. The cells were washed three times again with PBS following this and 90 µl of Ibidi Mounting Media was added to each flow channel and their corresponding reservoirs. The Ibidi slides were then wrapped in aluminium foil and stored in the fridge detailed in table 3.5 at 4^{o} C until microscope imaging.

A Nikon AIR confocal microscope at the Bio-Imaging Unit, William Leech Building, Newcastle University was used at 20x magnification for capturing cell images. The microscope images were then analysed using ImageJ software. Cell number was analysed using the DAPI nucleus staining as shown in figure 3.15 and 3.16.

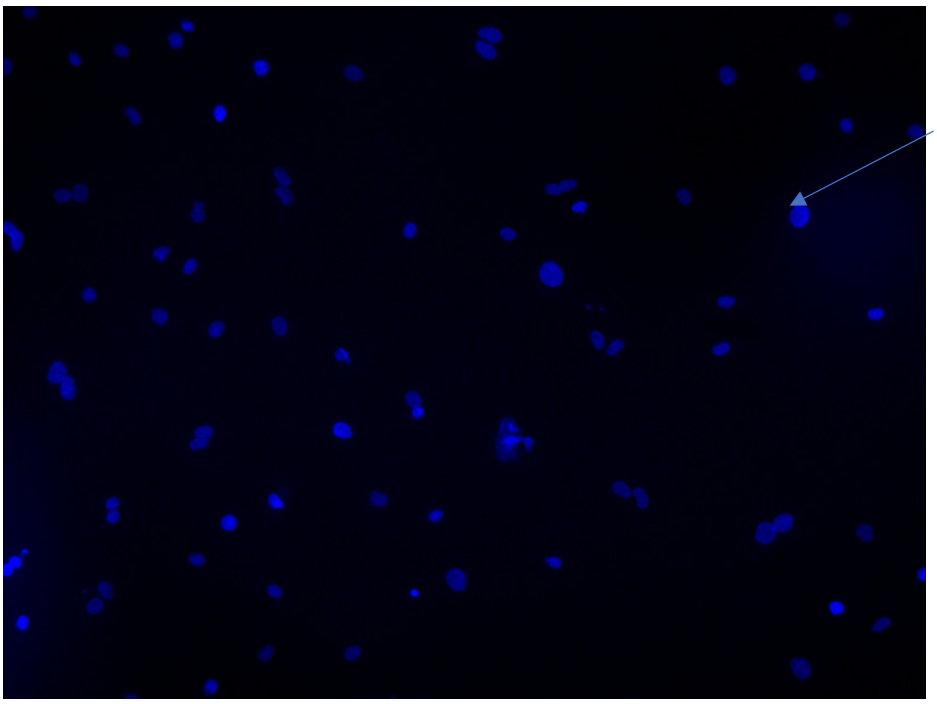

Figure 3.15 DAPI staining of cell nuclei

Cell numbers were counted using the following sequence of operations in ImageJ:

1. File → Open (To load image)
2. Options → conversions “scale when converting”
3. Image → adjust → threshold
4. Sliders were used to highlight the nuclei to be counted
5. Apply
6. Analyse → Analyse particles
7. Add to manager

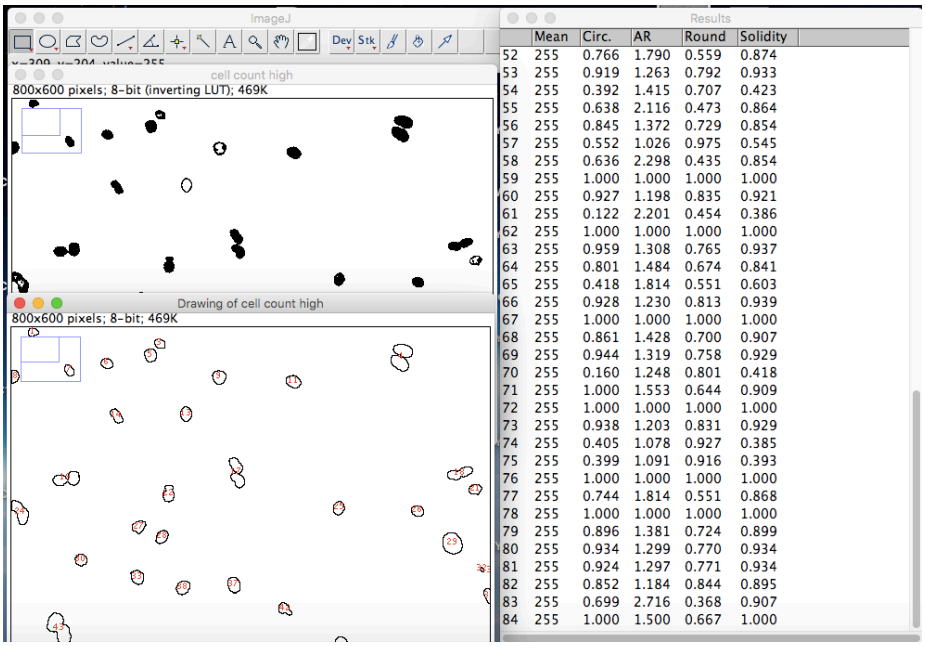

Figure 3.16 Screenshot of ImageJ for DAPI staining (cell number). Top left shows the original microscope image converted to greyscale, bottom left shows ‘analyse particles’ image and the right-hand side shows ‘add to manager’ option.

The focal adhesion number was determined using ImageJ as shown in figure 3.17 and 3.18.

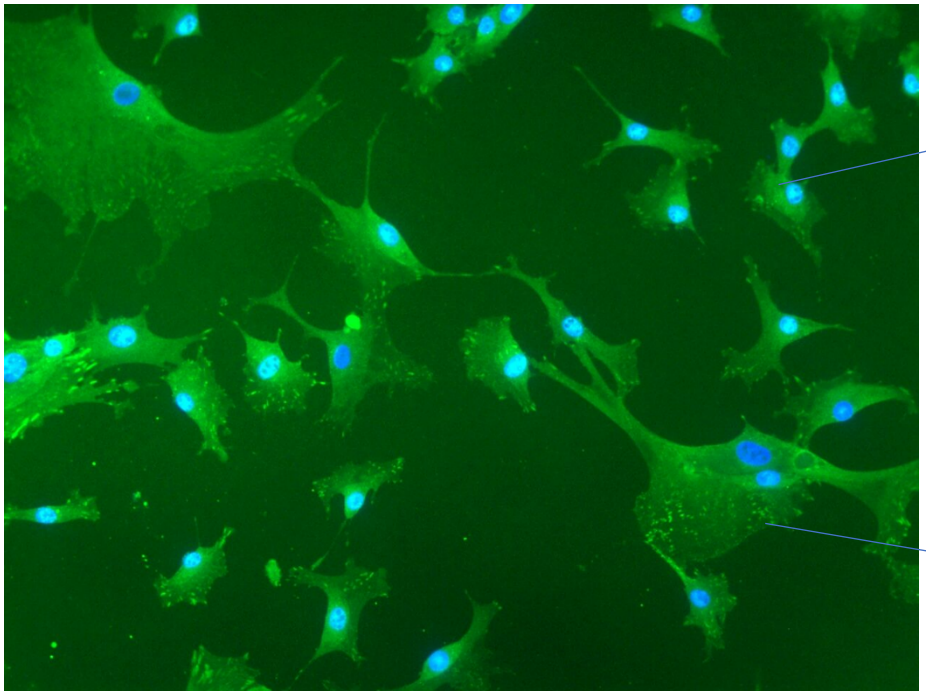

Figure 3.17 Vinculin staining to show cell focal adhesions

1. File → Open (To load image)
2. Options conversions “scale when converting”
3. Image → adjust → threshold
4. Sliders were used to highlight the focal adhesions to be counted
5. Apply
6. Analyse → Analyse particles
7. Add to manager

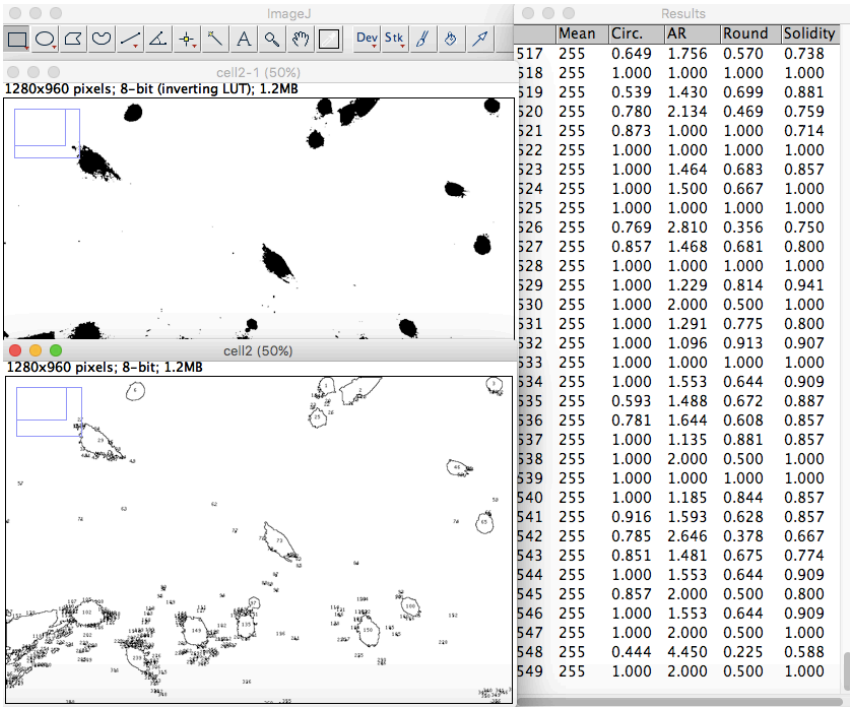

Figure 3.18 Screenshot of ImageJ for vinculin (Focal adhesion number). Top left shows original image converted to greyscale, bottom left shows 'analyse particles', right hand side shows 'add to manager' option.

Cell circularity is quantified between 0-1, where 1 is a circle and 0 is a straight line. Circularity was calculated using image J as shown in figure 3.11 and 3.12

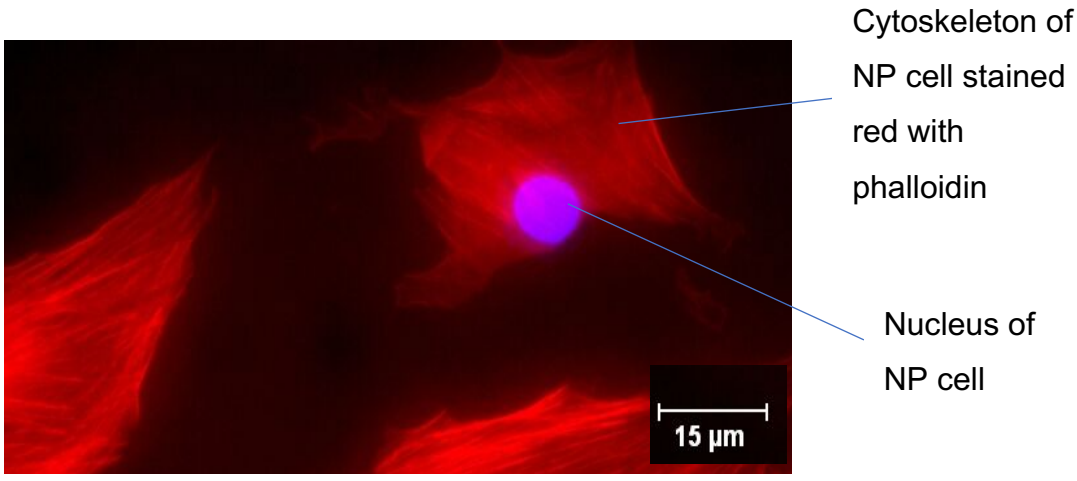

Figure 3.19 Phalloidin staining of cytoskeleton in red to show shape of cell for cell circularity measurement.

1. File → Open (To load image)

2. Options → conversions “scale when converting”
3. Image → adjust → threshold
4. Sliders were used to highlight the nuclei to be counted
5. Apply
6. Analyse → Circularity → Measure
7. Add to manager

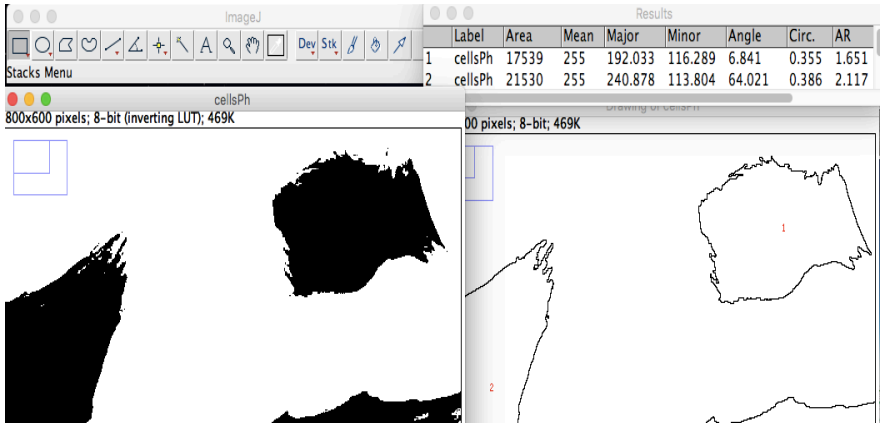

Figure 3.20 Screenshot of image J for phalloidin (cell circularity). Left hand side shows original image converted to greyscale, bottom right shows ‘analyse circularity’, top right shows ‘add to manager’ option.

3.8 Cell Gene Expression Analysis

3.8.1 Materials and methods

Equipment	Make	Model	Serial No
Refrigeration centrifuge	Labnet	Prism	K61112
Thermocycler	VWR	Uno	B3425
Heated water bath	VWR	1213	677455
Nanodrop	Thermofisher	1000	2777708
qRT-PCR	Applied Biosystems	HT9600	45537

Table 3.8 Equipment used in qRT-PCR analysis

Reagent	Role	Manufacturer
PBS	Wash the cells	Sigma-Aldrich
Trizol	Lyse the cells	Invitrogen
Chloroform	Separation of RNA	Sigma-Aldrich
Isopropanol	Aggregation of pellet	Sigma-Aldrich
Ethanol	Precipitation of nucleic acids	Sigma-Aldrich
Ultrapure water	Wash the pellet	Sigma-Aldrich

Table 3.9 Reagents used in RNA isolation

After testing under flow, RNA was extracted from the cell by undergoing acid guanidinium thiocyanate-phenol-chloroform extraction (Wang and Seed, 2003). The cells were washed three times with PBS and then lysed using the reagent Trizol which breaks down the proteins in the cell. Chloroform was then added which results in separating the RNA in the aqueous phase (on the top of the suspension) and protein partitions in the organic phase (at the lower part of the suspension). A volume of 1ml Trizol was added to each channel and lysed inside the channel using 1ml syringes at each reservoir port. The cells were lysed for 3-4 mins to ensure extensive removal and breakdown of the cell contents. Following this the lysed contents in Trizol were placed into a 1.5 ml Eppendorf and 0.2 ml chloroform was added. The contents were shaken for 15 seconds, then left for 5 mins prior to centrifuging at 13000 rpm for 15 mins at 4^{o} C. A temperature of 4^{o}C is used to promote flocculation of the RNA to form a pellet. 13000 rpm has been demonstrated to be adequate to separate the aqueous phase from the organic phase. The clear liquid was aspirated from the top and transferred to a clean 1.5 ml Eppendorf where 0.5 ml of isopropanol was added and then left for 15 minutes before centrifuging again at 13000 rpm and 4^{o} C. RNA is insoluble in isopropanol so aggregated to leave a pellet. The liquid was removed following centrifugation and 1 ml 70% ethanol was added to the pellet. The Eppendorfs were then centrifuged again at 13000 rpm for 15 mins at 4^{o} C to remove any salt remaining around the pellet. The pellet was then left to air dry. At this point 15 µl of ultrapure water was added and then heated to 65 ^{o}C for 10 mins to dissolve the pellet, immediately after the eppendorfs were chilled on ice for 5 mins to condense the contents.

The solution was then centrifuged for a final time for 13000 rpm at 4° C for 15 mins to ensure all the liquid was at the bottom of the Eppendorf and this RNA was then tested for nucleic acid concentration using a Thermofisher Nanodrop. A Nanodrop is a spectrophotometer, it analyses nucleic acids concentration by absorbing UV light at a maximum of 260 nm. The nucleic acid absorbs up to 260 nm of light and the rest passes through, allowing quantification of the nucleic acid present. A drop of 1.5 µl of RNA sample was pipetted on to the spectrophotometer through which UV light was shone. Once the presence of RNA in the sample had been verified then the single stranded RNA was turned into the double stranded cDNA for PCR for analysis. 8 µl of RNA was transferred to a 0.6 ml Eppendorf and mixed with the components shown in table 3.9.

Mix	Component	Manufacturer	Volume
1	Deoxynucleotides (dNTP)	Sigma Aldrich	3µl
	Random hexamers	Sigma Aldrich	1µl
2	5x First strand buffer	Thermofisher	4µl
	Dithiothreitol (DTT)	Thermofisher	2µl
	Moloney Murine Leukemia Virus (MMLV)	Invitrogen	0.5µl
	PCR grade water	Roche	1.5µl

Table 3.10 Regent mixtures used in cDNA synthesis

4 µl of Mix 1 was added to each Eppendorf, pulse centrifuged, heated to in a VWR water bath at 70° C for 5 mins, then chilled on ice for 2 mins. Following this 8 µl of mix 2 was added to the Eppendorf and then incubated in a VWR Thermocycler at 37° C for 50 mins and then 70° C for 15mins. The cDNA was then diluted by adding 30 µl of PCR grade water to each lysate and then prepared for RT-PCR by combining with bovine primers and components shown in table 3.10.

SYBR green Advantage Premix was added to a 96 well PCR plate followed by Mix 1 for each primer (King, 2002). The plate was pulse centrifuged to ensure all liquid was

at the bottom of the well and the plate was then placed in the Applied Biosystems HT9600 qPCR-RT machine for analysis.

Mix	Component	Manufacturer	Volume
1	Forward primer	Sigma Aldrich	0.4μl
	Reverse primer	Sigma Aldrich	0.4μl
	dH2O	-	7.2μl
	cDNA	-	2.0μl
2	SYBR Advantage qPCR Premix	Invitrogen	10.0μl

Table 3.11 Reagent mixtures used in PCR amplification

There were six bovine genes tested in this research, the genes and their primer sequences are shown in table 3.6. Gene primers are short strands of RNA which are the starting point for DNA synthesis. RNA is synthesized from the cells and then Biosystems HT9600 qRT-PCR works was used to quantify the DNA. qRT-PCR works by creating cycles of temperature change to break down the DNA from the cells into RNA then adding RNA primers which would join to any RNA which has been produced from the cell. qRT-PCR then multiplies these DNA strands using, temperature cycles, to amplify them to a point where they can be quantified by the qRT-PCR equipment.

Gene	Sequence
GAPDH	5'-ACCCAGAAGACTGTGGATGG-3' (Forward) 5'-CAACAGACACGTTGGGAGTG-3' (Reverse)
Aggrecan	5'-ACAGCGCCTACCAAGACAAG-3' (Forward) 5'-ACGATGCCTTTTACCACGAC-3' (Reverse)
Collagen I	5'-TGAGAGAGGGGTTGTTGGAC-3' (Forward) 5'-AGGTTCACCCTTCACACCTG-3' (Reverse)
Collagen II	5'-CCTGTAGGACCTTTGGGTCA-3' (Forward) 5'-ATAGCGCCGTTGTGTAGGAC-3' (Reverse)
Aggrecanase I	5'-GAAGCAATGCACTGGTCTGA-3' (Forward) 5'-CTAGGAGACAGTGCCCGAAG-3' (Reverse)
Aggrecanase II	5'-CTCCCATGACGATTCCAAGT-3' (Forward) 5'-TACCGAGACCATCATCCAGA-3' (Reverse)

Table 3.12 Primer sequences for bovine genes used in qRT-PCR

Glyceraldehyde 3-phosphate dehydrogenase (GAPDH) is known as a 'house-keeping', it is expressed in normal and pathophysiological conditions so is used as a baseline for gene expression against which the expression of other genes is analysed. Aggrecan, Collagen 1 and Collagen II are indicators of anabolic metabolism. Aggrecanase 1 and aggrecanase II are indicators of catabolism as discussed in chapter 2 (section 2.4.5). Aggrecan is essential for the healthy functioning of the nucleus pulposus (NP) matrix. Healthy NP cells synthesis aggrecan and their synthesis has been shown to be downregulated under catabolic metabolism (Ishihara et al., 1996, Handa et al., 1997). Therefore, the analysis of aggrecan gene expression is important in analysing the effect of shear stress on NP cells. Collagen I is the main collagen type present in the annulus fibrous of the disc, but is also present in the nucleus pulposus, Collagen I fibres are oriented obliquely and facilitates the extra-cellular matrix's (ECM's) organized structure. Collagen II is the main collagen present in the nucleus pulposus and other gel like structures. Aggrecanase 1 and II have been shown to have the highest aggrecan cleavage in vitro (Roberts et al., 2000, Tortorella et al., 2002, Carlos Rodríguez-Manzaneque et al., 2002), so have been chosen as a marker for degradation. As aggrecan reduction is an early marker in nucleus pulposus degradation, aggrecanases, rather than collagenases have been the focus of gene expression of catabolism (Pockert et al., 2009). Temperature cycles for amplification of cDNA were recommended by Sigma-Aldrich and shown in table 3.11.

Stage	Temp (°C)	Time (secs)	Cycles
1	94	120	
2	94 60	15 60	40
Dissociation Curve	95 60 95	15 15 15	

Table 3.13 Temperature cycles for DNA amplification

qRT-PCR analysis generates threshold cycle (Ct) values, from which the GADPH Ct value is subtracted to give a dCt value. Subtracting the control Ct value from the treatment group (steady or unsteady flow) leads to a ddCt value. PCR is an exponential amplification and the amount of target gene is 2^{-ddCt} , the derivation of

this is detailed by (Livak and Schmittgen, 2001), 2^{-ddCt} values have been plotted on a logarithmic scale where the x-axis crosses at 1, which is the 2^{-ddCt} value for the control samples.

3.9 Statistical Analysis

In total there were three independent variables; flow type (steady and pulsed), shear stress rate (0.1 dyne/cm^2, 0.4 dyne/cm^{2}and 4 dyne/cm^2 and time interval (1-hr, 4-hr, 8-hr and 24-hr) in the study and 8 dependent variables (cell number, cell circularity, focal adhesions, aggrecan, collagen I, collagen II, aggrecanase I and aggrecanase II. Each flow study had a control consisting of cells seeded onto Ibidi Slides with no flow.

As discussed in section 3.5.4, there were 4 technical replicates for each experiment, means were taken from these technical replicates, as shown in figure 3.21. There were 4 biological replicates for each experiment, again means were taken to arrive at one value which is displayed on graphs in the results chapter, but all values for biological replicates were included in the statistical analysis of the results to allow for biological variations between specimens. A significance threshold was set at 0.05 and error bars on the graphs plots in the Results Chapter 4 were calculated for confidence intervals of 95%.

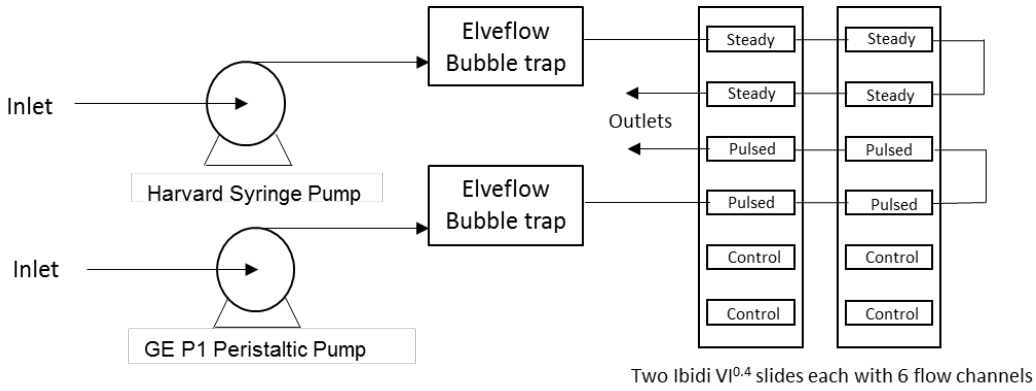

Figure 3.21 Schematic showing experimental set-up for each condition tested. Two Ibidi VI$^{0.4}$ slides in situ, each with 6 flow channels and both pumps. Leading to 4 control slides, 4 steady flow slides and 4 pulsed flow slides; Experiment carried out for immunostaining (for morphological analysis) and for qRT-PCR (for gene expression analysis) for each of the 12 flow conditions and for each biological replicate.

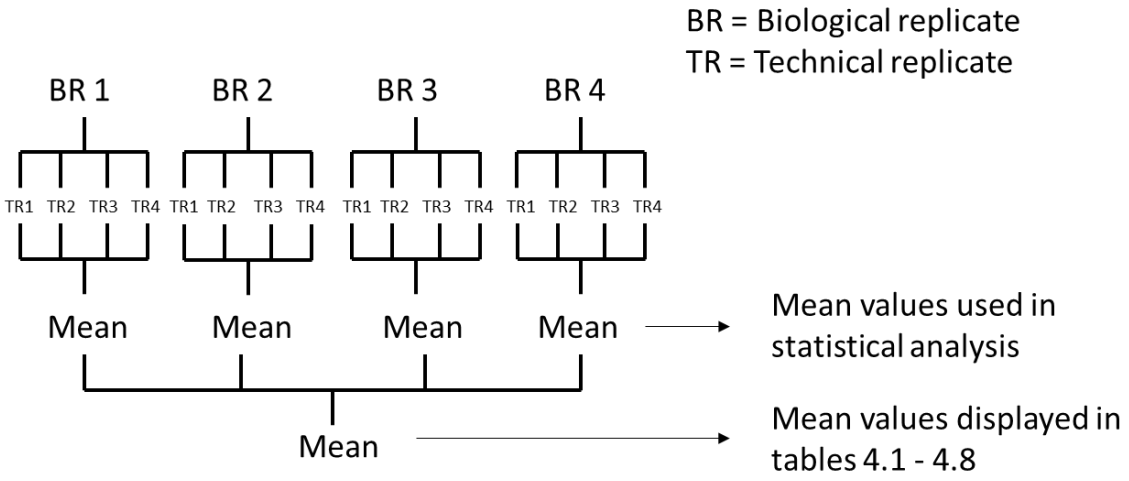

Figure 3.22 4 biological specimens (bovine coccygeal tails) were included in the research, cells from each tail went through the same test conditions. For each test condition there were 4 technical replicates carried out. The mean from these 4 technical replicate values were taken which left 4 values for each test condition, these values were used in statistical analysis. The means were taken of the values for the biological replicates which are shown in tables 4.1-4.8 in the results chapter.

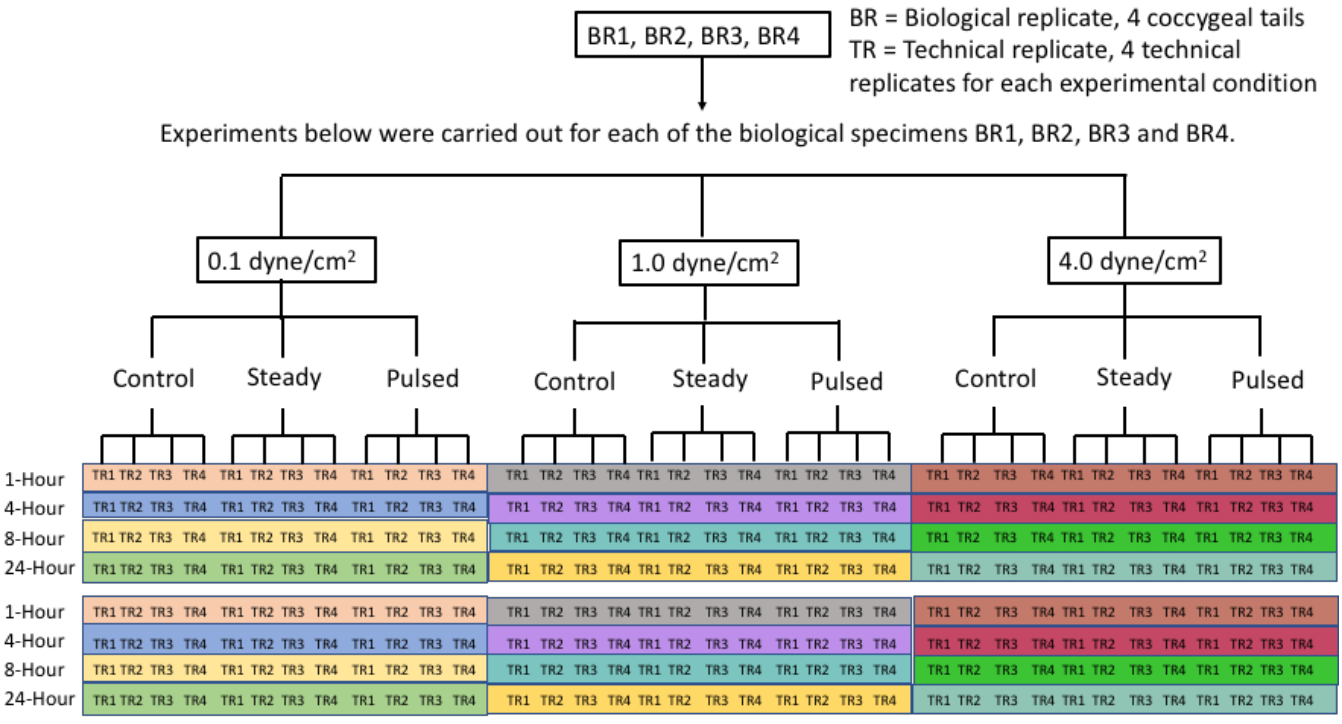

Figure 3.23 Colour coded figure 3.11 from section 3.5.4, showing flow studies 1-12, this is detailed further in the following table

Table 3.14 The 12 flow studies and 8 variables measured for each test condition. Controls was carried out for each of the flow studies and immunofluorescent and qRT-PCR performed simultaneously for each study.

Flow study	Flow Type	Shear Stress (dyne/cm^2)	Time Interval (Hours)	Dependent Variables Measured
1	Control	-	1	**Morphology:** 1. Cell Number 2. Focal Adhesions 3. Cell Circularity **Gene Expression:** 1. Collagen I 2. Collagen II 3. Aggrecanase I 4. Aggrecanase II 5. Aggrecan
	Steady	0.1	1	
	Pulsed	0.1	1	
2	Control	-	1	
	Steady	1	1	
	Pulsed	1	1	
3	Control	-	1	
	Steady	4	1	
	Pulsed	4	1	
4	Control	-	4	
	Steady	0.1	4	
	Pulsed	0.1	4	
5	Control	-	4	
	Steady	1	4	
	Pulsed	1	4	
6	Control	-	4	
	Steady	4	4	
	Pulsed	4	4	
7	Control	-	8	
	Steady	0.1	8	
	Pulsed	0.1	8	
8	Control	-	8	
	Steady	1	8	
	Pulsed	1	8	
9	Control	-	8	
	Steady	4	8	
	Pulsed	4	8	
10	Control	-	24	
	Steady	0.1	24	
	Pulsed	0.1	24	
11	Control	-	24	
	Steady	1	24	
	Pulsed	1	24	
12	Control	-	24	
	Steady	4	24	
	Pulsed	4	24	

The research questions to be answered were; firstly, does the shear stress rate affect any of the 8 dependent variables considered and if so, do these effects change over the time points covered? Secondly, does the flow type affect any of the 8 variables considered and if so, do these effects change over the time points covered?

Research question	Method of analysis	Flow Study	Post-hoc testing
1. Does flow type effect morphology or gene expression in bovine NP cells? (Objectives 2 & 5)	One-way ANOVA	1-12	If significance shown, post-hoc Tukey
2. Does the shear stress rate affect morphology or gene expression in bovine NP cells? (Objectives 4 & 6)	One-way ANOVA	1-12	If significance shown, post-hoc Tukey
3. Does the duration of time cells are exposed to the shear stress affect morphology or gene expression in bovine NP cells? (Objectives 5 & 7)	One-way ANOVA	1-12	If significant shown, post-hoc Tukey

Table 3.15 Research question and method of results analysis

Question 1 was answered using a one-way ANOVA, which allowed the investigation of differences between all 3 groups. Firstly, was there a difference between the steady flow group and control group (no flow), secondly, was there a difference between the pulsed flow group and control group (no flow) and finally was there a difference between the steady flow group and the pulsed flow group? Questions 2 and 3 were answered through a one-way ANOVA which allowed the analysis of the independent variables flow type, shear stress rate and time interval to be analysed simultaneously.

The statistical package SPSS was used to analyse the results. If a significant result was found through the ANOVA a post-hoc test was carried out to see which groups the significant differences were likely to be between. Tukey was used for post-hoc tests following the one-way ANOVAs due to its greater power than other post-hoc tests under most circumstances when all possible pairwise comparisons are being made (Holm and Christman, 1985, Dytham, 2003).

Chapter 4. Results

4.1 Data Analysis and Assumptions

To answer the research questions three independent variables; flow type, shear stress rate and duration, were investigated. As discussed in Methodology, the experimental set-up was such that for each experimental run there were 12 slides in total, 4 slides as the control with no flow on them, 4 slides with flow from the Harvard pump for steady flow and 4 slides for the Peristaltic pump for pulsed flow. The 4 slides for each group were technical replicates and the run would be repeated like this for each of the shear stress rate and duration conditions and repeated for morphology and gene expression analysis for each of the 4 biological cell specimens. This set up allowed the direct comparison of the flow types with the control for each experimental run, they are the between-subjects group in the analysis. The flow type was an independent variable with 3 categorical factors as mentioned; no flow (this was the control), steady flow and pulsed flow. The experimental set up was then repeated for each of the shear stress conditions and at each of the time intervals. The shear stress was therefore an independent variable with 3 categorical factors; 0.1, 1 and 4 dyne/cm^2. The duration was also an independent variable with 4 categorical factors; 1, 4, 8 and 24 hours. However, as cells in 1 dyne/cm^2 and 4 dyne/cm^2 at 24 hours were detached from the slides analyses for focal adhesion, cell circularity or gene expression was not possible, so the 24-hour data set was not included in the analysis. The 8 dependent variables are continuous and consist of cell number, focal adhesion number and cell circularity (to assess the morphology) and collagen 1, collagen 2, aggrecan, aggrecanase 1 and aggrecanase 2 (to assess gene expression). The statistical results were generated using SPSS and Microsoft Excel was used to generate the graphs shown. Levene's test showed homogenous variances for all groups.

4.1.1 Morphology

Sections 4.2-4.4 detail the results for the dependent variables used to assess morphology of the NP cells; cell number, focal adhesion number and cell circularity. There are 3 analyses detailed for each section, a one-way ANOVA for flow type analysis with post-hoc Tukey, a one-way ANOVA for shear stress rate analysis with

post-hoc Tukey and a one-way ANOVA for duration of flow analysis with post-hoc Tukey.

4.1.2 Gene expression

Sections 4.5-4.9 detail the results for the dependent variables used to assess gene expression of the NP cells; collagen 1, collagen 2, aggrecan, aggrecanase 1, aggrecanase 2. As for morphology there are 3 analyses detailed for each section, a one-way ANOVA for flow type analysis with post-hoc Tukey, a one-way ANOVA for shear stress rate analysis with post-hoc Tukey and a one-way ANOVA for duration of flow analysis with post-hoc Tukey. Statistical analysis for gene expression was carried out on dCt values, as they have normalized distribution, however graphical representation is 2^{-ddCt}, which is dCt values normalized to control dCt values. The graphs are shown on a logarithmic scale as this gives a more realistic visual representation of the amount that a gene is upregulated or downregulated compared to the control condition. Confidence intervals are shown, however due to the logarithmic scale, the presence of overlapping does not necessarily mean no statistical significance between the groups. The control value is depicted at y-axis=1, due to the values of dCt (control)-dCt (control) = 0 and $2^{-0} = 1$. Log base 2 is used as the Ct values are generated from qRT-PCR which involves the quantification of gene expression, which occurs as an exponential process. Every cycle of PCR doubles the amount of gene product, therefore generating the results in a graphical representation as log base 2 allows the visual representation of gene expression to be more meaningful. Any significant differences between the steady or pulsed flow compared to the control are shown above or below the confidence interval bar and differences between the steady and pulsed flow are depicted by a line between the two with the corresponding *p* value written above.

4.2 Cell Number

4.2.1 Descriptive statistics

Shear Stress (dyne/cm^2)	Time (hours)	Control		Steady		Pulsed	
		Mean	*Standard Deviation*	*Mean*	*Standard Deviation*	*Mean*	*Standard Deviation*
0.1	**1**	558	*6.83*	547	*13.18*	564	*14.41*
	4	576	*16.05*	598	*9.42*	593	*3.16*
	8	620	*9.03*	605	*19.52*	604	*9.78*
	24	726	*16.03*	722	*8.10*	723	*19.60*
1.0	**1**	564	*2.71*	560	*19.47*	566	*19.33*
	4	590	*4.11*	492	*23.20*	505	*15.73*
	8	626	*25.94*	406	*16.19*	404	*8.66*
	24	718	*5.51*	0	-	0	-
4.0	**1**	566	*12.96*	575	*14.11*	542	*8.68*
	4	588	*6.19*	336	*18.04*	337	*1.29*
	8	618	*16.97*	234	*14.82*	214	*8.77*
	24	717	*7.75*	0	-	0	-

Table 4.1 Mean and standard deviation values for cell number for all 3 independent variables; flow type (control, steady and pulsed), shear stress (01, 1.0 and 4.0 dyne/cm^2) and time points (1, 4, 8 and 24 hours).

4.2.2 Effect of flow type on cell number

One-way ANOVAs were used to analyse the effect of flow types; no flow, steady flow and pulsed flow, on cell number. Results and statistically significant findings are shown in figure 4.1.

There was no statistically significant effect of flow type on cell number at the $p < 0.05$ level at 0.1 dyne/cm^2 after 1-hour flow, [F (2, 9) = 1.967, p = 0.196]. There was a statistically significant effect of flow type on cell number at the p < 0.05 level at 0.1 dyne/cm^2 after 4-hour flow, [F (2, 9) = 4.590, p = 0.042]. Post-hoc comparisons using Tukey HSD indicated that the mean score for the steady flow conditions was significantly higher than the control (p = 0.043), but not significantly different from the pulsed flow (p = 0.798). The pulsed flow did not differ significantly from the control (p

= 0.118). There was no statistically significant effect of flow type on cell number at the $p < 0.05$ level at 0.1 dyne/cm^2 after 8-hour flow, [F (2, 9) = 1.727, $p = 0.232$]. There was no statistically significant effect of flow type on cell number at the $p < 0.05$ level at 0.1 dyne/cm^2 after 24-hour flow, [F (2, 9) = 0.074, $p = 0.930$].

There was no statistically significant effect of flow type on cell number at the $p < 0.05$ level at 1.0 dyne/cm^2 after 1-hour flow, [F (2, 9) = 0.140, $p = 0.871$]. There was a statistically significant effect of flow type on cell number at the $p < 0.05$ level at 1 dyne/cm^2 after 4-hour flow, [F (2, 9) = 41.895, $p < 0.001$]. Post-hoc comparisons using Tukey HSD indicated that the mean score for the steady flow conditions was significantly lower than the control ($p < 0.001$), but not significantly different from the pulsed flow ($p = 0.524$), but the cell number following pulsed flow was significantly lower than the control ($p < 0.001$). There was a statistically significant effect of flow type on cell number at the $p < 0.05$ level at 1 dyne/cm^2 after 8-hour flow, [F (2, 9) = 193.001, $p < 0.001$]. Post-hoc comparisons using Tukey HSD indicated that the mean score for the steady flow conditions was significantly lower than the control ($p < 0.001$), and the pulsed flow was also significantly lower than the control ($p < 0.001$), but the steady flow was not significantly different from the pulsed flow ($p = 0.980$).

There was a statistically significant effect of flow type on cell number at the $p < 0.05$ level at 4.0 dyne/cm^2 after 1-hour flow, [F (2, 9) = 7.707, $p = 0.011$]. Post-hoc comparisons using Tukey HSD indicated that the mean score for the steady flow conditions was significantly higher than the control ($p < 0.001$) and significantly higher than the pulsed flow ($p = 0.011$). The pulsed flow did not differ significantly from the control ($p = 0.05$). There was a statistically significant effect of flow type on cell number at the $p < 0.05$ level at 4.0 dyne/cm^2 after 4-hour flow, [F (2, 9) = 691.167, $p < 0.001$]. Post-hoc comparisons using Tukey HSD indicated that the mean score for the steady flow conditions was significantly lower than the control ($p < 0.001$), but not significantly different from the pulsed flow ($p = 0.998$), the cell number for pulsed flow was also significantly lower than the control ($p < 0.001$). There was a statistically significant effect of flow type on cell number at the $p < 0.05$ level at 4.0 dyne/cm^2 after 8-hour flow, [F (2, 9) = 1064.775, $p < 0.001$]. Post-hoc comparisons using Tukey HSD indicated that the mean score for the steady flow conditions was significantly lower than the control ($p < 0.001$), but not significantly different from the

pulsed flow (p = 0.180). The pulsed flow was also significantly lower than the control (p < 0.001).

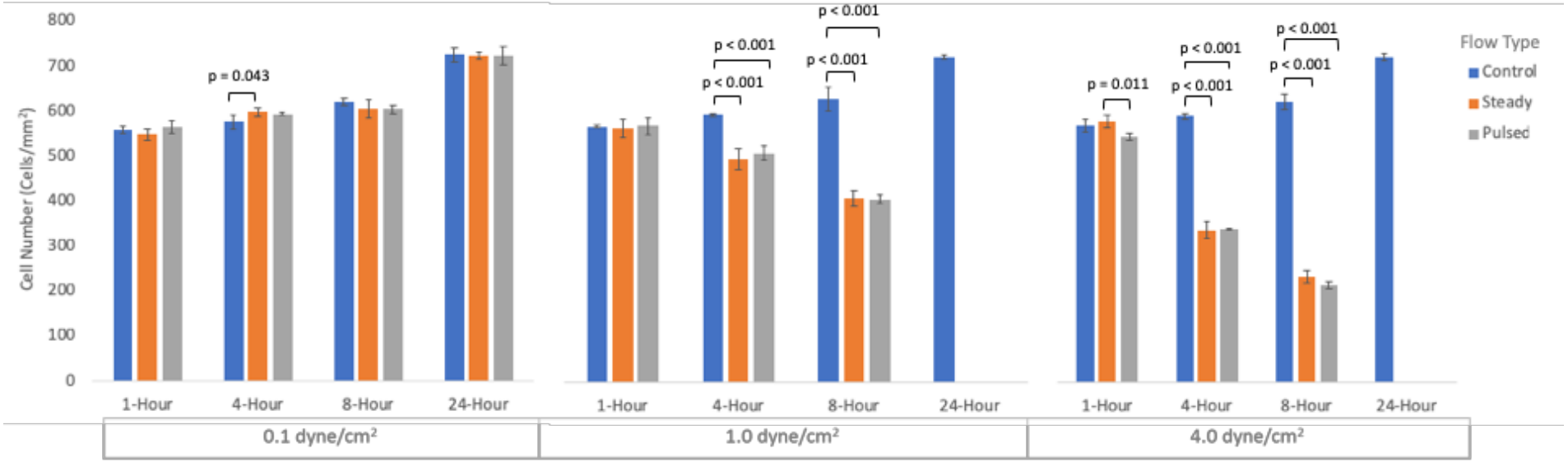

Figure 4.1 Bovine nucleus pulposus cell number as determined from DAPI immunostaining of nuclei following 12 test conditions: 1, 4, 8 and 24-hour flow experiments in Ibidi VI$^{0.4}$ flow chamber at shear stress conditions of 0.1, 1.0 and 4.0 dyne/cm^2. Results are shown for three flow types; control (no flow), steady flow and pulsed flow. Means and 95 % confidence interval error bars are shown based on 4 technical replicates and sample size (n) of 4 bovine subjects. Statistically significant results at level $p < 0.05$ are shown for one-way ANOVA with post-hoc Tukey HSD comparing control vs steady vs pulsed flow for each of the 12 test conditions. No results shown for 1.0 and 4.0 dyne/cm^2 after 24 hours as no cells present on Ibidi VI$^{0.4}$ slide following flow experiments, due to detachment of cells from slide.

4.2.3 Effect of shear stress on cell number

One-way ANOVAs were used to analyse the effect of shear stress rates; 0.1, 1.0 and 4.0 dyne/cm^2, on cell number. Results and statistically significant findings are shown in figure 4.2.

After 1 hour there was no statistically significant difference shown between the three shear stress rates in the control group; 0.1 dyne/cm^2, 1.0 dyne/cm^2 or 4.0 dyne/cm^2 at the $p < 0.05$ level [F (2, 9) = 0.937, p = 0.427]. After 1 hour in the steady flow group again there was no statistically significant difference between the three shear stress rates; 0.1 dyne/cm^2, 1.0 dyne/cm^2 and 4.0 dyne/cm^2 at the $p < 0.05$ level, [F (2, 9) = 2.971, p = 0.102]. After 1 hour in the pulsed group, again no statistically significant difference was shown between the three shear stress rates 0.1 dyne/cm^2, 1.0 dyne/cm^2 and 4.0 dyne/cm^2 at the $p < 0.05$ level [F (2, 9) = 3.133, p = 0.093].

After 4 hours there was no statistically significant difference shown between the shear stress rates for the control group; 0.1 dyne/cm^2, 1.0 dyne/cm^2 and 4.0 dyne/cm^2 at the $p < 0.05$ level, [F (2, 9) = 2.168, p = 0.170]. There was a statistically significant difference between the shear stress rate groups for the steady flow group [F (2, 9) = 218.936, $p < 0.001$]. Post-hoc Tukey HSD showed a significantly higher cell number after 0.1 dyne/cm^2 compared to 1.0 dyne/cm^2 ($p < 0.001$), a significantly higher cell number at 0.1 dyne/cm^2 compared to 4.0 dyne/cm^2 ($p < 0.001$), and a significantly higher cell number after 1 dyne/cm^2 compared to and 4.0 dyne/cm^2 ($p < 0.001$). For the pulsed flow group there was a statistically significance difference at the $p < 0.05$ level [F (2, 9) = 786.645, $p < 0.001$]. Post-hoc Tukey HSD showed a significantly higher cell number at 0.1 dyne/cm^2 compared to 1.0 dyne/cm^2 ($p < 0.001$), a significantly higher cell number at 0.1 dyne/cm^2 compared to 4.0 dyne/cm^2 ($p < 0.001$), and a significantly higher cell number after 1.0 dyne/cm^2 shear stress rate compared to 4.0 dyne/cm^2 ($p < 0.001$).

After 8 hours there was no statistically significant difference between the shear stress rates for the control group; 0.1 dyne/cm^2, 1.0 dyne/cm^2 and 4.0 dyne/cm^2 at the $p < 0.05$ level, [F (2, 9) = 0.177, p = 0.840]. There was a statistically significant difference between shear stress rates for the steady flow group, [F (2, 9) = 480.149, $p < 0.001$].

Post-hoc Tukey HSD showed significantly higher cell number after 0.1 dyne/cm^2 compared to 1.0 dyne/cm^2 ($p < 0.001$), significantly higher cell number after 0.1 dyne/cm^2 compared to 4.0 dyne/cm^2 ($p < 0.001$), and significantly higher cell number after 1.0 dyne/cm^2 compared to 4.0 dyne/cm^2 ($p < 0.001$). There was a statistically significance difference between shear stress rates for the pulsed flow group [F (2, 9) = 1839.401, $p < 0.001$]. Post-hoc Tukey HSD showed significantly higher cell number after 0.1 dyne/cm^2 compared to 1.0 dyne/cm^2 ($p < 0.001$), significantly higher cell number after 0.1 dyne/cm^2 compared to 4.0 dyne/cm^2 ($p < 0.001$), and significantly higher cell number after 1.0 dyne/cm^2 compared to 4.0 dyne/cm^2 ($p < 0.001$).

After 24 hours the control flow group only was analysed as all cells had detached from the Ibidi VI$^{0.4}$ slides for 1.0 dyne/cm^2 and 4.0 dyne/cm^2 for steady and pulsed flow groups. There was no statistically significant difference shown between the shear stress rates for the control group; 0.1 dyne/cm^2, 1.0 dyne/cm^2 and 4.0 dyne/cm^2 at the $p < 0.05$ level, [F (2, 9) = 0.834, $p = 0.465$].

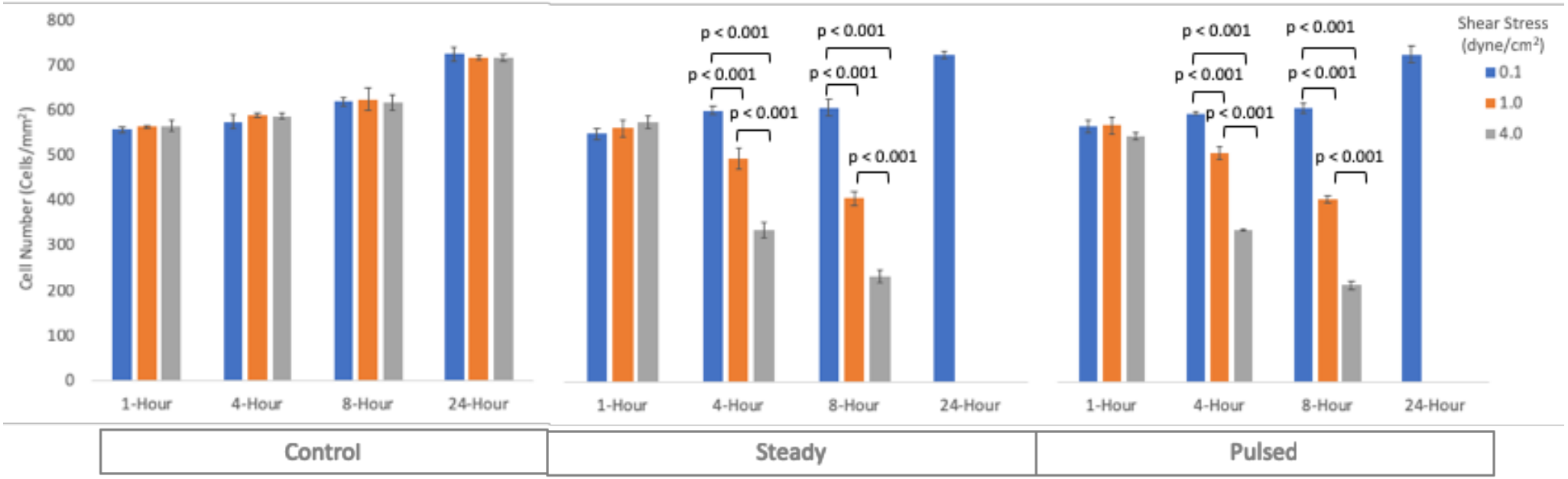

Figure 4.2 Bovine nucleus pulposus cell number as determined from DAPI immunostaining of nuclei following 12 test conditions: 1, 4, 8 and 24-hour flow experiments in Ibidi VI$^{0.4}$ flow chamber at shear stress conditions of 0.1, 1.0 and 4.0 dyne/cm^2. Results are shown for three flow groups; control (no flow), steady flow and pulsed flow. Means and 95 % confidence interval error bars are shown based on 4 technical replicates and sample size (n) of 4 bovine subjects. Statistically significant results at level $p < 0.05$ are shown for one-way ANOVA with post-hoc Tukey HSD comparing results of shear stress conditions of 0.1, 1.0 and 4.0 dyne/cm^2 for each of the time conditions and flow types. No results shown for 1.0 and 4.0 dyne/cm^2 after 24 hours as no cells present on Ibidi VI$^{0.4}$ slide following flow experiments, due to detachment of cells from slide.

4.2.4 Effect of duration of flow on cell number

One-way ANOVAs were used to analyse the effect of the duration of time cells were exposed to shear stress; 1, 4, 8 and 24 hours, on cell number. Results and statistically significant findings are shown in figure 4.3.

For the control group at 0.1 dyne/cm^2 there was a statistically significant result at the $p < 0.05$ level, [F (3, 12) = 140.936, $p < 0.001$]. Post-hoc Tukey HSD showed significantly lower cell number after 1 hour compared with 8 hours ($p < 0.001$), significantly lower cell number at 1 hour compared with 24 hours ($p < 0.001$), significantly lower cell number at 4 hours compared with 24 hours ($p = 0.012$), significantly lower cell number after 8 hours compared with 24 hours ($p = 0.008$) and significantly higher cell number at 8 hours compared to 4 hours ($p = 0.002$). No significant difference was seen between 1 hour and 4 hours ($p = 0.248$). For the steady group at 0.1 dyne/cm^2 a statistically significant difference was seen for cell numbers at different time intervals [F (3, 12) = 122.997, $p < 0.001$]. Post-hoc Tukey HSD showed significantly lower cell number after 1 hour flow compared with 4 hours flow ($p = 0.001$), significantly lower cell number after 4 hours flow compared with after 24 hours flow ($p < 0.001$), significantly lower cell number after 8 hours flow compared to after 24 hours flow ($p < 0.001$), significantly higher cell number at 8 hours compared to 1 hour ($p < 0.001$) and statistically significant higher cell number at 24 hours compared to 24 hours ($p < 0.001$). No significant difference was seen between 4 hour and 8 hours ($p = 0.888$). A statistically significant difference was seen between time intervals for the pulsed group at 0.1 dyne/cm^2, [F (3, 12) = 112.507, $p < 0.001$]. Post-hoc Tukey HSD showed a significantly higher cell number after 4 hours compared to 1 hour (p = 0.038), significantly higher cell number after 8 hour flow compared to after 1 hours flow ($p = 0.005$), significantly higher cell number after 24 hours flow compared to 1 hour ($p < 0.001$), significantly lower cell number after 4 hours compared to 24 hours ($p = <0.001$) and significantly lower cell number after 8 hours flow compared to after 24 hours flow ($p < 0.001$). No significant difference was seen between 4 hours and 8 hours ($p = 0.667$).

A statistically significant difference was seen between time intervals for the control group at 1.0 dyne/cm^2, [F (3, 12) = 99.085, $p < 0.001$]. Post-hoc Tukey HSD showed a significantly lower cell number after 1 hour compared to 8 hours ($p < 0.001$), significantly lower cell number after 1 hr compared to 24 hours ($p < 0.001$), significantly lower cell

number after 4 hours compared to 8 hours ($p = 0.013$), significantly lower cell number after 4 hours compared to 24 hours ($p < 0.001$) and significantly lower cell number after 8 hours compared to 24 hours ($p < 0.001$). No significant difference was seen between 1 hour and 4 hours ($p = 0.079$). For the steady group at 1.0 dyne/cm^2 a statistically significant difference was seen between time intervals [F (3, 12) = 854.955, $p < 0.001$]. Post-hoc Tukey HSD showed significantly higher cell numbers after 1 hour flow compared with 4 hour flow ($p = 0.001$), significantly higher cell numbers between 1 hour compared with 8 hour flow ($p < 0.001$), significantly higher cell number between 4 hours compared with 24 hours flow ($p < 0.001$), significantly higher cell numbers between after 4 hours flow compared with 8 hours flow ($p < 0.001$), significantly higher cell numbers after 1 hour compared to 24 hours (p < 0.001) and significantly higher cell numbers after 8 hours compared to 24 hours ($p < 0.001$). A statistically significant difference was seen between time intervals for the pulsed group at 1.0 dyne/cm^2 [F (3, 12) = 1490.092, $p < 0.001$]. Post-hoc Tukey HSD showed significantly higher cell numbers after 1 hour flow compared with 4 hour flow ($p < 0.001$), significantly higher cell numbers between 1 hour compared with 8 hour flow ($p < 0.001$), significantly higher cell number between 4 hours and 24 hours ($p < 0.001$), significantly higher cell numbers between after 4 hours flow compared with 8 hours flow ($p < 0.001$), significantly higher cell numbers after 1 hour compared to 24 hours (p < 0.001) and significantly higher cell numbers after 8 hours compared to 24 hours ($p < 0.001$).

A statistically significant difference was seen between time intervals for the control group at 4.0 dyne/cm^2 [F (3, 12) = 128.608, $p < 0.001$]. Post-hoc Tukey HSD showed significantly lower cell number after 1 hour compared to 24 hours ($p < 0.001$), significantly lower cell number after 1 hour compared to 8 hours ($p < 0.001$), significantly lower cell number after 4 hour compared to 8 hours ($p = 0.015$), significantly lower cell number after 4 hours compared to 24 hours ($p < 0.001$) and significantly lower cell number after 8 hours compared to 24 hours ($p < 0.001$). No significant difference was seen between 1 hour and 4 hours ($p = 0.096$). For the steady group at 4.0 dyne/cm^2 a statistically significant difference was seen between time intervals for the steady group [F (3, 12) = 1220.677, $p < 0.001$]. Post-hoc Tukey HSD showed significantly higher cell number after 1-hour flow compared with 8 hours flow ($p < 0.001$), significantly higher cell number after 4 hours compared with after 8 hours ($p < 0.001$), significantly higher cell number after 1 hour

compared with 4 hours ($p < 0.001$), significantly higher cell number after 1-hour flow compared with 8 hours flow ($p < 0.001$), significantly higher cell number after 4 hours compared with after 24 hours ($p < 0.001$) and significantly higher cell number after 1 hours compared with after 24 hours. Statistically significant differences were seen between time intervals for the pulsed group at 4.0 dyne/cm^2, [F (3, 12) = 5349.169, $p < 0.001$]. Post-hoc Tukey HSD showed statistically significant ($p < 0.001$) high cell number after 1-hour flow compared with 8 hours flow, statistically significant ($p < 0.001$) higher cell number after 4 hours compared with after 8 hours, statistically significant higher cell number ($p < 0.001$) after 1 hour compared with 4 hours, statistically significant ($p < 0.001$) high cell number after 1-hour flow compared with 8 hours flow, statistically significant ($p < 0.001$) higher cell number after 4 hours compared with after 24 hours and statistically significant ($p = 0.001$) higher cell number after 1 hours compared with after 24 hours ($p = 0.001$).

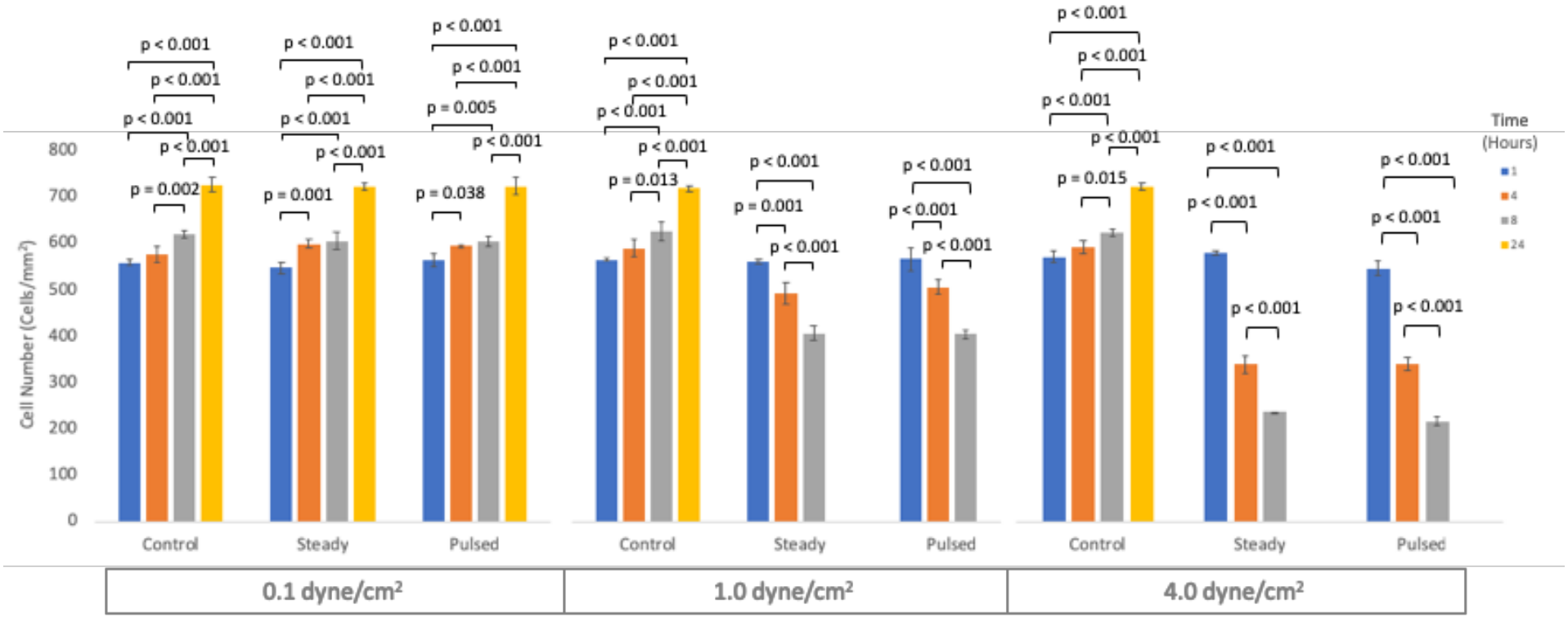

Figure 4.3 Bovine nucleus pulposus cell number as determined from DAPI immunostaining of nuclei following 12 test conditions: 1, 4, 8 and 24-hour flow experiments in Ibidi VI$^{0.4}$ flow chamber at shear stress conditions of 0.1, 1.0 and 4.0 dyne/cm^2. Results are shown for three flow groups; control (no flow), steady flow and pulsed flow. Means and 95 % confidence interval error bars are shown based on 4 technical replicates and sample size (n) of 4 bovine subjects. Statistically significant results at level $p < 0.05$ are shown for one-way ANOVA with post-hoc Tukey HSD comparing results after 1, 4, 8 and 24 hours, for each of the shear stress conditions and flow types. No results shown for 1.0 and 4.0 dyne/cm^2 after 24 hours as no cells present on Ibidi VI$^{0.4}$ slide following flow experiments, due to detachment of cells from slide.

4.3 Focal Adhesion Number

4.3.1 Descriptive statistics

Shear Stress (dyne/cm^2)	Time (hours)	Control		Steady		Pulsed	
		Mean	*Standard Deviation*	*Mean*	*Standard Deviation*	*Mean*	*Standard Deviation*
0.1	**1**	36	*6.95*	34	*12.69*	30	*2.63*
	4	45	*5.31*	47	*8.76*	45	*4.99*
	8	50	*1.83*	47	*8.76*	45	*4.99*
	24	53	*1.29*	48	*1.29*	50	*2.08*
1.0	**1**	32	*2.75*	31	*2.65*	30	*1.26*
	4	52	*4.03*	40	*2.99*	38	*2.08*
	8	55	*1.71*	34	*0.82*	32	*0.50*
	24	55	*0.58*	-	-	-	-
4.0	**1**	29	*2.36*	24	*1.83*	25	*0.50*
	4	49	*2.22*	24	*0.96*	27	*2.16*
	8	59	*5.94*	22	*1.91*	23	*1.71*
	24	52	*4.24*	-	-	-	-

Table 4.2 Mean and standard deviation values for focal adhesion number per cell for all 3 independent variables; flow type (control, steady and pulsed), shear stress (01, 1.0 and 4.0 dyne/cm^2) and time points (1, 4, 8 and 24 hours).

4.3.2 Effect of flow type on FA number

One-way ANOVAs were used to analyse the effect of flow types; no flow, steady flow and pulsed flow, on focal adhesion (FA) number. Results and statistically significant findings are shown in figure 4.4. No statistical analysis was carried out at 24 hours for the steady and pulsed groups at 1.0 and 4.0 dyne/cm^2 as noted previously due to the detachment of all cells from the slides.

There was no statistically significant effect of flow type on focal adhesion (FA) number at the $p < 0.05$ level at 0.1 dyne/cm^2 after 1-hour flow; control, steady, pulsed, [F (2, 9) = 0.541, p = 0.600]. There was no significant effect of flow type on focal adhesion number at the $p < 0.05$ level at 0.1 dyne/cm^2 after 4-hour flow, [F (2, 9) = 0.156, p = 0.858]. There was no significant effect of flow type on FA number at

the $p < 0.05$ level for the three flow conditions at 0.1 dyne/cm^2 after 8-hour flow, [F (2, 9) = 2.077, p = 0.181]. There was a statistically significant effect of flow type on FA number at the $p < 0.05$ level at 0.1 dyne/cm^2 after 24-hour flow, [F (2, 9) = 9.913, p = 0.005]. Post-hoc comparisons using Tukey HSD indicated that the mean score for the control was significantly higher than the mean score for the steady flow (p = 0.004), but not significantly different to the pulsed flow (p = 0.062) and there was no significant difference between the steady and pulsed flow mean values (p = 0.234).

There was no statistically significant effect of flow type on FA number at the $p < 0.05$ level for the three flow conditions at 1.0 dyne/cm^2 after 1-hour flow, [F (2, 9) = 0.881, p = 0.447]. There was a statistically significant effect of flow type on FA number at the $p < 0.05$ level for the three flow conditions at 1 dyne/cm^2 after 4-hour flow, [F (2, 9) = 25.686, $p < 0.001$]. Post-hoc comparisons using Tukey HSD indicated that the mean score for the steady flow condition was significantly lower than the control (p = 0.001), but not significantly different compared to the pulsed flow (p = 0.587), and the FA number following pulsed flow was significantly lower than the control ($p < 0.001$). There was a statistically significant effect of flow type on FA number at the $p < 0.05$ level for the three flow conditions at 1 dyne/cm^2 after 8 hours flow, [F (2, 9) = 503.283, $p < 0.001$]. Post-hoc comparisons using Tukey HSD indicated that the mean score for the steady flow conditions was significantly lower than the control ($p <$ 0.001), and the pulsed was significantly lower than the control ($p < 0.001$) and the pulsed was significantly lower than the steady flow (p = 0.048).

There was a statistically significant effect of flow type on FA number at the $p < 0.05$ level for the three flow conditions at 4.0 dyne/cm^2 after 1-hour flow, [F (2, 9) = 10.555, p = 0.004]. Post-hoc comparisons using Tukey HSD indicated that the mean score for the steady flow conditions was significantly lower than the control (p = 0.005), and the pulsed was significantly lower than the control (p = 0.013). The pulsed flow did not significantly differ from the pulsed (p = 0.820). There was a statistically significant effect of flow type on FA number at the $p < 0.05$ level for the three flow conditions at 4.0 dyne/cm^2 after 4-hour flow, [F (2, 9) = 211.167, $p <$ 0.001]. Post-hoc comparisons using Tukey HSD indicated that the mean score for the steady flow conditions was significantly lower than the control ($p < 0.001$), and the pulsed was significantly lower than the control ($p < 0.001$). The pulsed flow did

not significantly differ from the pulsed (p = 0.084). There was a statistically significant effect of flow type on FA number at the $p < 0.05$ level for the three flow conditions at 4.0 dyne/cm^2 after 8-hour flow, [F (2, 9) = 129.871, $p < 0.001$]. Post-hoc comparisons using Tukey HSD indicated that the mean for the steady flow conditions was significantly lower than the control ($p < 0.001$), and the pulsed was significantly lower than the control ($p < 0.001$). The pulsed flow did not significantly differ from the pulsed (p = 0.886).

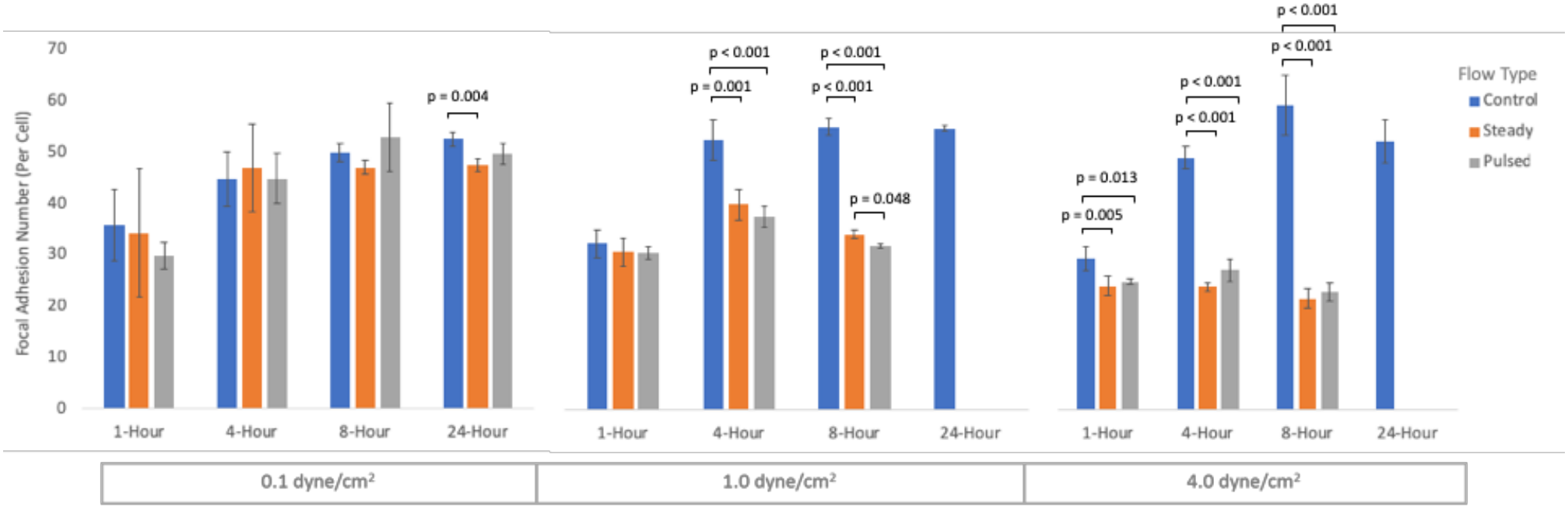

Figure 4.4 Bovine nucleus pulposus focal adhesion number as determined from vinculin immunostaining of focal adhesions following 12 test conditions: 1, 4, 8 and 24-hour flow experiments in Ibidi VI$^{0.4}$ flow chamber at shear stress conditions of 0.1, 1.0 and 4.0 dyne/cm^2. Results are shown for three flow types; control (no flow), steady flow and pulsed flow. Means and 95 % confidence interval error bars are shown based on 4 technical replicates and sample size (n) of 4 bovine subjects. Statistically significant results at level $p < 0.05$ are shown for one-way ANOVA with post-hoc Tukey HSD comparing control vs steady vs pulsed flow for each of the 12 test conditions. No results shown for 1.0 and 4.0 dyne/cm^2 after 24 hours as no cells present on Ibidi VI$^{0.4}$ slide following flow experiments, due to detachment of cells from slide.

4.3.3 Effect of shear stress on FA number

One-way ANOVAs were used to analyse the effect of shear stress rates; 0.1, 1.0 and 4.0 dyne/cm^2, on focal adhesion number. Results and statistically significant findings are shown in figure 4.5. No statistical analysis was carried out at 24 hours for the steady and pulsed groups at 1.0 and 4.0 dyne/cm^2 as noted previously due to the detachment of all cells from the slides.

After 1 hour there was no statistically significant difference shown between the three shear stress rates in the control group; 0.1 dyne/cm^2, 1.0 dyne/cm^2 or 4.0 dyne/cm^2 at the $p < 0.05$ level, [F (2, 9) = 2.068, p = 0.182]. After 1 hour in the steady flow group again there was no statistically significant difference between the three shear stress rates; 0.1 dyne/cm^2, 1.0 dyne/cm^2 and 4.0 dyne/cm^2 at the $p < 0.05$ level, [F (2, 9) = 1.885, p = 0.207]. After 1 hour in the pulsed group, statistically significant differences were shown between the three shear stress rates 0.1 dyne/cm^2 ,1.0 dyne/cm^2 and 4.0 dyne/cm^2 at the $p < 0.05$ level [F (2, 9) = 12.686, p = 0.002]. Post-hoc Tukey showed a significantly lower FA number after 4.0 dyne/cm^2 compared to 0.1 dyne/cm^2 (p = 0.006) and significantly lower FA number after 4.0 dyne/cm^2 compared to 1.0 dyne/cm^2 (p = 0.004), no significant difference was seen between 0.1 dyne/cm^2 and 1 dyne/cm^2 (p = 0.911).

After 4 hours for the control group, there was no significant difference between the shear stress rates for the control group; 0.1 dyne/cm^2, 1.0 dyne/cm^2 and 4.0 dyne/cm^2 at the $p < 0.05$ level [F (2, 9) = 3.420, p = 0.079]. There was a statistically significance difference between the shear stress rate groups for the steady flow group, [F (2, 9) = 19.633, p = 0.001]. Post-hoc Tukey showed a significantly lower FA number after 4.0 dyne/cm^2 compared to 0.1 dyne/cm^2 ($p < 0.001$) and a significantly lower FA number at 4.0 dyne/cm^2 compared to 1.0 dyne/cm^2 (p = 0.006), no significant difference was seen between 0.1 dyne/cm^2 and 1 dyne/cm^2 (p = 0.191). For the pulsed flow group, there was a statistically significant difference between groups at the $p < 0.05$ level [F (2, 9) = 28.179, $p < 0.001$]. Post-hoc Tukey showed a significantly lower FA number at 1.0 dyne/cm^2 compared to 0.1 dyne/cm^2 (p = 0.033), significantly lower FA number at 4.0 dyne/cm^2 compared to 0.1 dyne/cm^2 ($p < 0.001$) and significantly lower FA number between 4.0 dyne/cm^2 compared to 1.0 dyne/cm^2 (p = 0.004).

After 8 hours there was a statistically significant difference between the shear stress rates for the control group at the $p < 0.05$ level, [F (2, 9) = 5.850, p = 0.024]. Post-hoc Tukey showed a significantly higher FA number in 4 dyne/cm^2 flow compared to 0.1 dyne/cm^2 (p = 0.019), no significant difference (p = 0.222) was seen between 0.1 dyne/cm^2 and 1 dyne/cm^2 and no significant difference (p = 0.289) was seen between 4.0 dyne/cm^2 and 1 dyne/cm^2. There was a statistically significant difference between shear stress rates for the steady flow group, [F (2, 9) = 308.053, $p < 0.001$]. Post-hoc Tukey showed significantly lower FA number after 1.0 dyne/cm^2 compared to 0.1 dyne/cm^2 ($p < 0.001$), significantly lower FA number after 4.0 dyne/cm^2 compared to 1.0 dyne/cm^2 ($p < 0.001$) and significantly lower FA number after 4.0 dyne/cm^2 compared to 0.1 dyne/cm^2 ($p < 0.001$). There was a statistically significance difference between shear stress rates for the pulsed flow group at the $p < 0.05$ level, [F (2, 9) = 58.099, $p < 0.001$]. Post-hoc Tukey showed significantly lower FA number after 1.0 dyne/cm^2 compared to 0.1 dyne/cm^2 ($p < 0.001$), significantly lower FA number after 4.0 dyne/cm^2 compared to 0.1 dyne/cm^2 ($p < 0.001$) and significantly lower FA number after 4.0 dyne/cm^2 compared to 1.0 dyne/cm^2 (p = 0.030).

After 24 hours the control flow group only was analysed as all cells had detached from the Ibidi VI$^{0.4}$ slides for 1.0 dyne/cm^2 and 4.0 dyne/cm^2 for steady and pulsed flow groups. There was no statistical significance shown between the shear stress rates for the control group; 0.1 dyne/cm^2, 1.0 dyne/cm^2 and 4.0 dyne/cm^2 at the $p < 0.05$ level, [F (2, 9) = 1.050, p = 0.389].

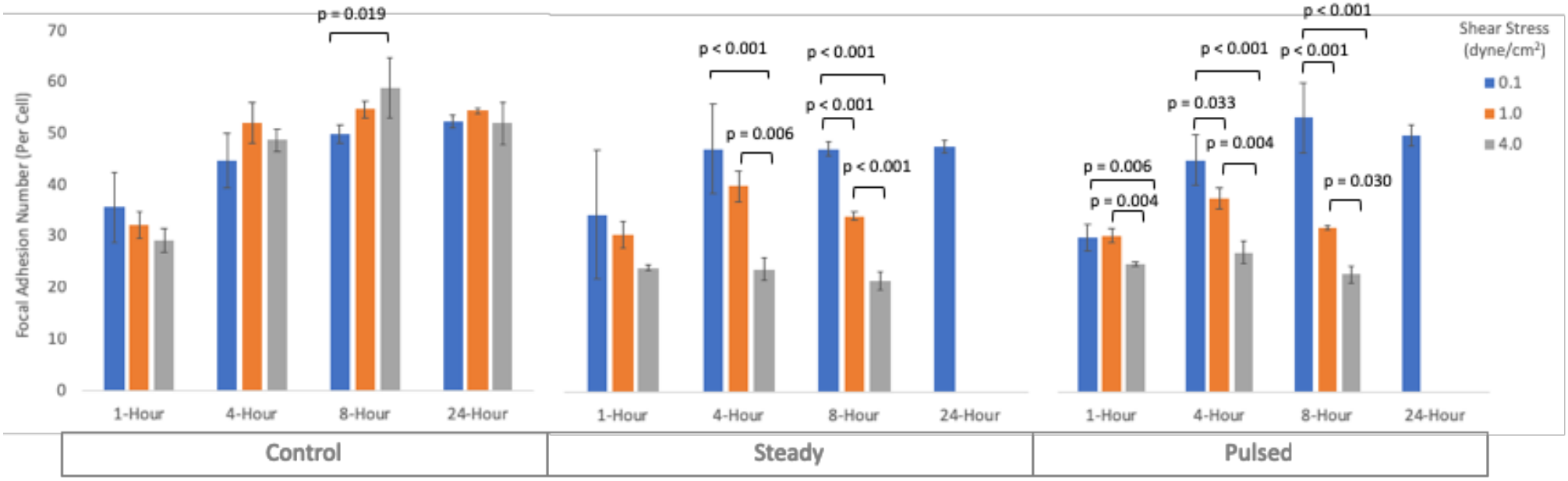

Figure 4.5 Bovine nucleus pulposus focal adhesion number as determined from vinculin immunostaining of focal adhesions following 12 test conditions: 1, 4, 8 and 24-hour flow experiments in Ibidi VI$^{0.4}$ flow chamber at shear stress conditions of 0.1, 1.0 and 4.0 dyne/cm^2. Results are shown for three flow groups; control (no flow), steady flow and pulsed flow. Means and 95 % confidence interval error bars are shown based on 4 technical replicates and sample size (n) of 4 bovine subjects. Statistically significant results at level $p < 0.05$ are shown for one-way ANOVA with post-hoc Tukey HSD comparing results of shear stress conditions of 0.1, 1.0 and 4.0 dyne/cm^2 for each of the time conditions and flow types. No results shown for 1.0 and 4.0 dyne/cm^2 after 24 hours as no cells present on Ibidi VI$^{0.4}$ slide following flow experiments, due to detachment of cells from slide.

4.3.4 Effect of flow duration on FA number

One-way ANOVAs were used to analyse the effect of the duration of time cells were exposed to shear stress; 1, 4, 8 and 24 hours, on focal adhesion number. Results and statistically significant findings are shown in figure 4.6. No statistical analysis was carried out at 24 hours for the steady and pulsed groups at 1.0 and 4.0 dyne/cm^2 as noted previously due to the detachment of all cells from the slides.

For the control group at 0.1 dyne/cm^2 there was a statistically significant results at the $p < 0.05$ level, [F (3, 12) = 10.773, p = 0.001]. Post-hoc Tukey HSD showed significantly higher FA number after 8 hours compared with 1 hour (p = 0.004) and significantly higher FA number after 24 hours compared with 1 hour (p = 0.001). No significant difference was seen between 1 hour and 4 hours (p = 0.065), no significant difference was seen between 4 hours and 8 hours (p = 0.392), no significant difference was seen between 4 hours and 24 hours (p = 0.124) and no significant difference was seen between 8 hours and 24 hours (p = 0.861). For the steady group at 0.1 dyne/cm^2 there was no statistically significant difference seen for FA number at different time intervals, [F (3, 12) = 2.770, p = 0.087]. A statistically significant difference was seen between time intervals for the pulsed group at 0.1 dyne/cm^2, [F (3, 12) = 20.258, $p < 0.001$]. Post-hoc Tukey HSD showed significantly higher FA number after 4 hours flow compared to after 1 hour flow (p = 0.003), significantly higher FA number after 8 hours flow compared to after 1 hour flow ($p <$ 0.001) and significantly higher FA number after 24 hours flow compared to after 1 hour flow ($p < 0.001$). No significant difference was seen between 4 hours and 8 hours (p = 0.099), no significant difference was seen between 8 hours and 24 hours (p = 0.703) and no significant difference was seen between 4 hours and 24 hours (p = 0.480).

A statistically significant difference was seen between time intervals for the control group at 1.0 dyne/cm^2, [F (3, 12) = 69.548, $p < 0.001$]. Post-hoc Tukey HSD showed significantly higher FA number after 4 hours compared to 1 hour ($p < 0.001$), significantly higher FA number after 8 hours compared to 1 hour ($p < 0.001$) and significantly higher FA number after 24 hours compared to 1 hour ($p < 0.001$). No significance difference was seen between 8 hours and 4 hours (p = 0.546), or between 24 hours and 4 hours (p = 0.625) or between 24 hours and 8 hours (p =

0.999). For the steady group at 1.0 dyne/cm^2 a statistically significant difference was seen between time intervals [F (2, 11) =15.784, p < 0.001]. Post-hoc Tukey HSD showed statistically significant higher FA number after 4 hour flow compared with 1 hour flow (p = 0.001), statistically significant lower FA number after 8 hours flow compared with 4 hours flow (p = 0.008). No significant difference was seen between 1 hour and 8 hours (p = 0.144). A statistically significant difference was seen between time intervals for the pulsed group at 1.0 dyne/cm^2 [F (2, 11) =28.500, p < 0.001]. Post-hoc Tukey HSD showed statistically significant higher FA number after 4 hours flow compared with 1 hour flow (p < 0.001) and statistically significant lower FA number after 8 hours flow compared with 4 hours flow (p < 0.001), no significant difference was seen between 1 hour and 8 hours flow (p = 0.345).

A statistically significant difference was seen between time intervals for the control group at 4.0 dyne/cm^2 [F (3, 12) = 40.679, p < 0.001]. Post-hoc Tukey showed significantly higher FA number after 4 hours compared to 1 hour (p < 0.001), significantly higher FA number after 8 hours compared to 1 hour (p < 0.001) and significantly higher FA number after 24 hours compared to 1 hour (p < 0.001), no statistically significant differences were seen between 4 hours and 8 hours (p = 0.016), between 8 hours and 24 hours (p = 0.114) or between 4 and 24 hours (p = 0.667). For the steady group at 4.0 dyne/cm^2 there were no statistically significant differences seen between time intervals for the steady group [F (2, 11) = 2.874, p = 0.108]. There was a statistically significant difference seen between time intervals for the pulsed group at 4.0 dyne/cm^2 [F (2, 11) = 6.926, p = 0.015]. Post-hoc Tukey HSD showed significantly high FA number after 4 hours compared to 8 hours (p = 0.005).

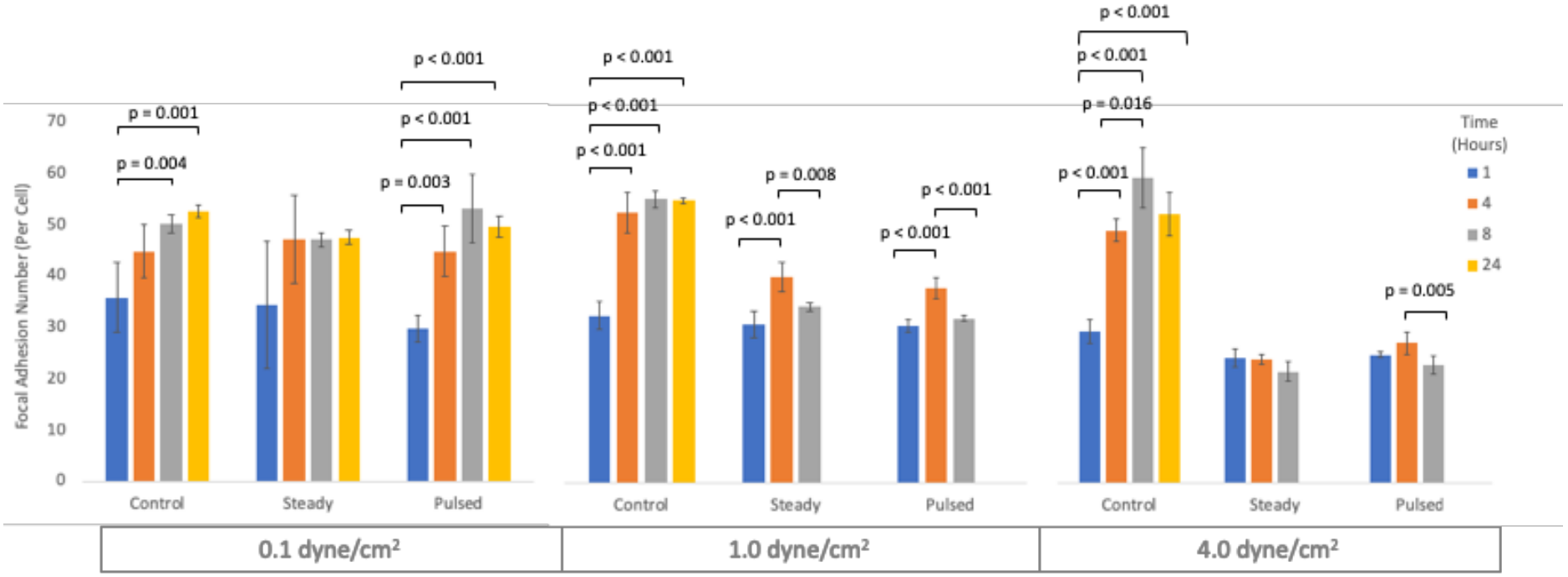

Figure 4.6 Bovine nucleus pulposus focal adhesion number as determined from vinculin immunostaining of focal adhesions following 12 test conditions: 1, 4, 8 and 24-hour flow experiments in Ibidi VI$^{0.4}$ flow chamber at shear stress conditions of 0.1, 1.0 and 4.0 dyne/cm^2. Results are shown for three flow groups; control (no flow), steady flow and pulsed flow. Means and 95 % confidence interval error bars are shown based on 4 technical replicates and sample size (n) of 4 bovine subjects. Statistically significant results at level $p < 0.05$ are shown for one-way ANOVA with post-hoc Tukey HSD comparing results after 1, 4, 8 and 24 hours, for each of the shear stress conditions and flow types. No results shown for 1.0 and 4.0 dyne/cm^2 after 24 hours as no cells present on Ibidi VI$^{0.4}$ slide following flow experiments, due to detachment of

4.4 Cell Circularity

4.4.1 Descriptive statistics

Shear Stress (dyne/cm^2)	Time (hours)	Control		Steady		Pulsed	
		Mean	*Standard Deviation*	*Mean*	*Standard Deviation*	*Mean*	*Standard Deviation*
0.1	**1**	0.34	*0.048*	0.32	*0.028*	0.32	*0.015*
	4	0.30	*0.033*	0.30	*0.016*	0.31	*0.015*
	8	0.31	*0.013*	0.27	*0.010*	0.29	*0.014*
	24	0.28	*0.012*	0.29	*0.014*	0.29	*0.010*
1.0	**1**	0.30	*0.025*	0.32	*0.043*	0.29	*0.019*
	4	0.32	*0.043*	0.37	*0.013*	0.35	*0.014*
	8	0.30	*0.013*	0.37	*0.022*	0.43	*0.037*
	24	0.28	*0.029*	-	-	-	-
4.0	**1**	0.32	*0.022*	0.30	*0.008*	0.32	*0.026*
	4	0.31	*0.008*	0.39	*0.029*	0.41	*0.026*
	8	0.26	*0.017*	0.16	*0.033*	0.44	*0.030*
	24	0.29	*0.013*	-	-	-	-

Table 4.3 Mean and standard deviation values for cell circularity for all 3 independent variables; flow type (control, steady and pulsed), shear stress (01, 1.0 and 4.0 dyne/cm^2) and time points (1, 4, 8 and 24 hours).

4.4.2 Effect of flow type on cell circularity

One-way ANOVAs were used to analyse the effect of flow types; no flow, steady flow and pulsed flow, on cell circularity. Results and statistically significant findings are shown in figure 4.7. No statistical analysis was carried out at 24 hours for the steady and pulsed groups at 1.0 and 4.0 dyne/cm^2 as noted previously due to the detachment of all cells from the slides.

There was no statistically significant effect of flow type on cell circularity at the $p < 0.05$ level for the three flow conditions at 0.1 dyne/cm^2 after 1-hour flow, [F (2, 11) = 0.373, p = 0.699]. There was no statistically significant effect of flow type on cell

circularity at the $p < 0.05$ level for the three flow conditions at 0.1 dyne/cm^2 after 4-hour flow, [F (2, 11) = 0.047, p = 0.954]. There was a statistically significant effect of flow type on cell circularity at the $p < 0.05$ level for the three flow conditions at 0.1 dyne/cm^2 after 8-hour flow, [F (2, 11) = 6.927, p = 0.015]. Post-hoc comparisons using Tukey HSD indicated that the mean score for the control was significantly higher than the mean score for the steady flow (p = 0.012), but not significantly different to the pulsed flow (p=0.252) and no significant difference was seen between steady and pulsed flow mean values (p = 0.167). There was no statistically significant effect of flow type on cell circularity at the $p < 0.05$ level for the three flow conditions at 0.1 dyne/cm^2 after 24-hour flow; control, steady pulsed, [F (2, 11) = 2.745, p = 0.117].

There was no statistically significant effect of flow type on cell circularity at the $p < 0.05$ level for the three flow conditions at 1.0 dyne/cm^2 after 1-hour flow; control steady pulsed, [F (2, 11) = 1.167, p = 0.354]. There was no statistically significant effect of flow type on cell circularity at the $p < 0.05$ level for the three flow conditions at 1 dyne/cm^2 after 4-hour flow, [F (2, 11) = 2.544, p = 0.133]. There was a statistically significant effect of flow type on cell circularity at the $p < 0.05$ level for the three flow conditions at 1 dyne/cm^2 after 8 hour flow, [F (2, 11) = 24.434, $p < 0.001$]. Post-hoc comparisons using Tukey HSD indicated that the mean score for the steady flow conditions was significantly higher than the control (p = 0.007), and the pulsed was significantly higher than the control ($p < 0.001$) and the pulsed was significantly higher than the steady flow (p = 0.045).

There was no statistically significant effect of flow type on cell circularity at the $p < 0.05$ level for the three flow conditions at 4.0 dyne/cm^2 after 1-hour flow, [F (2, 11) = 1.163, p = 0.355]. There was a statistically significant effect of flow type on cell circularity at the $p < 0.05$ level for the three flow conditions at 4.0 dyne/cm^2 after 4-hour flow, [F (2, 11) = 19.1632, p = 0.001]. Post-hoc comparisons using Tukey HSD indicated that the mean score for the steady flow conditions was significantly higher than the control (p = 0.002), and the pulsed was significantly higher than the control (p = 0.001). The pulsed flow did not significantly differ from the steady flow (p = 0.648). There was a statistically significant effect of flow type on cell number at the $p < 0.05$ level for the three flow conditions at 4.0 dyne/cm^2 after 8-hour flow, [F (2, 11)

= 59.551, $p < 0.001$]. Post-hoc comparisons using Tukey HSD indicated that the mean score for the steady flow conditions was significantly higher than the control ($p < 0.001$), and the pulsed was significantly higher than the control ($p < 0.001$). The pulsed flow did not significantly differ from the steady flow ($p = 0.655$).

4.4.2 Effect of shear stress rate on cell circularity

One-way ANOVAs were used to analyse the effect of shear stress rates; 0.1, 1.0 and 4.0 dyne/cm^2, on cell circularity. Results and statistically significant findings are shown in figure 4.8. No statistical analysis was carried out at 24 hours for the steady and pulsed groups at 1.0 and 4.0 dyne/cm^2 as noted previously due to the detachment of all cells from the slides.

After 1 hour there was no statistically significant difference seen between the three shear stress rates in the control group; 0.1 dyne/cm^2, 1.0 dyne/cm^2 or 4.0 dyne/cm^2 at the $p < 0.05$ level, [F (2, 9) = 1.260, $p = 0.329$]. After 1 hour in the steady flow group there was no statistically significant difference between the three shear stress rates; 0.1 dyne/cm^2, 1.0 dyne/cm^2 and 4.0 dyne/cm^2 at the $p < 0.05$ level, [F (2, 9) = 0.529, $p = 0.606$]. After 1 hour in the pulsed group no statistically significant differences were seen between the three shear stress rates 0.1 dyne/cm^2 ,1.0 dyne/cm^2 and 4.0 dyne/cm^2 at the $p < 0.05$ level [F (2, 9) = 2.824, $p = 0.112$].

After 4 hours for the control group, there was no significant difference seen between the shear stress rates for the control group; 0.1 dyne/cm^2, 1.0 dyne/cm^2 and 4.0 dyne/cm^2 at the $p < 0.05$ level, [F (2, 9) = 0.760, $p = 0.495$]. There was a statistically significance difference between the shear stress rate groups for the steady flow group [F (2, 9) = 19.923, $p < 0.001$]. Post-hoc Tukey HSD showed significantly higher cell circularity after 1.0 dyne/cm^2 compared to 0.1 dyne/cm^2 ($p = 0.004$), significantly higher cell circularity at 4.0 dyne/cm^2 compared to 0.1 dyne/cm^2 ($p < 0.001$) and no significant difference between 1 dyne/cm^2 and 4.0 dyne/cm^2 ($p = 0.258$). For the pulsed flow group, there was a statistically significant difference at the $p < 0.05$ level [F (2, 9) = 30.822, $p < 0.001$]. Post-hoc Tukey HSD showed significantly higher cell circularity at 4.0 dyne/cm^2 compared to 0.1 dyne/cm^2 ($p < 0.001$), significantly higher in cell circularity at 4.0 dyne/cm^2 compared to 1.0 dyne/cm^2 (p = 0.008), and

significantly higher cell circularity at 1.0 dyne/cm^2 compared to 0.1 dyne/cm^2 (p = 0.010).

After 8 hours there was a statistically significance difference between the shear stress rates for the control group; 0.1 dyne/cm^2, 1.0 dyne/cm^2 and 4.0 dyne/cm^2 at the $p < 0.05$ level, [F (2, 9) = 10.014, p = 0.005]. Post-hoc Tukey HSD showed significantly lower cell circularity at 4.0 dyne/cm^2 compared to 1.0 dyne/cm^2 (p = 0.018), significantly lower cell circularity at 4.0 dyne/cm^2 compared to 0.1 dyne/cm^2 (p = 0.006) and no significant difference between 0.1 dyne/cm^2 and 1.0 dyne/cm^2 (p = 0.747). There was a statistically significant difference between shear stress rates for the steady flow group at the $p < 0.05$ level, [F (2, 9) = 59.540, $p < 0.001$]. Post-hoc Tukey HSD showed significantly higher cell circularity after 1.0 dyne/cm^2 compared to 0.1 dyne/cm^2 (p = 0.001), significantly higher cell circularity after 4.0 dyne/cm^2 compared to 0.1 dyne/cm^2 ($p < 0.001$) and significantly higher cell circularity at 4.0 dyne/cm^2 compared to 1.0 dyne/cm^2 (p = 0.002). There was a statistically significant difference between shear stress rates for the pulsed flow group, [F (2, 9) = 32.654, $p < 0.001$]. Post-hoc Tukey HSD showed significantly higher cell circularity after 1.0 dyne/cm^2 compared to 0.1 dyne/cm^2 ($p < 0.001$), significantly higher cell circularity after 4.0 dyne/cm^2 compared to 0.1 dyne/cm^2 ($p < 0.001$) and no significant difference between 4.0 dyne/cm^2 and 1.0 dyne/cm^2 (p = 0.814).

After 24 hours the control flow group only was analysed as all cells had detached from the Ibidi VI$^{0.4}$ slides for 1.0 dyne/cm^2 and 4.0 dyne/cm^2 for steady and pulsed flow groups. There was no statistical significance shown between the shear stress rates for the control group; 0.1 dyne/cm^2, 1.0 dyne/cm^2 and 4.0 dyne/cm^2 at the $p < 0.05$ level [F (2, 9) = 0.265, p = 0.773].

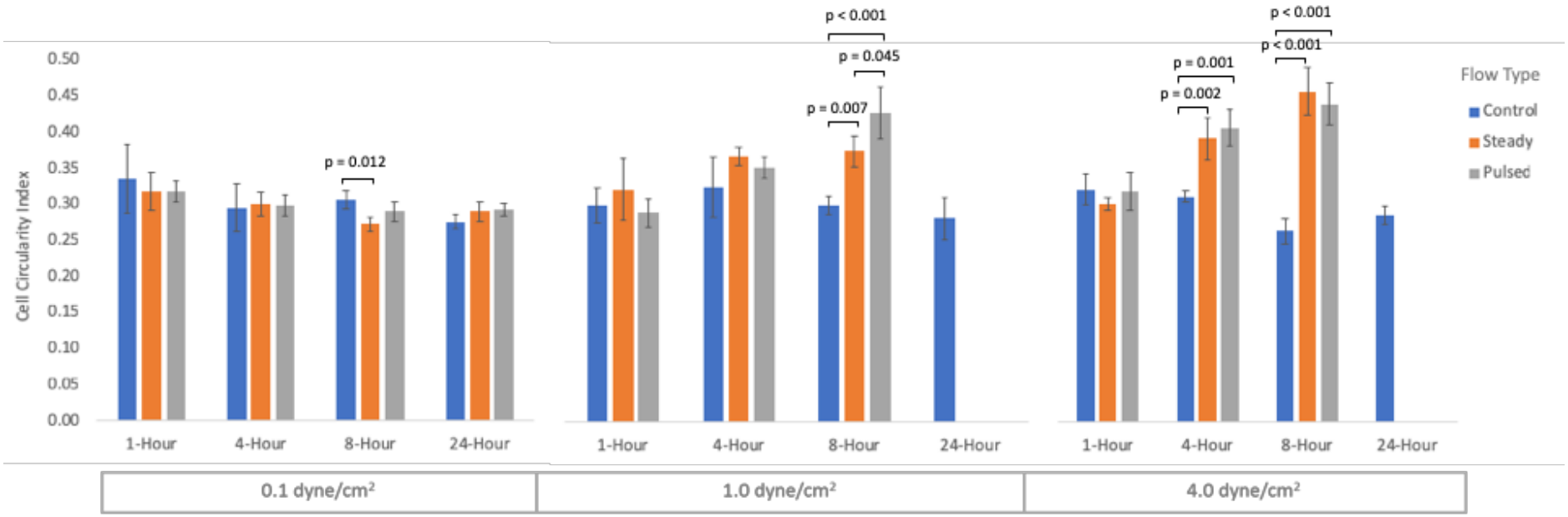

Figure 4.7 Bovine nucleus pulposus circularity as determined from phalloidin immunostaining of F-actin following 12 test conditions: 1, 4, 8 and 24-hour flow experiments in Ibidi VI$^{0.4}$ flow chamber at shear stress conditions of 0.1, 1.0 and 4.0 dyne/cm^2. Results are shown for three flow types; control (no flow), steady flow and pulsed flow. Means and 95 % confidence interval error bars are shown based on 4 technical replicates and sample size (n) of 4 bovine subjects. Statistically significant results at level $p < 0.05$ are shown for one-way ANOVA with post-hoc Tukey HSD comparing control vs steady vs pulsed flow for each of the 12 test conditions. No results shown for 1.0 and 4.0 dyne/cm^2 after 24 hours as no cells present on Ibidi VI$^{0.4}$ slide following flow experiments, due to detachment of cells from slide.

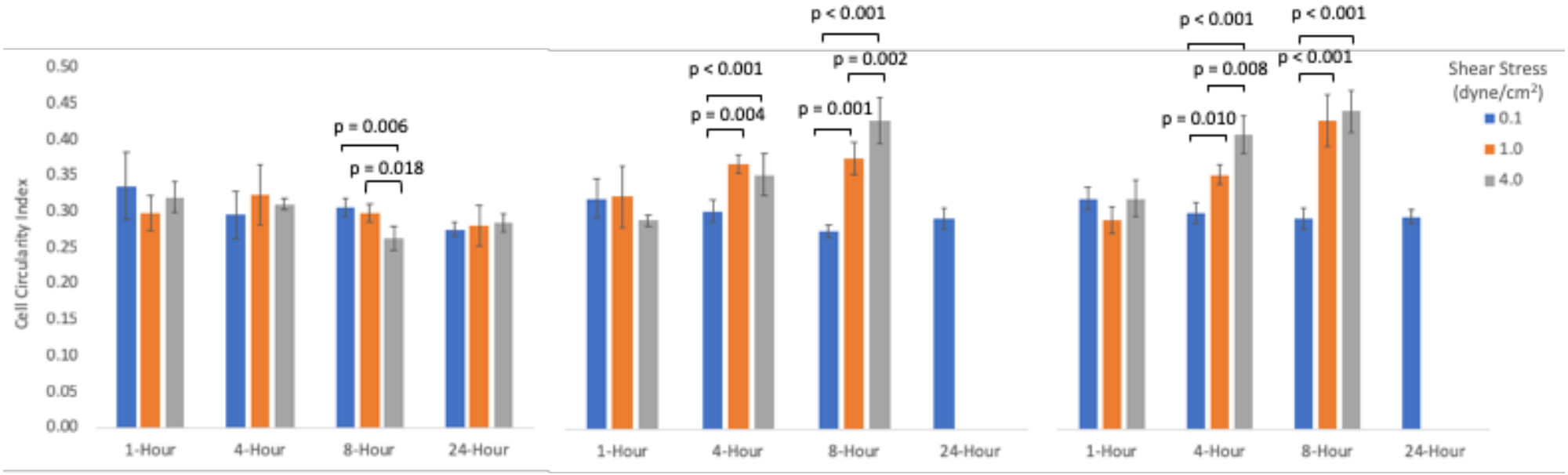

Figure 4.8 Bovine nucleus pulposus cell circularity as determined from phalloidin immunostaining of F-actin following 12 test conditions: 1, 4, 8 and 24-hour flow experiments in Ibidi VI$^{0.4}$ flow chamber at shear stress conditions of 0.1, 1.0 and 4.0 dyne/cm^2. Results are shown for three flow groups; control (no flow), steady flow and pulsed flow. Means and 95 % confidence interval error bars are shown based on 4 technical replicates and sample size (n) of 4 bovine subjects. Statistically significant results at level $p < 0.05$ are shown for one-way ANOVA with post-hoc Tukey HSD comparing results of shear stress conditions of 0.1, 1.0 and 4.0 dyne/cm^2 for each of the time conditions and flow types. No results shown for 1.0 and 4.0 dyne/cm^2 after 24 hours as no cells present on Ibidi VI$^{0.4}$ slide following flow experiments, due to detachment of cells from slide.

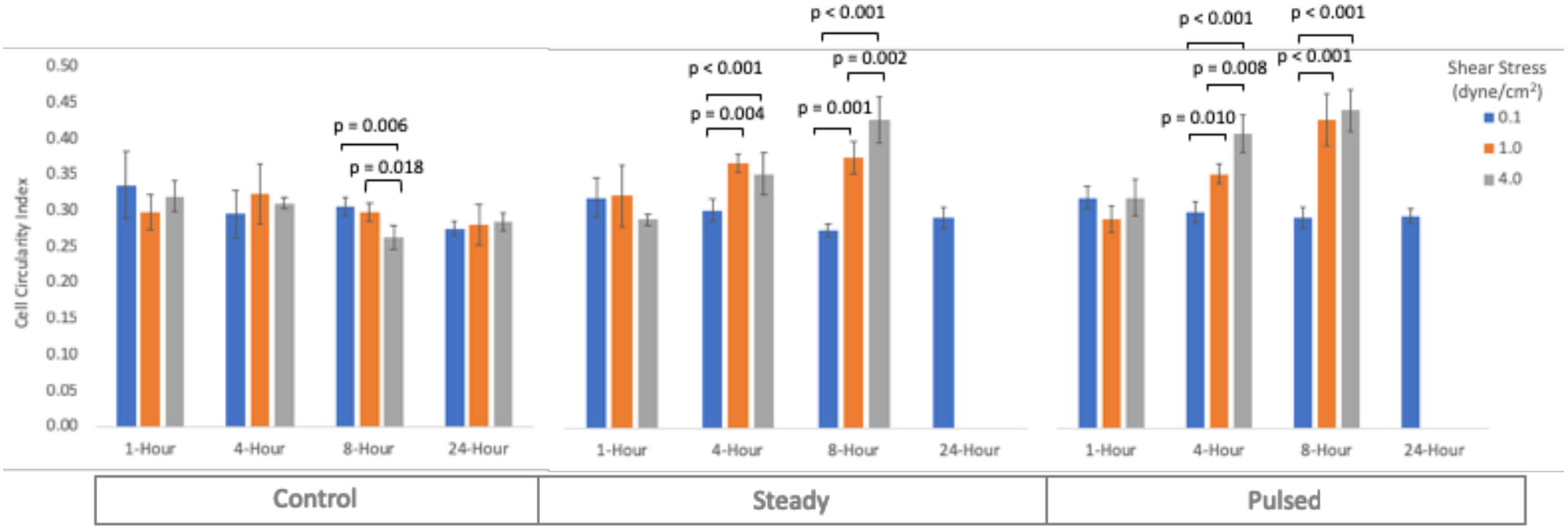

Figure 4.8 Bovine nucleus pulposus cell circularity as determined from phalloidin immunostaining of F-actin following 12 test conditions: 1, 4, 8 and 24-hour flow experiments in Ibidi VI$^{0.4}$ flow chamber at shear stress conditions of 0.1, 1.0 and 4.0 dyne/cm^2. Results are shown for three flow groups; control (no flow), steady flow and pulsed flow. Means and 95 % confidence interval error bars are shown based on 4 technical replicates and sample size (n) of 4 bovine subjects. Statistically significant results at level $p < 0.05$ are shown for one-way ANOVA with post-hoc Tukey HSD comparing results of shear stress conditions of 0.1, 1.0 and 4.0 dyne/cm^2 for each of the time conditions and flow types. No results shown for 1.0 and 4.0 dyne/cm^2 after 24 hours as no cells present on Ibidi VI$^{0.4}$ slide following flow experiments, due to detachment of cells from slide.

4.4.3 Effect of duration of flow on cell circularity

One-way ANOVAs were used to analyse the effect of the duration of time cells were exposed to shear stress; 1, 4, 8 and 24 hours, on cell circularity. Results and statistically significant findings are shown in figure 4.9. No statistical analysis was carried out at 24 hours for the steady and pulsed groups at 1.0 and 4.0 dyne/cm^2 as noted previously due to the detachment of all cells from the slides.

For the control group at 0.1 dyne/cm^2 there were no statistically significant results at the $p < 0.05$ level, [F (3, 12) = 2.727, p = 0.091]. Statistically significant differences were seen between time intervals for the steady group at 0.1 dyne/cm^2, [F (3, 12) = 4.304, p = 0.028). Post-hoc Tukey HSD showed significantly lower cell circularity after 8 hours compared with 1 hour (p = 0.020). No significant differences between 1 and 4 hours (p = 0.543), between 1 and 24 hours (p = 0.195), between 4 and 8 hours (p = 0.195), between 4 and 24 hours (p = 0.962) or between 8 and 24 hours (p = 0.543). No statistically significant differences were seen between time intervals for the pulsed group at 0.1 dyne/cm^2, [F (3, 12) = 3.360, p = 0.055].

No statistically significant difference was seen between time intervals for the control group at 1.0 dyne/cm^2, [F (3, 12) = 1.408, p = 0.289]. For the steady group at 1.0 dyne/cm^2 no statistically significant difference was seen between time intervals [F (2, 11) = 3.832, p = 0.063]. Statistically significant differences were seen between time intervals for the pulsed group at 1.0 dyne/cm^2 [F (2, 11) = 29.545, $p < 0.001$]. Post-hoc Tukey HSD showed significantly higher cell circularity after 4 hours flow compared with 1 hour flow (p = 0.008) and significantly higher cell circularity after 8 hours flow compared with 1 hours flow ($p < 0.001$) and significantly higher cell circularity was seen after 8 hours flow compared with 4 hours flow (p = 0.002).

Statistically significant differences were seen between time intervals for the control group at 4.0 dyne/cm^2 [F (3, 12) = 10.782, $p < 0.001$]. Post-hoc Tukey showed statistically significant (p = 0.005) lower cell circularity after 8 hours compared to 4 hours, statistically significant (p = 0.001) lower cell circularity after 8 hours compared to 1 hour and statistically significant (p = 0.037) lower cell circularity after 24 hours compared to 1 hours. No statistically significant differences (p = 0.806) between 4 hours compared to 1 hour, no statistically significant differences (p = 0.166) between

4 hours compared to 24 hours, no statistically significant differences were seen between 8 hours and 24 hours ($p = 0.234$). For the steady group at 4.0 dyne/cm^2 a statistically significant difference was seen between time intervals for the steady group [F (2, 11) = 35.754, $p < 0.001$]. Post-hoc Tukey HSD showed significantly higher cell circularity after 4 hours flow compared with 1 hour flow ($p = 0.001$) and significantly higher cell circularity after 8 hours flow compared with 1 hours flow ($p = 0.007$), and significantly higher cell circularity between 4 hour and 8 hours flow ($p < 0.001$). A statistically significant difference was seen between time intervals for the pulsed group at 4.0 dyne/cm^2 [F (2, 11) = 20.245, $p < 0.001$]. Post-hoc Tukey HSD showed significantly higher cell circularity after 4 hours flow compared with 1 hour flow ($p = 0.001$) and significantly higher cell circularity after 8 hours flow compared with 1 hours flow ($p < 0.001$), no significant difference was seen between 4 hour and 8 hours flow ($p = 0.269$).

4.5 Collagen 1

4.5.1 Descriptive statistics

Shear Stress (dyne/cm^2)	Time (hours)	Control		Steady		Pulsed	
		Mean	*Standard Deviation*	*Mean*	*Standard Deviation*	*Mean*	*Standard Deviation*
0.1	**1**	-4.52	*0.51*	-1.75	*0.90*	-5.77	*1.00*
	4	-3.25	*1.06*	-1.64	*0.71*	-3.66	*1.02*
	8	-2.51	*0.72*	-3.84	*1.03*	-5.17	*0.60*
	24	-1.72	*0.25*	-2.60	*0.80*	-3.96	*0.76*
1.0	**1**	-4.02	*1.00*	-4.68	*0.91*	-2.40	*0.55*
	4	-0.76	*1.01*	-2.32	*0.39*	-2.27	*0.66*
	8	-4.12	*1.11*	-2.84	*1.55*	-2.54	*0.47*
	24	-2.22	*0.62*	-	-	-	-
4.0	**1**	-2.26	*1.02*	-0.96	*0.81*	1.99	*2.32*
	4	-3.01	*0.48*	-1.91	*0.14*	-1.36	*0.85*
	8	-1.43	*0.45*	-0.79	*0.21*	-0.84	*0.68*
	24	-3.67	*0.77*	-	-	-	-

Table 4.4 Mean and standard deviation dCt values (normalized to GAPDH) for gene expression of collagen 1 for all 3 independent variables; flow type (control, steady and pulsed), shear stress (01, 1.0 and 4.0 dyne/cm^2) and time points (1, 4, 8 and 24 hours).

4.5.2 Effect of flow type on GE of collagen 1

One-way ANOVAs were used to analyse the effect of flow types; no flow, steady flow and pulsed flow, on gene expression of Collagen 1. Results and statistically significant findings are shown in figure 4.10. No statistical analysis was carried out at 24 hours for the steady and pulsed groups at 1.0 and 4.0 dyne/cm^2 as noted previously due to the detachment of all cells from the slides.

There was a statistically significant effect of flow type on gene expression dCt values for collagen 1 at the $p < 0.05$ level for the three flow conditions at 0.1 dyne/cm^2 after 1 hour flow, [F (2, 11) = 24.677, $p < 0.001$]. Post-hoc comparisons using Tukey HSD indicated

that the mean score for the steady flow conditions was significantly different than for the control (p = 0.003), and the steady flow was significantly different from the pulsed flow (p < 0.001), but the pulsed flow did not significantly differ from the control (p = 0.139).There was a statistically significant effect of flow type on gene expression dCt values for collagen 1 at the p < 0.05 level for the three flow conditions at 0.1 dyne/cm^2 after 4 hour flow, [F (2, 11) = 5.154, p = 0.032]. Post-hoc comparisons using Tukey HSD indicated that the mean score for the steady flow conditions was significantly different than the pulsed (p = 0.034), the control was not significantly different the steady flow (p = 0.089), or to the pulsed flow (p = 0.817). There was a statistically significant effect of flow type on gene expression dCt values for collagen 1 at the p < 0.05 level for the three flow conditions at 0.1 dyne/cm^2 after 8 hour flow, [F (2,11) = 10.970, p = 0.004]. Post-hoc comparisons using Tukey HSD indicated that the mean score for the pulsed flow conditions was significantly different than the control (p = 0.003), and there was no significant differences between the control and steady flow (p = 0.102) or between the pulsed flow and steady flow (p = 0.099). There was a statistically significant effect of flow type on gene expression dCt values for collagen 1 at the p < 0.05 level for the three flow conditions at 0.1 dyne/cm^2 after 24 hour flow, [F (2, 11) = 11.904, p = 0.003]. Post-hoc comparisons using Tukey HSD indicated that the mean score for the pulsed flow conditions was significantly different than the control (p = 0.002), and pulsed flow was significantly different from the steady flow (p = 0.040), but the steady flow did not significantly differ from the control (p = 0.193).

There was a statistically significant effect of flow type on gene expression dCt values for collagen 1 at the p < 0.05 level for the three flow conditions at 1.0 dyne/cm^2 after 1 hour flow, [F (2, 11) = 7.707, p = 0.011]. Post-hoc comparisons using Tukey HSD indicated that the mean score for the pulsed flow conditions was significantly different than the steady (p = 0.010), there was no significant difference between the control and pulsed flow (p = 0.057), or between the control and steady flow (p = 0.532). There was a statistically significant effect of flow type on gene expression dCt values for collagen 1 at the p < 0.05 level for the three flow conditions at 1.0 dyne/cm^2 after 4 hour flow, [F(2, 11) = 5.889, p = 0.023]. Post-hoc comparisons using Tukey HSD indicated that the mean score for the steady flow condition was significantly different than the control (p = 0.035), and control was significantly different from the pulsed flow (p = 0.041), but the pulsed flow did not significantly differ from the steady (p = 0.994). There was no statistically significant effect

of flow type on gene expression dCt values for collagen 1 at the $p < 0.05$ level for the three flow conditions at 1.0 dyne/cm^2 after 8 hour flow, [F (2, 11) = 2.209, p = 0.166].

There was a statistically significant effect of flow type on gene expression dCt values for collagen 1 at the $p < 0.05$ level for the three flow conditions at 4.0 dyne/cm^2 after 1 hour flow, [F (2, 11) = 8.034, p = 0.010]. Post-hoc comparisons using Tukey HSD indicated that the mean score for the pulsed flow conditions was significantly different than the control (p = 0.009), there was no statistically significant difference between the control and steady flow (p = 0.483), or between pulsed flow and steady flow (p = 0.057). There was a statistically significant effect of flow type on gene expression dCt values for collagen 1 at the $p < 0.05$ level for the three flow conditions at 4.0 dyne/cm^2 after 4 hours flow, [F (2, 11) = 8.775, p = 0.008]. Post-hoc comparisons using Tukey HSD indicated that the mean score for the pulsed flow conditions was significantly different than the control (p = 0.007), but there was no significantly difference between control and steady flow (p = 0.054) or between steady and pulsed flow (p = 0.397). There was no statistically significant effect of flow type on gene expression dCt values for collagen 1 at the $p < 0.05$ level for the three flow conditions at 4.0 dyne/cm^2 after 8 hour flow, [F (2, 11) = 2.117, p = 0.176].

4.5.3 Effect of shear stress rate on GE of collagen 1

One-way ANOVAs were used to analyse the effect of shear stress rates; 0.1, 1.0 and 4.0 dyne/cm^2, on gene expression of collagen 1. Results and statistically significant findings are shown in figure 4.11. No statistical analysis was carried out at 24 hours for the steady and pulsed groups at 1.0 and 4.0 dyne/cm^2 as noted previously due to the detachment of all cells from the slides.

There was a statistically significant effect on gene expression dCt values for collagen 1 at the $p < 0.05$ level between the three shear stress conditions 0.1, 1.0 and 4.0 dyne/cm^2 after 1 hour for control [F (2, 9) = 7.344, p = 0.013]. Post-hoc tests using Tukey HSD showed no significant difference between 0.1 dyne/cm^2 and 4.0 dyne/cm^2 (p = 0.013), no significant difference between 1.0 dyne/cm^2 and 4.0 dyne/cm^2 (p = 0.047) and no significant difference between 0.1 dyne/cm^2 and 1.0 dyne/cm^2 (p = 0.703). After 1 hour for steady flow a statistically significant difference was seen, [F (2, 9) = 20.223, $p < 0.001$]. Post-hoc tests using Tukey HSD indicated that there was a significant difference between

0.1 dyne/cm^2 and 1 dyne/cm^2 shear stress (p = 0.003), significant difference between 1.0 dyne/cm^2 and 4.0 dyne/cm^2 (p = 0.001), and no significant difference between 0.1 dyne/cm^2 and 4.0 dyne/cm^2 (p = 0.438). After 1 hour for pulsed flow, [F (2, 9) = 27.293, p < 0.001]. Post-hoc tests using Tukey HSD indicated that there was a significant difference between 0.1 dyne/cm^2 and 4.0 dyne/cm^2 (p < 0.001), a significant difference between 0.1 dyne/cm^2 and 1.0 dyne/cm^2 (p = 0.027) and a significant difference between 1.0 dyne/cm^2 and 4.0 dyne/cm^2 (p = 0.006).

A one-way ANOVA determined that there was a statistically significant effect on gene expression dCt values for collagen 1 at the p<0.05 level between the three shear stress conditions 0.1, 1.0 and 4.0 dyne/cm^2 after 4 hours for control, [F (2, 9) = 9.568, p = 0.006]. Post-hoc tests using Tukey HSD showed a significant difference between 1.0 dyne/cm^2 and 4.0 dyne/cm^2 (p = 0.015), a significant difference between 0.1 dyne/cm^2 and 1.0 dyne/cm^2 (p = 0.008) and no significant difference between 0.1 dyne/cm^2 and 4.0 dyne/cm^2 (p = 0.926). There was no statistically significant difference between groups after 4 hours for steady flow, [F (2, 9) = 2.150, p = 0.172]. There was a statistically significant difference between groups after 4 hours for pulsed, [F (2, 9) = 7.323, p = 0.013]. Post-hoc tests using Tukey HSD showed a significant difference between 0.1 dyne/cm^2 and 4.0 dyne/cm^2 (p = 0.011), but no significant difference between 0.1 dyne/cm^2 and 1.0 dyne/cm^2 (p = 0.108) or between 1.0 dyne/cm^2 and 4.0 dyne/cm^2 (p = 0.332).

A one-way ANOVA determined that there was a statistically significant effect on gene expression dCt values for collagen 1 at the p < 0.05 level between the three shear stress conditions 0.1, 1.0 and 4.0 dyne/cm^2 after 8 hours for control, [F (2, 9) = 11.387, p = 0.003]. Post-hoc tests using Tukey HSD showed a significant difference between 1.0 dyne/cm^2 and 4.0 dyne/cm^2 (p = 0.003), a significant difference between 0.1 dyne/cm^2 and 1.0 dyne/cm^2 (p = 0.047) and no significant difference between 0.1 dyne/cm^2 and 4.0 dyne/cm^2 (p = 0.192). A statistically significant difference was seen after 8 hours for steady flow, [F (2, 9) = 8.299, p = 0.009]. Post-hoc tests using Tukey HSD indicated that there was a significant difference between 0.1 dyne/cm^2 and 4.0 dyne/cm^2 shear stress (p = 0.008), no significant difference was seen between 0.1 dyne/cm^2 and 1.0 dyne/cm^2 (p = 0.423), and no significance between 1.0 dyne/cm^2 and 4.0 dyne/cm^2 (p = 0.059). A statistically significant difference was seen after 8 hours for pulsed, [F (2, 9) = 54.316, p <

0.001]. Post-hoc tests using Tukey HSD indicated that there was a significant difference between 0.1 dyne/cm^2 and 1.0 dyne/cm^2 ($p < 0.001$), a significant difference between 0.1 dyne/cm^2 and 4.0 dyne/cm^2 ($p < 0.001$) and a significant difference between 1.0 dyne/cm^2 and 4.0 dyne/cm^2 ($p = 0.007$).

After 24 hours the control flow group only was analysed as all cells had detached from the Ibidi VI$^{0.4}$ slides for 1.0 dyne/cm^2 and 4.0 dyne/cm^2 for steady and pulsed flow groups. There was a statistically significant difference shown between the shear stress rates for the control group; 0.1 dyne/cm^2, 1.0 dyne/cm^2 and 4.0 dyne/cm^2 at the $p < 0.05$ level, [$F(2, 9) = 11.889$, $p = 0.003$]. Post-hoc tests using Tukey HSD showed a significant difference between 0.1 dyne/cm^2 and 4.0 dyne/cm^2 ($p = 0.003$), and a significant difference between 1.0 dyne/cm^2 and 4.0 dyne/cm^2 ($p = 0.017$), and no significant difference was seen between 0.1 dyne/cm^2 and 1.0 dyne/cm^2 ($p = 0.487$).

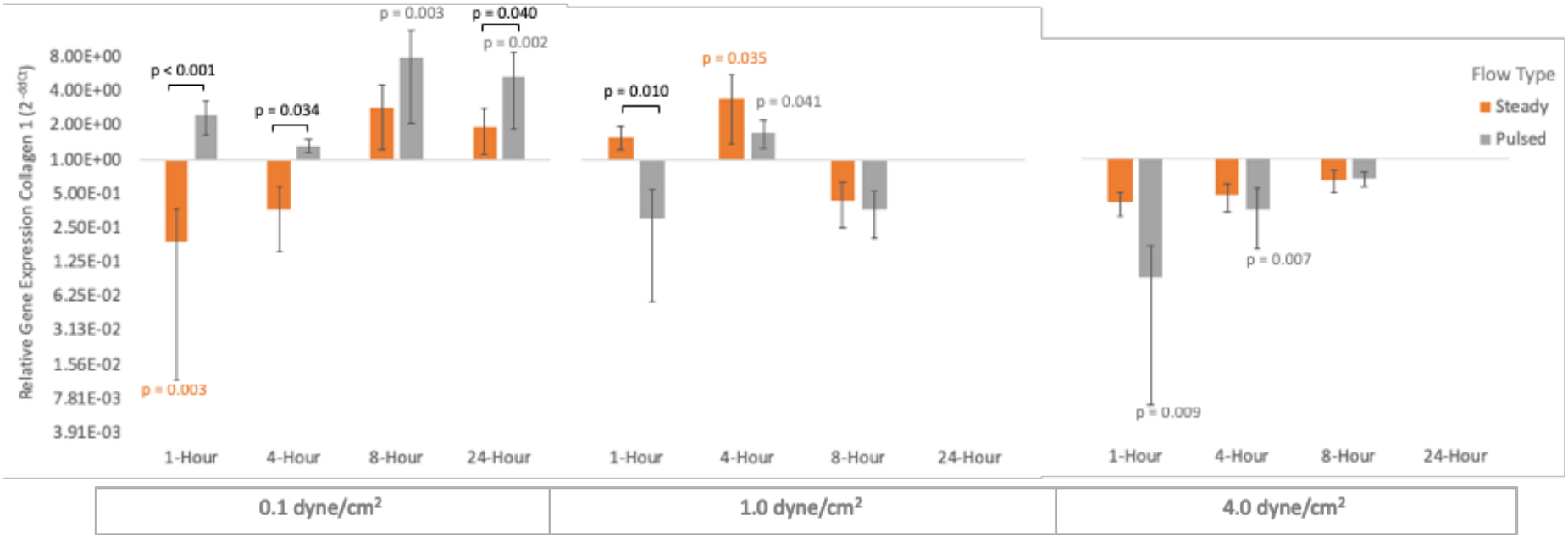

Figure 4.10 Gene expression of collagen 1 in Bovine nucleus pulposus cells relative to housekeeping gene (GAPDH) and control (no flow) as determined by qRT-PCR following 12 test conditions: 1, 4, 8 and 24-hour flow experiments in Ibidi VI$^{0.4}$ flow chamber at shear stress conditions of 0.1, 1.0 and 4.0 dyne/cm^2. Results are shown for three flow types; control (no flow), steady flow and pulsed flow. Control is shown at y-axis = 1. Means and 95 % confidence interval error bars are shown based on 4 technical replicates and sample size (n) of 4 bovine subjects. Statistically significant results at level $p < 0.05$ are shown for one-way ANOVA with post-hoc Tukey HSD comparing control vs steady vs pulsed flow for each of the 12 test conditions. p value above or below error bar corresponds to Tukey HSD post-hoc test result between control and flow condition (steady or pulsed). p value above comparison bar corresponds to Tukey HSD post-hoc test result between steady vs pulsed flow. No results shown for 1.0 and 4.0 dyne/cm^2 after 24 hours as no cells present on Ibidi VI$^{0.4}$ slide following flow experiments, due to detachment of cells from slide.

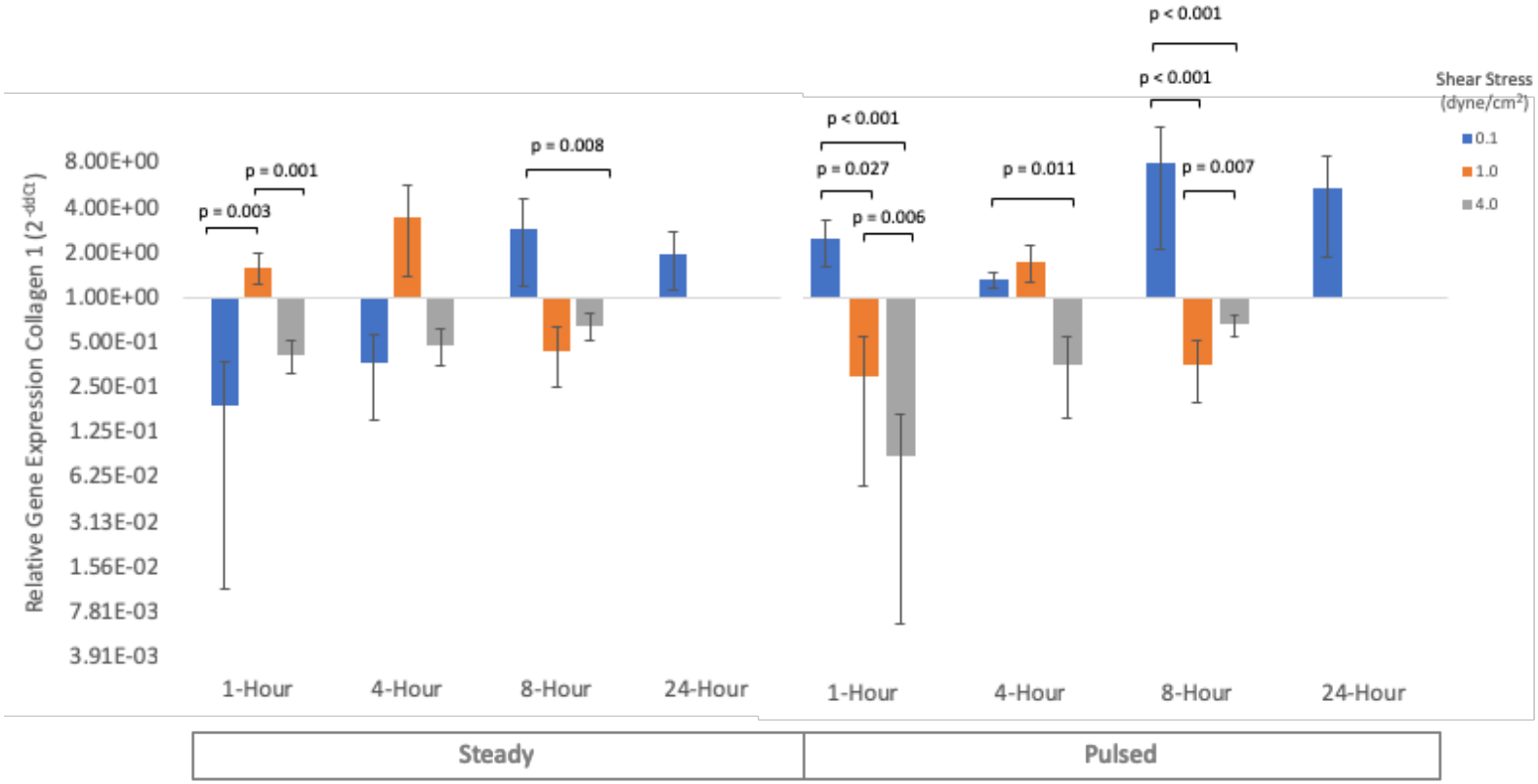

Figure 4.11 Gene expression of collagen 1 in bovine nucleus pulposus cells relative to GAPDH and control (no flow) as determined by qRT-PCR following 12 test conditions: 1, 4, 8 and 24-hour flow experiments in Ibidi VI$^{0.4}$ flow chamber at shear stress conditions of 0.1, 1.0 and 4.0 dyne/cm^2. Results are shown for three flow types; control (no flow), steady flow and pulsed flow. Control is shown at y-axis = 1. Means and 95 % confidence interval error bars are shown based on 4 technical replicates and sample size (n) of 4 bovine subjects. Statistically significant results at level $p < 0.05$ are shown for one-way ANOVA with post-hoc Tukey HSD comparing shear stress conditions 0.1 vs 1.0 vs 4.0 dyne/cm^2 flow for each of the time conditions and flow types. No results shown for 1.0 and 4.0 dyne/cm^2 after 24 hours as no cells present on Ibidi VI$^{0.4}$ slide following flow experiments, due to detachment of cells from slide.

4.5.4 Effect of duration of flow on GE of collagen 1

One-way ANOVAs were used to analyse the effect of the duration of time cells were exposed to shear stress; 1, 4, 8 and 24 hours, on gene expression of collagen 1. Results and statistically significant findings are shown in figure 4.12. No statistical analysis was carried out at 24 hours for the steady and pulsed groups at 1.0 and 4.0 dyne/cm^2 as noted previously due to the detachment of all cells from the slides.

For the control group at 0.1 dyne/cm^2 there was a statistically significant result at the $p < 0.05$ level [F (3, 12) = 11.628, p = 0.001]. Post-hoc Tukey HSD showed a significant difference after 24 hours compared to 1 hour (p = 0.001), a significant difference was seen between 8 hours and 1 hour (p = 0.007) and between 4 hours and 24 hours (p = 0.041). No significant differences were seen between 8 hours and 4 hours (p = 0.473), between 4 hours and 1 hour (p = 0.096) or between 8 hours and 24 hours (p = 0.415). A statistically significant difference was seen between time intervals for the steady group at 0.1 dyne/cm^2, [F (3, 12) = 5.536, p = 0.013). Post-hoc Tukey HSD showed significant differences between 1 hour and 8 hours (p = 0.023), and between 4 hours and 8 hours (p = 0.017). There were no significant differences between 1 hour and 4 hours (p = 0.998), between 1 hour and 24 hours (p = 0.524) between 4 hours and 24 hours (p = 0.426) or between 8 hours and 24 hours (p = 0.233). A statistically significant difference was seen between time intervals for the pulsed group at 0.1 dyne/cm^2, [F (3, 12) = 5.350, p = 0.015]. Post-hoc Tukey HSD showed significant differences after 4 hours compared to 1 hour (p = 0.021) and after 24 hours compared to 1 hour (p = 0.050), no significant differences were seen between 24 hours compared to 8 hours (p = 0.246) or between 8 hours and 1 hour (p = 0.763), or between 8 hours and 4 hours (p = 0.114) or between 4 hours and 24 hours (p = 0.959).

A statistically significant difference was seen between time intervals for the control group at 1.0 dyne/cm^2, [F (3, 12) = 11.340, p = 0.001]. Post-hoc Tukey HSD showed significant differences after 4 hours compared to 1 hour (p = 0.002) and after 8 hours compared to 1 hour (p = 0.002), no significant differences were seen after 8 hours compared to 1 hour (p = 0.999), after 24 hours compared to 1 hour (p = 0.083), after 24 hours compared to 4 hours (p = 0.189) or after 8 hours compared to 1 hour (p = 0.999). For the steady group at 1.0 dyne/cm^2 a statistically significant difference was

seen between time intervals [F (2, 11) = 5.466, p = 0.028]. Post-hoc Tukey HSD showed significant difference after 4 hours compared with 1 hour (p = 0.029), and no significant difference was seen after 8 hours compared to 1 hour (p = 0.084) or after 8 hours compared with 4 hours (p = 0.778). For the pulsed group, no statistically significant difference was seen between time intervals at 1.0 dyne/cm^2 [F (2, 11) = 0.235, p = 0.795].

A statistically significant difference was seen between time intervals for the control group at 4.0 dyne/cm^2, [F (3, 12) = 7.241, p = 0.005]. Post-hoc Tukey HSD showed significant differences after 8 hours compared to 4 hours (p = 0.039) and between 8 hours and 24 hours (p = 0.004), no significant difference was seen between 4 hours compared to 1 hour (p = 0.474), between 8 hours compared to 1 hour (p = 0.401), between 4 hours and 24 hours (p = 0.582) or between 1 hours and 24 hours (p = 0.069). For the steady group at 4.0 dyne/cm^2 a statistically significant difference was seen between time intervals for the steady group [F (2, 11) = 6.096, p = 0.021]. Post-hoc Tukey HSD showed a significant difference after 8 hours flow compared with 4 hour flow (p = 0.025), no significant difference was seen between 1 hour and 4 hours (p = 0.053) or between 1 hour and 8 hours (p = 0.884). A statistically significant difference was seen between time intervals for the pulsed group at 4.0 dyne/cm^2 [F (2, 11) = 5.954, p = 0.023]. Post-hoc Tukey HSD showed a significant difference between 4 hours and 1 hour (p = 0.026) and no significant difference between 8 hours and 1 hour (p = 0.057) and no significant difference between 8 hours and 4 hours (p = 0.877).

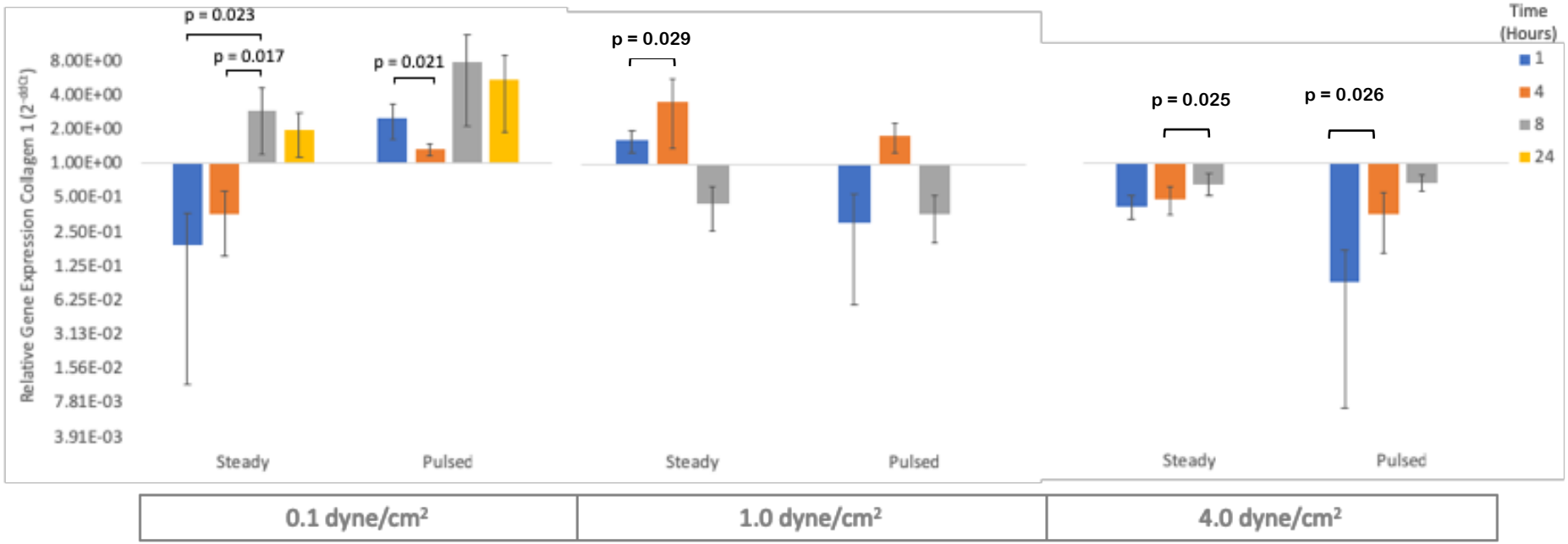

Figure 4.12 Gene expression of collagen 1 in bovine nucleus pulposus cells relative to GAPDH and control (no flow) as determined by qRT-PCR following 12 test conditions: 1, 4, 8 and 24-hour flow experiments in Ibidi VI$^{0.4}$ flow chamber at shear stress conditions of 0.1, 1.0 and 4.0 dyne/cm^2. Results are shown for three flow types; control (no flow), steady flow and pulsed flow. Control is shown at y-axis = 1. Means and 95 % confidence interval error bars are shown based on 4 technical replicates and sample size (n) of 4 bovine subjects. Statistically significant results at level $p < 0.05$ are shown for one-way ANOVA with post-hoc Tukey HSD comparing results after 1, 4, 8 and 24 hours, for each of the shear flow conditions and flow groups. No results shown for 1.0 and 4.0 dyne/cm^2 after 24 hours as no cells present on Ibidi VI$^{0.4}$ slide following flow experiments, due to detachment of cells from slide.

4.6 Collagen 2

4.6.1 Descriptive statistics

Shear Stress (dyne/cm^2)	Time (hours)	Control		Steady		Pulsed	
		Mean	*Standard Deviation*	*Mean*	*Standard Deviation*	*Mean*	*Standard Deviation*
0.1	**1**	3.11	*1.07*	2.34	*0.84*	4.85	*0.19*
	4	7.00	*1.18*	3.73	*0.42*	5.11	*1.09*
	8	5.21	*0.77*	3.53	*0.88*	3.43	*1.14*
	24	5.70	*1.14*	6.27	*1.20*	4.53	*1.37*
1.0	**1**	3.30	*1.41*	1.25	*0.56*	6.13	*1.23*
	4	4.94	*0.90*	5.52	*0.56*	7.02	*1.10*
	8	2.58	*0.29*	5.56	*1.86*	5.92	*0.69*
	24	2.10	*0.88*	-	-	-	-
4.0	**1**	5.44	*0.61*	7.72	*0.92*	7.17	*0.84*
	4	3.47	*0.89*	5.54	*1.17*	5.09	*1.31*
	8	4.44	*0.92*	5.63	*0.43*	6.36	*1.56*
	24	3.51	*0.93*	-	-	-	-

Table 4.5 Mean and standard deviation dCt values (normalized to GAPDH) for gene expression of collagen 2 for all 3 independent variable, flow type (control, steady and pulsed), shear stress (01, 1.0 and 4.0 dyne/cm^2) and time points (1, 4, 8 and 24 hours).

4.6.2 Effect of flow type on GE of collagen 2

One-way ANOVAs were used to analyse the effect of flow types; no flow, steady flow and pulsed flow, on gene expression of collagen 2. Results and statistically significant findings are shown in figure 4.13. No statistical analysis was carried out at 24 hours for the steady and pulsed groups at 1.0 and 4.0 dyne/cm^2 as noted previously due to the detachment of all cells from the slides.

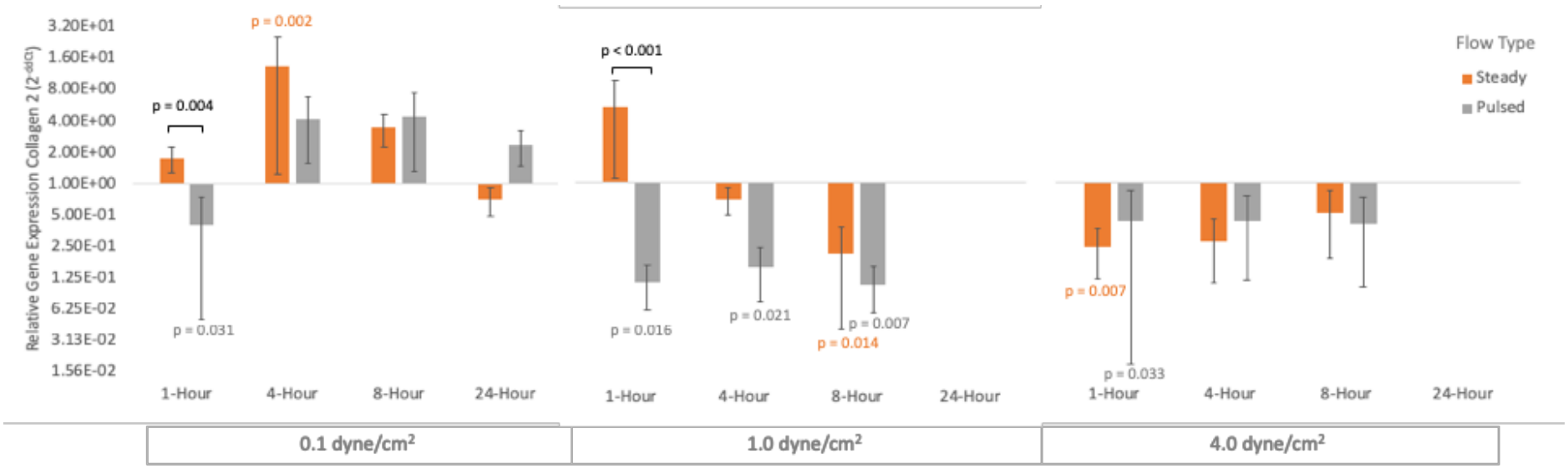

Figure 4.13 Gene expression of collagen 2 in bovine nucleus pulposus cells relative to GAPDH and control (no flow) as determined by qRT-PCR following 12 test conditions: 1, 4, 8 and 24-hour flow experiments in Ibidi VI$^{0.4}$ flow chamber at shear stress conditions of 0.1, 1.0 and 4.0 dyne/cm^2. Results are shown for three flow types; control (no flow), steady flow and pulsed flow. Control is shown at y-axis = 1. Means and 95 % confidence interval error bars are shown based on 4 technical replicates and sample size (n) of 4 bovine subjects. Statistically significant results at level $p < 0.05$ are shown for one-way ANOVA with post-hoc Tukey HSD comparing control vs steady vs pulsed flow for each of the 12 test conditions. p value above or below error bar corresponds to Tukey HSD post-hoc test result between control and flow condition (steady or pulsed). p value above comparison bar corresponds to Tukey HSD post-hoc test result between steady vs pulsed flow. No results shown for 1.0 and 4.0 dyne/cm^2 after 24 hours as no cells present on Ibidi VI$^{0.4}$ slide following flow experiments, due to detachment of cells from slide.

There was a statistically significant effect of flow type on gene expression dCt values for collagen 2 at the $p < 0.05$ level for the three flow conditions at 0.1 dyne/cm^2 after 1 hour flow, [F (2, 9) = 10.422, p = 0.005]. Post-hoc comparisons using Tukey HSD indicated that the mean score for the pulsed flow condition was significantly different than for the control (p = 0.031), and the steady flow was significantly different from the pulsed flow (p = 0.004), but the steady flow did not significantly differ from the control (p = 0.400). There was a statistically significant effect of flow type on gene expression dCt values for collagen 2 at the $p < 0.05$ level for the three flow conditions at 0.1 dyne/cm^2 after 4 hour flow, [F (2, 9) = 11.702, p = 0.003]. Post-hoc comparisons using Tukey HSD indicated that the mean score for the steady flow condition was significantly different from the control (p = 0.002), the control was not significantly different from the pulsed flow (p = 0.050), and the steady was not significantly different from the pulsed flow (p = 0.160). There was a statistically significant effect of flow type on gene expression dCt values for collagen 2 at the $p <$ 0.05 level for the three flow conditions at 0.1 dyne/cm^2 after 8 hour flow, [F (2,9) = 4.530, p = 0.044]. Post-hoc comparisons using Tukey HSD indicated that the mean score for the steady flow condition was significantly different than the control (p = 0.032), and there was a significant difference between from the control and pulsed flow (p = 0.025) and no significant difference between the pulsed flow and steady flow (p = 0.891).There was no statistically significant effect of flow type on gene expression dCt values for collagen 2 at the $p < 0.05$ level for the three flow conditions at 0.1 dyne/cm^2 after 24 hour flow, [F (2, 9) = 2.040, p =0.186].

There was a statistically significant effect of flow type on gene expression dCt values for collagen 2 at the $p < 0.05$ level for the three flow conditions at 1.0 dyne/cm^2 after 1 hour flow, [F (2, 9) = 18.818, p = 0.001]. Post-hoc comparisons using Tukey HSD indicated that the mean score for the pulsed flow condition was significantly different than the control (p = 0.016), there was a significant difference between the steady and pulsed flow ($p < 0.001$), and no significant difference between the steady and pulsed flow (p = 0.071). There was a statistically significant effect of flow type on gene expression dCt values for collagen 2 at the $p < 0.05$ level for the three flow conditions at 1.0 dyne/cm^2 after 4 hours flow, [F (2, 9) = 5.947, p = 0.023]. Post-hoc comparisons using Tukey HSD indicated that the mean score for the pulsed flow

condition was significantly different than the control (p = 0.021), and control was significantly different from the steady flow (p = 0.635), but the pulsed flow did not significantly differ from the steady (p = 0.091). There was a statistically significant effect of flow type on gene expression dCt values for collagen 2 at the $p < 0.05$ level for the three flow conditions at 1.0 dyne/cm^2 after 8 hours flow, [F (2, 9) = 9.990, p = 0.005]. Post-hoc comparisons using Tukey HSD indicated that the mean score for the steady flow conditions was significantly different than the control (p = 0.014), and control was significantly different from the pulsed flow (p = 0.007), but the pulsed flow did not significantly differ from the steady (p = 0.897).

There was a statistically significant effect of flow type on gene expression dCt values for collagen 2 at the $p < 0.05$ level for the three flow conditions at 4.0 dyne/cm^2 after 1 hour flow. [F (2, 9) = 8.933, p = 0.007]. Post-hoc comparisons using Tukey HSD indicated that the mean score for the steady flow condition was significantly different than the control (p = 0.007), there was a significant difference between the control and pulsed flow (p = 0.033), there was no significant difference between pulsed flow and steady flow (p = 0.604). There was no statistically significant effect of flow type on gene expression dCt values for collagen 2 at the $p < 0.05$ level for the three flow conditions at 4.0 dyne/cm^2 after 4 hour flow, [F (2, 9) = 3.698, p = 0.067]. There was no statistically significant effect of flow type on gene expression dCt values for collagen 2 at the $p < 0.05$ level for the three flow conditions at 4.0 dyne/cm^2 after 8 hour flow, [F (2, 9) = 3.268, p = 0.086].

4.6.3 Effect of shear stress rate on GE of collagen 2

One-way ANOVAs were used to analyse the effect of shear stress rates; 0.1, 1.0 and 4.0 dyne/cm^2, on gene expression of collagen 2. Results and statistically significant findings are shown in figure 4.14. No statistical analysis was carried out at 24 hours for the steady and pulsed groups at 1.0 and 4.0 dyne/cm^2 as noted previously due to the detachment of all cells from the slides.

There was a statistically significant effect on gene expression dCt values for collagen 2 at the $p < 0.05$ level between the three shear stress conditions 0.1, 1.0 and 4.0 dyne/cm^2 after 1 hour for control, [F (2, 9) = 5.704, p = 0.025]. Post-hoc tests using Tukey HSD indicated that there was a significant difference between 0.1 dyne/cm^2

and 4 dyne/cm^2 shear stress (p = 0.034) and no statistically significant difference between 1.0 dyne/cm^2 and 4.0 dyne/cm^2 (p = 0.050), and no significance between 0.1 dyne/cm^2 and 1.0 dyne/cm^2 (p = 0.967). There was a statistically significant effect on gene expression dCt values for collagen 2 at the $p < 0.05$ level between the three shear stress conditions 0.1, 1.0 and 4.0 dyne/cm^2 after 1 hour for steady, [F (2, 9) = 77.056, $p < 0.001$]. Post-hoc tests using Tukey HSD indicated that there was a significant difference between 0.1 dyne/cm^2 and 4 dyne/cm^2 shear stress ($p < 0.001$), a significant difference between 1.0 dyne/cm^2 and 4.0 dyne/cm^2 ($p < 0.001$), and no significance between 0.1 dyne/cm^2 and 1.0 dyne/cm^2 (p = 0.178). A statistically significant difference was seen after 1 hour for pulsed, [F (2, 9) = 7.183, p = 0.014]. Post-hoc tests using Tukey HSD showed a significant difference between 0.1 dyne/cm^2 and 4.0 dyne/cm^2 (p = 0.011), no statistically significant difference was seen between 0.1 dyne/cm^2 and 1.0 dyne/cm^2 (p = 0.148) or between 1.0 dyne/cm^2 and 4.0 dyne/cm^2 (p = 0.258).

A one-way ANOVA determined that there was a statistically significant effect on gene expression dCt values for collagen 2 at the $p < 0.05$ level between the three shear stress conditions 0.1, 1.0 and 4.0 dyne/cm^2 after 4 hours for control [F (2, 9) = 12.604, p = 0.002]. Post-hoc tests using Tukey HSD showed that there was a significant difference between 0.1 dyne/cm^2 and 4.0 dyne/cm^2 (p = 0.002), a significant difference between 0.1 dyne/cm^2 and 1.0 dyne/cm^2 (p = 0.041) and no significant difference between 1.0 dyne/cm^2 and 4.0 dyne/cm^2 (p = 0.150). A statistically significant difference was seen after 4 hours for steady flow, [F (2, 9) = 6.998, p = 0.015]. Post-hoc tests using Tukey HSD showed a significant difference between 0.1 dyne/cm^2 and 1.0 dyne/cm^2 (p = 0.026), a significant difference between 0.1 dyne/cm^2 and 4.0 dyne/cm^2 (p = 0.024), and no significant difference between 1.0 dyne/cm^2 and 4.0 dyne/cm^2 (p = 0.999). No statistically significant difference was seen between group means after 4 hours for pulsed flow, [F (2, 9) = 3.601, p = 0.071].

A one-way ANOVA determined that there was a statistically significant effect on gene expression dCt values for collagen 2 at the $p < 0.05$ level between the three shear stress conditions 0.1, 1.0 and 4.0 dyne/cm^2 after 8 hours for control, [F (2, 9) = 14.390, p = 0.002]. Post-hoc tests using Tukey HSD showed that there was a

significant difference between 0.1 dyne/cm^2 and 1.0 dyne/cm^2 (p = 0.001), a significant difference between 1.0 dyne/cm^2 and 4.0 dyne/cm^2 (p = 0.013) and no significant difference between 0.1 dyne/cm^2 and 4.0 dyne/cm^2 (p = 0.321). No statistically significant difference was seen after 8 hours steady flow, [F (2, 9) = 3.869, p = 0.061]. A statistically significant difference was seen after 8 hours for pulsed flow, [F (2, 9) = 7.119, p = 0.014]. Post-hoc tests using Tukey HSD showed that there was a significant difference between 0.1 dyne/cm^2 and 1.0 dyne/cm^2 (p = 0.038), a significant difference between 0.1 dyne/cm^2 and 4.0 dyne/cm^2 (p = 0.017) and no significant difference between 1.0 dyne/cm^2 and 4.0 dyne/cm^2 (p = 0.859).

After 24 hours the control flow group only was analysed as all cells had detached from the Ibidi VI$^{0.4}$ slides for 1.0 dyne/cm^2 and 4.0 dyne/cm^2 for steady and pulsed flow groups. There was a statistically significant difference shown between the shear stress rates for the control group; 0.1 dyne/cm^2, 1.0 dyne/cm^2 and 4.0 dyne/cm^2 at the $p < 0.05$ level, [F (2, 9) = 13.331, p = 0.002]. Post-hoc tests using Tukey HSD showed a significant difference between 0.1 dyne/cm^2 and 1.0 dyne/cm^2 (p = 0.002), and a significant difference between 0.1 dyne/cm^2 and 4.0 dyne/cm^2 (p = 0.030) and no significant difference was seen between 1.0 dyne/cm^2 and 4.0 dyne/cm^2 (p = 0.166).

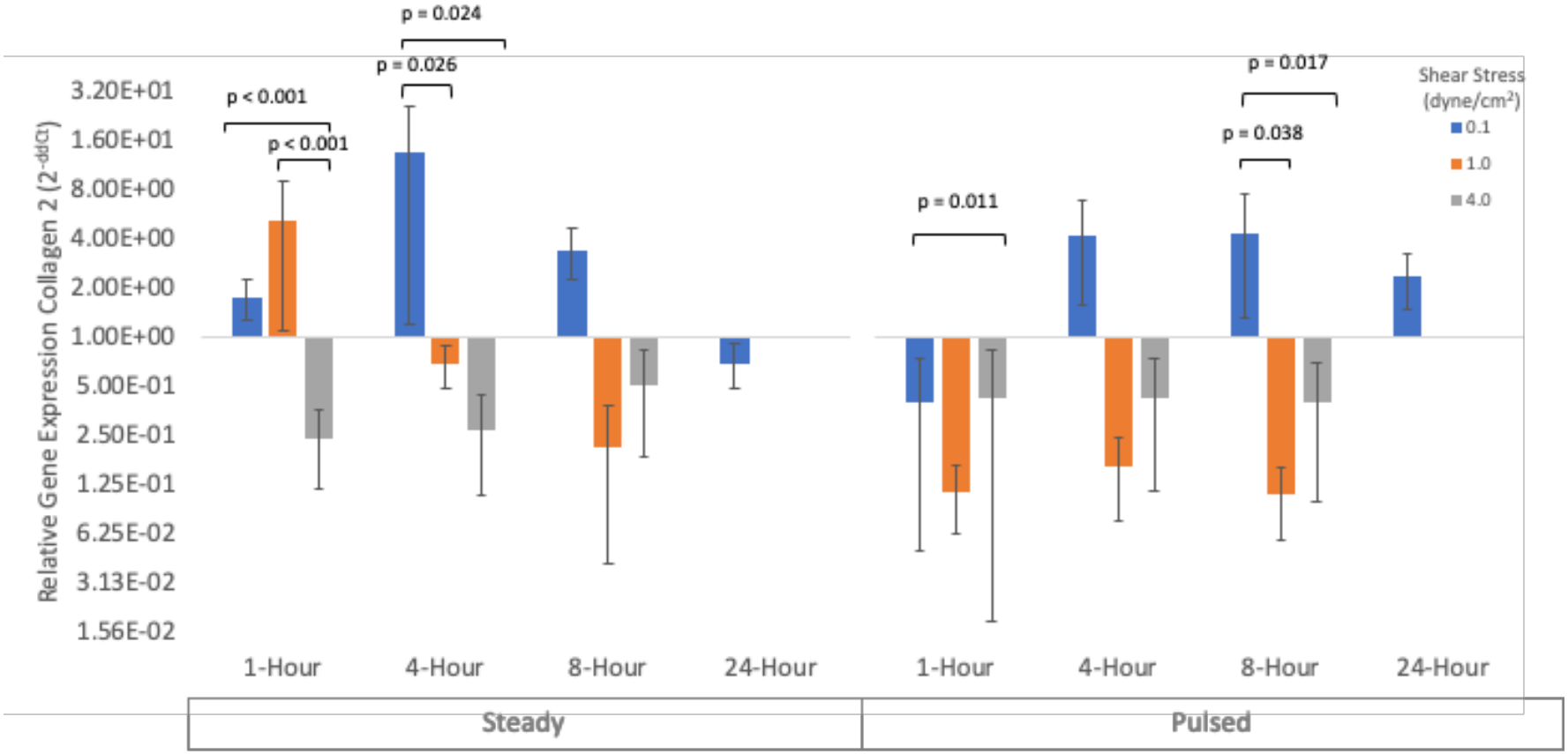

Figure 4.14 Gene expression of collagen 2 in bovine nucleus pulposus cells relative to GAPDH and control (no flow) as determined by qRT-PCR following 12 test conditions: 1, 4, 8 and 24-hour flow experiments in Ibidi VI$^{0.4}$ flow chamber at shear stress conditions of 0.1, 1.0 and 4.0 dyne/cm^2. Results are shown for three flow types; control (no flow), steady flow and pulsed flow. Control is shown at y-axis = 1. Means and 95 % confidence interval error bars are shown based on 4 technical replicates and sample size (n) of 4 bovine subjects. Statistically significant results at level $p < 0.05$ are shown for one-way ANOVA with post-hoc Tukey HSD comparing shear stress conditions 0.1 vs 1.0 vs 4.0 dyne/cm^2 flow for each of the time conditions and flow types. No results shown for 1.0 and 4.0 dyne/cm^2 after 24 hours as no cells present on Ibidi VI$^{0.4}$ slide following flow experiments, due to detachment of cells from slide.

4.6.4 Effect of duration of flow on GE of collagen 2

One-way ANOVAs were used to analyse the effect of the duration of time cells were exposed to shear stress; 1, 4, 8 and 24 hours, on gene expression of collagen 2. Results and statistically significant findings are shown in figure 4.15. No statistical analysis was carried out at 24 hours for the steady and pulsed groups at 1.0 and 4.0 dyne/cm^2 as noted previously due to the detachment of all cells from the slides.

For the control group at 0.1 dyne/cm^2 there was a statistically significant results at the $p < 0.05$ level, [F (3, 12) = 9.435, p = 0.002]. Post-hoc Tukey HSD showed a significant difference after 4 hours compared to 1 hour (p = 0.001), a significant difference was seen between 24 hours and 1 hour (p = 0.021), no significant difference between 8 hours and 1 hour (p = 0.064) or between 24 hours and 4 hours (p = 0.342) or between 8 hours and 4 hours (p = 0.130) or between 8 hours and 24 hours (p = 0.914). A statistically significant difference was seen between time intervals for the steady group at 0.1 dyne/cm^2, [F (3, 12) = 14.043, $p < 0.001$). Post-hoc Tukey HSD showed significant differences after 24 hours compared to 1 hour ($p < 0.001$), between 4 hours and 24 hours (p = 0.007) and between 8 hours and 24 hours (p = 0.004), and no significant differences were seen between 1 hours and 4 hours (p = 0.170), no significant differences between 1 hour and 8 hours (p = 0.279), no significant difference between 4 hours and 8 hours (p = 0.987). No statistically significant differences were seen between time intervals for the pulsed group at 0.1 dyne/cm^2, [F (3, 12) = 1.980, p = 0.171].

A statistically significant difference was seen between time intervals for the control group at 1.0 dyne/cm^2, [F (3, 12) = 6.688, p = 0.007]. Post-hoc Tukey HSD showed significant differences after 24 hours compared to 1 hour (p = 0.334) and after 4 hours compare to 8 hours (p = 0.021) and after 4 hours compared to 24 hours (p = 0.006), no significant differences were seen between 1 hour and 4 hours (p = 0.127), between 1 hour and 8 hours (p = 0.719) and between 8 hours and 24 hours (p = 0.893). For the steady group at 1.0 dyne/cm^2 statistically significant differences were seen between time intervals, [F (2, 9) = 17.980, p = 0.001]. Post-hoc Tukey HSD showed statistically significant differences after 4 hours compared with 1 hour (p = 0.002), and after 8 hours compared to 1 hour (p = 0.001), no significant differences

were seen after 8 hours compared with 4 hours (p = 0.999). For the pulsed group no statistically significant differences were seen between time intervals at 1.0 dyne/cm^2, [F (2, 11) = 1.273, p = 0.326].

A statistically significant difference was seen between time intervals for the control group at 4.0 dyne/cm^2 [F (3, 12) = 4.812, p = 0.020]. Post-hoc Tukey HSD showed a significant difference after 4 hours compared to 1 hour (p = 0.029), a significant difference between 24 hours compared to 1 hour (p = 0.033), no significant difference between 8 hours compared to 1 hour (p = 0.382), no significant difference was seen between 8 hours and 24 hours (p = 0.441) or between 4 hours and 8 hours (p = 0.406), or between 4 hours and 24 hours (p = 1.000). For the steady group at 4.0 dyne/cm^2 statistically significant differences seen between time intervals for the steady group [F (2, 11) = 7.647, p = 0.011]. Post-hoc Tukey HSD showed statistically significant differences after 4 hours flow compared with 1 hour flow (p = 0.018), statistically significant differences were seen between 8 hour and 1 hours (p = 0.022) and no significant differences were seen between 4 hours and 8 hours (p = 0.990). No statistically significant differences seen between time intervals for the pulsed group at 4.0 dyne/cm^2 [F (2, 11) = 2.740, p = 0.118].

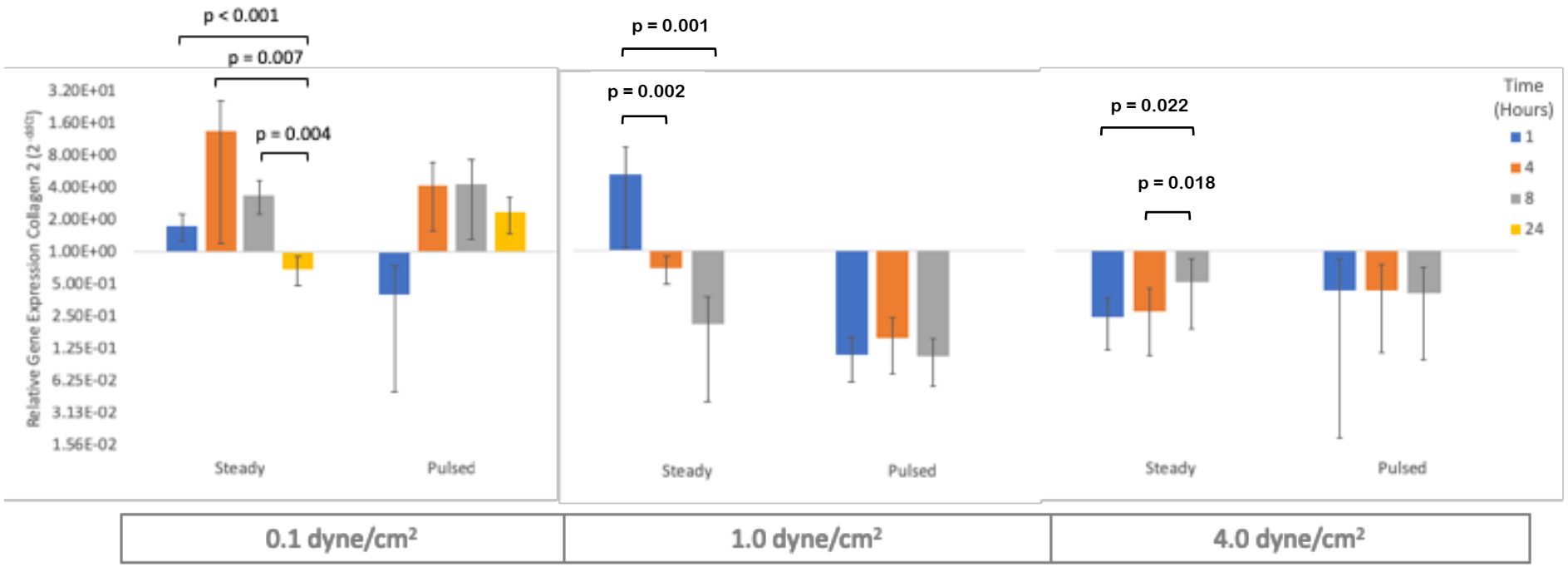

Figure 4.15 Gene expression of collagen 2 in bovine nucleus pulposus cells relative to GAPDH and control (no flow) as determined by qRT-PCR following 12 test conditions: 1, 4, 8 and 24-hour flow experiments in Ibidi VI$^{0.4}$ flow chamber at shear stress conditions of 0.1, 1.0 and 4.0 dyne/cm^2. Results are shown for three flow types; control (no flow), steady flow and pulsed flow. Control is shown at y-axis = 1. Means and 95 % confidence interval error bars are shown based on 4 technical replicates and sample size (n) of 4 bovine subjects. Statistically significant results at level $p < 0.05$ are shown for one-way ANOVA with post-hoc Tukey HSD comparing results after 1, 4, 8 and 24 hours, for each of the shear flow conditions and flow groups. No results shown for 1.0 and 4.0 dyne/cm^2 after 24 hours as no cells present on Ibidi VI$^{0.4}$ slide following flow experiments, due to detachment of cells from slide.

4.7 Aggrecan

4.7.1 Descriptive statistics

Shear Stress (dyne/cm^2)	Time (hours)	Control		Steady		Pulsed	
		Mean	*Standard Deviation*	*Mean*	*Standard Deviation*	*Mean*	*Standard Deviation*
0.1	**1**	-1.50	*1.30*	-2.02	*1.19*	-1.95	*1.01*
	4	7.24	*0.52*	5.58	*0.73*	3.91	*2.01*
	8	0.39	*0.91*	-0.65	*0.75*	-0.80	*0.47*
	24	5.14	*1.96*	3.23	*1.13*	3.09	*2.53*
1.0	**1**	2.89	*1.50*	0.48	*0.87*	4.02	*1.28*
	4	2.76	*1.15*	4.85	*1.04*	4.09	*1.55*
	8	0.36	*1.26*	0.79	*1.36*	4.29	*0.88*
	24	1.61	*0.95*	-	-	-	-
4.0	**1**	1.98	*1.80*	5.46	*1.02*	6.25	*1.37*
	4	1.80	*1.44*	2.34	*1.30*	3.84	*1.73*
	8	0.36	*0.46*	1.89	*0.90*	5.14	*1.59*
	24	1.34	*0.46*	-	-	-	-

Table 4.6 Mean and standard deviation dCt values (normalized to GAPDH) for gene expression of aggrecan for all 3 independent variables; flow type (control, steady and pulsed), shear stress (01, 1.0 and 4.0 dyne/cm^2) and time points (1, 4, 8 and 24 hours).

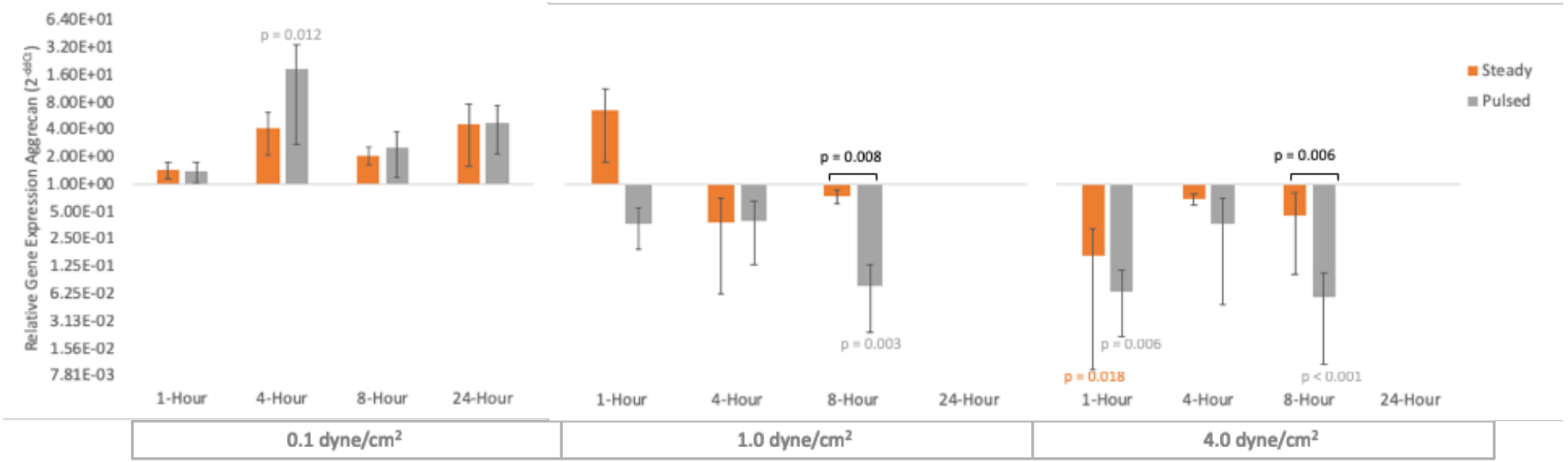

Figure 4.16 Gene expression of aggrecan in bovine nucleus pulposus cells relative to GAPDH and control (no flow) as determined by qRT-PCR following 12 test conditions: 1, 4, 8 and 24-hour flow experiments in Ibidi VI$^{0.4}$ flow chamber at shear stress conditions of 0.1, 1.0 and 4.0 dyne/cm^2. Results are shown for three flow types; control (no flow), steady flow and pulsed flow. Control is shown at y-axis = 1. Means and 95 % confidence interval error bars are shown based on 4 technical replicates and sample size (n) of 4 bovine subjects. Statistically significant results at level $p < 0.05$ are shown for one-way ANOVA with post-hoc Tukey HSD comparing control vs steady vs pulsed flow for each of the 12 test conditions. p value above or below error bar corresponds to Tukey HSD post-hoc test result between control and flow condition (steady or pulsed). p value above comparison bar corresponds to Tukey HSD post-hoc test result between steady vs pulsed flow. No results shown for 1.0 and 4.0 dyne/cm^2 after 24 hours as no cells present on Ibidi VI$^{0.4}$ slide following flow experiments, due to detachment of cells from slide.

4.7.2 Effect of flow type on GE of aggrecan

One-way ANOVAs were used to analyse the effect of flow types; no flow, steady flow and pulsed flow, on gene expression of aggrecan. Results and statistically significant findings are shown in figure 4.16. No statistical analysis was carried out at 24 hours for the steady and pulsed groups at 1.0 and 4.0 dyne/cm^2 as noted previously due to the detachment of all cells from the slides.

There was no statstically significant effect of flow type on gene expression dCt values for aggrecan at the $p < 0.05$ level for the three flow conditions at 0.1 dyne/cm^2 after 1 hour flow, [F (2, 9) = 0.233, p = 0.797]. There was a statistically significant effect of flow type on gene expression dCt values for aggrecan at the $p < 0.05$ level for the three flow conditions at 0.1 dyne/cm^2 after 4 hour flow, [F (2, 9) = 6.837, p = 0.016]. Post-hoc comparisons using Tukey HSD indicated that the mean score for the pulsed flow condition was significantly different than the control (p = 0.012), and no significant difference between control and pulsed flow (p = 0.209), and the pulsed flow did not significantly differ from the steady (p = 0.209). There was no statistically significant effect of flow type on gene expression dCt values for aggrecan at the p < 0.05 level for the three flow conditions at 0.1 dyne/cm^2 after 8 hour flow, [F (2, 9) = 3.123, p = 0.093]. There was no statistically significant effect of flow type on gene expression dCt values for aggrecan at the $p < 0.05$ level for the three flow conditions at 0.1 dyne/cm^2 after 24 hour flow, [F (2, 9) = 1.360, p = 0.305].

There was a statistically significant effect of flow type on gene expression dCt values for aggrecan at the $p < 0.05$ level for the three flow conditions at 1.0 dyne/cm^2 after 1 hour flow, [F (2, 9) = 8.478, p = 0.009]. Post-hoc comparisons using Tukey HSD indicated that the mean score for the steady flow condition was significantly different than the pulsed (p = 0.008), and no significant differences were seen between control and steady flow (p = 0.054), or between the control and pulsed flow (p = 0.435). There was no statistically significant effect of flow type on gene expression dCt values for aggrecan at the $p < 0.05$ level for the three flow conditions at 1.0 dyne/cm^2 after 4 hour flow, [F (2, 9) = 2.806, p = 0.113]. There was a statistically significant effect of flow type on gene expression dCt values for aggrecan at the $p < 0.05$ level for the three flow conditions at 1.0 dyne/cm^2 after 8 hour flow, [F (2, 9) = 13.203, p =

0.002]. Post-hoc comparisons using Tukey HSD indicated that the mean score for the control was significantly different than for pulsed flow ($p = 0.003$) and the steady flow condition was significantly different than the pulsed ($p = 0.006$), and no significant difference was seen between control and steady flow ($p = 0.867$).

There was a statistically significant effect of flow type on gene expression dCt values for aggrecan at the $p < 0.05$ level for the three flow conditions at 4.0 dyne/cm^2 after 1 hour flow, [F (2, 9) = 10.062, $p = 0.005$]. Post-hoc comparisons using Tukey HSD indicated that the mean score for the control was significantly different than the steady ($p = 0.018$), and the control was significantly different from the pulsed flow ($p = 0.006$), but the pulsed flow did not significantly differ from the steady flow ($p = 0.722$). There was no statistically significant effect of flow type on gene expression dCt values for aggrecan at the $p < 0.05$ level for the three flow conditions at 4.0 dyne/cm^2 after 4 hour flow, [F (2, 9) = 1.977, $p = 0.194$]. There was a statistically significant effect of flow type on gene expression dCt values for aggrecan at the $p < 0.05$ level for the three flow conditions at 4.0 dyne/cm^2 after 8 hour flow, [F (2, 9) = 20.156, $p < 0.001$]. Post-hoc comparisons using Tukey HSD indicated that the mean score for the control was significantly different than the pulsed ($p < 0.001$), and the steady was significantly different from the pulsed flow ($p = 0.006$), but the control did not significantly differ from the steady ($p = 0.172$).

4.7.3 Effect of shear stress rate on GE of aggrecan

One-way ANOVAs were used to analyse the effect of shear stress rates; 0.1, 1.0 and 4.0 dyne/cm^2, on gene expression of aggrecan. Results and statistically significant findings are shown in figure 4.17. No statistical analysis was carried out at 24 hours for the steady and pulsed groups at 1.0 and 4.0 dyne/cm^2 as noted previously due to the detachment of all cells from the slides.

There was a statistically significant effect on gene expression dCt values for aggrecan at the $p < 0.05$ level between the three shear stress conditions 0.1, 1.0 and 4.0 dyne/cm^2 after 1 hour for control, [F (2, 9) = 9.012, $p = 0.007$]. Post-hoc tests using Tukey HSD showed there was a significant difference between 0.1 dyne/cm^2 and 1.0 dyne/cm^2 ($p = 0.008$), and significant difference between 0.1 dyne/cm^2 and 4.0 dyne/cm^2 ($p = 0.027$), and no significant difference between 1.0 dyne/cm^2 and 4.0

dyne/cm^2 (p = 0.693). A statistically significant difference was seen after 1 hour for steady flow, [F (2, 9) = 54.340, p < 0.001]. Post-hoc tests using Tukey HSD showed there was a significant difference between 0.1 dyne/cm^2 and 4.0 dyne/cm^2 (p < 0.001), a significant difference between 1.0 dyne/cm^2 and 4.0 dyne/cm^2 (p < 0.001) and a significant difference was seen between 0.1 dyne/cm^2 and 1.0 dyne/cm^2 (p = 0.019). A statistically significant difference was seen after 1 hour for pulsed flow, [F (2, 9) = 47.537, p < 0.001]. Post-hoc tests using Tukey HSD showed there was a significant difference between 0.1 dyne/cm^2 and 1.0 dyne/cm^2 (p < 0.001), a significant difference between 0.1 dyne/cm^2 and 4.0 dyne/cm^2 (p < 0.001), no significant difference was seen between 1.0 dyne/cm^2 and 4.0 dyne/cm^2 (p = 0.072).

A one-way ANOVA determined that there was a statistically significant effect on gene expression dCt values for aggrecan at the p < 0.05 level between the three shear stress conditions 0.1, 1.0 and 4.0 dyne/cm^2 after 4 hours for control, [F (2, 9) = 27.744, p < 0.001]. Post-hoc tests using Tukey HSD showed there was a significant difference between 0.1 dyne/cm^2 and 1.0 dyne/cm^2 (p = 0.001), a significant difference between 0.1 dyne/cm^2 and 4.0 dyne/cm^2 (p < 0.001), and no significant difference between 1.0 dyne/cm^2 and 4.0 dyne/cm^2 (p = 0.461). A statistically dignificant difference was seen after 4 hours for steady flow, [F (2, 9) = 10.436, p = 0.005]. Post-hoc tests using Tukey HSD showed there was a significant difference between 0.1 dyne/cm^2 and 4.0 dyne/cm^2 (p = 0.005), a significant difference between 1.0 dyne/cm^2 and 4.0 dyne/cm^2 (p = 0.020) and no significant difference between 0.1 dyne/cm^2 and 1.0 dyne/cm^2 (p = 0.610). No statistically significant difference was seen after 4 hours for pulsed flow, [F (2, 9) = 0.021, p = 0.979].

A one-way ANOVA determined that there was no statistically significant effect on gene expression dCt values for aggrecan at the p < 0.05 level between the three shear stress conditions 0.1, 1.0 and 4.0 dyne/cm^2 after 8 hours for control, [F (2, 9) = 0.001, p = 0.999]. A statistically significant differences was seen after 8 hours steady flow, [F (2, 9) = 6.026, p = 0.022]. Post-hoc tests using Tukey HSD showed there was a significant difference between 0.1 dyne/cm^2 and 4.0 dyne/cm^2 (p = 0.018), and no significant difference between 0.1 dyne/cm^2 and 1.0 dyne/cm^2 (p = 0.175), and no significant difference between 1.0 dyne/cm^2 and 4.0 dyne/cm^2 (p = 0.341).

A statistically significant difference was seen after 8 hours for pulsed, [F (2, 9) = 35.157, $p < 0.001$]. Post-hoc tests using Tukey HSD showed there was a significant difference between 0.1 dyne/cm^2 and 1.0 dyne/cm^2 ($p < 0.001$), a significant difference between 0.1 dyne/cm^2 and 4.0 dyne/cm^2 ($p < 0.001$), and no significant difference between 1.0 dyne/cm^2 and 4.0 dyne/cm^2 ($p = 0.535$).

After 24 hours the control flow group only was analysed as almost all cells had detached from the Ibidi VI$^{0.4}$ slides for 1.0 dyne/cm^2 and 4.0 dyne/cm^2 for steady and pulsed flow groups. There was a statistically significant difference shown between the shear stress rates for the control group; 0.1 dyne/cm^2, 1.0 dyne/cm^2 and 4.0 dyne/cm^2 at the $p < 0.05$ level, [F (2, 9) = 10.806, $p = 0.004$]. Post-hoc tests using Tukey HSD showed a significant difference between 0.1 dyne/cm^2 and 1.0 dyne/cm^2 ($p = 0.010$), and significant difference between 0.1 dyne/cm^2 and 4.0 dyne/cm^2 ($p = 0.006$), and no significance difference between 1.0 dyne/cm^2 and 4.0 dyne/cm^2 ($p = 0.951$).

4.7.4 Effect of duration of flow on GE of aggrecan

One-way ANOVAs were used to analyse the effect of the duration of time cells were exposed to shear stress; 1, 4, 8 and 24 hours, on gene expression of aggrecan. Results and statistically significant findings are shown in figure 4.18. No statistical analysis was carried out at 24 hours for the steady and pulsed groups at 1.0 and 4.0 dyne/cm^2 as noted previously due to the detachment of all cells from the slides.

For the control group at 0.1 dyne/cm^2 there was a statistically significant result at the $p < 0.05$ level, [F (3, 12) = 39.793, $p < 0.001$]. Post-hoc Tukey HSD showed a significant difference after 4 hours compared to 1 hour ($p < 0.001$), a significant difference between 24 hours and 1 hours ($p < 0.001$) and a significant difference between 4 hour and 8 hours ($p < 0.001$) and between 8 hours and 24 hours ($p = 0.001$). No significant difference was seen between 1 hours and 8 hours ($p = 0.217$) or between 4 hours and 24 hours ($p = 0.150$). A statistically significant difference was seen between time intervals for the steady group at 0.1 dyne/cm^2, [F (3, 12) = 51.876, $p < 0.001$). Post-hoc Tukey HSD showed a significant difference after 4 hours compared to 1 hour ($p < 0.001$) and a significant difference was seen between 4 hours and 24 hours ($p = 0.023$), between 8 and 24 hours ($p = 0.001$), between 8

hour and 4 hours ($p < 0.001$) and between 4 hours and 24 hours ($p = 0.023$). No significant difference was seen between 1 hour and 8 hours ($p = 0.242$). A statistically significant difference was seen between time intervals for the pulsed group at 0.1 dyne/cm^2, [F (3, 12) = 11.340, $p = 0.001$]. Post-hoc Tukey HSD showed a significant difference after 4 hours compared to 1 hour ($p = 0.002$) and between 1 hours and 24 hours ($p = 0.006$), between 4 hours and 8 hours ($p = 0.010$) and between 8 hours and 24 hours ($p = 0.032$). No significant differences were seen between 8 hours and 1 hours ($p = 0.778$) or between 4 hours and 24 hours ($p = 0.900$).

No statistically significant differences were seen between time intervals for the control group at 1.0 dyne/cm^2, [F (3, 12) = 2.933, $p = 0.092$]. For the steady group at 1.0 dyne/cm^2 statistically significant differences were seen between time intervals [F (2, 11) = 19.316, $p = 0.001$]. Post-hoc Tukey HSD showed a significant difference after 4 hours compared to 1 hour ($p = 0.001$), and between 4 hours and 8 hours ($p = 0.002$), no significant difference was seen between 8 hours and 1 hours ($p = 0.918$). For the pulsed group no statistically significant differences were seen between time intervals at 1.0 dyne/cm^2, [F (2, 11) = 0.049, $p = 0.952$].

No statistically significant differences were seen between time intervals for the control group at 4.0 dyne/cm^2 [F (3, 12) = 1.467, $p = 0.273$]. For the steady group at 4.0 dyne/cm^2 a statistically significant difference was seen between time intervals for the steady group [F (2, 11) = 12.795, $p = 0.002$]. Post-hoc Tukey HSD showed significant differences after 8 hours compared to 1 hour ($p = 0.018$), no significant differences were seen between 4 hours and 1 hours ($p = 0.062$), or between 4 hours and 8 hours ($p = 1.000$). No statistically significant differences seen between time intervals for the pulsed group at 4.0 dyne/cm^2 [F (2, 11) = 2.364, $p = 0.150$].

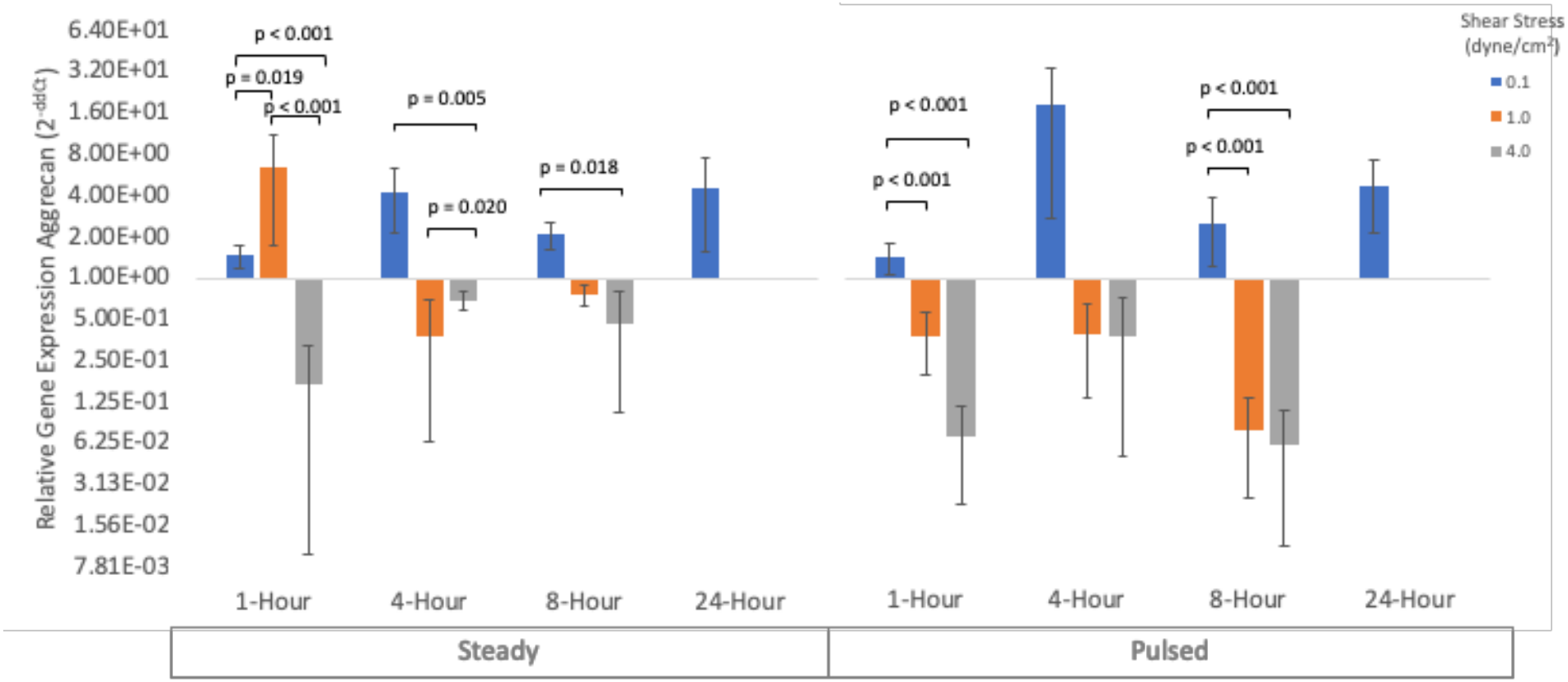

Figure 4.17 Gene expression of aggrecan in bovine nucleus pulposus cells relative to GAPDH and control (no flow) as determined by qRT-PCR following 12 test conditions: 1, 4, 8 and 24-hour flow experiments in Ibidi VI$^{0.4}$ flow chamber at shear stress conditions of 0.1, 1.0 and 4.0 dyne/cm^2. Results are shown for three flow types; control (no flow), steady flow and pulsed flow. Control is shown at y-axis = 1. Means and 95 % confidence interval error bars are shown based on 4 technical replicates and sample size (n) of 4 bovine subjects. Statistically significant results at level p<0.05 are shown for one-way ANOVA with post-hoc Tukey HSD comparing shear stress conditions 0.1 vs 1.0 vs 4.0 dyne/cm^2 flow for each of the time conditions and flow types. No results shown for 1.0 and 4.0 dyne/cm^2 after 24 hours as no cells present on Ibidi VI$^{0.4}$ slide following flow experiments, due to detachment of cells from slide.

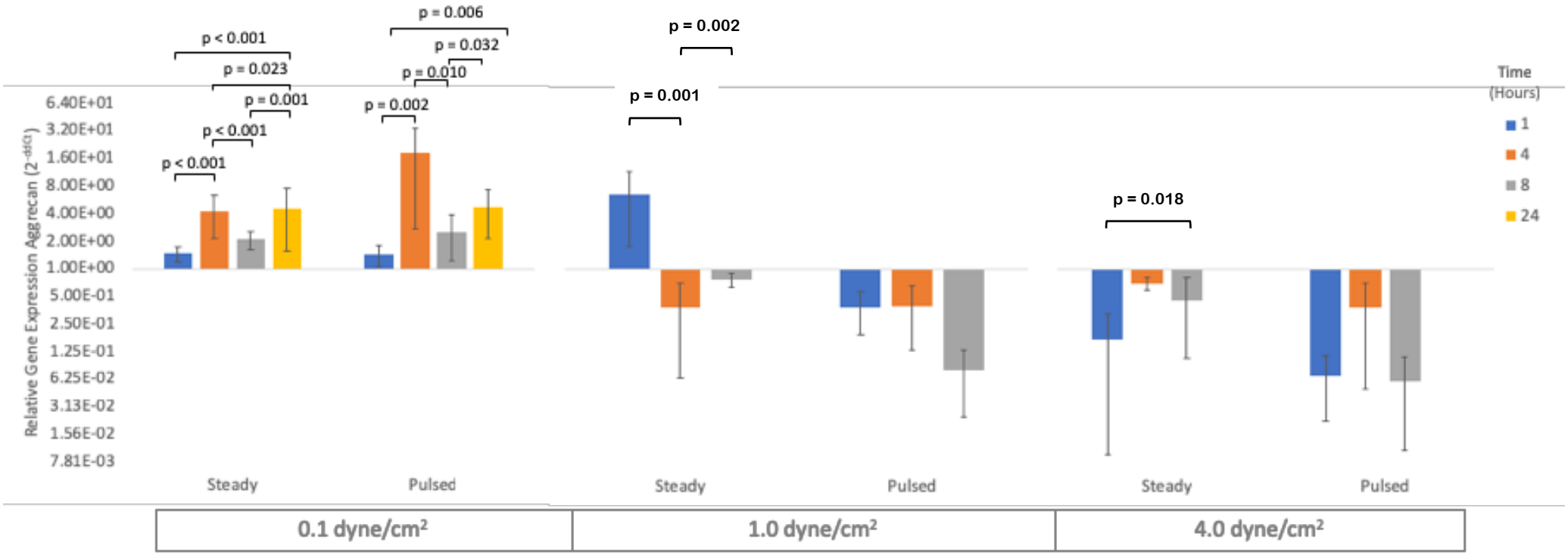

Figure 4.18 Gene expression of aggrecan in bovine nucleus pulposus cells relative to GAPDH and control (no flow) as determined by qRT-PCR following 12 test conditions: 1, 4, 8 and 24-hour flow experiments in Ibidi VI$^{0.4}$ flow chamber at shear stress conditions of 0.1, 1.0 and 4.0 dyne/cm^2. Results are shown for three flow types; control (no flow), steady flow and pulsed flow. Control is shown at y-axis = 1. Means and 95 % confidence interval error bars are shown based on 4 technical replicates and sample size (n) of 4 bovine subjects. Statistically significant results at level p<0.05 are shown for one-way ANOVA with post-hoc Tukey HSD comparing results after 1, 4, 8 and 24 hours, for each of the shear flow conditions and flow groups. No results shown for 1.0 and 4.0 dyne/cm^2 after 24 hours as no cells present on Ibidi VI$^{0.4}$ slide following flow experiments, due to detachment of cells from slide.

4.8 Aggrecanase 1

4.8.1 Descriptive statistics

Shear Stress (dyne/cm^2)	Time (hours)	Control		Steady		Pulsed	
		Mean	*Standard Deviation*	*Mean*	*Standard Deviation*	*Mean*	*Standard Deviation*
0.1	**1**	0.70	*0.77*	-0.30	*0.38*	-0.15	*0.37*
	4	2.16	*1.15*	0.20	*0.41*	1.62	*0.87*
	8	-0.03	*0.49*	1.24	*0.79*	0.64	*0.59*
	24	0.80	*1.32*	0.09	*1.03*	0.54	*1.17*
1.0	**1**	-1.17	*0.83*	1.39	*3.14*	0.97	*1.28*
	4	-0.46	*1.18*	2.13	*1.42*	3.86	*0.71*
	8	0.14	*0.96*	-0.41	*0.65*	1.14	*0.78*
	24	-0.55	*1.35*	-	-	-	-
4.0	**1**	1.62	*1.75*	2.76	*1.38*	0.93	*1.94*
	4	-0.56	*0.89*	-1.37	*1.13*	-1.22	*0.82*
	8	0.84	*0.54*	0.15	*0.21*	2.10	*1.39*
	24	0.75	*1.06*	-	-	-	-

Table 4.7 Mean and standard deviation dCt values (normalized to GAPDH) for gene expression of aggrecanase 1 for all 3 independent variables; flow type (control, steady and pulsed), shear stress (01, 1.0 and 4.0 dyne/cm^2) and time points (1, 4, 8 and 24 hours).

4.8.2 Effect of flow type on GE of aggrecanase 1

One-way ANOVAs were used to analyse the effect of flow types; no flow, steady flow and pulsed flow, on gene expression of aggrecanase 1. Results and statistically significant findings are shown in figure 4.19. No statistical analysis was carried out at 24 hours for the steady and pulsed groups at 1.0 and 4.0 dyne/cm^2 as noted previously due to the detachment of all cells from the slides.

There was no statistically significant effect of flow type on gene expression dCt values for aggrecanase 1 at the $p < 0.05$ level for the three flow conditions at 0.1 dyne/cm^2 after 1 hour flow, [F (2, 9) = 3.913, p = 0.060]. There was a statistically significant effect of flow type on gene expression dCt values for aggrecanase 1 at the $p < 0.05$ level for the three flow conditions at 0.1 dyne/cm^2 after 4 hours flow, [F (2, 9)

= 5.459, p = 0.028]. Post-hoc comparisons using Tukey HSD indicated that the mean score for the steady flow conditions was significantly different than the control (p = 0.027), there was no significant difference between the control and pulsed flow (p = 0.665), or between the pulsed and steady flow (p = 0.104). There was no statistically significant effect of flow type on gene expression dCt values for aggrecanase 1 at the $p < 0.05$ level for the three flow conditions at 0.1 dyne/cm^2 after 8 hours flow, [F (2, 9) = 3.967, p = 0.058]. There was no statistically significant effect of flow type on gene expression dCt values for aggrecanase 1 at the $p < 0.05$ level for the three flow conditions at 0.1 dyne/cm^2 after 24 hours flow, [F (2, 11) = 0.371, p = 0.700].

There was no statistically significant effect of flow type on gene expression dCt values for aggrecanase 1 at the $p < 0.05$ level for the three flow conditions at 1.0 dyne/cm^2 after 1 hour flow, [F (2, 9) = 1.855, p = 0.212]. There was a statistically significant effect of flow type on gene expression dCt values for aggrecanase 1 at the $p < 0.05$ level for the three flow conditions at 1.0 dyne/cm^2 after 4 hour flow, [F (2, 9) = 14.479, p = 0.002]. Post-hoc comparisons using Tukey HSD indicated that the mean score for the steady flow conditions was significantly different than the control (p = 0.026), and the mean score for pulsed was significantly different from the control (p = 0.001), but the pulsed flow did not significantly differ from the steady (p = 0.135). There was no statistically significant effect of flow type on gene expression dCt values for aggrecanase 1 at the $p < 0.05$ level for the three flow conditions at 1.0 dyne/cm^2 after 8 hours flow, [F (2, 9) = 3.826, p = 0.063].

There was no statistically significant effect of flow type on gene expression dCt values for aggrecanase 1 at the $p < 0.05$ level for the three flow conditions at 4.0 dyne/cm^2 after 1 hour flow, [F (2, 9) = 1.172, p = 0.353]. There was no statistically significant effect of flow type on gene expression dCt values for aggrecanase 1 at the $p < 0.05$ level for the three flow conditions at 4.0 dyne/cm^2 after 4 hours flow, [F (2, 9) = 0.803, p = 0.477]. There was a statistically significant effect of flow type on gene expression dCt values for aggrecanase 1 at the $p < 0.05$ level for the three flow conditions at 4.0 dyne/cm^2 after 8 hours flow, [F (2, 9) = 5.189, p = 0.032]. Post-hoc comparisons using Tukey HSD indicated that the mean score for the steady flow conditions was significantly different than the pulsed (p = 0.027), there was no

significant difference between the steady flow and control (p = 0.524) or between the pulsed flow and control (p = 0.155).

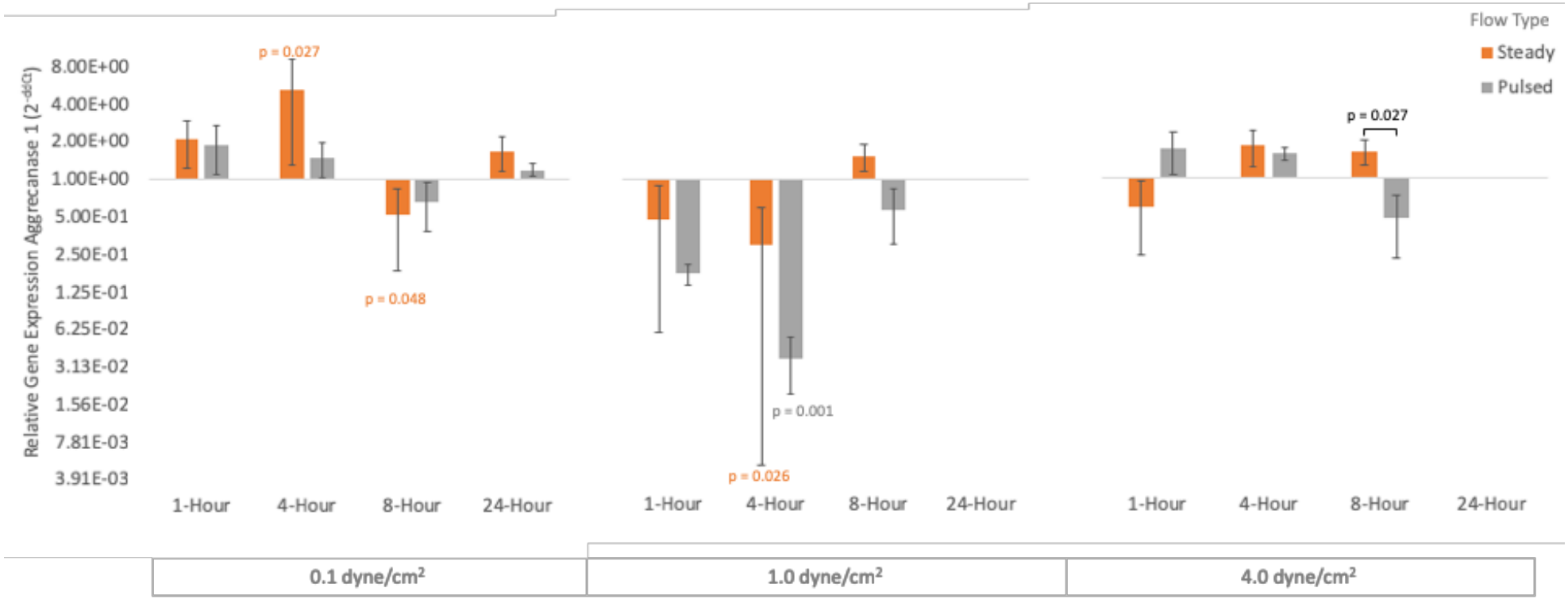

Figure 4.19 Gene expression of aggrecanase 1 in bovine nucleus pulposus cells relative to GAPDH and control (no flow) as determined by qRT-PCR following 12 test conditions: 1, 4, 8 and 24-hour flow experiments in Ibidi VI$^{0.4}$ flow chamber at shear stress conditions of 0.1, 1.0 and 4.0 dyne/cm^2. Results are shown for three flow types; control (no flow), steady flow and pulsed flow. Control is shown at y-axis = 1. Means and 95 % confidence interval error bars are shown based on 4 technical replicates and sample size (n) of 4 bovine subjects. Statistically significant results at level p<0.05 are shown for one-way ANOVA with post-hoc Tukey HSD comparing control vs steady vs pulsed flow for each of the 12 test conditions. p value above or below error bar corresponds to Tukey HSD post-hoc test result between control and flow condition (steady or pulsed). p value above comparison bar corresponds to Tukey HSD post-hoc test result between steady vs pulsed flow. No results shown for 1.0 and 4.0 dyne/cm^2 after 24 hours as no cells present on Ibidi VI$^{0.4}$ slide following flow experiments, due to detachment of cells from slide.

4.8.3 Effect of shear stress rate on GE of aggrecanase 1

One-way ANOVAs were used to analyse the effect of shear stress rates; 0.1, 1.0 and 4.0 dyne/cm^2, on gene expression of aggrecanase 1. Results and statistically significant findings are shown in figure 4.20. No statistical analysis was carried out at 24 hours for the steady and pulsed groups at 1.0 and 4.0 dyne/cm^2 as noted previously due to the detachment of all cells from the slides.

A one-way ANOVA determined that there was a statistically significant effect on gene expression dCt values for aggrecanase 1 at the $p < 0.05$ level between the three shear stress conditions 0.1, 1.0 and 4.0 dyne/cm^2 after 1 hour for control, [F (2, 9) = 5.600, p = 0.026]. Post-hoc Tukey HSD showed a significant difference between 1.0 dyne/cm^2 and 4.0 dyne/cm^2 (p = 0.023), no significant difference between 0.1 dyne/cm^2 and 1.0 dyne/cm^2 (p = 0.126), and no significance between 0.1 dyne/cm^2 and 4.0 dyne/cm^2 (p = 0.543). No statistically significant difference was seen after 1 hour for steady flow, [F (2, 9) = 2.363, p = 0.150]. No statistically significant difference was seen after 1 hour for pulsed flow [F (2, 9) = 0.874, p = 0.450].

A one-way ANOVA determined that there was a statistically significant effect on gene expression dCt values for aggrecanase 1 at the $p < 0.05$ level between the three shear stress conditions 0.1, 1.0 and 4.0 dyne/cm^2 after 4 hours for control, [F (2, 6) = 8.068, p = 0.010]. Post-hoc tests using Tukey HSD showed that there was a significant difference between 0.1 dyne/cm^2 and 1.0 dyne/cm^2 (p = 0.019), a significant difference between 0.1 dyne/cm^2 and 4.0 dyne/cm^2 (p = 0.016), and no significant difference between 1.0 dyne/cm^2 and 4.0 dyne/cm^2 (p = 0.989). A statistically significant difference was seen after 4 hours for steady flow, [F (2, 9) = 10.601, p = 0.004]. Post-hoc tests using Tukey HSD showed there was a significant difference between 1.0 dyne/cm^2 and 4.0 dyne/cm^2 (p = 0.003), no significant difference between 0.1 dyne/cm^2 and 1.0 dyne/cm^2 (p = 0.074), and no significance difference between 0.1 dyne/cm^2 and 4.0 dyne/cm^2 (p = 0.154). A statistically significant difference was seen after 4 hours for pulsed flow, [F (2, 6) = 40.403, $p < 0.001$]. Post-hoc tests using Tukey HSD showed that there was a significant difference between 1.0 dyne/cm^2 and 4.0 dyne/cm^2 ($p < 0.001$), a significant difference between 0.1 dyne/cm^2 and 1.0 dyne/cm^2 (p = 0.008), and a significant difference between 0.1 dyne/cm^2 and 4.0 dyne/cm^2 (p = 0.002).

A one-way ANOVA determined that there was no statistically significant effect on gene expression dCt values for aggrecanase 1 at the $p < 0.05$ level between the three shear stress conditions 0.1, 1.0 and 4.0 dyne/cm^2 after 8 hours for control, [F (2, 9) = 1.758, p = 0.227]. A statistically significant differences was seen after 8 hours steady flow, [F (2, 9) = 7.721, p = 0.011]. Post-hoc tests using Tukey HSD showed there was a significant difference between 0.1 dyne/cm^2 and 1.0 dyne/cm^2 (p = 0.010). no significant difference was seen between 0.1 dyne/cm^2 and 4.0 dyne/cm^2 (p = 0.072) and no significant difference between 1.0 dyne/cm^2 and 4.0 dyne/cm^2 (p = 0.428). No statistically significant differences were seen after 8 hours for pulsed flow, [F (2, 9) = 2.286, p = 0.157].

After 24 hours the control flow group only was analysed as all cells had detached from the Ibidi VI$^{0.4}$ slides for 1.0 dyne/cm^2 and 4.0 dyne/cm^2 for steady and pulsed flow groups. There was no statistically significant difference shown between the shear stress rates for the control group; 0.1 dyne/cm^2, 1.0 dyne/cm^2 and 4.0 dyne/cm^2 at the $p < 0.05$ level, [F (2, 9) = 1.500, p = 0.274].

4.8.4 Effect of duration of flow on GE of aggrecanase 1

One-way ANOVAs were used to analyse the effect of the duration of time cells were exposed to shear stress; 1, 4, 8 and 24 hours, on gene expression of aggrecanase 1. Results and statistically significant findings are shown in figure 21. No statistical analysis was carried out at 24 hours for the steady and pulsed groups at 1.0 and 4.0 dyne/cm^2 as noted previously due to the detachment of all cells from the slides.

For the control group at 0.1 dyne/cm^2 there was no statistically significant result at the $p < 0.05$ level, [F (3, 12) = 3.409, p = 0.053]. No statistically significant difference was seen between time intervals for the steady group at 0.1 dyne/cm^2, [F (3, 12) = 3.444, p = 0.052). No statistically significant difference was seen between time intervals for the pulsed group at 0.1 dyne/cm^2, [F (3, 12) = 3.219, p = 0.061].

No statistically significant difference was seen between time intervals for the control group at 1.0 dyne/cm^2, [F (3, 12) = 0.954, p = 0.446]. For the steady group at 1.0 dyne/cm^2 no statistically significant difference was seen between time intervals, [F (2,

11) = 1.666, $p = 0.242$]. For the pulsed group a statistically significant difference was seen between time intervals at 1.0 dyne/cm^2, [F (2, 11) = 11.442, $p = 0.003$]. Post-hoc Tukey HSD showed a significant difference after 4 hours flow compared with 1 hour flow ($p = 0.005$), a significant difference was seen between 4 hours and 8 hours ($p = 0.008$), no significant difference was seen between 8 hour and 1 hours ($p = 0.965$).

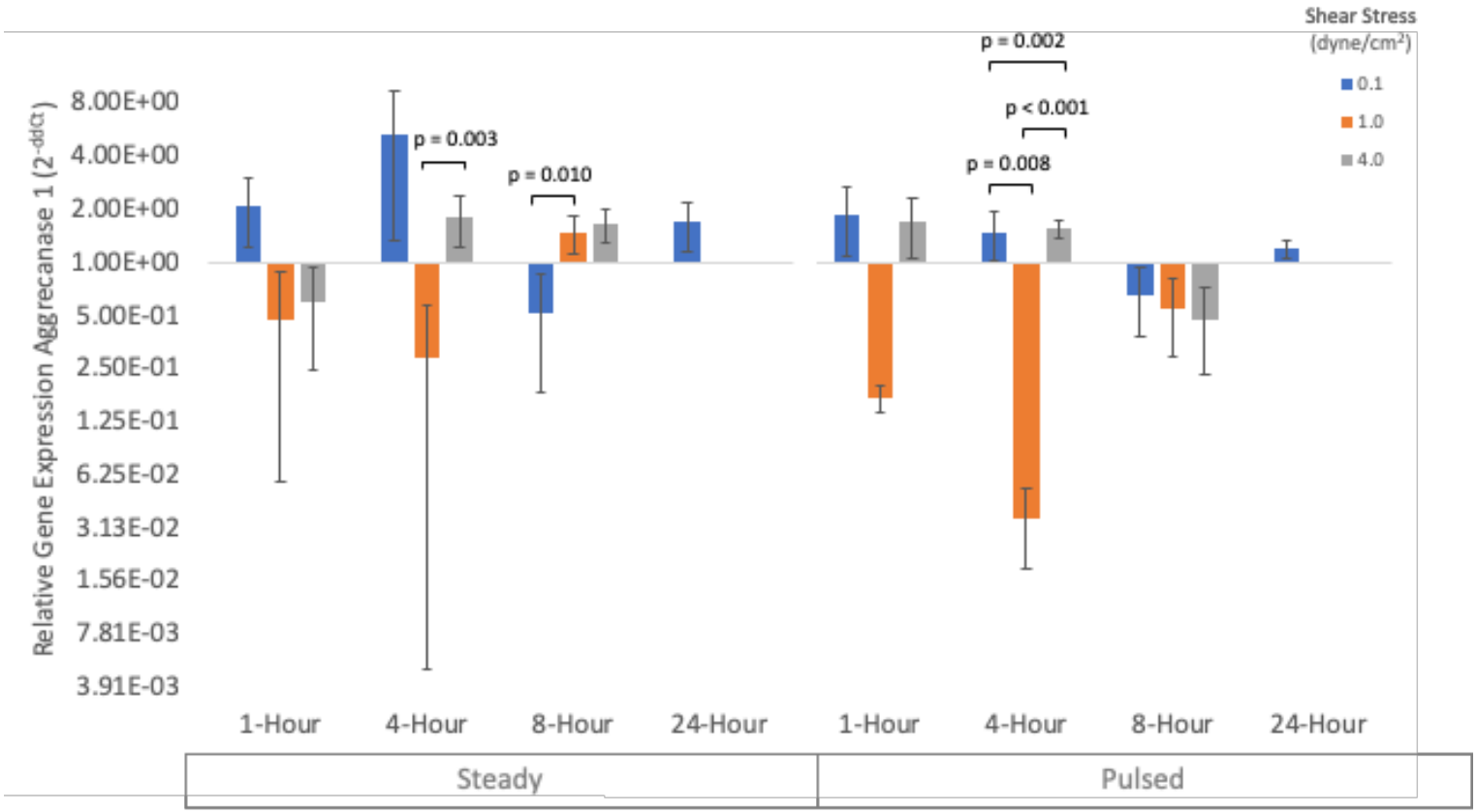

Figure 4.20 Gene expression of aggrecanase 1 in bovine nucleus pulposus cells relative to GAPDH and control (no flow) as determined by qRT-PCR following 12 test conditions: 1, 4, 8 and 24-hour flow experiments in Ibidi VI$^{0.4}$ flow chamber at shear stress conditions of 0.1, 1.0 and 4.0 dyne/cm^2. Results are shown for three flow types; control (no flow), steady flow and pulsed flow. Control is shown at y-axis = 1. Means and 95 % confidence interval error bars are shown based on 4 technical replicates and sample size (n) of 4 bovine subjects. Statistically significant results at level $p < 0.05$ are shown for one-way ANOVA with post-hoc Tukey HSD comparing shear stress conditions 0.1 vs 1.0 vs 4.0 dyne/cm^2 flow for each of the time conditions and flow types. No results shown for 1.0 and 4.0 dyne/cm^2 after 24 hours as no cells present on Ibidi VI$^{0.4}$ slide following flow experiments, due to detachment of cells from slide.

No statistically significant difference was seen between time intervals for the control group at 4.0 dyne/cm^2, [F (3, 12) = 2.498, p = 0.109]. For the steady group at 4.0 dyne/cm^2 a statistically significant difference was seen between time intervals for the steady group, [F (2, 11) = 16.119, p = 0.001]. Post-hoc Tukey HSD showed a significant difference after 4 hours flow compared with 1 hour flow (p = 0.001), no significant difference was seen between 8 hour and 1 hours (p = 0.154) and no significant difference was seen between 4 hours and 8 hours (p = 0.290). A statistically significant difference was seen between time intervals for the pulsed group at 4.0 dyne/cm^2, [F (2, 11) = 5.359, p = 0.029]. Post-hoc Tukey HSD showed a significant difference after 4 hours flow compared with 8 hours flow (p = 0.025), no significant difference was seen between 8 hour and 1 hours (p = 0.519) and no significant difference was seen between 4 hours and 1 hours (p = 0.146)

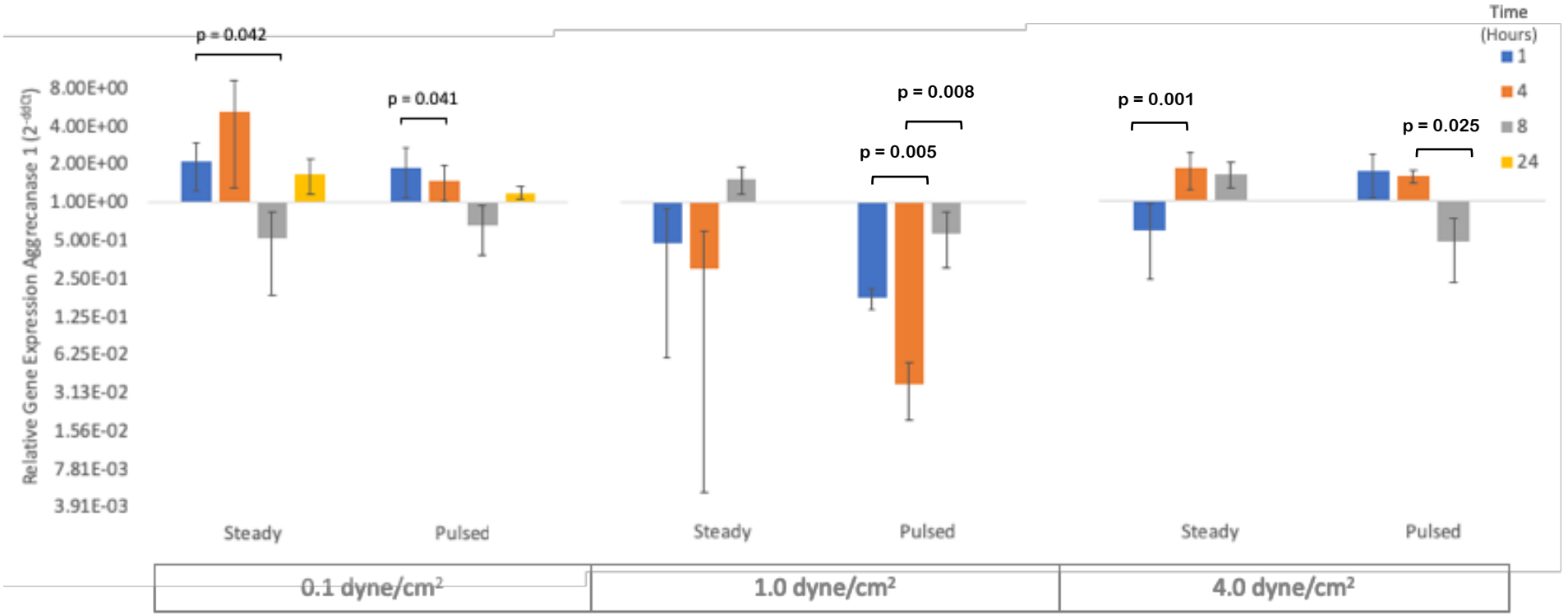

Figure 4.21 Gene expression of aggrecanase 1 in bovine nucleus pulposus cells relative to GAPDH and control (no flow) as determined by qRT-PCR following 12 test conditions: 1, 4, 8 and 24-hour flow experiments in Ibidi VI$^{0.4}$ flow chamber at shear stress conditions of 0.1, 1.0 and 4.0 dyne/cm^2. Results are shown for three flow types; control (no flow), steady flow and pulsed flow. Control is shown at y-axis = 1. Means and 95 % confidence interval error bars are shown based on 4 technical replicates and sample size (n) of 4 bovine subjects. Statistically significant results at level $p < 0.05$ are shown for one-way ANOVA with post-hoc Tukey HSD comparing results after 1, 4, 8 and 24 hours, for each of the shear flow conditions and flow groups. No results shown for 1.0 and 4.0 dyne/cm^2 after 24 hours as no cells present on Ibidi VI$^{0.4}$ slide following flow experiments, due to detachment of cells from slide.

4.9 Aggrecanase 2

4.9.1 Descriptive statistics

Shear Stress (dyne/cm^2)	Time (hours)	Control		Steady		Pulsed	
		Mean	*Standard Deviation*	*Mean*	*Standard Deviation*	*Mean*	*Standard Deviation*
0.1	**1**	0.67	*0.81*	1.45	*0.46*	0.25	*0.94*
	4	5.92	*0.87*	2.48	*0.49*	4.91	*0.78*
	8	2.69	*1.50*	2.00	*1.15*	-1.53	*1.04*
	24	0.08	*0.08*	4.96	*0.81*	-0.75	*0.52*
1.0	**1**	0.33	*1.01*	-1.22	*0.82*	1.84	*0.85*
	4	-1.06	*2.06*	1.61	*1.48*	1.09	*0.80*
	8	1.28	*1.25*	0.43	*1.33*	-0.22	*0.95*
	24	4.03	*0.76*	-	-	-	-
4.0	**1**	3.84	*1.73*	3.16	*1.48*	1.40	*2.31*
	4	3.52	*0.56*	2.52	*0.53*	-0.07	*0.62*
	8	0.85	*1.70*	0.36	*1.61*	-0.42	*1.44*
	24	4.53	*1.36*	-	-	-	-

Table 4.8 Mean and standard deviation dCt values (normalized to GAPDH) for gene expression of aggrecanase 2 for all 3 independent variable, flow type (control, steady and pulsed), shear stress (01, 1.0 and 4.0 dyne/cm^2) and time points (1, 4, 8 and 24 hours).

4.9.2 Effect of flow type on GE of aggrecanase 2

One-way ANOVAs were used to analyse the effect of flow types; no flow, steady flow and pulsed flow, on gene expression of aggrecanase 2. Results and statistically significant findings are shown in figure 4.22. No statistical analysis was carried out at 24 hours for the steady and pulsed groups at 1.0 and 4.0 dyne/cm^2 as noted previously due to the detachment of all cells from the slides.

There was no statistically significant effect of flow type on gene expression dCt values for aggrecanase 2 at the $p < 0.05$ level for the three flow conditions at 0.1 dyne/cm^2 after 1 hour flow, [F (2, 9) = 2.551, p = 0.133]. There was a statistically significant effect of flow type on gene expression dCt values for aggrecanase 2 at the

$p < 0.05$ level for the three flow conditions at 0.1 dyne/cm^2 after 4 hours flow, [F (2, 9) = 23.693, $p < 0.001$]. Post-hoc comparisons using Tukey HSD indicated that the mean score for the steady flow conditions was significantly different than the control ($p < 0.001$), and significantly different from the pulsed flow ($p = 0.003$), but the pulsed flow did not significantly differ from the control ($p = 0.171$). There was a significant effect of flow type on gene expression dCt values for aggrecanase 2 at the $p < 0.05$ level for the three flow conditions at 0.1 dyne/cm^2 after 8 hours flow, [F (2, 9) = 13.203, $p = 0.002$]. Post-hoc comparisons using Tukey HSD indicated that the mean score for the pulsed flow conditions was significantly different than the control ($p = 0.003$), and the steady was significantly different from the pulsed flow ($p = 0.008$), but the steady flow did not significantly differ from the control ($p = 0.724$). There was a statistically significant effect of flow type on gene expression dCt values for aggrecanase 2 at the $p < 0.05$ level for the three flow conditions at 0.1 dyne/cm^2 after 24 hours flow, [F (2, 9) = 121.101, $p < 0.001$]. Post-hoc comparisons using Tukey HSD indicated that the mean score for the steady flow conditions was significantly different than the control ($p <0.001$), and steady significantly different from the pulsed flow ($p < 0.001$), but the pulsed flow did not significantly differ from the control ($p = 0.142$).

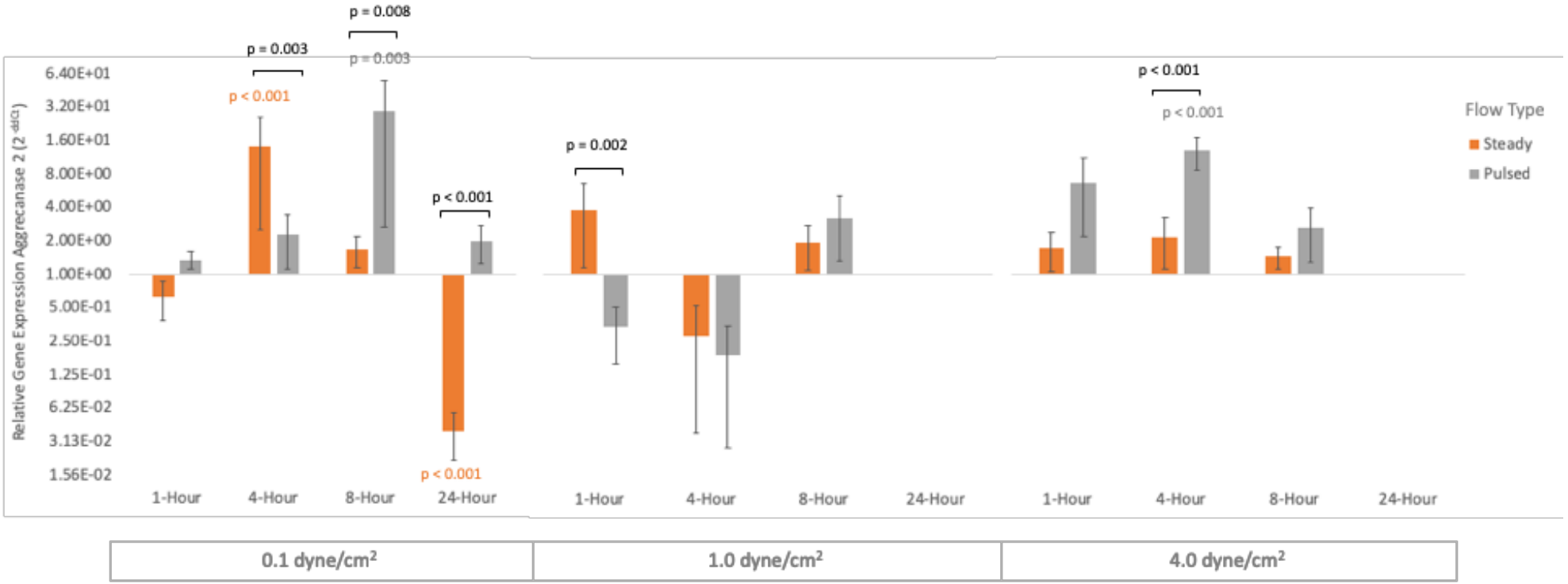

Figure 4.22 Gene expression of aggrecanase 2 in bovine nucleus pulposus cells relative to GAPDH and control (no flow) as determined by qRT-PCR following 12 test conditions: 1, 4, 8 and 24-hour flow experiments in Ibidi VI$^{0.4}$ flow chamber at shear stress conditions of 0.1, 1.0 and 4.0 dyne/cm^2. Results are shown for three flow types; control (no flow), steady flow and pulsed flow. Control is shown at y-axis = 1. Means and 95 % confidence interval error bars are shown based on 4 technical replicates and sample size (n) of 4 bovine subjects. Statistically significant results at level $p < 0.05$ are shown for one-way ANOVA with post-hoc Tukey HSD comparing control vs steady vs pulsed flow for each of the 12 test conditions. p value above or below error bar corresponds to Tukey HSD post-hoc test result between control and flow condition (steady or pulsed). p value above comparison bar corresponds to Tukey HSD post-hoc test result between steady vs pulsed flow. No results shown for 1.0 and 4.0 dyne/cm^2 after 24 hours as no cells present on Ibidi VI$^{0.4}$ slide following flow experiments, due to detachment of cells from slide.

There was a statistically significant effect of flow type on gene expression dCt values for aggrecanase 2 at the $p < 0.05$ level for the three flow conditions at 1.0 dyne/cm^2 after 1 hour flow, [F (2, 9) = 11.569, p = 0.003]. Post-hoc comparisons using Tukey HSD indicated that the mean score for the steady flow conditions was significantly different than the pulsed (p = 0.002), no significant difference was seen between the control and steady flow (p = 0.086) and the control and pulsed flow (p = 0.097). There was no statistically significant effect of flow type on gene expression dCt values for aggrecanase 2 at the $p < 0.05$ level for the three flow conditions at 1.0 dyne/cm^2 after 4 hours flow, [F (2, 9) = 3.401, p = 0.079]. There was no statistically significant effect of flow type on gene expression dCt values for aggrecanase 2 at the $p < 0.05$ level for the three flow conditions at 1.0 dyne/cm^2 after 8 hours flow, [F (2, 9) = 1.598, p = 0.255].

There was no statistically significant effect of flow type on gene expression dCt values for aggrecanase 2 at the $p < 0.05$ level for the three flow conditions at 4.0 dyne/cm^2 after 1 hour flow, [F (2, 9) = 0.217, p = 0.628]. There was a statistically significant effect of flow type on gene expression dCt values for aggrecanase 2 at the $p < 0.05$ level for the three flow conditions at 4.0 dyne/cm^2 after 4 hours flow, [F (2, 9) = 42.086, $p < 0.001$]. Post-hoc comparisons using Tukey HSD indicated that the mean score for the pulsed flow conditions was significantly different than the control (p <0.001), and steady was significantly different from the pulsed flow ($p < 0.001$), but the steady flow did not significantly differ from the control (p = 0.080). There was no statistically significant effect of flow type on gene expression dCt values for aggrecanase 2 at the $p < 0.05$ level for the three flow conditions at 4.0 dyne/cm^2 after 8 hours flow, [F (2, 9) = 0.649, p = 0.545].

4.9.3 Effect of shear stress rate on GE of aggrecanase 2

One-way ANOVAs were used to analyse the effect of shear stress rates; 0.1, 1.0 and 4.0 dyne/cm^2, on gene expression of aggrecanase 2. Results and statistically significant findings are shown in figure 4.23. No statistical analysis was carried out at 24 hours for the steady and pulsed groups at 1.0 and 4.0 dyne/cm^2 as noted previously due to the detachment of all cells from the slides.

There was a statistically significant effect on gene expression dCt values for aggrecanase 2 at the $p < 0.05$ level between the three shear stress conditions 0.1, 1.0 and 4.0 dyne/cm^2 after 1 hour for control, [F (2, 9) = 9.628, p = 0.006]. Post-hoc tests using Tukey HSD showed there was a significant difference between 0.1 dyne/cm^2 and 4.0 dyne/cm^2 (p = 0.014) and between 1.0 dyne/cm^2 and 4.0 dyne/cm^2 (p = 0.008) and no significant difference between 0.1 dyne/cm^2 and 1.0 dyne/cm^2 (p = 0.922). A statistically significant difference was seen after 1 hour for steady flow, [F (2, 9) = 19.012, p = 0.001]. Post-hoc tests using Tukey HSD showed there was a difference between 0.1 dyne/cm^2 and 1.0 dyne/cm^2 (p = 0.012), a significant difference between 1.0 dyne/cm^2 and 4.0 dyne/cm^2 ($p < 0.001$), no significant difference was seen between 0.1 dyne/cm^2 and 4.0 dyne/cm^2 (p = 0.094). No statistically significant difference was seen after 1 hour for pulsed flow, [F (2, 9) = 1.163, p = 0.355].

A one-way ANOVA determined that there was a statistically significant effect on gene expression dCt values for aggrecanase 2 at the $p < 0.05$ level between the three shear stress conditions 0.1, 1.0 and 4.0 dyne/cm^2 after 4 hours for control, [F (2, 9) = 28.409*,* $p < 0.001$]. Post-hoc tests using Tukey HSD showed there was a significant difference between 0.1 dyne/cm^2 and 1.0 dyne/cm^2 ($p < 0.001$) and between 1.0 dyne/cm^2 and 4.0 dyne/cm^2 (p = 0.002), no statistically significant difference was seen between 0.1 dyne/cm^2 and 4.0 dyne/cm^2 (p = 0.073). No statistically significant difference was seen after 4 hours for steady flow, [F (2, 9) = 1.155, p = 0.358]. A statistically significant difference was seen after 4 hours for pulsed flow, [F (2, 9) = 50.066, $p < 0.001$]. Post-hoc tests using Tukey HSD showed that there was a significant difference between 0.1 dyne/cm^2 and 1.0 dyne/cm^2 ($p < 0.001$), and a significant difference between 0.1 dyne/cm^2 and 4.0 dyne/cm^2 ($p < 0.001$), and no significant difference between 1.0 dyne/cm^2 and 4.0 dyne/cm^2 (p = 0.117).

A one-way ANOVA determined that there was no statistically significant effect on gene expression dCt values for aggrecanase 2 at the $p < 0.05$ level between the three shear stress conditions 0.1, 1.0 and 4.0 dyne/cm^2 after 8 hours for control, [F (2, 9) = 1.659, p = 0.244]. No statistically significant differences were seen after 8 hours steady flow [F (2, 9) = 1.824, p = 0.216]. No statistically significant differences were seen after 8 hours for pulsed flow, [F (2, 9) = 1.482*,* p = 0.278].

After 24 hours the control flow group only was analysed as all cells had detached from the Ibidi VI$^{0.4}$ slides for 1.0 dyne/cm^2 and 4.0 dyne/cm^2 for steady and pulsed flow groups. There was a statistically significant difference between the shear stress rates for the control group; 0.1 dyne/cm^2, 1.0 dyne/cm^2 and 4.0 dyne/cm^2 at the $p < 0.05$ level, [F (2, 9) = 29.453, $p < 0.001$]. Post-hoc tests using Tukey HSD showed that there was a difference between 0.1 dyne/cm^2 and 1.0 dyne/cm^2 ($p < 0.001$), and statistically significant difference between 0.1 dyne/cm^2 and 4.0 dyne/cm^2 ($p < 0.001$), and no significance between 1.0 dyne/cm^2 and 4.0 dyne/cm^2 ($p = 0.724$).

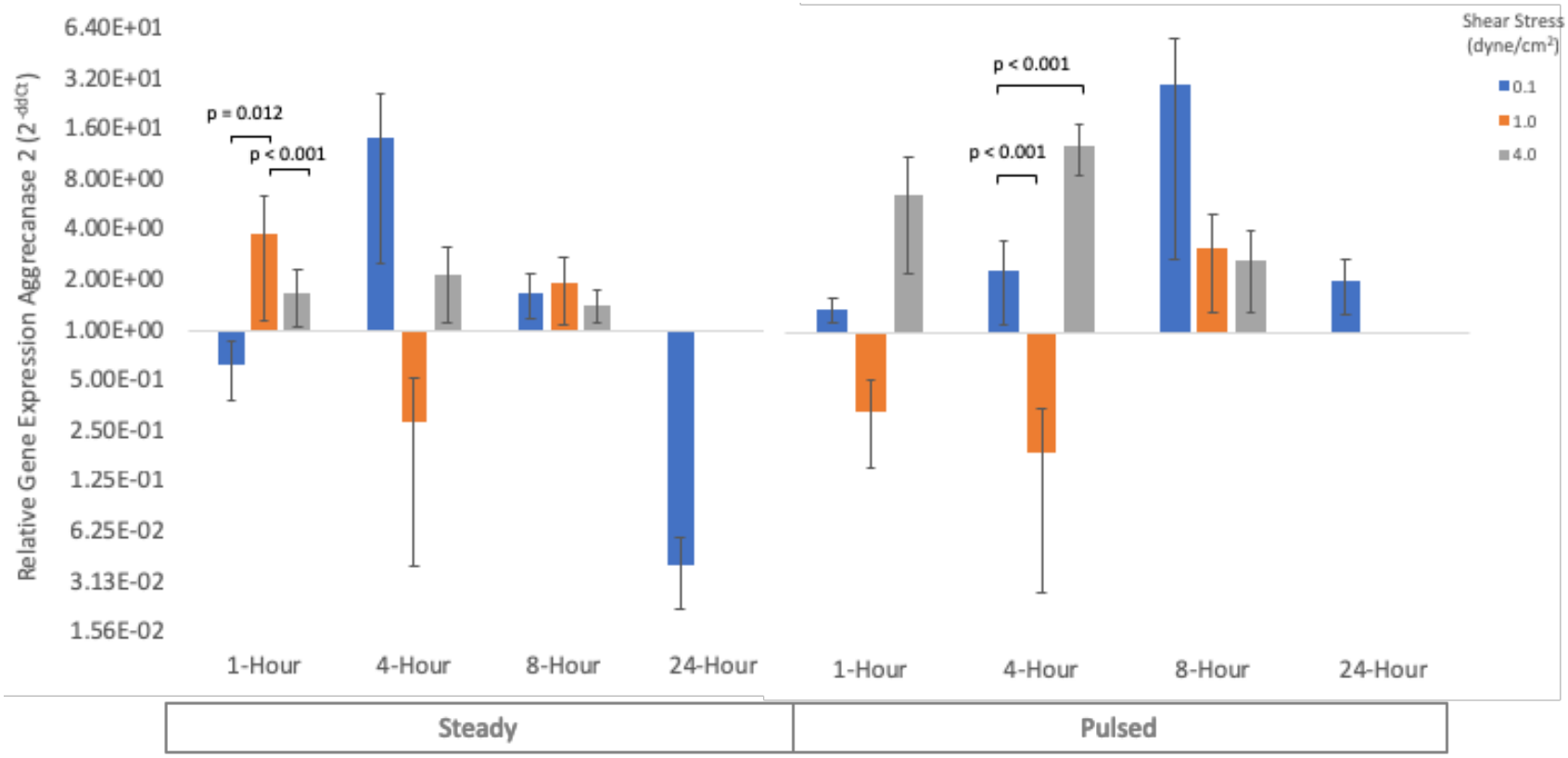

Figure 4.23 Gene expression of aggrecanase 2 in bovine nucleus pulposus cells relative to GAPDH and control (no flow) as determined by qRT-PCR following 12 test conditions: 1, 4, 8 and 24-hour flow experiments in Ibidi VI$^{0.4}$ flow chamber at shear stress conditions of 0.1, 1.0 and 4.0 dyne/cm^2. Results are shown for three flow types; control (no flow), steady flow and pulsed flow. Control is shown at y-axis = 1. Means and 95 % confidence interval error bars are shown based on 4 technical replicates and sample size (n) of 4 bovine subjects. Statistically significant results at level $p < 0.05$ are shown for one-way ANOVA with post-hoc Tukey HSD comparing shear stress conditions 0.1 vs 1.0 vs 4.0 dyne/cm^2 flow for each of the time conditions and flow types. No results shown for 1.0 and 4.0 dyne/cm^2 after 24 hours as no cells present on Ibidi VI$^{0.4}$ slide following flow experiments, due to detachment of cells from slide.

4.9.4 Effect of duration of flow on GE of aggrecanase 2

One-way ANOVAs were used to analyse the effect of the duration of time cells were exposed to shear stress; 1, 4, 8 and 24 hours, on gene expression of aggrecanase 2. Results and statistically significant findings are shown in figure 4.24. No statistical analysis was carried out at 24 hours for the steady and pulsed groups at 1.0 and 4.0 dyne/cm^2 as noted previously due to the detachment of all cells from the slides.

For the control group at 0.1 dyne/cm^2 there were statistically significant results at the $p < 0.05$ level, [F (3, 12) = 30.427, $p < 0.001$]. Post-hoc Tukey HSD shows a significant difference after 4 hours compared to 1 hour ($p < 0.001$) and a significant difference between 1 hour and 8 hours ($p = 0.049$), and a significant difference between 4 hours and 8 hours ($p = 0.002$) and between 8 hours and 24 hours ($p = 0.011$) and between 4 hours and 24 hours ($p < 0.001$). No significant difference was seen between 1 hour and 24 hours ($p = 0.819$). A statistically significant difference was seen between time intervals for the steady group at 0.1 dyne/cm^2, [F (3, 12) = 15.779 $p < 0.001$). Post-hoc Tukey HSD showed a significant difference after 24 hours compared to 1 hour ($p < 0.001$) and a significant difference was seen between 4 hours and 24 hours ($p = 0.004$), and between 8 hours and 24 hours ($p = 0.001$). No significant difference was seen between 1 hour and 4 hours ($p = 0.292$) or between 1 hours and 8 hours ($p = 0.754$) or between 4 hours and 8 hours ($p = 0.821$). A statistically significant difference was seen between time intervals for the pulsed group at 0.1 dyne/cm^2, [F (3, 12) = 46.763, $p < 0.001$]. Post-hoc Tukey HSD showed a significant difference after 4 hours compared to 1 hour ($p < 0.001$) and a significant difference between 8 hours and 1 hour ($p = 0.049$), and between 4 hours and 24 hours ($p < 0.001$) and between 4 hours compared to 8 hours ($p < 0.001$). No significant difference was seen between 1 hour and 24 hours ($p = 0.375$) or between 8 hours and 24 hours ($p = 0.578$).

A statistically significant difference was seen between time intervals for the control group at 1.0 dyne/cm^2, [F (3, 12) = 9.989, $p = 0.001$]. Post-hoc Tukey HSD showed a significant difference after 24 hours compared to 1 hour ($p = 0.011$) and a significant difference between 4 hours and 24 hours ($p = 0.001$). No significant difference was seen between 8 hours and 24 hours ($p = 0.060$), or between 1 hour and 4 hours ($p =$

0.495) or between 1 hours and 8 hours (p = 0.763) or between 4 hours and 8 hours (p = 0.124). For the steady group at 1.0 dyne/cm^2 a statistically significant difference was seen between time intervals [F (2, 11) = 5.233, p = 0.031]. Post-hoc Tukey HSD showed a significant difference after 4 hours flow compared with 1 hour flow (p = 0.026), no significant difference was seen between 8 hour and 1 hours (p = 0.200) and no significant difference was seen between 4 hours and 8 hours (p = 0.409). For the pulsed group a statistically significant difference was seen between time intervals at 1.0 dyne/cm^2, [F (2, 11) = 5.759, p = 0.025]. Post-hoc Tukey HSD showed a significant difference after 8 hours flow compared with 1 hour flow (p = 0.021), no significant difference was seen between 4 hour and 1 hours (p = 0.478) and no significant difference was seen between 4 hours and 8 hours (p = 0.136).

A statistically significant difference was seen between time intervals for the control group at 4.0 dyne/cm^2, [F (3, 12) = 5.182, p = 0.016]. Post-hoc Tukey HSD showed significant differences after 24 hours compared to 8 hour (p = 0.015) and significant differences were seen between 1 hour and 8 hours (p = 0.049), and no significant differences were seen between 1 hours and 4 hours (p = 0.988), no significant differences between 1 hour and 24 hours (p = 0.900) or between 4 hours and 8 hours (p = 0.084) or between 4 hours and 24 hours (p = 0.750). For the steady group at 4.0 dyne/cm^2 a statistically significant difference was seen between time intervals for the steady group [F (2, 11) = 5.119, p = 0.033]. Post-hoc Tukey HSD showed a significant difference after 8 hours flow compared with 1 hour flow (p = 0.033), no significant difference was seen between 4 hour and 1 hours (p = 0.772) and no significant difference was seen between 4 hours and 8 hours (p = 0.098). No statistically significant difference was seen between time intervals for the pulsed group at 4.0 dyne/cm^2, [F (2, 11) = 1.428, p = 0.289].

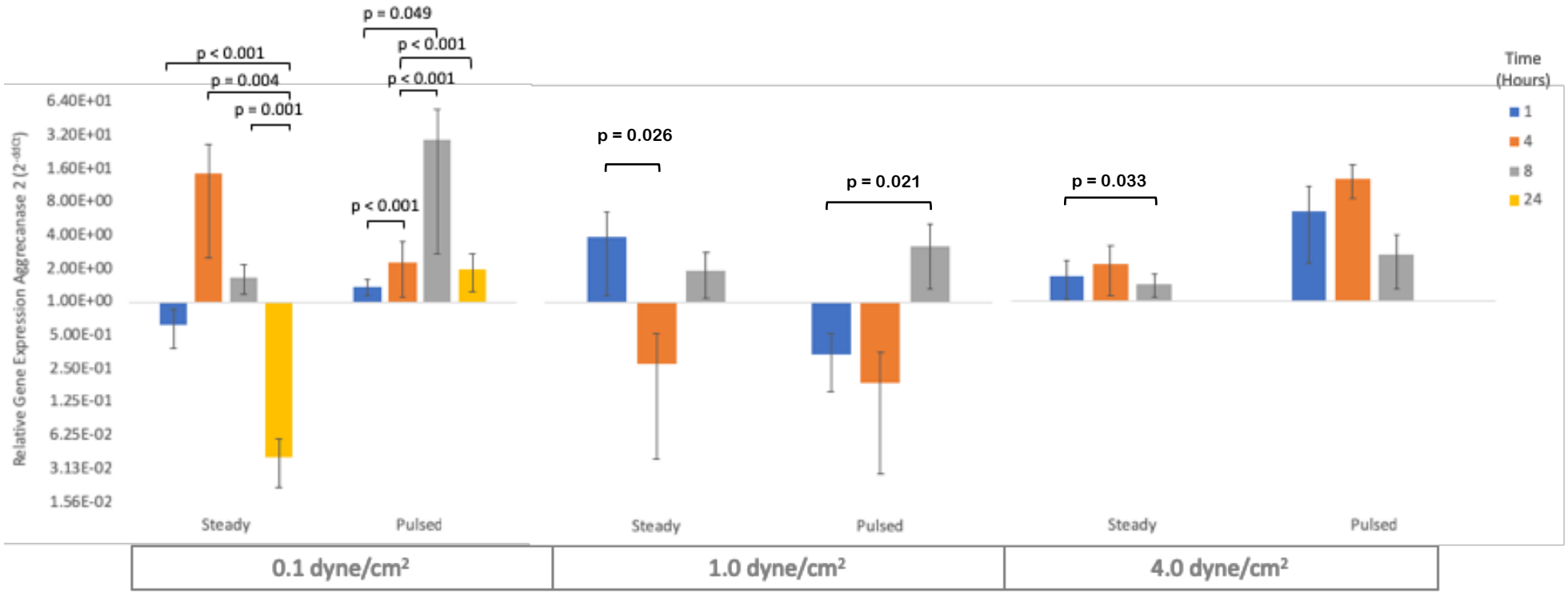

Figure 4.24 Gene expression of aggrecanase 2 in bovine nucleus pulposus cells relative to GAPDH and control (no flow) as determined by qRT-PCR following 12 test conditions: 1, 4, 8 and 24-hour flow experiments in Ibidi VI$^{0.4}$ flow chamber at shear stress conditions of 0.1, 1.0 and 4.0 dyne/cm^2. Results are shown for three flow types; control (no flow), steady flow and pulsed flow. Control is shown at y-axis = 1. Means and 95 % confidence interval error bars are shown based on 4 technical replicates and sample size (n) of 4 bovine subjects. Statistically significant results at level $p < 0.05$ are shown for one-way ANOVA with post-hoc Tukey HSD comparing results after 1, 4, 8 and 24 hours, for each of the shear flow conditions and flow groups. No results shown for 1.0 and 4.0 dyne/cm^2 after 24 hours as no cells present on Ibidi VI$^{0.4}$ slide following flow experiments, due to detachment of cells from slide.

Chapter 5. Discussion and Limitations

5.1 Does shear stress affect bovine nucleus pulposus morphology?

Figures 4.1, 4.4 and 4.7 demonstrate that respectively, cell number, focal adhesion number and cell circularity are all affected by shear stress in bovine NP cells when exposed to some of the shear stress conditions in this research study. Cell number was shown to increase after 4 hours flow at 0.1 dyne/cm^2 for steady flow compared to no flow and decrease after 4 hours and 8 hours at 1 dyne/cm^2 and 4 dyne/cm^2 for steady and pulsed flow compared to no flow. Focal adhesion number decreased after 24 hours in steady flow at 0.1 dyne/cm^2 compared to control and decreased after 4 and 8 hours in steady and pulsed flow after 1.0 dyne/cm^2 compared to control and in 4.0 dyne/cm^2 focal adhesions were found to decrease after 1, 4 and 8 hours in steady and pulsed flow. Cell circularity was shown to decrease after 8 hours in steady flow at 0.1 dyne/cm^2 and increase after 8 hours at 1 dyne/cm^2 for steady and pulsed flow and increase after 4 hours and 8 hours at 4.0 dyne/cm^2 for steady and pulsed flow.

These findings appear to show that shear stress can have an anabolic and catabolic effect on cell morphology. The effect after 4 hours flow at 0.1 dyne/cm^2 of an increase in cell number indicates shear stress at the lower rates could be beneficial in promoting cell proliferation. Similar findings have been shown in studies on osteoblasts but at a shear stress rate of 12 dyne/cm^2 (Ding et al., 2018). However, at the higher shear stress rates of 1.0 and 4.0 dyne/cm^2 the cell number was shown to be lower than that for the control, which indicates either detachment of the cells from the slides or a reduction in the rate of proliferation. A previous study of shear stress 35 dyne/cm^2 on chondrocytes showed cell proliferation (Malaviya and Nerem, 2002), so the bovine NP cells used here appear to show a greater sensitivity to shear flow than chondrocytes. As the cell number dropped below that seen for the previous time period, it may be most likely that the decreased cell number was due mainly to cell detachment from the slide, not just a decreased rate of proliferation. This has been shown in the study of cancer cells, where detachment was shown to begin at higher shear stresses of 20-50 dyne/cm^2 (Couzon et al., 2009). For cells which lie within an extra-cellular matrix (ECM), such as nucleus pulposus cells, attachment to the cell

surface is an inherent property essential for mechanotransduction interaction with the surroundings to maintain a healthy ECM. The focal adhesions are an integral part of mechanotransduction their number was shown to decrease in focal adhesions per cell in all shear stress rates; after 24hours in 0.1 dyne/cm^2, after 4 and 8 hours at 1.0 dyne/cm^2 and 1, 4 and 8 hours at 4.0 dyne/cm^2. Changes in focal adhesion number have been associated with cell remodeling as focal adhesions are broken down and rebuilt in the stream of flow. Studies have shown that when the shear stress is above the strength of the focal adhesion connection then the focal adhesion will breakdown (Biton and Safran, 2010, Verma et al., 2015). The decrease in number in these studies show that all the shear stress rates chosen have a catabolic effect on nucleus pulposus cells, for 0.1 dyne/cm^2 this happened only at the 24 hour duration, for 1.0 dyne/cm^2 this happened at 4 and 8 hours and in 4.0 dyne/cm^2 this happened at 1, 4 and 8 hours. No cells were left attached at 24 hours in 1.0 and 4.0 dyne/cm^2. In other studies shear stress levels have been shown to increase focal adhesion activity (Li et al., 1997), but this research only analysed focal adhesion number so cannot comment on the activity of the FA, this would be an interesting area of future research. The decrease in cell circularity at 8 hours of 0.1 dyne/cm^2 is indicative of the cell becoming more elongated as it adheres more strongly to the surface of the Ibidi VI$^{0.4}$ slide, this has been shown in studies on osteoblasts (Liu et al., 2010) and endothelial cells (Schilling et al., 1992). The increase in cell circularity after 8 hours in 1.0 dyne/cm^2 and 4 and 8 hours in 4.0 dyne/cm^2 is indicative of cells becoming more circular and losing their adherence to the slide surface. No cells were present at 24 hours 1.0 dyne/cm^2 and 4.0 dyne/cm^2 the obvious reason being detachment from the slide which would fit with the increased cell circularity at the short duration in these two shear stress rates.

5.1.1 Does the type of flow have an effect on cell morphology?

In-vivo, steady flow could be implicated in flow into the disc through diurnal changes and pulsed flow could be more indicative of changes caused by frequent intradiscal pressure changes, for example when walking or running. Analysing the effect of steady flow compared to pulsed flow could give a greater understanding of the response of nucleus pulposus cells to these types of flow changes. Cell number was seen to differ for flow type after 1 hours at 4.0 dyne/cm^2. Pulsed flow showed a significant decrease compared to steady flow, see figure 4.1. The focal adhesion

number was seen to differ for flow type after 8 hours in 1.0 dyne/cm^2 with the focal adhesions in the pulsed flow being significantly less than that for steady flow. Cell circularity was also shown to differ significantly after 8 hours at 1.0 dyne/cm^2 with pulsed flow showing slightly significantly higher cell circularity values to steady flow.

The decrease in cell number after 1 hour at 4.0 dyne/cm^2 pulsed flow could be indicative of the oscillating acceleration and deceleration in the flow having a greater effect on cell detachment than a steady flow. Oscillatory shear stress has been shown to induce an inflammatory response in endothelial cells (Dabagh et al., 2017). Differences in flow type were not seen after a greater duration which could be explained by the cells requiring a longer duration to become detached in the steady flow, but once detachment begins to occur then it occurs at the same rate in steady and pulsed flow. The reduction in focal adhesion number in pulsed flow compared to steady flow, could again be an indication of the pulsed flow having a greater effect on the breakdown of focal adhesions and subsequent detachment of cells from the surface of the slide. The increase in cell circularity after 8 hours at 1.0 dyne/cm^2 is indicative of a greater roundness of the cell, which is a sign of detachment from the Ibidi slide. The fact that this occurs at the same condition as focal adhesion number decreased in the pulsed flow and not in the steady flow, could be linked in that a reduction in focal adhesion attachment to the Ibidi Slide is seen at the same time that the cell becomes more round. This has been seen in several other studies on other types of cells, and is not particularly remarkable as it is expected, however what may be of interest is why this happens only in pulsed flow at this condition and not in steady flow and why these changes are not seen together at any other condition.

5.1.2 Does the rate of shear stress have an effect on cell morphology?

Significant decreases in cell number was seen for steady flow and pulsed low after 4 hours from 0.1 vs 1.0 dyne/cm^2 and from 1.0 to 4.0 dyne/cm^2 and from 0.1 to 4.0 dyne/cm^2. These changes were also seen after 8 hours and to a greater statistical significance. These changes were not seen in the control group which was not exposed to flow. Significant decreases in focal adhesion numbers were seen for both steady and pulsed flow at 4 hours from 0.1 to 4.0 dyne/cm^2 and from 1.0 to 4.0 dyne/cm^2 and at 8 hours from 0.1 to 1.0 dyne/cm^2, 1.0 to 4.0 dyne/cm^2 and from 0.1 to 4.0 dyne/cm^2. In addition, significant decreases in focal adhesion number were

seen after 1 hour from 0.1 to 4.0 dyne/cm^2 in pulsed flow which was not seen in steady flow. Cell circularity increased significantly after 4 hours from 0.1 to 4.0 dyne/cm^2 shear stress in steady flow, not other changes were seen at 4 hours. After 8 hours flow significant increases in circularity were seen from 0.1 to 1.0 dyne/cm^2 and from 0.1 to 4.0 dyne/cm^2 in both steady and pulsed flow.

The decrease in cell number as the shear stress rate increases is an indication of increased cell detachment as the shear stress rate increases. The decreases in focal adhesion number as the shear stress rate increased demonstrates that the shear stress rate does effect cell morphology and a higher shear stress rate leads to greater detachment of focal adhesions. Increases in cell circularity with increasing shear stress rates demonstrate cell detachment increasing as the cell becomes less adhered and spread out across the surface and more round in appearance.

5.1.3 Does the duration of flow have an effect on cell morphology?

Cell number significantly increased in the control groups for all 3 shear stress rates from 1 hour to 24 hours. Increases in cell number were also seen from 1 hour to 8 hours and from 4 hours to 24 hours and from 8 hours to 24 hours in the 0.1 dyne/cm^2 control group. Increases were seen from 1 hour to 4 hours, from 4 hours to 24 hours and from 8 hours to 24 hours in the 1.0 dyne/cm^2 control group. Increases were also seen from 4 hours to 24 hours and from 8 hours to 24 hours in the 4.0 dyne/cm^2 control group. Cell number for the steady flow groups significantly increased from 1 hour to 4 hours and 1 hour to 24 hours and from 4 hours to 24 hours and 8 hours to 24 hours at 0.1 dyne/cm^2 and decreased significantly from 1 hour to 8 hours and 4 hours to 8 hours until all cells had detached after 24 hours at the 1.0 dyne/cm2 shear stress rate and decreased from 1 hour to 4 hours and from 1 hour to 8 hours and from 4 hours to 8 hours at the 4.0 dyne/cm^2 shear stress rate. Cell number for pulsed flow increased significantly from 1 hour to 24 hours and from 4 hours to 24 hours and from 8 hours to 24 hours at 0.1 dyne/cm^2 shear stress rate and decreased significantly from 1 hour to 4 hours and from 1 hour to 8 hours and from 4 hours to 8 hours until all cells had detached after 24 hours at the 1.0 dyne/cm^2 shear stress rate and cell number decreased from 1 hour to 4 hours, from 1 hour to 8 hours and from 4 hour to 8 hours until all cells had detached at 24 hours at the 4.0 dyne/cm^2 shear stress rate.

Focal adhesion number for the 3 control groups showed the same trends for the control groups for 1.0 and 4.0 dyne/cm^2 with an increase from 1 hour to 4 hours, 8 hours and 24 hours. However, there were no significant changes in the control group for 0.1 dyne/cm^2, which is confusing. It can be seen that the confidence interval for 1 hour at 0.1 dyne/cm^2 is relatively large, this could affect the relative comparison of the 4, 8 and 24 hour groups. A larger sample size would help to give more reliability to the results gained. The steady flow groups showed no significant differences in focal adhesion number over time points. The pulsed group showed significant increase in focal adhesion number from 1 hour to 24 hours in the 0.1 dyne/cm^2 group, however, although this change was not seen in the control for the 0.1 dyne/cm^2 group it was seen in the control groups for the 1.0 dyne/cm^2 and the 4.0 dyne/cm^2 groups, so caution must be used when drawing conclusions from these results. An increase in focal adhesion number was also seen from 1 hour to 4 hours in the pulsed 1.0 dyne/cm^2 group and then a significant decrease from 4 hours to 8 hours.

Only one significant change in cell circularity was seen in the control groups which was a slightly significant decrease in cell circularity from 4 hours to 8 hours in the 4.0 dyne/cm^2 however this was not seen in the other two control groups, so caution must be taking in drawing any conclusions surrounding this finding, no significant changes were seen in the other control groups or over any of the other time points. At 1.0 dyne/cm^2 there was only significant changes seen in pulsed flow with significant increases seen from 1 hour to 4 hours and from 1 hour to 8 hours. At 4.0 dyne/cm^2 changes were seen in both steady and pulsed flow. Steady flow showed significant increases from 1 hour to 4 hours, 1 hour to 8 hours and 4 hours to 8 hours. Pulsed flow showed increases in circularity from 1 hour to 4 hours and 1 hour to 8 hours.

The increase in cell number in the three control groups, which were not exposed to flow, is expected as the cells would be expected to proliferate exponentially over a 24 hour period until they were confluent at which point proliferation would reduce in rate. The control groups were exposed to the exactly the same conditions and no flow. Therefore, any differences between the groups, for example the increase in cell number from 1 hour to hours in the 0.1 dyne/cm^2 group which was not seen in the 1.0

and 4.0 dyne/cm^2 groups, and the increase from 1 hour to 4 hour in the 1.0 dyne/cm^2 which was not seen in the 0.1 and 4.0 dyne/cm^2. These differences were not as an effect of any conditional change and gives some indication of the differences that could be present due to differences in biological samples. This lack of consistency in results between control groups could be improved with a greater sample size and is discussed further in the limitations section of this chapter. Significant increases in cell number in the steady flow group at 0.1 dyne/cm^2 were also seen in the control groups so could be assumed not have been affected by the shear stress. The decreases in cell number in the steady flow group are indicative of the detachment of cells from the Ibidi Slide VI$^{0.4}$ surface which becomes more pronounced with increased duration of shear flow, the effects seen at 1.0 dyne/cm^2 were more pronounced at 4.0 dyne/cm^2. These same decreases in cell number were seen in the pulsed flow group and again became more pronounced as the shear stress rate increased.

The results for focal adhesion number are inconclusive, it would be expected that the control groups for each shear stress rate would show the same trends, but the 0.1 dyne/cm^2 group did not, the large confidence interval is most likely the cause of this and an increase in sample number may have helped give more conclusive results. Based on the two control groups from 1.0 and 4.0 dyne/cm^2, focal adhesion number appears to increase in the control groups, this would be expected as the cells further adhere to the slide and lay down more focal adhesions over a 24 hour period. The lack of this increase in focal adhesions per cell in the steady flow groups for all three shear stress rates could then be seen as a decrease in the rate of focal adhesion formation in comparison to the control groups. The increase in focal adhesions in the pulsed flow at 0.1 dyne/cm^2 was seen in the control groups for 1 dyne and 4.0 dyne/cm^2 so caution should be taken in concluding that this could be a difference to the control group. The increase in pulsed flow at 1.0 dyne/cm^2 and then subsequent decrease in focal adhesions per cell could an indication of the time at which focal adhesion number increases but the increase at 4 hours was still reduced compared to the control at 4 hours, so although it was an increase from 1hour it was still not an overall increase in focal adhesion number.

The increases in cell circularity seen in pulsed flow at 1.0 dyne/cm^2 show that the longer the cells are exposed to shear stress the ore circular they become, and this effect is seen at lower shear stress rates in pulsed flow than in steady flow, whereby significant changes were not seen until 4.0 dyne/cm^2. This could be due to the pulsatile motion having a greater effect on the detachment of cells from the slide so an increase in cell circularity.

5.1.4 Implications for researchers

Key findings that would be useful to the body of knowledge surrounding NP cells response to flow is that the NP cells used in this study respond to shear stress at relatively low shear stress rate. Shear stress rates cited in studies for IVD cells of 1 and 10 dyne/cm^2 (Chou et al., 2016) and 1 dyne/cm^2 (Wang et al., 2011) and for other cell types shear stress rates of 20-50 dyne/cm^2 and 35 dyne/cm^2 (Malaviya and Nerem, 2002) are relatively high for shear stress values that may be most beneficial for NP cells. Increases in cell proliferation were seen at 0.1 dyne/cm^2 in a steady flow, but not in a pulsed flow. Therefore, for increased cell growth in bioreactors a shear stress rate of not more than 0.1 dyne/cm^2 is recommended. Shear stress rates of 1.0 dyne/cm^2 and 4.0 dyne/cm^2 could have detrimental effects on cell proliferation. Durations on flow at 1.0 and 4.0 dyne/cm^2 had a cumulatively detrimental effect on cell proliferation and focal adhesion number, so if increased shear stress rates were required for periods of time in a bioreactor, reducing the duration to a minimum would be advisable. Significant increases in cell circularity occurred at 1.0 dyne/cm^2 and 4.0 dyne/cm^2 after 8 hours and could be a precursor to cell detachment or decreases in proliferation so if imaging was available during bioreactor cell growth then cell circularity could be used as an indication of cell health during the time in situ.

5.2 Does shear stress affect bovine nucleus pulposus gene expression?

Significant upregulation was seen for collagen 1 gene expression after 8 hours and 24 hours at 0.1 dyne/cm^2 pulsed flow compared and for steady and pulsed flow after 4 hours at 1.0 dyne/cm^2 and downregulation was seen after 1 hour and 4 hours in pulsed flow at 4.0 dyne/cm^2. Significant downregulation of collagen 2 was seen after 1 hour exposed to 0.1 dyne/cm^2 in pulsed flow and upregulation after 4 hours in steady flow at 0.1 dyne/cm^2. At 1.0 dyne/cm^2 collagen 2 was significantly downregulated after 8 hours in steady flow and downregulated at all time points, 1, 4

and 8 hours at 1.0 dyne/cm^2 in pulsed flow and then significantly downregulated in steady and pulsed flow after 1 hour exposure to 4.0 dyne/cm^2 shear stress. Aggrecanase 1 was significantly upregulated after 4 hours exposure to 0.1 dyne/cm^2 steady flow and then downregulated after 8 hours exposure. At 1.0 dyne/cm^2 exposure to steady and pulsed flow aggrecanase 1 was significantly downregulated after 4 hours. Aggrecanase 2 was significantly upregulated when exposed to steady flow for 4 hours and pulsed flow for 8 hours. Aggrecanase 2 was also upregulated when exposed to pulsed flow at 4.0 dyne/cm^2 for 4 hours. Aggrecan was upregulated when exposed to pulsed flow at 0.1 dyne/cm^2 for 4 hours and downregulated when exposed to pulsed flow at 1.0 dyne/cm for 8 hours. When exposed to 4.0 dyne/cm^2 aggrecan was significantly downregulated in pulsed and steady flow after 1 hour and in pulsed flow after 8 hours.

Upregulation of collagen 1 was generally seen at the lowest two flow rates and down regulation at the higher flow rate when compared to no flow. Only significant down regulation of collagen 2 was seen in flow, healthy nucleus pulposus cells produce more collagen 2 than collagen 1 (Bogduk, 2011), so this finding is not in keeping with the literature. One explanation for this could be the growth of nucleus pulposus cells as a monolayer rather than in a 3-D matrix where they could maintain their spherical shape. Nucleus pulposus cells are classified as chondrite-like, in-vivo nucleus pulposus cells synthesize more collagen II than collagen I. However, chondrocyte cells grown in a monolayer have been shown to synthesize more collagen I than collagen II (Tekari et al., 2014) and further studies showed that annulus fibrosus disc cells synthesized collagen I and II only when grown in 3D culture and not in a monolayer (Gruber and Hanley, 2000). The downregulation of collagen II compared to collagen I may be due to the growth of these nucleus pulposus cells in a monolayer and further flow studies in a 3D environment would be beneficial in further determining the role of fluid flow on cells in-vivo.

5.2.1 Does the type of flow have an effect on cell gene expression?

A highly significant difference was shown between steady and pulsed flow at 0.1 dyne/cm^2 after 1 hour with cells exposed to steady flow showing down regulation of collagen 1 and cells exposed to pulsed flow showing upregulation of collagen 1. The same difference was seen after 4 hours, but this difference was only moderately

significant. At 24 hours both steady and pulsed flow were upregulated, but pulsed flow was upregulated significantly more than steady flow. At 1.0 dyne/cm^2 there was a significant difference between steady flow and pulsed flow after 1 hour, collagen 1 was upregulated in steady flow and downregulated in pulsed flow. A significant difference was seen in collagen 2 gene expression between steady and pulsed flow after 1 hour at 0.1 dyne/cm^2, upregulation was seen in steady flow and downregulation in pulsed flow. The same difference was seen at 1.0 dyne/cm^2 after 1 hour. The only difference between flow type was seen in aggrecanase 1 gene expression was after 8 hours in 4.0 dyne/cm^2 shear stress, upregulation was seen in steady flow and downregulation in pulsed flow. Significant changes were seen between steady and pulsed flow at after exposure to 0.1 dyne/cm, upregulation of aggrecanase 2 was seen at both time points, and higher levels of upregulation were seen in steady flow at 4 hours and in pulsed flow at 8 hours. After 24 hours exposure to 0.1 dyne/cm^2 significant changes in flow type were seen with down regulation in steady flow and upregulation in pulsed flow. After 1 hour exposure to 1.0 dyne/cm^2 significant differences were seen in flow type with upregulation seen in pulsed flow and downregulation seen in steady flow. 4 hours exposure to 4.0 dyne/cm^2 flow again showed a significant difference in flow type for gene expression of aggrecanase 2, both steady and pulsed flow caused upregulation, but there was a significant increase in pulsed flow over steady flow. Significance differences in flow type were shown under two conditions for the gene expression of aggrecan. These conditions were after 8 hours exposure to 1.0 dyne/cm^2 and 4.0 dyne/cm^2, both steady and pulsed flow showed downregulation of aggrecan, but with an increase in downregulation in pulsed flow compared to steady flow in both conditions.

5.2.2 Does the rate of shear stress have an effect on cell gene expression?

The rate of shear stress does appear to have had an effect on the gene expression of bovine nucleus pulposus cells. In steady flow Collagen 1 was downregulated at 0.1 dyne/cm2 after 1 hour exposure and then the was a significant difference in upregulation of collagen 1 at 1.0 dyne/cm^2 and then further downregulation at 4.0 dyne/cm^2 which again was a significant difference. A significant difference between collagen 1 expression in steady flow after 8 hours exposure was also seen between 0.1 and 4.0 dyne/cm^2 with upregulation at 0.1 dyne/cm^{2}and downregulation at 4.0 dyne/cm^2. For pulsed flow, significant differences were seen after 8 hours exposure

between 0.1 and 1.0 dyne/cm^2 shear stress and 0.1 and 4.0 dyne/cm^2 shear stress with upregulation at 0.1 dyne/cm^2 and downregulation at 1.0 and 4.0 dyne/cm^2. For collagen 2 gene expression there were significant differences seen for pulsed flow only, after 1 hour exposure between upregulation at 0.1 dyne/cm^2 and downregulation at 4.0 dyne/cm^2 and between upregulation at 1.0 dyne/cm^2 and downregulation at 4.0 dyne/cm^2. For aggrecanase 1 there was only significant differences seen in steady flow following 1 hour exposure between upregulation at 0.1 dyne/cm^2 and downregulation at 4.0 dyne/cm^2. Expression of aggrecanase 2 was shown to differ significantly after 1 hour exposure to steady flow 0.1 dyne/cm^2 where it was downregulated compare to 1.0 dyne/cm^2 where it was upregulated. And after 1 hour exposure to steady flow at 1.0 dyne/cm^2 which saw a significant decrease in upregulation. Pulsed flow rate showed significant differences after 4 hours exposure to 0.1 dyne/cm^2 where it was upregulated compared to 1.0 dyne/cm^2 where it was downregulated and compared to 4.0 dyne/cm^2 which saw a significant increase in upregulation. Aggrecan was upregulated after exposure to 0.1 dyne/cm^2 shear stress in steady flow which significantly differed from expression after exposure to 4.0 dyne/cm^2 which saw downregulation of aggrecan. Significant differences were also seen after 1 hour exposure to 1.0 dyne/cm^2 steady flow which again showed upregulation compared to downregulation at 4.0 dyne/cm^2. Aggrecan was upregulated after 4 hours in 0.1 dyne/cm^2 steady flow which was significantly different to downregulation of aggrecan seen after 4 hours of steady flow at 1.0 dyne/cm^2. This is significantly different to the downregulation seen after 4 hours exposure to 4.0 dyne/cm^2 steady flow. Pulsed flow saw significant differences between cells exposed to 0.1 dyne/cm^2 for 1 hour which saw upregulation of aggrecan and 1.0 dyne/cm^2 for 1 hour which showed downregulation and significantly different to 1 hour exposure to 4.0 dyne/cm^2 which also showed downregulation. The same trend was seen after 4 hours exposure which saw upregulation of aggrecan after exposure to 0.1 dyne/cm^2 and downregulation after exposure to 4.0 dyne/cm^2. Significant differences were seen between exposure to 0.1 dyne/cm^2 after 8 hours, which showed upregulation compared to downregulation seen after 8 hours exposure to 1.0 dyne/cm^2 and downregulation of aggrecan after 8 hours exposure to 4.0 dyne/cm^2.

5.2.3 Does the duration of flow have an effect on cell gene expression?

The only significant difference in expression of collagen across time points was seen in steady flow at 4.0 dyne/cm^2 where a significant increase in downregulation was seen at 4 hours compared to 8 hours exposure. The only significant difference seen for expression of collagen 2 was in 0.1 dyne/cm^2 flow where upregulation after 1 hour exposure differed significantly from downregulation seen after 24 hours exposure. For expression of aggrecanase 1 significant differences were seen in exposure to pulsed 1.0 dyne/cm^2 from 1 hour downregulation to 4 hours which saw a significant increase in downregulation and for steady slow there was a slightly significant change seen at 4.0 dyne/cm^2 between downregulation after 1 hour exposure and upregulation at 4 hours exposure. For expression of aggrecanase 2 the only significant changes between time points were seen at 0.1 dyne/cm^2 pulsed flow. Aggrecanase 2 was upregulated after 1 hour exposure which significantly increased after 4 hours and significantly increased again from 4 hours to 8 hours and then upregulation significant increased from 1 hours to 24 hours, but this was actually a decrease from 4 and 8 hours, although not a significant one. Expression of aggrecan was significantly affected by exposure time in steady flow at 0.1 dyne/cm^2, upregulation was seen at all time points. There was a significant increase in upregulation from 1 hour to 4 hours exposure and a significant decrease in upregulation from 4 hours to 8 hours and a significant difference from 4 hours to 24 hours and a significant increase was seen from 1 hour to 24 hours exposure. In - pulsed flow at 0.1 dyne/cm^2 a significant increase in upregulation was seen from 1hour exposure to 4 hours exposure. Significant changes in steady flow were also seen after exposure to 1.0 dyne/cm^2 upregulation after 1 hour saw a significant change to downregulation after 4 hours, and in 4.0 dyne/cm^2 exposure down regulation after 1 hour was significantly reduced, but still downregulated after 4 hours.

5.2.4 Implications for researchers

Key findings regarding gene expression of bovine NP cells under shear stress are that cells significantly upregulate collagen 2 in steady flow compared to pulsed flow at 0.1 and 1.0 dyne/cm^2, however there was no change compared to the control. If flow needed to be created due to the replenishments of nutrients, then a steady flow rather than a pulsed flow would be recommended. However, after 24 hours collagen

2 was significantly downregulated so a shorter duration, even at 0.1 dyne/cm^2 would be recommended. Aggrecanase 1 was upregulated at 4.0 dyne/cm^2 after 4 hours, and aggrecanase 2 was upregulated after only 1 hour. Furthermore, aggrecan was upregulated at 0.1 dyne/cm^2, this gives further weight to the discussion that shear stress rates of higher than 1.0 dyne/cm^2 may have a catabolic effect on NP cells, so if cell and matrix growth are required from a bioreactor then shear stress rates of below 1.0 dyne/cm^2 would be recommended. However, this increase in aggrecan was in pulsed flow, not steady flow and cell morphology was seen to show better cell health in steady flow.

5.3 Implications for the wider research community and clinicians

Commonly, shear stress studies have investigated red blood cells, endothelial cells and osteoblasts and the flow rate, and shear stress rate experienced by these cells in vivo would be significantly higher compared to those in the matrix of the nucleus pulposus. The key findings of this research show that shear stress rates of 1.0 dyne/cm^2 and higher may have detrimental effects on cell morphology, causing increased cell circularity, decreased focal adhesion number and decreased cell proliferation and eventually detachment of cells. Furthermore, shear stress rates of 1.0 dyne/cm^2 can also have a catabolic effect on bovine NP cells, upregulating aggrecanase 1 and 2 and downregulating aggrecan. These findings could be useful in guiding researchers working towards developing successful cell-seeded scaffolds for nucleus pulposus regeneration. Growing cell-seeded scaffolds in a perfusion bioreactor where the infusion rate can be controlled could create the most beneficial environment for matrix production by the cells. Shear stress rates of 1.0 dyne/cm^2 and above could change the phenotype of the nucleus pulposus cell and be detrimental to matrix production. However, lower shear stress rates of around 0.1 dyne/cm^2 could have a beneficial effect on matrix production. Taking this into account when designing the environment for scaffold growth may prove advantageous.

Relating these findings to in-vivo research may also be interesting in research for measures to prevent low back pain through exercise therapy. As discussed in Chapter 2, heavy repetitive loading of the spine creates relatively high intradiscal pressures (Nachemson and Morris, 1964a) which can lead to microtrauma in the disc. Weightlifters have been shown to have degenerative changes throughout the

spine when compared with runners (Videman et al., 1995), however normal physiological loading through movement and exercise has been shown to have a beneficial effect, runners have been shown to have less spinal degeneration than controls (Belavý et al., 2017). The pressure changes created during weightlifting could lead to greater fluid flow rates and therefore higher fluid shear stress in the disc than lower pressure changes created through beneficial exercise modalities which have been shown to be beneficial for low back pain, such as running, walking, yoga, Pilates and tai chi. Furthermore, disc degeneration could be responsible for an increase in shear stress rates within the disc. In a structurally intact disc, the permeability of the disc tissue is low, due to the densely packed collagen structure. In a degraded disc, in which the disc has lost its structure and annular fissures are present, higher fluid flow rates could be present and therefore higher shear stress rates. This could lead to an escalation of catabolic metabolism by the disc cells and further degradation of the disc. The anabolic metabolism seen at the lower shear stress rates investigated in this study could be related to the beneficial effects of exercises modalities discussed in the literature and could be the key to determining the types of exercises which as beneficial for prevention of low back pain. Further research incorporating fluid shear stress onto nucleus pulposus cells in a 3D matrix, rather than a monolayer would be a useful development in assessing the role of shear stress in the possible prevention of early degeneration of the intervertebral disc.

5.4 Limitations

5.4.1 Sample size

Four biological samples were used in this research based on the power analysis carried out using G*Power3 prior to starting which calculated 3-7 replicates to be sufficient. As the specimens were of the same age, 18 months, and same breed and from the same slaughterhouse, there was an assumption made that the cells would likely be biologically very similar. Four technical replicates were used and any outliers in the technical replicates were disregarded. However, all values for the biological replicates were included, and these values were used for statistical analysis and means were taken which are represented on the graphs in the results chapter. It is clear from some of the confidence intervals that there was a large spread on some of the results, particularly for the gene expression. Following the experiments another

power analysis was carried out using the Partial Eta Squared values generated in SPSS and calculations in G*Power3.1 determined a sample size of between 6-16 would be recommended for the studies carried out. A reduced number of flow conditions and a greater sample size would have been a more effective means of resources of these cell studies if they were to be repeated to give greater reliability in the results gained.

5.4.2 Pump accuracy

The accuracy of the peristaltic pump was a limitation to the accuracy of the flow rate that could be delivered. The pumps were calibrated using a weighted water method and a flow rate accurate to 2 decimal places had been chosen based on the syringe pump. However, for the peristaltic pump (pulsed flow) set up, the flowrate of 0.08 ml/min an accuracy of 75% over 20 readings was observed, meaning that 15 out of 20 readings were between 0.076-0.084ml/min. Flowrate 0.78 ml/min an accuracy of 80% was observed meaning that for 16 out of 20 readings were between 0.776-0.784ml/min. For 3.12 ml/min an accuracy of 85% was recorded meaning for 18 out of the 20 readings were between 3.116-3.124ml/min. Measuring the accuracy to one decimal place, resulted in 95% accuracy for all peristaltic pump measurements. For the syringe pump (steady flow) set up the respective accuracies for 0.08 ml/min, 0.79 ml/min and 3.15 ml/min were 95% over the 20 calibrations taken meaning that all 20 readings were between 0.076-0.084ml/min, 0.776-0.784ml/min and 3.116-.3.124 ml/min respectively. However, taking to 0.1 decimal place increased the accuracy to 100%. To ensure a minimum of 95% accuracy of the peristaltic pump flowrates and shear stress rates were recorded accurate to one decimal place, hence 0.1, 1.0 and 4.0 dyne/cm^2. The lowest flow rate was also limited by the lowest flow rate that the peristaltic pump could deliver. An alternative pumping system could have included another Harvard syringe pump if one had been available, programmed to deliver a step flow. An alternative to the weighted water calibration could have been the use of a microfluidic flow sensor, such as the Elveflow BFS flow sensor which could measure ranges of between 1.6µL/min to 3 mL/min, or Elveflow MFS which measures lower flow rates, however, due to expense these were not available.

5.4.3 Selection of shear stress conditions

The selection of shear stress rates to use was limited to a choice based on previous published studies and experimental practicalities. It would be much more ideal to know the shear stress rates that the cells may experience in vivo and mimic those shear stress rates in vitro. However, due to the complexity of the fluid flow through the disc, as discussed in chapter 2, and there currently being no direct way to measure the fluid velocity through the disc, this was not possible. There are some drives to model the flow through the disc and future research may find the answers. In vitro experimental methods and computer modelling using biphasic, triphasic and quadphasic models incorporating Darcy's Law (Ferguson et al., 2004, Gu et al., 2004), Biot's Law (Biot, 1955, Laible et al., 1993) and Carmen-Kozeny (Nield and Bejan, 2013) for flow through porous media with consolidation have been used to attempt to quantify fluid flow through biological material and advances are being made in this area of research in the IVD by Schroeder et al (2006). Early research in this area investigated flow through articular cartilage and due to the similarities in the poroelastic nature this existing research has been useful in proposing fluid flow through the IVD. Models have been based on original work by (Mow et al., 1980) for flow through cartilage as a biphasic material, this model assumed the solid and fluid to be incompressible and calculated a fluid velocity of 13.7μm/s after loading. Their model did not take into account the ionic nature of the fluid and only the pressure-driven flow. (1984) developed a triphasic theory incorporating the fluid ion concentration and its effect on swelling potential in articular cartilage. (Lai and Mow, 1999) and (Gu et al., 1998) included the effect of electric potentials and electrochemical influence of fluid flow through charged biological tissues. Ferguson et al. (2004), used a poroelastic model of the IVD and an iterative approach to calculate fluid velocities in the IVD of 5 μm/s with application of 0.5 MPa load. (Gu and Yao, 2003) found that fixed charge density affects the fluid transport in the IVD and (Farrell and Riches, 2011) found that ionic effects of the fluid in the IVD account for approximately 50% of the fluid flow in disc. When testing fluid flow velocities on IVD cells in vitro, it would therefore be a reasonable assumption to test flow velocity values around the range 5-13.7μm/s while keeping in mind the findings by (Gu and Yao, 2003) and (Farrell and Riches, 2011) on the significance of electro-kinetic effects on fluid transport, which strengthen the justification for continued research into quadphasic models of fluid movement of in the IVD to include these more

complex phenomenon. Translating these velocities into shear stress rates is complex as the pore size of the ECM would be required and this changes with hydration of the disc and degeneration of the disc, so ascertaining effective shear stress values would not be possible at present.

5.4.4 Maintaining incubator conditions

In the longer duration experiments it was necessary to replace the media in the Harvard pump syringe, this required opening the incubator door during the experiment. As the incubator was hypoxic to maintain the cells at a 2% O_2 concentration then opening the door resulted in raising the oxygen content of the incubator briefly until it was closed again and the incubator reached its desired O_2. The whole process took approximately 3 minutes and was unavoidable with the apparatus being used. A larger syringe would have meant the door would have to be opened less would have reduced the accuracy of the syringe pump.

5.4.5 Cell detachment

For the flow rates chosen cells detached from the slide in large number at 1.0 and 4.0 dyne/cm^2, is it assumed that detachment of the cells was due to the shear stress having a negative effect on the cells, however, as the cells were washed away in the flow and discarded; the state of the detached cells was not tested. Analysing the cells following detachment by collecting them in the fluid and attempting to grow them and analyse their morphology and gene expression would be interesting to see if the function of the cell had been affected in the long term by shear stress or just in the short term. This could lead to studies involving regeneration of NP cells and would be useful as future research.

Chapter 6. Conclusions

Cell-based treatments for pain arising from intervertebral disc problems are on the rise. Perfusion bioreactors are more commonly being used in the development of cell-based scaffolds as a possible future treatment for intervertebral disc problems. Perfusion bioreactors have the advantages of allowing a continuous supply of nutrients to the cells but also as the importance of mechanotransduction has been realised in maintaining the in vivo morphology and gene expression of cells, so the importance of utilising mechanical stresses in bioreactors has been realised. The aim of this thesis was to investigate if shear stresses caused by fluid flow influences nucleus pulposus cells. The animal model, bovine, was used for its advantages of bovine tails being readily available for cell harvesting and Ibidi VI$^{0.4}$ slides were used to create a chamber over which to flow fluid over a monolayer of bovine nucleus pulposus cells. The research questions to be answered from this research fill a gap in current knowledge, there has only been one other study on shear stress which investigated cells under exposure to 1 dyne/cm^2 for 1 hour and found increased gene expression of the keratan sulphate protein, lumican. The questions of does shear stress affect bovine NP cell morphology and gene expression and if so, does the type of fluid flow effect bovine NP cell morphology and gene expression, does the shear stress rate effect bovine NP cell morphology and gene expression and does the duration of time the cells are exposed to shear stress effect NP cell morphology and gene expression? These questions were answered by using two pumps, a Harvard syringe pump; to create a steady flow, and a GE peristaltic pump; to create a pulsed flow, and by testing the response of NP bovine cells to the different types of flow over 3 different shear stress rates; 0.1, 1.0 and 4.0 dyne/cm^2 and over 4 time points; 1, 4, 8 and 24 hours.

Changes in morphology were analysed by immunostaining the cells following the flow condition, compared to the control which was not exposed to flow. Immunostaining was carried on the nucleus; used to count the cell number, vinculin; used to count focal adhesion number and phalloidin; used to quantify the shape of the cell (cell circularity). Gene expression was analysed using RT-qPCR, 5 genes were analysed, Collagen 1, collagen 2, aggrecanase 1, aggrecanase 2 and aggrecan. The Ct values gained for RT-qPCR analysed were normalized to the GAPDH (housekeeping gene)

to give dCt values and statistical analysis was carried out on these values. Graphical representations of the results were shown on logarithmic scale of 2^{-ddCt} and justification for this was discussed in the results chapter. One-way ANOVAs were then used to assess the effects of flow type, shear stress rates and duration of exposure on cell morphology and gene expression.

The main findings were that shear stress can have both anabolic and catabolic effects on bovine NP cell morphology and gene expression. Shear stress of 0.1 dyne/cm^2 for 4 hours was shown to increase the gene expression of aggrecan compared to a control in a pulsed flow have a significant, but steady flow of 0.1 dyne/cm^2 for 4 hours showed a significant increase in proliferation of cells, so there is inconclusive evidence to show whether steady or pulsed flow is preferential for cell health. The results for the rate of shear stress were more conclusive with shear stress rates of 1.0 dyne/cm^2 and 4.0 dyne/cm^2 having a detrimental effect on cell morphology and anabolic gene expression and these effects were cumulative over a 24 hour period, showing that the duration that the cells were exposed to shear stress was important. Further studies with larger sample sizes would be needed to recommend a conclusive regime which could be used in bioreactors to improve cell health, but the general trend appears to be shear stress rates lower than 1 dyne/cm^2, for less than 8 hours and in either steady or pulsed flow may be beneficial. The development of computer modelling to develop quadphasic models to determine the in vivo shear stress rates in the IVD matrix would further enhance this research. Allowing the development of shear stress regimes which could take into account pressure changes and thereby flow rates which are created through exercises. This would then allow not only testing of bioreactor regimes for novel cell-based treatments but also recommendations for in vivo exercise regimes for the prevention of disc degeneration.

References

ACCADBLED, F., LAFFOSSE, J.-M., AMBARD, D., GOMEZ-BROUCHET, A., DE GAUZY, J. S. & SWIDER, P. 2008. Influence of location, fluid flow direction, and tissue maturity on the macroscopic permeability of vertebral end plates. *Spine,* 33**,** 612-619.

ADAMS, M. A., BOGDUK, N., BURTON, K., DOLAN, P. 2013. *The Biomechanics of Back Pain*, Elsevier Churchill Livingstone.

ADAMS, M. A., DOLAN, P. & HUTTON, W. C. 1986a. The stages of disc degeneration as revealed by discograms. *Journal of Bone & Joint Surgery, British Volume,* 68**,** 36-41.

ADAMS, M. A., DOLAN, P. & HUTTON, W. C. 1986b. The stages of disc degeneration as revealed by discograms. *Bone & Joint Journal,* 68**,** 36-41.

ADAMS, M. A. & HUTTON, W. C. 1982. Prolapsed Intervertebral Disc: A Hyperflexion Injury. *Spine,* 7**,** 184-191.

ADAMS, M. A. & HUTTON, W. C. 1983. The Effect of Posture on the Fluid Content of Lumbar Intervertebral Discs. *Spine,* 8**,** 665-671.

ADAMS, M. A. & ROUGHLEY, P. J. 2006. What is intervertebral disc degeneration, and what causes it? *Spine,* 31**,** 2151-2161.

ALINI, M., EISENSTEIN, S. M., ITO, K., LITTLE, C., KETTLER, A. A., MASUDA, K., MELROSE, J., RALPHS, J., STOKES, I. & WILKE, H. J. 2008. Are animal models useful for studying human disc disorders/degeneration? *European Spine Journal,* 17**,** 2-19.

ANDERSSON, G. B. 1999. Epidemiological features of chronic low-back pain. *Lancet,* 354**,** 581-5.

BACABAC, R. G., SMIT, T. H., COWIN, S. C., VAN LOON, J. J. W. A., NIEUWSTADT, F. T. M., HEETHAAR, R. & KLEIN-NULEND, J. 2005. Dynamic shear stress in parallel-plate flow chambers. *Journal of Biomechanics,* 38**,** 159-167.

BANCROFT, G. N., SIKAVITSAS, V. I. & MIKOS, A. G. 2003. Technical note: Design of a flow perfusion bioreactor system for bone tissue-engineering applications. *Tissue engineering,* 9**,** 549-554.

BELAVÝ, D. L., QUITTNER, M. J., RIDGERS, N., LING, Y., CONNELL, D. & RANTALAINEN, T. 2017. Running exercise strengthens the intervertebral disc. *Sci Rep,* 7**,** 45975.

BERG, S., TULLBERG, T., BRANTH, B., OLERUD, C. & TROPP, H. 2009. Total disc replacement compared to lumbar fusion: a randomised controlled trial with 2-year follow-up. *European spine journal,* 18**,** 1512-1519.

BERTRAM, H., KROEBER, M., WANG, H., UNGLAUB, F., GUEHRING, T., CARSTENS, C. & RICHTER, W. 2005. Matrix-assisted cell transfer for intervertebral disc cell therapy. *Biochemical and Biophysical Research Communications,* 331**,** 1185-1192.

BIOT, M. A. 1955. Theory of elasticity and consolidation for a porous anisotropic solid. *Journal of applied physics,* 26**,** 182-185.

BITON, Y. Y. & SAFRAN, S. A. 2010. Theory of the mechanical response of focal adhesions to shear flow. *J Phys Condens Matter,* 22**,** 194111.

BOGDUK, N. 2011. *Clinical Anatomy of the Lumbar Spine and Sacrum*, Elsevier.

BOOS, N., WEISSBACH, S., ROHRBACH, H., WEILER, C., SPRATT, K. F. & NERLICH, A. G. 2002. Classification of age-related changes in lumbar intervertebral discs: 2002 Volvo Award in basic science. *Spine (Phila Pa 1976),* 27**,** 2631-44.

BOYAN, B. D., SYLVIA, V. L., DEAN, D. D. & SCHWARTZ, Z. 1996. Cell biology of calcified tissues: experimental models of differentiation and mechanisms by which local and systemic factors exert their effects. *Connect Tissue Res,* 35**,** 63-70.

BROOKS, A. R., LELKES, P. I. & RUBANYI, G. M. 2002. Gene expression profiling of human aortic endothelial cells exposed to disturbed flow and steady laminar flow. *Physiological genomics,* 9**,** 27-41.

BROWN, D. C. & LARSON, R. S. 2001. Improvements to parallel plate flow chambers to reduce reagent and cellular requirements. *BMC immunology,* 2**,** 9.

BUCKWALTER, J. A. 1995. Aging and degeneration of the human intervertebral disc. *Spine (Phila Pa 1976),* 20**,** 1307-14.

BUSHELL, G. R., GHOSH, P., TAYLOR, T. F. & AKESON, W. H. 1977. Proteoglycan chemistry of the intervertebral disks. *Clin Orthop Relat Res***,** 115-23.

CAMPISI, J. 2013. Aging, cellular senescence, and cancer. *Annu Rev Physiol,* 75**,** 685-705.

CAO, H., CAO, F., ROUSSEL, A.-M. & ANDERSON, R. A. 2013. Quantitative PCR for glucose transporter and tristetraprolin family gene expression in cultured mouse adipocytes and macrophages. *In Vitro Cellular & Developmental Biology-Animal,* 49**,** 759-770.

CARLOS RODRÍGUEZ-MANZANEQUE, J., WESTLING, J., THAI, S. N. M., LUQUE, A., KNAUPER, V., MURPHY, G., SANDY, J. D. & IRUELA-ARISPE, M. L. 2002. ADAMTS1 cleaves aggrecan at multiple sites and is differentially inhibited by metalloproteinase inhibitors. *Biochemical and Biophysical Research Communications,* 293**,** 501-508.

CHATZIZISIS, Y. S., COSKUN, A. U., JONAS, M., EDELMAN, E. R., FELDMAN, C. L. & STONE, P. H. 2007. Role of endothelial shear stress in the natural history of coronary atherosclerosis and vascular remodeling: molecular, cellular, and vascular behavior. *Journal of the American College of Cardiology,* 49**,** 2379-2393.

CHIANG, Y. F., CHIANG, C. J., YANG, C. H., ZHONG, Z. C., CHEN, C. S., CHENG, C. K. & TSUANG, Y. H. 2012. Retaining intradiscal pressure after annulotomy by different annular suture techniques, and their biomechanical evaluations. *Clin Biomech (Bristol, Avon),* 27**,** 241-8.

CHOU, P.-H., WANG, S.-T., YEN, M.-H., LIU, C.-L., CHANG, M.-C. & LEE, O. K.-S. 2016. Fluid-induced, shear stress-regulated extracellular matrix and matrix metalloproteinase genes expression on human annulus fibrosus cells. *Stem Cell Research & Therapy,* 7**,** 1-8.

CHOU, R., QASEEM, A., SNOW, V., CASEY, D., CROSS, J. J. T., SHEKELLE, P. & OWENS, D. K. 2007. Diagnosis and Treatment of Low Back Pain: A Joint Clinical Practice Guideline from the American College of Physicians and the American Pain Society. *Annals of Internal Medicine,* 147**,** 478-491.

CHUNG, S. S., LEE, C. S. & KANG, C. S. 2006. Lumbar total disc replacement using ProDisc II: a prospective study with a 2-year minimum follow-up. *Clinical Spine Surgery,* 19**,** 411-415.

CORNISH, R. J. 1928. Flow in a Pipe of Rectangular Cross-Section. *Proceedings of the Royal Society of London. Series A,* 120**,** 691.

COSTI, J. J., STOKES, I. A., GARDNER-MORSE, M., LAIBLE, J. P., SCOFFONE, H. M. & IATRIDIS, J. C. 2007. Direct measurement of intervertebral disc maximum shear strain in six degrees of freedom: motions that place disc tissue at risk of injury. *Journal of biomechanics,* 40**,** 2457-2466.

COUZON, C., DUPERRAY, A. & VERDIER, C. 2009. Critical stresses for cancer cell detachment in microchannels. *Eur Biophys J,* 38**,** 1035-47.
COVENTRY, M. B., GHORMLEY, R. K. & KERNOHAN, J. W. 1945. The intervertebral disc: its microscopic anatomy and pathology. *The Journal of Bone & Joint Surgery,* 27**,** 460-474.
CROCK, H. V., YOSHIZAWA, H. & KAME, S. K. 1973. Observations on the venous drainage of the human vertebral body. *J Bone Joint Surg Br,* 55**,** 528-33.
DABAGH, M., JALALI, P., BUTLER, P. J., RANDLES, A. & TARBELL, J. M. 2017. Mechanotransmission in endothelial cells subjected to oscillatory and multi-directional shear flow. *J R Soc Interface,* 14.
DARLING, E. M. & ATHANASIOU, K. A. 2005. Rapid phenotypic changes in passaged articular chondrocyte subpopulations. *Journal of Orthopaedic Research,* 23**,** 425-432.
DEPALMA, M. J., KETCHUM, J. M. & SAULLO, T. 2011. What is the source of chronic low back pain and does age play a role? *Pain Med,* 12**,** 224-33.
DI LUCA, A., OSTROWSKA, B., LORENZO-MOLDERO, I., LEPEDDA, A., SWIESZKOWSKI, W., VAN BLITTERSWIJK, C. & MORONI, L. 2016. Gradients in pore size enhance the osteogenic differentiation of human mesenchymal stromal cells in three-dimensional scaffolds. *Scientific Reports,* 6**,** 22898.
DING, M., HENRIKSEN, S. S., WENDT, D. & OVERGAARD, S. 2016. An automated perfusion bioreactor for the streamlined production of engineered osteogenic grafts. *J Biomed Mater Res B Appl Biomater,* 104**,** 532-7.
DING, N., GENG, B., LI, Z., YANG, Q., YAN, L., WAN, L., ZHANG, B., WANG, C. & XIA, Y. 2018. Fluid shear stress promotes osteoblast proliferation through the NFATc1-ERK5 pathway. *Connect Tissue Res***,** 1-10.
DYTHAM, C. 2003. *Choosing and using statistics : a biologist's guide,* Malden, Mass. ; Oxford, Blackwell Pub.
EGAN, J. J., GRONOWICZ, G. & RODAN, G. A. 1991. Cell density-dependent decrease in cytoskeletal actin and myosin in cultured osteoblastic cells: Correlation with cyclic AMP changes. *Journal of Cellular Biochemistry,* 45**,** 93-100.
ELFERVIG, M. K., MINCHEW, J. T., FRANCKE, E., TSUZAKI, M. & BANES, A. J. 2001. IL-1β sensitizes intervertebral disc annulus cells to fluid-induced shear stress. *Journal of cellular biochemistry,* 82**,** 290-298.
ENKER, P., STEFFEE, A., MCMILLIN, C., KEPPLER, L., BISCUP, R. & MILLER, S. 1993. Artificial Disc Replacement: Preliminary Report With a 3-Year Minimum Follow-up. *Spine,* 18**,** 1061-1070.
ESKIN, S. G., IVES, C. L., MCINTIRE, L. V. & NAVARRO, L. T. 1984. Response of cultured endothelial cells to steady flow. *Microvascular Research,* 28**,** 87-94.
FARRELL, M. & RICHES, P. 2011. Ionic osmotic effects increase fluid flow during permeation tests. *Journal of Mechanics in Medicine and Biology*.
FENG, G., LI, L., LIU, H., SONG, Y., HUANG, F., TU, C., SHEN, B., GONG, Q., LI, T., LIU, L., ZENG, J., KONG, Q., YI, M., GUPTE, M., MA, P. X. & PEI, F. 2013. Hypoxia differentially regulates human nucleus pulposus and annulus fibrosus cell extracellular matrix production in 3D scaffolds. *Osteoarthritis Cartilage,* 21**,** 582-8.
FERGUSON, S. J., ITO, K. & NOLTE, L.-P. 2004. Fluid flow and convective transport of solutes within the intervertebral disc. *Journal of Biomechanics,* 37**,** 213-221.

FERNANDEZ, C., MARIONNEAUX, A., GILL, S. & MERCURI, J. 2016. Biomimetic nucleus pulposus scaffold created from bovine caudal intervertebral disc tissue utilizing an optimal decellularization procedure. *J Biomed Mater Res A,* 104**,** 3093-3106.

FREEMONT, A. J., PEACOCK, T. E., GOUPILLE, P., HOYLAND, J. A., O'BRIEN, J. & JAYSON, M. I. V. 1997. Nerve ingrowth into diseased intervertebral disc in chronic back pain. *The lancet,* 350**,** 178-181.

FUJISAKI, K., TADANO, S. & ASANO, N. 2011. Relationship between streaming potential and compressive stress in bovine intervertebral tissue. *Journal of Biomechanics,* 44**,** 2477-2481.

GANEY, T., LIBERA, J., MOOS, V., ALASEVIC, O., FRITSCH, K.-G., MEISEL, H. J. & HUTTON, W. C. 2003. Disc chondrocyte transplantation in a canine model: a treatment for degenerated or damaged intervertebral disc. *Spine,* 28**,** 2609-2620.

GARCIA, R., YUE, J. J., BLUMENTHAL, S., CORIC, D., PATEL, V. V., LEARY, S. P., DINH, D. H., BUTTERMANN, G. R., DEUTSCH, H., GIRARDI, F., BILLYS, J. & MILLER, L. E. 2015. Lumbar Total Disc Replacement for Discogenic Low Back Pain: Two-year Outcomes of the activL Multicenter Randomized Controlled IDE Clinical Trial. *Spine (Phila Pa 1976),* 40**,** 1873-81.

GEIGER, B., SPATZ, J. P. & BERSHADSKY, A. D. 2009. Environmental sensing through focal adhesions. *Nat Rev Mol Cell Biol,* 10**,** 21-33.

GHARRAVI, A. M., ORAZIZADEH, M. & HASHEMITABAR, M. 2016. Fluid-induced low shear stress improves cartilage like tissue fabrication by encapsulating chondrocytes. *Cell and Tissue Banking,* 17**,** 117-122.

GILBERT, H. T., HODSON, N., BAIRD, P., RICHARDSON, S. M. & HOYLAND, J. A. 2016. Acidic pH promotes intervertebral disc degeneration: Acid-sensing ion channel -3 as a potential therapeutic target. *Sci Rep,* 6**,** 37360.

GILBERT, H. T., HOYLAND, J. A. & MILLWARD-SADLER, S. J. 2010. The response of human anulus fibrosus cells to cyclic tensile strain is frequency-dependent and altered with disc degeneration. *Arthritis Rheum,* 62.

GILCHRIST, C. L., DARLING, E. M., CHEN, J. & SETTON, L. A. 2011. Extracellular matrix ligand and stiffness modulate immature nucleus pulposus cell-cell interactions. *PloS one,* 6**,** e27170.

GOMES, M. E., BOSSANO, C. M., JOHNSTON, C. M., REIS, R. L. & MIKOS, A. G. 2006. In vitro localization of bone growth factors in constructs of biodegradable scaffolds seeded with marrow stromal cells and cultured in a flow perfusion bioreactor. *Tissue engineering,* 12**,** 177-188.

GRUBER, H. E. & HANLEY, E. N. 2000. Human disc cells in monolayer vs 3D culture: cell shape, division and matrix formation. *BMC Musculoskeletal Disorders,* 1**,** 1.

GRUNHAGEN, T., WILDE, G., SOUKANE, D. M., SHIRAZI-ADL, S. A. & URBAN, J. P. G. 2006. Nutrient supply and intervertebral disc metabolism. *The Journal of Bone & Joint Surgery,* 88**,** 30-35.

GU, W. Y., LAI, W. M. & MOW, V. C. 1998. A Mixture Theory for Charged-Hydrated Soft Tissues Containing Multi-electrolytes: Passive Transport and Swelling Behaviors. *Journal of Biomechanical Engineering,* 120**,** 169-180.

GU, W. Y. & YAO, H. 2003. Effects of hydration and fixed charge density on fluid transport in charged hydrated soft tissues. *Ann Biomed Eng,* 31**,** 1162-70.

GU, W. Y., YAO, H., VEGA, A. L. & FLAGLER, D. 2004. Diffusivity of Ions in Agarose Gels and Intervertebral Disc: Effect of Porosity. *Annals of Biomedical Engineering,* 32**,** 1710-1717.

GUEHRING, T., OMLOR, G. W., LORENZ, H., ENGELLEITER, K., RICHTER, W., CARSTENS, C. & KROEBER, M. 2006. Disc distraction shows evidence of regenerative potential in degenerated intervertebral discs as evaluated by protein expression, magnetic resonance imaging, and messenger ribonucleic acid expression analysis. *Spine (Phila Pa 1976),* 31**,** 1658-65.

GUEHRING, T., WILDE, G., SUMNER, M., GRÜNHAGEN, T., KARNEY, G. B., TIRLAPUR, U. K. & URBAN, J. P. G. 2009. Notochordal intervertebral disc cells: Sensitivity to nutrient deprivation. *Arthritis & Rheumatism,* 60**,** 1026-1034.

GUILAK, F., TING-BEALL, H. P., BAER, A. E., TRICKEY, W. R., ERICKSON, G. R. & SETTON, L. A. 1999. Viscoelastic properties of intervertebral disc cells: identification of two biomechanically distinct cell populations. *Spine,* 24**,** 2475.

GUYER, R. D., MCAFEE, P. C., BANCO, R. J., BITAN, F. D., CAPPUCCINO, A., GEISLER, F. H., HOCHSCHULER, S. H., HOLT, R. T., JENIS, L. G. & MAJD, M. E. 2009. Prospective, randomized, multicenter Food and Drug Administration investigational device exemption study of lumbar total disc replacement with the CHARITE artificial disc versus lumbar fusion: five-year follow-up. *The Spine Journal,* 9**,** 374-386.

HADDEN, W. J. & CHOI, Y. S. 2016. The extracellular microscape governs mesenchymal stem cell fate. *Journal of Biological Engineering,* 10**,** 16.

HALLORAN, D. O., GRAD, S., STODDART, M., DOCKERY, P., ALINI, M. & PANDIT, A. S. 2008. An injectable cross-linked scaffold for nucleus pulposus regeneration. *Biomaterials,* 29**,** 438-447.

HANDA, T., ISHIHARA, H., OHSHIMA, H., OSADA, R., TSUJI, H. & OBATA, K. I. 1997. Effects of hydrostatic pressure on matrix synthesis and matrix metalloproteinase production in the human lumbar intervertebral disc. *Spine,* 22**,** 1085-1091.

HARTMAN, R. A., YURUBE, T., NGO, K., MERZLAK, N. E., DEBSKI, R. E., BROWN, B. N., KANG, J. D. & SOWA, G. A. 2015. Biological responses to flexion/extension in spinal segments ex-vivo. *Journal of Orthopaedic Research,* 33**,** 1255-1264.

HELMLINGER, G., GEIGER, R. V., SCHRECK, S. & NEREM, R. M. 1991. Effects of Pulsatile Flow on Cultured Vascular Endothelial Cell Morphology. *Journal of Biomechanical Engineering,* 113**,** 123-131.

HICKEY, D. S. & HUKINS, D. W. 1980. Relation between the structure of the annulus fibrosus and the function and failure of the intervertebral disc. *Spine (Phila Pa 1976),* 5**,** 106-16.

HILIBRAND, A. S. & ROBBINS, M. 2004. Adjacent segment degeneration and adjacent segment disease: the consequences of spinal fusion? *The Spine Journal,* 4**,** S190-S194.

HILLSLEY, M. V. & FRANGOS, J. A. 1994. Review: Bone tissue engineering: The role of interstitial fluid flow. *Biotechnology and bioengineering,* 43**,** 573-581.

HOCHMUTH, R., DAS, N. M., SESHADRI, V. & SUTERA, S. 1971. Deformation of red cells in shear flow. *AIAA Paper No. 71-104*.

HOHAUS, C., GANEY, T. M., MINKUS, Y. & MEISEL, H. J. 2008. Cell transplantation in lumbar spine disc degeneration disease. *European Spine Journal,* 17**,** 492-503.

HOLM, K. & CHRISTMAN, N. J. 1985. Post hoc tests following analysis of variance. *Res Nurs Health,* 8**,** 207-10.

HOLM, S., MAROUDAS, A., URBAN, J. P. G., SELSTAM, G. & NACHEMSON, A. 1981. Nutrition of the intervertebral disc: solute transport and metabolism. *Connective tissue research,* 8**,** 101-119.
HONG, J., REED, C., NOVICK, D. & HAPPICH, M. 2013. Costs associated with treatment of chronic low back pain: an analysis of the UK General Practice Research Database. *Spine (Phila Pa 1976),* 38**,** 75-82.
HORNER, H. A., ROBERTS, S., BIELBY, R. C., MENAGE, J., EVANS, H. & URBAN, J. P. G. 2002. Cells from different regions of the intervertebral disc: effect of culture system on matrix expression and cell phenotype. *Spine,* 27**,** 1018-1028.
HORNER, H. A. & URBAN, J. P. G. 2001. 2001 Volvo Award Winner in Basic Science Studies: effect of nutrient supply on the viability of cells from the nucleus pulposus of the intervertebral disc. *Spine,* 26**,** 2543-2549.
HORZUM, U., OZDIL, B. & PESEN-OKVUR, D. 2014. Step-by-step quantitative analysis of focal adhesions. *MethodsX,* 1**,** 56-59.
HOSSAIN, M. S., BERGSTROM, D. J. & CHEN, X. B. 2015. Modelling and simulation of the chondrocyte cell growth, glucose consumption and lactate production within a porous tissue scaffold inside a perfusion bioreactor. *Biotechnology Reports,* 5**,** 55-62.
HOY, D., MARCH, L., BROOKS, P., BLYTH, F., WOOLF, A., BAIN, C., WILLIAMS, G., SMITH, E., VOS, T., BARENDREGT, J., MURRAY, C., BURSTEIN, R. & BUCHBINDER, R. 2014. The global burden of low back pain: estimates from the Global Burden of Disease 2010 study. *Annals of the Rheumatic Diseases,* 73**,** 968-974.
HUANG, N. F., OKOGBAA, J., LEE, J. C., JHA, A., ZAITSEVA, T. S., PAUKSHTO, M. V., SUN, J. S., PUNJYA, N., FULLER, G. G. & COOKE, J. P. 2013. The modulation of endothelial cell morphology, function, and survival using anisotropic nanofibrillar collagen scaffolds. *Biomaterials,* 34**,** 4038-4047.
IATRIDIS, J. C., FURUKAWA, M., STOKES, I. A. F., GARDNER-MORSE, M. G. & LAIBLE, J. P. 2009. Spatially Resolved Streaming Potentials of Human Intervertebral Disk Motion Segments Under Dynamic Axial Compression. *Journal of Biomechanical Engineering,* 131**,** 031006-031006-6.
IATRIDIS, J. C., LAIBLE, J. P. & KRAG, M. H. 2003. Influence of fixed charge density magnitude and distribution on the intervertebral disc: applications of a poroelastic and chemical electric (PEACE) model. *Journal of Biomechanical Engineering,* 125**,** 12-24.
IATRIDIS, J. C., WEIDENBAUM, M., SETTON, L. A. & MOW, V. C. 1996. Is the Nucleus Pulposus a Solid or a Fluid? Mechanical Behaviors of the Nucleus Pulposus of the Human Intervertebral Disc. *Spine,* 21**,** 1174-1184.
IBIDI 2015. u-slide VI$^{0.4}$ instructions. *In:* IBIDI (ed.).
INOUE, H. & TAKEDA, T. 1975. Three-dimensional observation of collagen framework of lumbar intervertebral discs. *Acta Orthopaedica Scandinavica,* 46**,** 949-956.
ISHIHARA, H., MCNALLY, D. S., URBAN, J. P. & HALL, A. C. 1996. Effects of hydrostatic pressure on matrix synthesis in different regions of the intervertebral disk. *J Appl Physiol (1985),* 80.
JOHNSEN, L. G., HELLUM, C., STORHEIM, K., NYGAARD, Ø., BROX, J. I., ROSSVOLL, I., RØ, M., ANDRESEN, H., LYDERSEN, S., GRUNDNES, O., PEDERSEN, M., LEIVSETH, G., OLAFSSON, G., BORGSTRÖM, F., FRITZELL, P. & GROUP, N. S. S. 2014. Cost-effectiveness of total disc

replacement versus multidisciplinary rehabilitation in patients with chronic low back pain: a Norwegian multicenter RCT. *Spine (Phila Pa 1976),* 39**,** 23-32.
JOHNSON, L., MORGAN, RAFF, ROBERTS, WALTER 2015. *Molecular Biology of The Cell*, Garland Science.
JÜNGER, S., GANTENBEIN-RITTER, B., LEZUO, P., ALINI, M., FERGUSON, S. J. & ITO, K. 2009. Effect of limited nutrition on in situ intervertebral disc cells under simulated-physiological loading. *Spine,* 34**,** 1264-1271.
KHISMATULLIN, D. B. & TRUSKEY, G. A. 2004. A 3D numerical study of the effect of channel height on leukocyte deformation and adhesion in parallel-plate flow chambers. *Microvascular research,* 68**,** 188-202.
KIM, K. W., HA, K. Y., LEE, J. S., NAM, S. W., WOO, Y. K., LIM, T. H. & AN, H. S. 2009. Notochordal cells stimulate migration of cartilage end plate chondrocytes of the intervertebral disc in in vitro cell migration assays. *Spine J,* 9**,** 323-9.
KIM, K. W., LIM, T. H., KIM, J. G., JEONG, S. T., MASUDA, K. & AN, H. S. 2003. The origin of chondrocytes in the nucleus pulposus and histologic findings associated with the transition of a notochordal nucleus pulposus to a fibrocartilaginous nucleus pulposus in intact rabbit intervertebral discs. *Spine (Phila Pa 1976),* 28**,** 982-90.
KING, N. 2002. *RT-PCR Protocols*, Humana press Inc.
KRAUS, P. & LUFKIN, T. 2016. Bovine annulus fibrosus cell lines isolated from intervertebral discs. *Genom Data,* 10**,** 83-84.
KROEBER, M., UNGLAUB, F., GUEHRING, T., NERLICH, A., HADI, T., LOTZ, J. & CARSTENS, C. 2005. Effects of controlled dynamic disc distraction on degenerated intervertebral discs: an in vivo study on the rabbit lumbar spine model. *Spine,* 30**,** 181-187.
LAI, W. M. & MOW, V. C. 1999. Transport of Multi-Electrolytes in Charged Hydrated Biological Soft Tissues. *Transport in Porous Media,* 34**,** 143-157.
LAIBLE, J. P., PFLASTER, D. S., KRAG, M. H., SIMON, B. R. & HAUGH, L. D. 1993. A Poroelastic-Swelling Finite Element Model With Application to the Intervertebral Disc. *Spine,* 18.
LATRIDIS, J. C., GODBURN, K., WUERTZ, K., ALINI, M. & ROUGHLEY, P. J. 2011. Region-dependent aggrecan degradation patterns in the rat intervertebral disc are affected by mechanical loading in vivo. *Spine (Phila Pa 1976),* 36**,** 203-9.
LE MAITRE, C. L., FRAIN, J., MILLWARD-SADLER, J., FOTHERINGHAM, A. P., FREEMONT, A. J. & HOYLAND, J. A. 2009. Altered integrin mechanotransduction in human nucleus pulposus cells derived from degenerated discs. *Arthritis & Rheumatism,* 60**,** 460-469.
LEE, J., S. 2016.
LEE, J. T., CHEUNG, K. M. & LEUNG, V. Y. 2015. Systematic study of cell isolation from bovine nucleus pulposus: Improving cell yield and experiment reliability. *J Orthop Res,* 33**,** 1743-55.
LEMAIRE, J. P., SKALLI, W., LAVASTE, F., TEMPLIER, A., MENDES, F., DIOP, A., SAUTY, V. & LALOUX, E. 1997. Intervertebral Disc Prosthesis: Results and Prospects for the Year 2000. *Clinical Orthopaedics and Related Research,* 337.
LEVESQUE, M. J. & NEREM, R. M. 1985. The Elongation and Orientation of Cultured Endothelial Cells in Response to Shear Stress. *Journal of Biomechanical Engineering,* 107**,** 341-347.

LI, D. 2001. Electro-viscous effects on pressure-driven liquid flow in microchannels. *Colloids and Surfaces A: Physicochemical and Engineering Aspects,* 195**,** 35-57.
LI, S., KIM, M., HU, Y. L., JALALI, S., SCHLAEPFER, D. D., HUNTER, T., CHIEN, S. & SHYY, J. Y. 1997. Fluid shear stress activation of focal adhesion kinase. Linking to mitogen-activated protein kinases. *J Biol Chem,* 272**,** 30455-62.
LINN, F. C. & SOKOLOFF, L. 1965. Movement and composition of interstitial fluid of cartilage. *Arthritis & Rheumatology,* 8**,** 481-494.
LIU, X., ZHANG, X. & LEE, I. 2010. A quantitative study on morphological responses of osteoblastic cells to fluid shear stress. *Acta Biochim Biophys Sin (Shanghai),* 42**,** 195-201.
LIVAK, K. J. & SCHMITTGEN, T. D. 2001. Analysis of Relative Gene Expression Data Using Real-Time Quantitative PCR and the 2−ΔΔCT Method. *Methods,* 25**,** 402-408.
LOTZ, J. C., FIELDS, A. J. & LIEBENBERG, E. C. 2013. The Role of the Vertebral End Plate in Low Back Pain. *Global Spine Journal,* 3**,** 153-164.
MALANDRINO, A., LACROIX, D., HELLMICH, C., ITO, K., FERGUSON, S. J. & NOAILLY, J. 2014. The role of endplate poromechanical properties on the nutrient availability in the intervertebral disc. *Osteoarthritis and Cartilage,* 22**,** 1053-1060.
MALAVIYA, P. & NEREM, R. M. 2002. Fluid-induced shear stress stimulates chondrocyte proliferation partially mediated via TGF-beta1. *Tissue Eng,* 8**,** 581-90.
MALEK, A. M. & IZUMO, S. 1996. Mechanism of endothelial cell shape change and cytoskeletal remodeling in response to fluid shear stress. *Journal of Cell Science,* 109**,** 713.
MALKO, J. A., HUTTON, W. C. & FAJMAN, W. A. 1999. An in vivo magnetic resonance imaging study of changes in the volume (and fluid content) of the lumbar intervertebral discs during a simulated diurnal load cycle. *Spine,* 24**,** 1015-1022.
MANNION, A. F., BROX, J. I. & FAIRBANK, J. C. 2016. Consensus at last! Long-term results of all randomized controlled trials show that fusion is no better than non-operative care in improving pain and disability in chronic low back pain. *Spine J,* 16**,** 588-90.
MATSIKO, A., GLEESON, J. P. & O'BRIEN, F. J. 2015. Scaffold mean pore size influences mesenchymal stem cell chondrogenic differentiation and matrix deposition. *Tissue Eng Part A,* 21**,** 486-97.
MATTEI, T. A., BEER, J., TELES, A. R., REHMAN, A. A., ALDAG, J. & DINH, D. 2017. Clinical Outcomes of Total Disc Replacement Versus Anterior Lumbar Interbody Fusion for Surgical Treatment of Lumbar Degenerative Disc Disease. *Global Spine J,* 7**,** 452-459.
MELROSE, J., ROBERTS, S., SMITH, S., MENAGE, J. & GHOSH, P. 2002. Increased Nerve and Blood Vessel Ingrowth Associated With Proteoglycan Depletion in an Ovine Anular Lesion Model of Experimental Disc Degeneration. *Spine,* 27.
MELROSE, J., SMITH, S. M., APPLEYARD, R. C. & LITTLE, C. B. 2008. Aggrecan, versican and type VI collagen are components of annular translamellar crossbridges in the intervertebral disc. *European Spine Journal,* 17**,** 314-324.
MILLIPORE 2009. Actin cytoskeleton and focal adhesion staining kit. *In:* INC, M. (ed.).

MINOGUE, B. M., RICHARDSON, S. M., ZEEF, L. A. H., FREEMONT, A. J. & HOYLAND, J. A. 2010. Characterization of the human nucleus pulposus cell phenotype and evaluation of novel marker gene expression to define adult stem cell differentiation. *Arthritis & Rheumatism,* 62**,** 3695-3705.
MITRA, S., K., AND CHAKRABORTY, S. 2012. *Microfluidics and Nanofluidics Handbook. Chemistry, Physics, and Life Science Principles*, CRC Press.
MORRISON, F. 2013. Introduction to fluid mechanics.
MOW, V. C., KUEI, S. C., LAI, W. M. & ARMSTRONG, C. G. 1980. Biphasic creep and stress relaxation of articular cartilage in compression? Theory and experiments. *J Biomech Eng,* 102**,** 73-84.
MYERS, E. R., LAI, W. M. & MOW, V. C. 1984. A Continuum Theory and an Experiment for the Ion-Induced Swelling Behavior of Articular Cartilage. *Journal of Biomechanical Engineering,* 106**,** 151-158.
NACHEMSON, A. L. F. & MORRIS, J. M. 1964a. In Vivo Measurements of Intradiscal Pressure. *The Journal of Bone & Joint Surgery,* 46**,** 1077.
NACHEMSON, A. L. F. & MORRIS, J. M. 1964b. In Vivo Measurements of Intradiscal Pressure. *The Journal of Bone & Joint Surgery,* 46**,** 1077.
NEIDLINGER-WILKE, C., WÜRTZ, K., URBAN, J. P. G., BÖRM, W., ARAND, M., IGNATIUS, A., WILKE, H.-J. & CLAES, L. E. 2006. Regulation of gene expression in intervertebral disc cells by low and high hydrostatic pressure. *European Spine Journal,* 15**,** 372-378.
NETTLES, D. L., RICHARDSON, W. J. & SETTON, L. A. 2004. Integrin expression in cells of the intervertebral disc. *J Anat,* 204**,** 515-20.
NICE 2016. Low Back Pain and Sciatica in over 16s: assessment and management.
NIELD, D. A. & BEJAN, A. 2013. *Mechanics of Fluid Flow Through a Porous Medium*, Springer.
NIKKHOO, M., WANG, J. L., ABDOLLAHI, M., HSU, Y. C., PARNIANPOUR, M. & KHALAF, K. 2016. A regenerative approach towards recovering the mechanical properties of degenerated intervertebral discs: Genipin and platelet-rich plasma therapies. *Proc Inst Mech Eng H***,** 954411916681597.
OHSHIMA, H., URBAN, J. P. G. & BERGEL, D. H. 1995. Effect of static load on matrix synthesis rates in the intervertebral disc measured in vitro by a new perfusion technique. *Journal of orthopaedic research,* 13**,** 22-29.
OLIVER, C. & JAMUR, M. C. 2010. *Immunocytochemical Methods and Protocols,* New York.
OSTI, O. L., VERNON-ROBERTS, B., MOORE, R. & FRASER, R. D. 1992. Annular tears and disc degeneration in the lumbar spine. A post-mortem study of 135 discs. *J Bone Joint Surg Br,* 74.
OUYANG, A., CERCHIARI, A. E., TANG, X., LIEBENBERG, E., ALLISTON, T., GARTNER, Z. J. & LOTZ, J. C. 2016. Effects of cell type and configuration on anabolic and catabolic activity in 3D co-culture of mesenchymal stem cells and nucleus pulposus cells. *J Orthop Res*.
PALASTANGA, N. F., D. SOAMES, R. 2012. *Anatomy and Human Movement: Structure and Function*, Butterworth-Heinemann Ltd.
PARK, J.-B. & PARK, E.-Y. 2016. Increased Apoptosis, Expression of Matrix Degrading Enzymes and Inflammatory Cytokines of Annulus Fibrosus Cells in Genetically Engineered Diabetic Rats: Implication for Intervertebral Disc Degeneration. *Global Spine J,* 06**,** GO238.
PARK, P., GARTON, H. J., GALA, V. C., HOFF, J. T. & MCGILLICUDDY, J. E. 2004. Adjacent segment disease after lumbar or lumbosacral fusion: review of the literature. *Spine,* 29**,** 1938-1944.

RAIMONDI, M. T., BERTOLDI, S., CADDEO, S., FARÈ, S., ARRIGONI, C. & MORETTI, M. 2016. The effect of polyurethane scaffold surface treatments on the adhesion of chondrocytes subjected to interstitial perfusion culture. *Tissue Engineering and Regenerative Medicine,* 13**,** 364-374.
RAINEY, S., BLUMENTHAL, S. L., ZIGLER, J. E., GUYER, R. D. & OHNMEISS, D. D. 2012. Analysis of adjacent segment reoperation after lumbar total disc replacement. *Int J Spine Surg,* 6**,** 140-4.
RICHARDSON, S. M., WALKER, R. V., PARKER, S., RHODES, N. P., HUNT, J. A., FREEMONT, A. J. & HOYLAND, J. A. 2006. Intervertebral Disc Cell–Mediated Mesenchymal Stem Cell Differentiation. *STEM CELLS,* 24**,** 707-716.
RIHN, J. A., RADCLIFF, K., NORVELL, D. C., EASTLACK, R., PHILLIPS, F. M., BERLAND, D., SHERRY, N., FREEDMAN, M. & VACCARO, A. R. 2017. Comparative Effectiveness of Treatments for Chronic Low Back Pain: A Multiple Treatment Comparison Analysis. *Clin Spine Surg,* 30**,** 204-225.
RINKLER, C., HEUER, F., PEDRO, M. T., MAUER, U. M., IGNATIUS, A. & NEIDLINGER-WILKE, C. 2010. Influence of low glucose supply on the regulation of gene expression by nucleus pulposus cells and their responsiveness to mechanical loading: Laboratory investigation. *Journal of Neurosurgery: Spine,* 13**,** 535-542.
RISBUD, M. V., SCHAER, T. P. & SHAPIRO, I. M. 2010. Toward an understanding of the role of notochordal cells in the adult intervertebral disc: from discord to accord. *Developmental Dynamics,* 239**,** 2141-2148.
ROBERTS, S., CATERSON, B., MENAGE, J., EVANS, E. H., JAFFRAY, D. C. & EISENSTEIN, S. M. 2000. Matrix metalloproteinases and aggrecanase: their role in disorders of the human intervertebral disc. *Spine,* 25.
ROLANDER, S. D. & BLAIR, W. E. 1975. Deformation and fracture of the lumbar vertebral end plate. *Orthop Clin North Am,* 6**,** 75-81.
ROUGHLEY, P., HOEMANN, C., DESROSIERS, E., MWALE, F., ANTONIOU, J. & ALINI, M. 2006. The potential of chitosan-based gels containing intervertebral disc cells for nucleus pulposus supplementation. *Biomaterials,* 27**,** 388-396.
SAKAI, D., MOCHIDA, J., YAMAMOTO, Y., NOMURA, T., OKUMA, M., NISHIMURA, K., NAKAI, T., ANDO, K. & HOTTA, T. 2003. Transplantation of mesenchymal stem cells embedded in Atelocollagen® gel to the intervertebral disc: a potential therapeutic model for disc degeneration. *Biomaterials,* 24**,** 3531-3541.
SCHILLING, W. P., MO, M. & ESKIN, S. G. 1992. Effect of shear stress on cytosolic Ca2+ of calf pulmonary artery endothelial cells. *Exp Cell Res,* 198**,** 31-5.
SCHROEDER, Y., WILSON, W., HUYGHE, J. M. & BAAIJENS, F. P. T. 2006. Osmoviscoelastic finite element model of the intervertebral disc. *European spine journal,* 15**,** 361-371.
SCHWARZER, A. C., APRILL, C. N., DERBY, R., FORTIN, J., KINE, G. & BOGDUK, N. 1995. The prevalence and clinical features of internal disc disruption in patients with chronic low back pain. *Spine (Phila Pa 1976),* 20**,** 1878-83.
SETTON, L. A. & CHEN, J. 2004. Cell mechanics and mechanobiology in the intervertebral disc. *Spine,* 29**,** 2710-2723.
SHARP, L. A., LEE, Y. W. & GOLDSTEIN, A. S. 2009. Effect of low-frequency pulsatile flow on expression of osteoblastic genes by bone marrow stromal cells. *Annals of biomedical engineering,* 37**,** 445-453.
SMOLDERS, L. A., BERGKNUT, N., GRINWIS, G. C., HAGMAN, R., LAGERSTEDT, A. S., HAZEWINKEL, H. A., TRYFONIDOU, M. A. & MEIJ, B. P. 2013.

Intervertebral disc degeneration in the dog. Part 2: chondrodystrophic and non-chondrodystrophic breeds. *Vet J,* 195**,** 292-9.
SONAM, S., SATHE, S. R., YIM, E. K. F., SHEETZ, M. P. & LIM, C. T. 2016. Cell contractility arising from topography and shear flow determines human mesenchymal stem cell fate. *Scientific Reports,* 6**,** 20415.
STOYANOV, J., GANTENBEIN, B., AEBLI, N., BAUR, M., ALINI, M. & GRAD, S. 2010. Role of Hypoxia on Differentiation of Human Mesenchymal Stem Cells Towards Intervertebral Disc-Like Cells.
SUNG, J. H. & SHULER, M. L. 2009. Prevention of air bubble formation in a microfluidic perfusion cell culture system using a microscale bubble trap. *Biomedical Microdevices,* 11**,** 731-738.
TATE, M. L. K., KNOTHE, U. L. F. & NIEDERER, P. 1998. Experimental elucidation of mechanical load-induced fluid flow and its potential role in bone metabolism and functional adaptation. *The American journal of the medical sciences,* 316**,** 189-195.
TEKARI, A., LUGINBUEHL, R., HOFSTETTER, W. & EGLI, R. J. 2014. Chondrocytes expressing intracellular collagen type II enter the cell cycle and co-express collagen type I in monolayer culture. *J Orthop Res,* 32**,** 1503-11.
TIAN, Y., YUAN, W., FUJITA, N., WANG, J., WANG, H., SHAPIRO, I. M. & RISBUD, M. V. 2013. Inflammatory cytokines associated with degenerative disc disease control aggrecanase-1 (ADAMTS-4) expression in nucleus pulposus cells through MAPK and NF-κB. *Am J Pathol,* 182**,** 2310-21.
TONG, W., LU, Z., QIN, L., MAUCK, R. L., SMITH, H. E., SMITH, L. J., MALHOTRA, N. R., HEYWORTH, M. F., CALDERA, F., ENOMOTO-IWAMOTO, M. & ZHANG, Y. 2016. Cell therapy for the degenerating intervertebral disc. *Transl Res*.
TORTORELLA, M. D., LIU, R.-Q., BURN, T., NEWTON, R. C. & ARNER, E. 2002. Characterization of human aggrecanase 2 (ADAM-TS5): substrate specificity studies and comparison with aggrecanase 1 (ADAM-TS4). *Matrix Biology,* 21**,** 499-511.
TRAUB, O. & BERK, B. C. 1998. Laminar shear stress mechanisms by which endothelial cells transduce an atheroprotective force. *Arteriosclerosis, thrombosis, and vascular biology,* 18**,** 677-685.
TROPIANO, P., HUANG, R. C., GIRARDI, F. P. & MARNAY, T. 2003. Lumbar disc replacement: preliminary results with ProDisc II after a minimum follow-up period of 1 year. *Clinical Spine Surgery,* 16**,** 362-368.
URBAN, J. 1977.
URBAN, J. P. G. & MAROUDAS, A. 1979. The measurement of fixed charged density in the intervertebral disc. *Biochimica et Biophysica Acta (BBA) - General Subjects,* 586**,** 166-178.
URBAN, J. P. G. & MAROUDAS, A. 1981. Swelling of the intervertebral disc in vitro. *Connective tissue research,* 9**,** 1-10.
VADALA, G., RUSSO, F., AMBROSIO, L., PAPALIA, R. & DENARO, V. 2016. Mesenchymal stem cells for intervertebral disc regeneration. *J Biol Regul Homeost Agents,* 30**,** 173-179.
VARKI, A., CUMMINGS, R., ESKO, J., FREEZE, H., HART, G. & MARTH, J. 1999. Proteoglycans and glycosaminoglycans.
VENNEMANN, P., LINDKEN, R. & WESTERWEEL, J. 2007. In vivo whole-field blood velocity measurement techniques. *Experiments in Fluids,* 42**,** 495-511.

VERMA, D., MENG, F., SACHS, F. & HUA, S. Z. 2015. Flow-induced focal adhesion remodeling mediated by local cytoskeletal stresses and reorganization. *Cell Adh Migr,* 9**,** 432-40.
VIDEMAN, T., SARNA, S., BATTIÉ, M. C., KOSKINEN, S., GILL, K., PAANANEN, H. & GIBBONS, L. 1995. The long-term effects of physical loading and exercise lifestyles on back-related symptoms, disability, and spinal pathology among men. *Spine (Phila Pa 1976),* 20**,** 699-709.
WALTER, B. A., ILLIEN-JÜNGER, S., NASSER, P. R., HECHT, A. C. & IATRIDIS, J. C. 2014. Development and validation of a bioreactor system for dynamic loading and mechanical characterization of whole human intervertebral discs in organ culture. *Journal of biomechanics,* 47**,** 2095-2101.
WAN, Q., KIM, S. J., YOKOTA, H. & NA, S. 2013. Differential activation and inhibition of RhoA by fluid flow induced shear stress in chondrocytes. *Cell biology international,* 37**,** 568-576.
WANG, D.-L., JIANG, S.-D. & DAI, L.-Y. 2007. Biologic response of the intervertebral disc to static and dynamic compression in vitro. *Spine,* 32**,** 2521-2528.
WANG, J., PAN, H., LI, X., ZHANG, K., LI, Z., WANG, H., ZHENG, Z. & LIU, H. 2016. Hypoxia suppresses serum deprivation-induced degradation of the nucleus pulposus cell extracellular matrix through the JNK and NF-kappaB pathways. *J Orthop Res*.
WANG, N., BUTLER, J. P. & INGBER, D. E. 1993. Mechanotransduction across the cell surface and through the cytoskeleton. *Science,* 260**,** 1124-1127.
WANG, N., TYTELL, J. D. & INGBER, D. E. 2009. Mechanotransduction at a distance: mechanically coupling the extracellular matrix with the nucleus. *Nature reviews Molecular cell biology,* 10**,** 75-82.
WANG, P., YANG, L. & HSIEH, A. H. 2011. Nucleus pulposus cell response to confined and unconfined compression implicates mechanoregulation by fluid shear stress. *Ann Biomed Eng,* 39**,** 1101-11.
WANG, X. & SEED, B. 2003. A PCR primer bank for quantitative gene expression analysis. *Nucleic acids research,* 31**,** e154-e154.
WHITED, B. M. & RYLANDER, M. N. 2014. The influence of electrospun scaffold topography on endothelial cell morphology, alignment, and adhesion in response to fluid flow. *Biotechnology and bioengineering,* 111**,** 10.1002/bit.24995.
WILKE, H.-J. 2008. Animal models for spinal research. *European Spine Journal,* 17**,** 1-1.
WILKE, H. J., NEEF, P., CAIMI, M., HOOGLAND, T. & CLAES, L. E. 1999. New In Vivo Measurements of Pressures in the Intervertebral Disc in Daily Life. *Spine,* 24**,** 755-762.
WOGNUM, S., HUYGHE, J. M. & BAAIJENS, F. P. T. 2006. Influence of osmotic pressure changes on the opening of existing cracks in 2 intervertebral disc models. *Spine,* 31**,** 1783-1788.
YOKOYAMA, W. M. 2001. Cryopreservation of Cells. *Current Protocols in Immunology.* John Wiley & Sons, Inc.
YOSHIZUMI, M., ABE, J.-I., TSUCHIYA, K., BERK, B. C. & TAMAKI, T. 2003. Stress and vascular responses: atheroprotective effect of laminar fluid shear stress in endothelial cells: possible role of mitogen-activated protein kinases. *Journal of pharmacological sciences,* 91**,** 172-176.
ZANDER, T., KRISHNAKANTH, P., BERGMANN, G. & ROHLMANN, A. 2010. Diurnal variations in intervertebral disc height affect spine flexibility, intradiscal

pressure and contact compressive forces in the facet joints. *Comput Methods Biomech Biomed Engin,* 13**,** 551-7.
ZHU, J., TANG, H., ZHANG, Z., ZHANG, Y., QIU, C., ZHANG, L., HUANG, P. & LI, F. 2016. Kaempferol slows intervertebral disc degeneration by modifying LPS-induced osteogenesis/adipogenesis imbalance and inflammation response in BMSCs. *Int Immunopharmacol,* 43**,** 236-242.
ZIGLER, J. E., BLUMENTHAL, S. L., GUYER, R. D., OHNMEISS, D. D. & PATEL, L. 2018. Progression of Adjacent-level Degeneration After Lumbar Total Disc Replacement: Results of a Post-hoc Analysis of Patients with Available Radiographs from a Prospective Study with 5-year Follow-up. *Spine (Phila Pa 1976)*.